NASA Contractor Report 159170

ANALYTIC MODELING OF AEROSOL SIZE DISTRIBUTIONS

ADARSH DEEPAK AND GAIL P. BOX

INSTITUTE FOR ATMOSPHERIC OPTICS & REMOTE SENSING
HAMPTON, VIRGINIA 23666

NASA CONTRACT NAS1-15198
NOVEMBER 1979

National Aeronautics and
Space Administration

Langley Research Center
Hampton, Virginia 23665

CONTENTS

SUMMARY

This paper presents the results of a parametric study of nine analytic models that are commonly used for representing aerosol size distributions; discusses methods by which best-fit estimates of these parameters can be obtained; describes a catalog of graphical plots, depicting the parametric behavior of the functions; and explains procedures for obtaining analytical representations of size distribution data by visual matching of the data with one of the plots. These analytic models consist of mathematical functions, with up to four adjustable parameters, which are referred to as follows: power law; regularized power law--in which singularities that occur in a simple power law as radius goes to zero are avoided; modified gamma distribution; inverse modified gamma distribution--in which the variable is the inverse of radius; log normal distribution; normal distribution; generalized distribution function; and, power law generalized distribution function. The mathematical properties of these distribution functions, such as, mode radius, modal value, limiting behavior of the distribution as radius goes to zero or infinity, moments of the distribution, and, the dominant role played by each parameter in the model. These properties are summarized in a table in the report. The model catalog consists of log-log graphs (6 x 4 cycles) and/or in some cases, semi-log graphs on which the model size distributions are separately plotted. For each of the nine models, sets of plots have been produced, each set depicting the behavior of the model as a function of only one of its parameters, the other parameters being kept constant. Thus, each catalog graph contains several plots, one

corresponding to each value of the parameter being varied, the parameter values being chosen to cover the range of variations in aerosol size distribution likely to be encountered.

The catalog is meant to assist researchers in obtaining an analytic representation for their empirical size distribution data. This is done by means of a relatively quick visual fit to one of the plots in the catalog; and, if the fit is not good enough, which is more likely to be the case, then use the parameters corresponding to the closest plot as initial estimates in a least-squares type program to obtain the best fit to the data. For this purpose, the experimental data should be plotted on transparencies provided with the catalog. The closer the initial estimates are to the best-fit values, the better the assurance of reaching a fast convergence.

In addition, it is shown that the same experimental data can often be represented with equal accuracy by more than one analytic function.

INTRODUCTION

Even though atmospheric aerosols are known to possess a variety of shapes, the description of their physical structure is immensely simplified if they are assumed to be spherical. The size spectrum of atmospheric aerosols is, in general, continuous and covers over four decades in radii, viz, 10^{-3} to 20 μm (Ref. 1). Of the basically four ways in which the empirical size distribution (SD) data can be represented, namely, tabular, histogram, graphical and analytical (Ref. 2), the last one is usually employed due to the fact that there exist regularities in the gross structure of atmospheric aerosols which exhibit behaviour similar to that of a variety of mathematical functions. An analytic function generally encompasses in a smooth way the main features of the aerosol physical structure

While admittedly unrealistic in its smoothness, the analytical representation has the following advantages, namely those of convenient adjustability to obtain a best fit to the experimental data; compact representation of the dependent variable (the SD) in the form of estimated parameters of the fitted distribution; construction of reasonable and convenient models; and, carrying out systematic, parametric modeling of the aerosol optical properties.

The success of the analytic representation approach depends upon the the selection of an appropriate mathematical function to approximate the actual size distribution data. This may not always be possible (Ref. 2); often a linear sum of mathematical functions may provide a good representation. Thus, there seems to be no "special" analytic function that can be said to be unique in representing aerosol SD's. The choice of the function is to some extent dictated by the modeler's taste. However, ultimately, it is only when the fitted analytic function leads to results that closely fit the experimental optical (scattering/extinction) data and at the same time falls within the typical physical domain of atmospheric aerosols, that the analytic function may be assumed to represent the aerosol SD.

The main purpose of this paper is to describe the use of a catalog, depicting graphically the parametric behavior of some analytic functions with up to 4 parameters, that could assist researchers in obtaining analytical representation of their empirical particle size distribution data. The terminology used, the distribution functions considered and the basis for their selection, and a description of the various models and their mathematical properties precede the discussion on the catalog.

The valuable discussions in connection with this work and the careful review of the paper by M. A. Box, Institute for Atmospheric Optics and Remote Sensing, and W. P. Chu and K. H. Crumbly, NASA-Langley Research Center, are gratefully acknowledged.

Terminology for Aerosol Size Distributions

For clarification, the terminology for the particle SD's used is discussed in this section. The physical structure of aerosols (atmospheric or artificial) can be represented, in general, in terms of the number, area, volume or mass of aerosol particles per unit volume per unit radius at r. However, in this paper the discussion will be restricted to the SD representation in terms of the particle number and radius, so that only the *radius-number distribution, log radius-number distribution* and *cumulative size distribution* will be considered. Their definitions, used in this report, follow those given in Ref. 3. (The dependence of the SD on factors such as altitude, composition, etc., will not be considered here.)

The *radius-number distribution n(r), ($cm^{-3}\mu m^{-1}$)*, is defined as the number of particles per unit volume (cm^3) within a unit radius range at r measured in μm. Thus,

$$n(r) = -dN(r) / dr = dN_u(r) / dr, \ (cm^{-3}\mu m^{-1}) \qquad (1)$$

where N(r) ($N_u(r)$) is the cumulative oversize (undersize) distribution function (Ref. 4).

The *log radius-number distribution* $n_L(r)$ (cm^{-3}) is defined by

$$n_L(r) = -dN(r) / d(\log_{10} r) = 2.3026\ r\ n(r), \ (cm^{-3}) \qquad (2)$$

Junge found it convenient to handle the wide range of atmospheric aerosol size distribution data by plotting $n_L(r)$ as a function of r, on a log-log scale. This method of plotting has the advantage that it represents the particle concentration as well as the size distribution.

The *cumulative size distribution* represents the total number of particles per cm^3 that have radii greater (less) than r, is represented by N(r) ($N_u(r)$) and is called the cumulative oversize (undersize) distribution function (Ref. 4). In essence

$$N(r) = \int_r^\infty n(r")dr" = \int_{\log_{10}(r)}^{\infty} n_L(r')\, d\log_{10}(r'), \ (cm^{-3}) \tag{3a}$$

$$N_u(r) = \int_0^r n(r")dr" = \int_{-\infty}^{\log_{10}(r)} n_L(r')\, d\log_{10}(r'), \ (cm^{-3}) \tag{3b}$$

In this paper, only the cumulative oversize distribution (COSD) will be discussed. Note that N(0) would then be the total *number density* (cm^{-3}) of the particles.

Distribution Functions and Selection Criteria

Given some empirical aerosol size distribution data, the problem is to find an analytic function that will most closely represent this data. Examples of mathematical functions of up to two parameters are the normal, gamma, binomial and exponential distribution functions; and of those with more than two parameters are the Weibull, Johnson and Pearson distribution families. These distributions are discussed in detail in many books on probability. (See Ref. 5.) These functions admit almost every type of probability distribution, except composite distributions made up of several distinct populations, such as multimodal distributions. In addition, there is another versatile

distribution, referred to as the generalized distribution function (GDF) (Refs. 6 and 7) which is derived from the Wood-Saxon function.

In the selection of an analytic function to represent the size distribution n(r), the following criteria must be taken into account:

1. The function is not singular for $0 \leq r \leq \infty$;
2. It is easily integrable over r;
3. It can represent the main features of the gross structure of the aerosols by a minimum number of adjustable parameters.

LIST OF SYMBOLS AND ACRONYMS

Symbols

a_j	adjustable constants (Defined in Eq. 18a)
$\bar{A}$	average particle surface area
DN(R)/DLOG10R	$n_L(r) = dN(r)/\log_{10} r$; notation used in the plot labels
DN(R)/DR	$n(r) = d\,N(r)/dr$; notation used in the plot labels
M_k	k^{th} moment
n(r)	radius-number size distribution $[cm^{-3}\ \mu m^{-1}]$
$n_j(r)$	n(r) for j^{th} mode (Defined in Eq. 18a)
$n_L(r)$	log radius-number size distribution $[cm^{-3}]$
N(0)	number density $[cm^{-3}]$
N(r) $[N_u(r)]$	cumulative oversize [undersize] distribution $[cm^{-3}]$
N(>r)	same as N(r); notation used in the plot labels
p_i, i = 1,2,3,4,...	adjustable parameters in mathematical functions; given values of parameters
p_i'	estimated values of parameters
p_i''	reestimated values of parameters
p_{24}	$(p_2 + 1)/p_4$
p_{42}	$(p_2 - 1)/p_4$

r	particle radius
$\bar{r}$	average particle radius
r_j	j^{th} value of r
r_m	mode radius for n(r)
r_{Lm}	mode radius for $n_L(r)$
r_1, r_2	limits of r
$\bar{V}$	average particle volume

Acronyms

CG	catalog graph
CP	catalog plot
COSD	cumulative oversize distribution, N(>r)
DT	data transparency
GD	generalized distribution
IMGD	inverse modified gamma distribution
LND	log normal distribution
MGD	modified gamma distribution
MODELR	represents model number
ND	normal distribution
NLLS	nonlinear least squares
PLD	power law distribution
PLGD	power law generalized distribution
QCM	quartz crystal measurement
RM	r_m, the mode radius
RPLD	regularized power law distribution
SD	size distribution
SD1, SD2	terms 1 and 2 of SD

SIZE DISTRIBUTION MODELS AND THEIR MATHEMATICAL PROPERTIES

Analytic models suitable for representing aerosol size distributions include the following mathematical functions:

1. Power Law Distribution (PLD)
2. Regularized Power Law Distribution (RPLD)
3. Modified Gamma Distribution (MGD)
4. Inverse Modified Gamma Distribution (IMGD)
5. Log-normal Distribution (LND)
6. Normal Distribution (ND)
7. Generalized Distribution (GD)
8. Power Law Generalized Distribution (PLGD)

The expressions and the mathematical properties of the functions will be described in this section. Here the model distributions represent the radius-number distribution n(r), from which the corresponding expressions for $n_L(r)$ and N(r) are derived. The properties of interest are: the mode radii for n(r) and $n_L(r)$; lower limit, asymptotic, and parametric behavior of the functions; and the k^{th} moment of the models. The mode radius r_m for n(r) is given by the solution of

$$\frac{d\ n(r)}{dr} = 0$$

and that for $n_L(r)$, by the solution of

$$\frac{d\ n_L(r)}{dr} = 0$$

The k^{th} moment is given by

$$M_k = \int_0^\infty r^k\ n(r)dr$$

The moments are useful for calculating properties of the distribution such as number (N(O)), average radius ($\bar{r}$), average area ($\bar{A}$), and average volume ($\bar{V}$) of aerosol particles in a unit volume, as shown here:

$$N(O) = M_0$$

$$\bar{r} = M_1/M_0$$

$$\bar{A} = \pi M_2/M_0$$

$$\bar{V} = \frac{4}{3}\pi\ M_3/M_0$$

These properties for the eight size distributions models for n(r) and N(>r) are summarized in Appendix I for quick reference.

A description of how one can determine good estimates of the parameters from the gradients, modal values and moments of the models will be given in a later section. In all these models, the adjustable parameters are represented by p_1, p_2, p_3, ..., where p_1 is the scaling parameter and is chosen so that the maximum value of the function is unity.

Model 1 -- The Power Law (PL) Model

This model, known as the Junge power law, was proposed by Junge to represent his continental aerosol SD data and is given by

$$n(r) = p_1\ r^{-p_2}\ ,\quad r_1 \leq r \leq r_2 \tag{4a}$$

or, alternately, by

$$n_L(r) = 2.3\ p_1 r^{(1-p_2)}\ ,\ r_1 \leq r \leq r_2 \tag{4b}$$

It has a COSD of the form

$$N(r) = \frac{p_1}{p_2-1} \left(r^{1-p_2} - r_2^{1-p_2}\right), \; r_1 \leq r \leq r_2 \qquad (4c)$$

Junge used 0.01μm for r_1 and 1.0μm for r_2 but other values could be used.

The k^{th} moment for the distribution is given by

$$M_k = p_1\left(r_1^{1+k-p_2} - r_2^{1+k-p_2}\right) / \left(p_2 - k - 1\right) \qquad (4d)$$

This model becomes singular at $r = 0$, if $r_1 = 0$; has all its moments infinite if $r_1 = 0$ and $r_2 = \infty$; and has no mode radius (r_m). Even though this model may not always represent a real situation, and does not meet the selection criteria, it is popularly used as it readily gives analytically tractable results. The model is graphically presented in Figs. (1A.1 - 1C.1).

Model 2 -- The Regularized Power Law (RPL) Model

In order to eliminate the singularity at $r = 0$ that occurs in Model 1, without losing its power law behaviour at large r, one may use a regularized form of the power law,

$$n(r) = \left(\frac{p_1}{p_2}\right) \frac{\left(r/p_2\right)^{p_3-1}}{\left[1 + \left(r/p_2\right)^{p_3}\right]^{p_4}} \qquad (5a)$$

The mode radius is given by

$$r_m = p_2 \left(\frac{p_3-1}{1 + p_3(p_4-1)}\right)^{\frac{1}{p_3}} \qquad (5b)$$

and the maximum value is

$$n(r_m) = \frac{p_1}{p_2} \frac{(p_3-1)^{1-\frac{1}{p_3}} (1+p_3(p_4-1))^{\frac{1+p_3(p_4-1)}{p_3}}}{(p_3p_4)^{p_4}} \tag{5c}$$

The limiting behavior of the function is as follows:

$$\text{As} \quad r \to 0, \; n(r) \simeq \frac{p_1}{p_2}(r/p_2)^{p_3-1} \tag{5d}$$

$$\text{and, as} \quad r \to \infty, \; n(r) \sim \frac{p_1}{p_2} (r/p_2)^{-(1+p_3(p_4-1))} \tag{5e}$$

The log radius number distribution is

$$n_L(r) = \frac{2.3 \; p_1 (r/p_2)^{p_3}}{(1+(r/p_2)^{p_3})^{p_4}} \tag{5f}$$

Its maximum value occurs at

$$r_{lm} = p_2 \; (p_4-1)^{-1/p_3} \tag{5g}$$

$$\text{so that } n_L(r_{lm}) = 2.3 \; p_1 \frac{(p_4-1)^{p_4-1}}{(p_4)^{p_4}}$$

The limiting behavior for this form of the distribution is as follows

$$\text{As} \quad r \to 0, \; n(r) \simeq 2.3 \; p_1 \; (r/p_2)^{p_3} \tag{5h}$$

$$\text{and, as} \quad r \to \infty, \; n(r) \sim 2.3 \; p_1 \; (r/p_2)^{-p_3(p_4-1)} \tag{5i}$$

The COSD is given by (Ref. 8, No. 3.194/2 and 9.121/1),

$$N(r) = \frac{p_1}{p_3(p_4-1)} \quad \frac{1}{(1 + (r/p_2)^{p_3})^{p_4-1}} \tag{5j}$$

The limiting behavior for this function is as follows,

$$\text{As} \quad r \to 0, \; N(r) \simeq \frac{p_1}{p_3(p_4-1)} \quad (1 - (p_4-1)\,(r/p_2)^{p_3}) \tag{5k}$$

$$\text{and, as} \quad r \to \infty, \; N(r) \sim \frac{p_1}{p_3(p_4-1)} \quad (r/p_2)^{-p_3(p_4-1)} \tag{5ℓ}$$

The moments for the RPL are given by (Ref. 8, No. 3.194/3 and Ref. 9, p. 103),

$$M_k = \frac{p_1\, p_2^{\,k}}{p_3} \quad \frac{\Gamma(1+k/p_3)\,\Gamma(p_4-1-k/p_3)}{\Gamma(p_4)}, \; k < p_3(p_4-1) \tag{5m}$$

where Γ is the complete gamma function.

The parameter p_2 has the main effect on mode radius, being a multiplicative factor, while p_3 and p_4 control the positive and negative gradients, and hence polydispersity. The parameter p_3 controls the positive gradient while both p_3 and p_4 influence the negative gradient. The model is graphically presented in Figs. (2A.1 - 2C.4).

Model 3 -- Modified Gamma Distribution (MGD) Model

Model 3 is the modified gamma distribution function. Deirmendjian (Ref. 10) has shown that this function can be used to describe various

types of realistic aerosol distributions. For instance, by assigning different values to the parameters p_2 and p_4 one obtains models such as Haze H, Haze M, Haze L, Cloud C3, etc.

The radius-number distribution is given by

$$n(r) = p_1 r^{p_2} \exp(-p_3 r^{p_4}) \tag{6a}$$

Its mode radius is

$$r_m = \left(\frac{p_2}{p_3 p_4}\right)^{1/p_4} \tag{6b}$$

and its maximum value is

$$n(r_m) = p_1 \left(\frac{p_2}{p_3 p_4}\right)^{p_2/p_4} \exp(-p_2/p_4) \tag{6c}$$

The limiting behavior of the distribution is as follows

$$\text{As} \quad r \to 0, \; n(r) \simeq p_1 r^{p_2} \tag{6d}$$

$$\text{and, as} \quad r \to \infty, \; n(r) \to 0 \quad \text{as} \quad p_1 \exp(-p_3 r^{p_4}) \tag{6e}$$

The log radius-number distribution is given by

$$n_L(r) = 2.3 \; p_1 r^{p_2+1} \exp(-p_3 r^{p_4}) \tag{6f}$$

It has a maximum value at

$$r_{lm} = (p_{24}/p_3)^{1/p_4} \quad \text{where} \quad p_{24} = (p_2+1)/p_4 \tag{6g}$$

so that

$$n_L(r_m) = 2.3\ p_1\ (p_{24}/p_3)^{p_{24}}\ \exp\ (-p_{24}) \tag{6h}$$

The limiting behavior of the function is as follows,

$$\text{As} \quad r \to 0,\ n_L(r) \simeq 2.3\ p_1\ r^{p_2+1} \tag{6i}$$

$$\text{and, as} \quad r \to \infty,\ n_L(r) \to 0 \quad \text{as} \quad 2.3\ p_1\ \exp(-p_3 r^{p_4}) \tag{6j}$$

The COSD is given by (Ref. 8, No. 3.381/3),

$$N(r) = p_1\ \Gamma(p_{24},\ p_3 r^{p_4})\ /\ p_4 p_3^{p_{24}} \quad p_3 > 0 \tag{6k}$$

The limiting behavior for the COSD is as follows (Ref. 11, 6.5.3, 6.5.12, 6.5.32),

$$\text{As} \quad r \to 0,\ N(r) \simeq p_1(\Gamma\ (p_{24}) - p_3^{p_{24}}\ r^{p_2+1}/p_{24})\ /\ p_4 p_3^{p_{24}} \tag{6l}$$

$$\text{and, as} \quad r \to \infty,\ N(r) \sim \frac{p_1}{p_3 p_4}\ r^{p_2-p_4+1}\ \exp(-p_3 r^{p_4}) \tag{6m}$$

The moments for the distribution are given by (Ref. 8, No. 3.381/4),

$$M_k = (p_1/p_4)\, p_3^{-(p_{24}+k/p_4)}\, \Gamma(p_{24}+k/p_4)\ ,\ p_2+k+1 > 0 \qquad (6n)$$

The parameter p_3 controls the mode radius and the parameters p_2 and p_4 control the polydispersity. The parameter p_2 determines the limiting behavior as $r \to 0$ while the parameter p_4 determines the limiting behavior as $r \to \infty$. The model is graphically presented in Figs. (3A.1 - 3C.5).

Model 4 -- Inverse Modified Gamma Distribution (IMGD) Model

This distribution has the same form as Model 3 except that the inverse radius is used. This results in an exponential fall-off at the small size end and power law behaviour at the large-radius end. Twomey (Ref. 12) suggests this form of the modified gamma distribution for dry aerosols.

The radius number distribution is given by

$$n(r) = p_1 \exp(-p_3/r^{p_4}) \,/\, r^{p_2} \qquad (7a)$$

Its mode radius is given by

$$r_m = \left(\frac{p_3 p_4}{p_2}\right)^{1/p_4} \qquad (7b)$$

and the maximum value is

$$n(r_m) = p_1 \left(\frac{p_2}{p_3 p_4}\right)^{p_2/p_4} \exp(-p_2/p_4) \qquad (7c)$$

The limiting behavior of the distribution is as follows,

$$\text{As} \quad r \to 0,\ n(r) \to 0 \quad \text{as} \quad p_1 \exp(-p_3/r^{p_4}) \tag{7d}$$

$$\text{and, as} \quad r \to \infty,\ n(r) \sim p_1\, r^{-p_2} \tag{7e}$$

The log-radius number distribution is given by

$$n_L(r) = 2.3\, p_1 \exp(-p_3/r^{p_4}) \,/\, r^{(p_2-1)} \tag{7f}$$

Its mode radius is given by

$$r_{1m} = (p_3/p_{42})^{1/p_4},\ p_{42} = (p_2 - 1)/p_4 \tag{7g}$$

and the maximum value is

$$n_L(r_{1m}) = 2.3\, p_1\, (p_{42}/p_3)^{p_{42}} \exp(-p_{42}) \tag{7h}$$

The limiting behavior of the distribution is as follows,

$$\text{As} \quad r \to 0,\ n_L(r) \to 0 \quad \text{as} \quad 2.3\, p_1 \exp(-p_3/r^{p_4}) \tag{7i}$$

$$\text{and, as} \quad r \to \infty,\ n_L(r) \sim 2.3\, p_1\, r^{-(p_2-1)} \tag{7j}$$

The COSD is given by (Ref. 8, No. 3.381/1)

$$N(r) = \frac{p_1}{p_4}\,(p_3)^{-p_{42}}\,\gamma\,(p_{42}, p_3\, r^{-p_4}),\ p_{42} > 0 \tag{7k}$$

where γ is the incomplete gamma function.

The limiting behavior of this distribution is as follows (Ref. 11, No. 6.1.1, 6.5.2, 6.5.12).

$$\text{As} \quad r \to 0, \; N(r) \approx \frac{p_1}{p_4} \left[p_3^{-p_{42}} \, \Gamma(p_{42}) - \exp(-p_3/r^{p_4}) \; / \; p_3 r^{p_4(p_{42}-1)} \right] \tag{7l}$$

$$\text{and, as} \quad r \to \infty, \; N(r) \sim p_1 \, r^{-(p_2-1)} \; / \; (p_2-1) \tag{7m}$$

The moments of the distribution are given by (Ref. 8, No. 3.381/4)

$$M_k = \frac{p_1}{p_4} \; p_3^{-(p_{42} - k/p_4)} \; \Gamma\,(p_{42} - k/p_4), \; k < p_2 - 1 \tag{7n}$$

The parameters p_2 and p_4 control the rate of fall-off at large and small radii, respectively, and hence control the polydispersity. The parameter p_3 controls the mode radius. This model is graphically presented in Figs. (4A.1 - 4C.4).

Model 5 -- The Log Normal Distribution (LND) Model

The log normal distribution generally provides a better description of particle size distribution than the normal distribuiton (discussed later on) because particle sizes, like many naturally occurring populations, are often asymmetric. In this distribution it is ln r rather than r which is normally distributed. An excellent discussion of this distribution is given by Kerker (Ref. 2).

The radius number distribution is given by

$$n(r) = \frac{p_1}{\sqrt{2\pi}\, p_3 r} \exp\left\{ -\frac{1}{2} \left(\frac{\ln r - \ln p_2}{p_3} \right)^2 \right\} \tag{8a}$$

The mode radius is

$$r_m = p_2 \exp(-p_3^2) \tag{8b}$$

and its maximum value is

$$n(r_m) = \frac{p_1}{\sqrt{2\pi}\, p_2 p_3} \exp(p_3^2/2) \tag{8c}$$

The parameter p_2 is the geometric mean of r and $\ln p_2$ is the mean of ln r. No series expansion could be found for the limiting behavior of this distribution which tends rapidly to zero at both extremities.

The log radius-number distribution is

$$n_L(r) = \frac{2.3\ p_1}{\sqrt{2\pi}\, p_3} \exp\left\{-\frac{1}{2}\left(\frac{\ln r - \ln p_2}{p_3}\right)^2\right\} \tag{8d}$$

It has a maximum at

$$r_{lm} = p_2 \tag{8e}$$

so that

$$n_L(r_{lm}) = 2.3\ p_1/(\sqrt{2\pi}\, p_3) \tag{8f}$$

No series expansion could be found for the limiting behavior of this distribution which tends rapidly to zero at both extremities.

The COSD is given by (Ref. 9, p. 183)

$$N(r) = \frac{p_1}{2} \operatorname{erfc}\left(\frac{\ln r - \ln p_2}{\sqrt{2}\ p_3}\right) \tag{8g}$$

where erfc is the complementary error function.

The limiting behavior of this function is as follows,

$$\text{As} \quad r \to 0, \; N(r) \to p_1 \tag{8h}$$

$$\text{and, as} \quad r \to \infty, \; N(r) \to 0 \tag{8i}$$

The parameter p_2 is the median for the COSD, i.e.,

$$N(p_2)/N(0) = 0.5$$

The moments for the distribution are given by (Ref. 8, No. 3.322/2)

$$M_k = p_1 p_2^{\,k} \exp\left(p_3^{\,2} k^2/2\right) \tag{8j}$$

The parameter p_3 controls the polydispersity of the model and the parameter p_2 has a multiplicative effect on mode radius. This model is graphically presented in Figs. (5A.1 - 5C.3).

Model 6 -- The Normal Distribution (ND) Model

The normal distribution is a symmetric distribution which is finite at r = 0 and, thus, strictly speaking cannot be used to represent aerosol SD's at small r. It can be used to represent SD's at other ranges of r, and since it is a Gaussian distribution, which has well known properties, such a model can be very useful in certain applications. It is given by

$$n(r) = \frac{p_1}{\sqrt{2\pi}\, p_3} \exp\left\{ -\frac{1}{2} \left[\frac{r-p_2}{p_3}\right]^2 \right\} \tag{9a}$$

Its mode radius is given by

$$r_m = p_2 \tag{9b}$$

and the maximum value is

$$n(r_m) = \frac{p_1}{\sqrt{2\pi}\, p_3} \tag{9c}$$

$$\text{As} \quad r \to 0 \ , \ n(r) \approx \frac{p_1}{\sqrt{2\pi}\, p_3} \exp\left\{ -\frac{1}{2} \left(\frac{p_2}{p_3}\right)^2 \right\} \left(1 + r p_2 / p_3^2\right) \tag{9d}$$

No series expansion could be found for the asymptotic behavior of this function which tends rapidly to zero.

The log radius-number distribution is given by

$$n_L(r) = \frac{2.3 \quad p_1 \, r}{\sqrt{2\pi}\, p_3} \quad \exp\left\{ -\frac{1}{2} \left(\frac{r-p_2}{p_3}\right)^2 \right\} \tag{9e}$$

Its mode radius is given by

$$r_{lm} = \frac{p_2 + \sqrt{p_2^2 + 4\, p_3^2}}{2} \tag{9f}$$

and the maximum value is

$$n_L(r_{lm}) = \frac{2.3\ p_1}{\sqrt{2\pi}\ p_3} \left(\frac{p_2 + \sqrt{p_2^2 + 4 p_3^2}}{2} \right) \exp\left\{ -1/2 \left[\frac{p_2^2 + 4 p_3^2}{p_3^2} \right] \right\} \tag{9g}$$

The limiting behavior of the distribution is as follows

$$\text{As} \quad r \to 0, \; n_L(r) \simeq \frac{2.3\, p_1\, r}{\sqrt{2\pi}\, p_3} \tag{9h}$$

$$\text{and, as} \quad r \to \infty, \; n_L(r) \to 0 \tag{9i}$$

The COSD is given by (Ref. 9 , p. 183)

$$N(r) = \frac{p_1}{2} \; \text{erfc} \left[\frac{r-p_2}{\sqrt{2}\, p_3}\right] \tag{9j}$$

The limiting behavior of the distribution is as follows (Ref. 9, p. 183),

$$\text{As} \quad r \to 0, \quad N(r) \simeq \frac{p_1}{2} \left[1 - \sqrt{\frac{2}{\pi}} \left(\frac{r-p_2}{p_3}\right)\right] \tag{9k}$$

$$\text{and, as} \quad r \to \infty, \; N(r) \sim \frac{p_1}{\sqrt{2\pi}} \left(\frac{p_3}{r-p_2}\right) \exp\left\{\left[\frac{r-p_2}{\sqrt{2}p_3}\right]\right\} \tag{9l}$$

The moments of the distribution are given by (Ref. 8, No. 3.462/1),

$$M_k = \frac{p_1}{\sqrt{2\pi}} \; p_3^{\,k} \; k! \exp\left(-p_2^{\,2}/4p_3^{\,2}\right) D_{-k+1}\left(p_2/2\right) \tag{9m}$$

where D_{-k+1} is a parabolic cylinder function.

In the normal distribution, the parameter p_2 controls the mode radius and the parameter p_3 controls the polydispersity. The model is graphically presented in Figs. (6A.1 - 6C.3).

Model 7 -- The Generalized Distribution Function (GDF) Model

This distribution is finite at r = 0 and thus does not, strictly speaking, represent particle size distribuitons at small r. However, it is a versatile function with a wide variety of applications, including altitude distributions, (Refs. 3 and 6) and is therefore included here as a potential representation of aerosol SD's.

The radius-number distribution is given by

$$n(r) = \frac{p_1 \ (1+p_2)^2 \ \exp \ (r/p_3)}{\{ p_2 + \exp \ (r/p_3) \}^2} \tag{10a}$$

Its mode radius is given by

$$r_m = p_3 \ \ln p_2 \tag{10b}$$

and the maximum is

$$n(r_m) = \frac{p_1 \ (1+p_2)^2}{4 \ p_2} \tag{10c}$$

The limiting behavior of the distribution is as follows

As $r \to 0$, $n(r) \simeq p_1(1 + r \ (p_2-1)/p_3(p_2+1))$ (10d)

and, as $r \to \infty$, $n(r) \to 0$ as $p_1(1+p_2)^2 \exp(- r/p_3)$ (10e)

The log radius-number distribution is given by

$$n_L(r) = 2.3 \ p_1 \ (1+p_2)^2 \ r \exp(r/p_3) \ / \ (p_2 + \exp(r/p_3))^2 \tag{10f}$$

Its mode radius r_{1m} is given by the solution of the equation

$$p_2(1 + r_{1m}/p_3) = (r_{1m}/p_3 - 1) \exp (r_{1m}/p_3) \tag{10g}$$

and the maximum is given by

$$n_L(r_{1m}) = 2.3\ p_1\ (1+p_2)^2\ (r_{1m}-p_3)\ (r_{1m}+p_3)\ /\ (4\ p_2 r_{1m}) \tag{10h}$$

The limiting behavior of the distribution is as follows

$$\text{As} \quad r \to 0,\ n(r) \simeq 2.3\ p_1\ (1+p_2)^2\ r \tag{10i}$$

$$\text{and, as} \quad r \to \infty,\ n(r) \to 0 \quad \text{as} \quad 2.3\ p_1\ (1+p_2)^2 \exp(-r/p_3) \tag{10j}$$

The COSD is given by

$$N(r) = \frac{p_1\ (1+p_2)^2\ p_3}{\left(p_2 + \exp(r/p_3)\right)} \tag{10k}$$

The limiting behavior of the distribution is as follows

$$\text{As} \quad r \to 0,\ N(r) \simeq p_1\ (1+p_2)\ p_3\ (1-r/p_3(p_2+1)) \tag{10ℓ}$$

$$\text{and, as} \quad r \to \infty,\ N(r) \to 0 \quad \text{as} \quad p_1 p_3\ (1+p_2)^2 \exp(-r/p_3) \tag{10m}$$

The analytic expression for the moments of the distribution could not be evaluated.

The parameter p_3 can be considered as a scale radius and the parameter p_2 determines the type of function. For $p_2 = 0$ the distribution becomes an exponential, and for small p_2 the function initially falls off more slowly than the exponential. As the parameter p_3 increases, the spread or polydispersity of the function increases. The model is graphically presented in Figs (7A.1 - 7C.3).

Model 8 -- Power Law Generalized Distribution Function (PLGDF) Model

This model is a versatile function which is most useful when the data to be fitted have broad peaks. The radius-number distribution is given by

$$n(r) = \frac{p_1 \exp\,(p_2/r^{p_4})}{r^{p_4+1}\,(1+p_3(\exp\,(p_2/r^{p_4}) - 1))^2} \qquad (11a)$$

Its mode radius is given by the solution of

$$(1-p_3)\,(p_2p_4 + (p_4+1)\,r_m^{p_4}) = p_3 \exp\,(p_2/r_m^{p_4})\,(p_2p_4-(p_4+1)r_m^{p_4}) \qquad (11b)$$

and the maximum is

$$n(r_m) = \frac{p_1\,(p_2p_4 + (p_4+1)\,r_m^{p_4})\,(p_2p_4 - (p_4+1)\,r_m^{p_4})}{4\,p_2^{\,2}\,p_3(1-p_3)\,p_4^{\,2}\,r_m^{\,p_4+1}} \qquad (11c)$$

The limiting behavior of the distribution is as follows

$$\text{As} \quad r \to 0,\ n(r) \to 0 \text{ as } p_1 \exp\,(-p_2/r^{p_4}) \qquad (11d)$$

$$\text{and, as} \quad r \to \infty,\ n(r) \sim p_1\, r^{-(p_4+1)} \qquad (11e)$$

The log radius-number SD is given by

$$n_L(r) = \frac{2.3\ p_1\ \exp\ (p_2/r^{p_4})}{r^{p_4}\ (1+p_3\ (\exp(p_2/r^{p_4})\ -1))^2} \tag{11f}$$

Its mode radius is given by the solution of

$$(1-p_3)\ (p_2+r_{1m}^{p_4}) \ = \ p_3\ \exp(p_2/r_{1m}^{p_4})\ (p_2-r_{1m}^{p_4}) \tag{11g}$$

and its maximum is given by

$$n_L(r_{1m}) = \frac{p_1\ (p_2+r_{1m}^{p_4})\ (p_2-r_{1m}^{p_4})}{4\ p_2^{\,2}\ p_3(1-p_3)\ r_{1m}^{p_4}} \tag{11h}$$

The limiting behavior of the distribution is as follows

$$\text{As} \quad r \to 0,\ n_L(r) \to 0 \quad \text{as} \quad 2.3\ p_1\ \exp\ (-p_2/r^{p_4}) \tag{11i}$$

$$\text{and, as} \quad r \to \infty,\ n_L(r) \sim 2.3\ p_1\ r^{-p_4} \tag{11j}$$

The COSD is given by

$$N(r) = \frac{p_1\ (\exp\ (p_2/r^{p_4}) - 1)}{p_2p_4\ (1+p_3\ (\exp(p_2/r^{p_4})\ -1))} \tag{11k}$$

The limiting behavior of the distribution is as follows

$$\text{As} \quad r \to 0,\ N(r) \simeq p_1/p_2p_3p_4(1+1/p_3(e^{p_2/r^2}-1)) \tag{11ℓ}$$

$$\text{and, as} \quad r \to \infty,\ N(r) \to 0 \quad \text{as} \quad \frac{p_1}{p_2p_4}\left\{\frac{(\exp(p_2/r^{p_4})-1)}{1+p_3(\exp(p_2/r^{p_4})-1)}\right\} \tag{11m}$$

The moments, other than the zeroeth moment (N(0)), cannot be calculated for this distribution. However, there is a special form of the function, referred to as Model 8B, for which higher moments can be calculated, but it has no analytic form for the COSD. The radius-number SD for this function is given by

$$n(r) = \frac{p_1 \exp(p_2/r^2)}{r^{p_4}\,(1+p_3\,(\exp(p_2/r^2)-1))^2} \tag{12a}$$

Its mode radius is obtained from the solution of the equation

$$(1-p_3)\,(2p_2+p_4 r_m^2) = p_3(2p_2-p_4 r_m^2)\exp(p_2/r_m^2) \tag{12b}$$

and its maximum is given by

$$n(r_m) = \frac{p_1(2p_2 + p_4 r^2)(2p_2 - p_4 r_m^2)}{16 p_2^2 p_3(1-p_3) r_m^{p_4}} \tag{12c}$$

The limiting behavior of this distribution is as follows

$$\text{As} \quad r \to 0,\ n(r) \to 0 \quad \text{as} \quad p_1 \exp(-p_2/r^{p_4}) \tag{12d}$$

$$\text{and, as} \quad r \to \infty,\ n(r) \sim p_1 r^{-p_4} \tag{12e}$$

The log radius-number distribution is given by

$$n_L(r) = \frac{2.3\ p_1 \exp(p_2/r^2)}{r^{p_4-1}\,(1+p_3\,(\exp(p_2/r^2) - 1))^2} \tag{12f}$$

Its mode radius is given by the solution of the equation

$$(1-p_3)(2p_2+(p_4-1)r_{1m}^2) = p_3(2p_2-(p_4-1)r_{1m}^2)\exp(p_2/r_{1m}^2) \qquad (12g)$$

and its maximum is given by

$$n_L(r_{1m}) = \frac{2.3\ p_1(2p_2+(p_4-1)r_{1m}^2)(2p_2-(p_4-1)r_{1m}^2)}{16\ p_2^2\ p_3(1-p_3)r_{1m}^{p_4-1}} \qquad (12h)$$

The limiting behavior of the distribution is as follows

As $r \to 0$, $n_L(r) \to 0$ as $2.3\ p_1 \exp(-p_2/r^2)$ (12i)

and, as $r \to \infty$, $n_L(r) \sim 2.3\ p_1\ r^{-(p_4-1)}$ (12j)

The moments for this distribution are given by (Ref. 13, No. 313.11)

$$M_k = \frac{p_1}{2p_3^2\ p_2^{p_{4k}}}\ \Gamma(p_{4k}) \sum_{i=0}^{\infty} \left(1 - \frac{1}{p_3}\right)^i (i+1)^{-(p_{4k}-1)} \qquad (12k)$$

where $p_{4k} = \frac{p_4-(k+1)}{2}$, $p_4 > k+1$.

The parameter behavior for both functions (Eqs. (11a) and (12a)) is similar. The parameter p_2 controls the rate of fall-off at small radii while the parameter p_4 controls the rate of fall-off at large radii. The parameter p_3 controls the spread of the distribution, the breadth of the peaks increasing with large values of p_3. The model is graphically presented in Figs. (8A.1 - 8F.3).

GRAPHICAL CATALOG OF SIZE DISTRIBUTION MODELS

Description of Model Catalog

The model catalog consists of log-log graphs (6 x 4 cycles), and/or in some cases, semi-log graphs, on which $n(r)$, $n_L(r)$ and $N(r)$ are separately plotted against radius (μm). For each of the aforementioned models, sets of plots have been produced, each set depicting the behavior of the model as a function of only one of its parameters, the other parameters being kept constant. Thus, each catalog graph (CG) contains several plots, one for each value of the parameter being varied, the parameter values being chosen to cover the range of variation in aerosol size distributions likely to be encountered. A CG with a p_2, p_3 or p_4 variation will be hereafter referred to as a p_2 CG, p_3 CG or p_4 CG, respectively. Each catalog plot (CP) is labeled by a different symbol against which are printed the value(s) of the parameter(s), outside the right-hand boundary of the graph. Also printed there, are the model number and the mode radius (RM). For the first plot all the parameters are listed; and for subsequent plots only the values of the varying parameter and RM are printed. In cases where the SD has no mode radius, the value RM has been set equal to 0.01. The annotation on logarithmic axes gives the power of 10.

For each set of parameter values, three corresponding CG's for $n(r)$, $n_L(r)$ and $N(r)$ are presented. The values of the parameters held constant in each case, in general, were selected so that they were near the middle of their likely range. In all cases, the parameter p_1 is a scaling factor which has been chosen so that the maximum values of $n(r)$, $n_L(r)$, or $N(r)$ are unity. This allows all of them to fit on one graph and facilitates estimation of parameters.

Use Of Model Catalog

In this section, a step-by-step procedure will be described illustrating how the catalog can be used to obtain the best-fit values of the model parameters.

Step 1: In case the two transparencies of log-log and semi-log graphs provided in the pocket on the back cover of this report are missing, take the blank log-log or semi-log graph provided at the end of the catalog and get some sharp photographic transparencies made of it. Xerox or vu-graph transparencies will not do as they generally distort the graph unevenly.

Step 2: Next, plot the experimental data for $n(r)$, $n_L(r)$ or $N(r)$ on the transparency, which is refered to as the data transparency (DT). If the data is not too noisy, one can visually detect some geometrical trend in the data points. A free-hand smooth line may be drawn through the data points to accentuate the shape of the geometrical curve or line.

Step 3: The DT should then be overlayed on the different CG's belonging to the selected analytical model until a visual matching of the data points to one of the plots is obtained. With some experience, such a match can quickly be obtained. However, one often finds that the visual fit of the data points to a CP is reasonably close but not exact. The values of the parameters corresponding to the closest plot are then read off the CG, and used as initial parameter estimates in a nonlinear least squares (NLLS) computer program or some other optimization code to obtain the best-fit values of the parameters.

Since all the CP's for $n(r)$, $n_L(r)$ and $N(r)$ are normalized to unity at their individual maxima, the experimental data points may not, in general, fall in the same range as that of the CP's; thus vertical translation of the

DT will be necessary to obtain the visual match. In addition, horizontal translations of the DT, where permissible, may sometimes be necessary. In any case, care should be taken to ensure that no rotation occurs between the CG and the DT.

As a rule, the horizontal translations are invalid when the parameter being varied controls the mode radius r_m and are valid if it controls the polydispersity or the rate of fall-off at the extremities.

PARAMETER ESTIMATION

There are three methods by which one can obtain, with relative ease, estimates of the parameters of the size distribution models that are close to the best-fit values. In each case, the experimental data is plotted on a log-log or semi-log graph paper. The first is based solely on the interpretation of the plotted data in terms of the mathematical properties (such as limiting behavior, mode radius, moments, etc.) of an analytic model; the second is based solely on the visual matching of the plotted data with a set of parameterized plots of that model; and the third, which is the most versatile, is simply a composite of the first two methods. It is the last methods, which will be discussed in this section. In this method, it is essential that the experimental data be plotted on the photographic transparency of the unused log-log graph provided with the catalog. In some cases it may be helpful to use the semi-log graph, also provided with the catalog.

A straight line on a log-log graph implies a power law, and on a semi-log graph, an exponential function. If for large r, the data points

on a log-log graph fall on a straight line, then the size distribution models which should be considered are those which vary as, say r^{-p_2} for $r \to \infty$, the slope being the value of the exponent, p_2. This would immediately suggest that models 1, 2, and 4 are the appropriate ones to work with. If, on the other hand, for large r, the data points on a semi-log graph fall on a straight line, the models which should be considered are those which vary as, say $e^{-p_2 r}$ as $r \to \infty$, the slope being the value of the coefficient p_2. This would suggest Model 3 with $p_4 = 1$ or Model 7. If, however, the experimental data do not fall on a straight line when plotted on either the log-log or the semi-log graph, then Models 3 and 5 are important. In the following discussion on parameter estimation, primed symbols will refer to the data estimates and unprimed symbols, to the CP values. The parameter p_1' is always the last parameter to be determined. Since the estimation of the scaling parameter p_1' is essentially the same for all models, it will be discussed before describing the procedures for estimating other parameters for each of the models. The estimates for p_1' can be obtained by one of the following three methods, after the estimates for p_2', p_3', etc. have been obtained.

(a) If one assumes a linear relationship between the observed (y_j^o) and calculated (y_j^c) values, i.e.,

$$y_j^o = p_1' \, y_j^c \tag{13a}$$

then by using linear regression methods it can be shown that

$$p_1' = \left(\sum_{j=1}^{J} y_j^o * y_j^c \right) \Big/ \sum_{j=1}^{J} (y_j^c)^2 \tag{13b}$$

where J = number of data points, y_j^o = observed SD value at r_j, and y_j^c = calculated SD value at r_j, using $p_1' = 1.0$ and the p_2', p_3', etc. already determined.

(b) $p_1' =$ (observed value at r_j/calculated value at r_j) (13c)

where the calculated value of the SD is obtained by substituting $p_1' = 1.0$ and p_2', p_3', etc. as estimated from the CP's, in the expression for the SD. If possible, the values at the maximum should be used.

(c) $p_1' =$ (observed value at r_j/catalog value at r_j) x p_1 (13d)

Even though the second method might perhaps be the easiest for estimating p_1', the first method is found to be more convenient when a computer optimization code is used, since the formula in Eq. (13b) can easily be incorporated into the program. The third method seems to be the most complicated since often several CP's with different p_1 values are used to estimate the parameters, p_2, p_3, etc.

The first step is to determine the other parameters p_2', p_3', etc. for each of the models. The procedures for estimating these parameters are described under the subheadings for the different models as follows.

Model 1: The slope of the straight line on a n(r), $n_L(r)$ or N(r) plot determines the parameter p_2'.

Model 2: This model behaves as a power law for both large and small r. Therefore, in general, it is best to determine p_3' and p_4' first, and then determine p_2'. The parameter estimation differs somewhat for the n(r), $n_L(r)$ or N(r) data plots.

(a) n(r) data. p_3' can be obtained from the positive slope ($= p_3' - 1$) of the data plot; p_4', from the negative slope ($= -1 - p_3'(p_4' - 1)$), after substituting for p_3'; and p_2' is found by substituting for r_m', p_3' and p_4' in Eq. (5b).

To obtain p_3' using the catalog, the DT is overlayed on the p_3- CG (Fig. 2A.3), and translated along x- and/or y- axes until the data points corresponding to the small limit of r match, as closely as possible, one of the CP's.

To obtain p_4', the DT is overlaid on the p_4 CG (Fig. 2A.4) and translated parallel to the x- and/or y- axes until the data points for large r closely match one of the plots. (Since both p_3 and p_4 affect the slope for $r \to \infty$, it may be necessary to adjust the p_4' value, using,

$$p_3' (p_4' - 1) = p_3 (p_4 - 1) \tag{14a}$$

if the p_3 value for the CP differs from p_3'.) Having obtained p_3' and p_4', estimates of p_2' can be obtained from Eq. (5b) or from the CP's. In the latter case, overlay the DT on the CG for which (p_3, p_4) are as close as possible to (p_3', p_4') (Fig. 2A.1 or 2A.2) so that the data maximum coincides with 1.0 on the CG y- scale (CP's are normalized so that their maximum value is 1.0). Translation of DT along the x-axis is not permitted, since the parameter being estimated controls r_m. If the data peak does not coincide with any of the CP peaks, but lies between two CP peaks then p_2' can be obtained by the following interpolation relations.

$$p_2'/r_m' = p_2/r_m \tag{14b}$$

(If p_3 and/or p_4 for the CG differ from those values for the DT, then use

$$p_2'' \left(\frac{p_3' - 1}{1 + p_3'(p_4' - 1)} \right)^{1/p_3'} = p_2' \left(\frac{p_3 - 1}{1 + p_3(p_4 - 1)} \right)^{1/p_3} \tag{14c}$$

to obtain a better estimate, p_2'', for p_2.)

(b) $n_L(r)$ data. The $n_L(r)$ data is plotted on the log-log transparency. The determination of the parameters is done in essentially the same manner as for the n(r) data. As $r \to 0$, p_3' = positive slope; as $r \to \infty$, p_4' = 1 + negative slope/p_3'; and p_2' is found by substituting for r_{1m}', p_3' and p_4' in Eq. (5g). The parameters p_3' and p_4' are determined from Figs. (2B.3 and 2B.4) respectively, in the same manner as for n(r). Similarly, p_2' is obtained in the manner described for n(r) data using Figs. (2B.1 or 2B.2), provided r_m and r_m' are replaced by r_{1m} and r_{1m}' in Eq. (14b) and (14c) is replaced by

$$p_2'' \left(p_4'-1\right)^{-1/p_3'} = p_2' \left(p_4-1\right)^{-1/p_3} \tag{14d}$$

(c) N(r) data. The parameter determination from the N(r) data is more difficult than from the n(r) data. Plot the N(r) data on the log-log transparency, visually fit a line through data points, and, if possible, extrapolate it to r = .01μm.

To obtain p_2', overlay the DT on the p_2- CG (Fig. 2C.1 or 2C.2) whose $r \to \infty$ behavior best matches that of the data, so that the N(0) for the data coincides with the N(0) for the CP. If data lies between two CP's, then use the following extrapolation formula to obtain p_2', viz.

$$\left(\frac{p_2'}{r'}\right)^{s'} = \left(\frac{p_2}{r}\right)^{s} \tag{14e}$$

where r and r' are radii with the same normalized value N(r) on the straight portion of the curve (Fig. 9) and s' and s are the slopes of

the straight portion of the curve. It is best to use the CP which turns closest to the data. P_4' can then be obtained from the relation

$$[N(r)]_{p_2'} \Big/ N(0) = 2^{p_4'-1} \qquad (14f)$$

To estimate p_3' overlay the DT on the p_3- CG (Fig. 2C.3) and translate along x- and y-axes to obtain the closest match between data points for $r \to \infty$ and one of the CP's. (If p_4 for the CG differs from p_4', then to obtain a better estimate for p_3', use Eq. (14a).)

Model 3: In representing the size distribution data with Model 3, one generally obtains estimates of the parameters p_2' and p_4' first and those of p_3' from them.

(a) n(r) data: If n(r) data is available for $r \to 0$, then one can obtain p_2' from the positive slope ($=p_2'$). To obtain p_2', overlay the DT on the p_2- CG (Fig. 3A.1), and translate it along x- and y- axes until a CP matches with the slope of the data for $r \to 0$, where the positive slope = p_2. To obtain p_4', overlay the DT on the p_4-CG (Fig. 3A.4), and translate it along x- and y- axes, until a CP matches with the data for $r \to \infty$, for which limiting behavior is an exponential type fall-off. P_3' can then be obtained by substituting r_m', p_4' and p_2' in Eq. (6b) or from the appropriate CP. In the latter case, overlay the DT on a CG with (p_2, p_4) closest to (p_2', p_4') (Fig. 3A.2, or 3A.3), so that the data maximum coincides with 1.0 on the CG y- scale. The following interpolation formula can be used to obtain the p_3' if the data do not coincide with one of the CP peaks.

$$\frac{p_3'}{p_3} = \left(\frac{r_m}{r_m'}\right)^{p_4} \tag{15a}$$

(If $p_2 \neq p_2'$ and/or $p_4 \neq p_4'$, then

$$\left(\frac{p_2'}{p_3'' p_4'}\right)^{1/p_4'} = \left(\frac{p_2}{p_3' p_4}\right)^{1/p_4} \tag{15b}$$

can be used to obtain a better estimate p_3'' for the p_3 parameter since p_2' and p_4' also influence the mode radius.)

(b) $n_L(r)$ data: Determination of the Model 3 parameters from the $n_L(r)$ data is similar to that described for the n(r) data, provided $(p_2' + 1)$ is used for the positive slope, p_3' is estimated from p_2' and p_4' using the expression for r_{1m} given in Eq. (6g), r_m and r_m' are replaced by r_{1m} and r_{1m}' in Eq. (15a), and Eq. (15b) is replaced by the relation

$$\left(\frac{p_2' + 1}{p_3'' p_4'}\right)^{1/p_4'} = \left(\frac{p_2 + 1}{p_3' p_4}\right)^{1/p_4} \tag{15c}$$

(c) N(r) data: Determination of the model parameters from the N(r) data is difficult. It will generally be necessary to extrapolate the data to r = 0.01μm.

To obtain p_2' overlay the DT on a CG with plots whose slopes for $r \to \infty$ (Fig. 3C.1 or 3C.2) are similar to that for the data, so that the extrapolated N(0) value for the data coincides with N(0) for the CP's. Then p_2' is the p_2- value for the CP which best fits the data particularly with regard to the curvature. It may be necessary to interpolate visually in order to obtain a better value for p_2.

To obtain p_4', overlay the DT on the p_4- CG (Fig. 3C.5) and translate it in a manner similar to that for the n(r) data, until a best fit to the data for $r \to \infty$ is obtained. Similarly, p_3' is obtained by overlaying the DT on the CG with (p_2, p_4) closest to (p_2', p_4') (Fig. 3C.3 or 3C.4), and translating vertically so that N(O) for the data and CPs coincide. Then determine which CP best fits the data, interpolation by eye may be necessary to give a better estimate of p_3'.

Model 4: Determination of parameters for this model is similar to that for Model 3. In general, determine p_2' and p_4' first, and then p_3'.

(a) n(r) data: The parameter p_2' can be determined from the slope of the data as $r \to \infty$ (slope = p_2'). To determine p_2' from the CG's, overlay the DT on the p_2- CG (Fig. 4A.1) and translate the DT parallel to the x- and/or y- axes until the data points as $r \to \infty$ lie on or close to one of the CP's. The p_2 value for this CP then becomes the estimate p_2'. To determine p_4', overlay the DT on the p_4- CG (Fig. 4A.4) and translate the DT vertically and horizontally until the data points as $r \to 0$ lie on one of the CP's.

The parameter p_3' can then be determined by substituting for p_2', p_4' and r_m' in Eq. (7b) or using the catalog graph. To determine p_3' from the catalog, overlay the DT on the p_3- CG which best matches the behavior of the data both as $r \to 0$ and $r \to \infty$ (Fig. 4A.2 or 4A.3) so that the data peak coincides with 1.0 on the CG y- scale. If interpolation between CP values is necessary, use the following relationship:

$$\frac{p_3'}{p_3} = \left(\frac{r_m'}{r_m}\right)^{p_4} \tag{16a}$$

(If the values of p_2 and/or p_4 for the CG differ from the estimates p_2' and p_4', then a better estimate p'_3 can be obtained by using the relationship:

$$\left(\frac{p_3'' \, p_4'}{p_2'}\right)^{1/p_4'} = \left(\frac{p_3' \, p_4}{p_2}\right)^{1/p_4} \tag{16b}$$

where p_3'' is the new estimate for p_3'.)

(b) $n_L(r)$ data: This is very similar to the parameter determination for n(r). The slope as $r \to \infty$ can be found from the data (slope $= p_2' - 1$). Using the catalog, p_2' and p_4' are determined from Figs. 4B.1 and 4B.4 respectively in the same way as p_2' and p_4' for n(r). The parameter p_3' is also determined in the same manner as for n(r) however, if interpolation between CP's is needed, r_{1m} and r'_{1m} should be used instead of r_m and r_m' in Eq. (16a). (If (p_2, p_4) for the CG differ from the estimates (p_2', p_4'), a better p_3' estimate can be obtained by using

$$\left(\frac{p_3'' \, p_4'}{p_2'-1}\right)^{1/p_4'} = \left(\frac{p_3' \, p_4}{p_2-1}\right)^{1/p_4} \tag{16c}$$

where p_3'' is defined as the new estimate for p_3'.)

(c) N(r) data: Determination of parameters is generally more difficult than for n(r) or $n_L(r)$. The slope as $r \to \infty$ is given by $-(p_2' - 1)$. Generally, it will be necessary to extrapolate the data to $r = 0.01\mu m$.

To determine p_2' from the catalog, overlay the DT on the p_2- CG (Fig. 4C.1) and translate the DT vertically and horizontally until the best fit CP for the region $r \to \infty$ is found. To determine p_4', overlay the DT on the p_4- CG (Fig. 4C.4) so that N(O) for the data coincides with N(O) for the CP's. The estimate for p_4' will be the p_4 value for the best CP, giving particular attention to the fit in the region of curvature. To determine p_3', overlay the DT on the p_3- CG which best approximates the behavior of the data as $r \to \infty$ (Fig. 4C.2 or 4C.3) so that N(O) for the data coincides with N(O) for the CP's. The estimate for p_3' is the value of p_3 for the CP which best fits the data. The point where the curve turns is of most importance here and some interpolation by eye may be necessary.

Model 5: In representing the size distribution data with Model 5, it is best to obtain an estimate of p_3' first and use it to determine p_2'.

(a) n(r) data: If sufficient data are available, both p_2' and p_3' can be determined from the mathematical properties as follows:

$$p_3' = 0.424 \ln(r_1/r_2), \quad r_1 > r_2 \tag{17a}$$

where r_1 and r_2 are the radii at half-maximum points. Then p_2' can be obtained by substituting for p_3' and r_m' in Eq. (8b). To determine the parameter using the catalog, overlay the DT on the p_3- CG (Fig. 5A.3) and translate it so that the maxima for the data and a CP coincide. Then p_3' is the same as the p_3 value for the plot which best fits the data. Attention should be paid to both the spread of the data, and the rate of fall-off as $r \to \infty$. Often some interpolation may be necessary.

Once p_3' is obtained, p_2' can be determined by substitution in Eq. (8b) or from the catalog. In the latter case, overlay the DT on the p_2- CG with p_3 closest to p_3' (Fig. 5A.1 or 5A.2) so that the data peak coincides with 1.0 on the y- scale of the CG. If the data do not coincide with one of the CP peaks, p_2' can be estimated from the closest one by using

$$\frac{p_2'}{p_2} = \frac{r_m'}{r_m} \tag{17b}$$

(If $p_3 \neq p_3'$, then a better estimate for p_2' can be obtained from

$$p_2'' \exp(-p_3'^2) = p_2' \exp(-p_3^2) \tag{17c}$$

where p_2'' is the new estimate of p_2 for the data.)

(b) $n_L(r)$ data: P_2' can easily be obtained from the data peak, since $p_2' = r_{1m}$. Determination of the model parameters from the CP's is essentially the same as for the n(r) data, provided r_m and r_m' are replaced by r_{1m} and r_{1m}' in Eq. (17b). Note that no adjustment of p_2' will be necessary if p_3 for the catalog differs from p_3'.

(c) N(r) data: Generally, it is best to extrapolate the N(r) data to r = 0.01μm to obtain an estimate of N(0). Then p_2' can be determined from the fact that p_2 is the median, i.e., $N(p_2) = 0.5$, or in the case of unnormalized data, $N(p_2)/N(0) = 0.5$.

To obtain p_3', overlay the DT on the p_3- CG (Fig. 5C.3), translate it horizontally and vertically until a match of the data for $r \to \infty$ with a CP is obtained. (If p_2' has been estimated as described

earlier, then the data point (p_2', 0.5 N(0)) should coincide with the point (p_2, 0.5) on the CP. If the median points for the data and the CP do not coincide it probably means that the original estimate for p_2' is not very good and a better one would be the radius on the DT which corresponds to the median point for the CP.)

To determine p_2' using the catalog, overlay the DT on the p_2- CG with p_3 closest to p_3' (Fig. 5C.1 or 5C.2) so that the N(0) values for the data and CP's coincide. p_2' is then the p_2- value of the CP with which data points match. Interpolation by eye may be necessary.

Model 6: Since this model was included in the catalog for completeness only, a description of how to determine parameters from the catalog will not be given. However, if the model is to be used, the data should be plotted on a semi-log graph and the procedure for determining the parameters will be similar to those described earlier.

Model 7: Data for this model should also be plotted on a semi-log graph. As in the case of Model 6, this model was included for the sake of completeness and will not be discussed here. However, determination of the parameters for this model is discussed by Green (Ref. 6).

Model 8: Two forms of this model were discussed earlier, but parameter determination is the same for both, so that separate discussions will not be necessary here.

(a) n(r) data: To determine p_2', overlay the DT on the p_2- CG (Fig. 8A.1 or 8D.1) so that the radii are aligned and the data peak coincides with 1.0 on the CG y- scale. p_2' is the same as p_2 for the

CP which coincides with the data peak. Interpolation by eye may be necessary to get a better estimate of p_2'.

To determine p_3' the DT is overlayed on the p_3- CG (Fig. 8A.2 or 8D.2) and translated vertically and horizontally until the CP which best matches the peak width is found. It is this parameter which controls the broadness of the peak and is of importance for data with broad flat peaks. The parameter p_4' can be found from the slope of the data for $r \to \infty$ ($= -(p_4' + 1)$ for Model 8, $= -p_4'$ for Model 8B) or from the catalog. Using the catalog, overlay the DT on the p_4- CG (Fig. 8A.3 or 8D.3) and translate vertically and horizontally until a CP which matches the data for $r \to \infty$ is found.

(b) $n_L(r)$ data: The procedure for determining p_2', p_3', p_4' is exactly the same as for n(r) except that in the case of Model 8 Figs. 8B.1 - 8B.3 are used and the slope for $r \to \infty$ is $-p_4'$ and in the case of Model 8B Figs. 8E.1 - 8E.3 are used and the slope for $r \to \infty$ is and $-p_4' - 1$.

(c) N(r) data: Extrapolate the data to r = 0.01μm, then to determine p_2', overlay the DT on the p_2- CG so that the radii are aligned and N(0) for the data coincides with N(0) for the CP's. The estimate for p_2' is given by the value of p_2 for the CP which best matches the data, particularly in the region where it turns.

To determine p_3' overlay the DT on the p_3- CG (Fig. 8C.2 or 8F.2) so that N(0) for the data and the CP's coincide. The estimate of p_3' is the value of p_3 for the CP which best matches the spread or polydispersity of the data. To determine p_4', overlay the DT on the p_4- CG (Fig. 8C.3 or 8F.3) and translate the DT vertically and horizontally until the CP which best matches the data for $r \to \infty$ is found.

Multimodal Size Distribution Models

Quite often the SD data may indicate that the distribution is multimodal (Refs. 14 and 15). Such SD's present no particular difficulty in representing them analytically in terms of the aforementioned SD models. One can represent multimodal size distributions simply by adding appropriate mathematical functions, each component term representing a peak in the size distribution data, such as,

$$n(r) = \sum_{j=1}^{J} a_j \, n_j(r) \tag{18a}$$

where J is the number of component terms and the a_j represent the adjustable constants and are equivalent to p_1 for the unimodal models.

In describing the procedure for fitting multimodal data using the catalog, a bimodal model will be condensed for simplicity.

Step 1: Plot the data on a log-log transparency and dot in the probable behavior of the two modes as illustrated in Fig. (10).

Step 2: Decide the most appropriate model for each mode using the guidelines already outlined for the unimodal models.

Step 3: Determine the parameters for each mode using the guidelines outlined earlier for unimodal models.

Step 4: Determine the scaling factors for each mode. The simplest method for determining the scaling factors is the solution of the simultaneous equations

$$n(r_1) = a_1 n_1(r_1) + a_2 n_2(r_1) \tag{18b}$$

$$n(r_2) = a_1 n_1(r_2) + a_2 n_2(r_2) \tag{18c}$$

where a_1, a_2 are the scaling factors required, and r_1 and r_2 are the mode radii for modes 1 and 2, respectively.

In some cases, it may be difficult to get good estimates for a_1 and a_2, either because of uncertainty in the accuracy of some estimates or because the scaling factors differ by several orders of magnitude. An alternative approach to determining the scaling factors under these circumstances would be to assume that each mode makes a negligible contribution to n(r) in the region where the other mode dominates and, thus, the scaling factors can be found by using the following relationships:

$$n(r_1) = a_1 n_1(r_1) \tag{18d}$$

$$n(r_2) = a_2 n_2(r_2) \tag{18e}$$

where r_1 and r_2 are radii at which modes 1 and 2, respectively, dominate.

Examples of Analytic Representation of SD Data

Tropospheric Aerosol Size Distributions (Junge Data): Junge's data (Ref. 1) for the average size distribution n(r) of continental aerosols in the altitude region (0-3 km) were plotted on the log-log graph transparency. One could readily see that for large radius particles, the n(r) data points lay along a straight line and suggest thereby a power law behavior. Thus, Models 2, 4, and 8 seemed appropriate. In the following, examples are given for fitting the SD data with these three models. Model 5 was also fitted to the data to illustrate the poor fit which can be obtained if an inappropriate model is chosen.

Model 2: According to our earlier prescription, the DT was overlaid on the p_4 - CG (Fig. 2A.4), and translated vertically

until the point (10^{-3}, 1.0) on the DT coincided with (10^{-2}, 0.1) on the CG. The data points for large radii fell on the $p_4 = 2.0$ plot; thus, $p_3 = 3.0$ and $p_4 = 2.0$ (the CP parameters) represent the data for large radii. Since there is not sufficient data at the smaller end to determine p_3' from the slope in that region, concentration will be on the curvature in the region of the peak.

Still using Fig. 2A.4, the DT was translated vertically and horizontally so that the point (0.5, 10^6) on the DT coincided with (100, 1.0) on the CG. Although $p_3' = 3.0$, $p_4' = 2.0$ represented the large r data well, the CP had a sharper peak than the data points and thus suggested that $p_3' = 3.0$ may be too high.

The DT was then overlaid on the p_3-CG (Fig. 2A.3), and translated vertically and horizontally so that the point (5.0, 10^6) on the DT coincided with the point (100, 1.0) on the CG. The plot for $p_3 = 2.0$ gave the best fit to the data. It did not fall off as sharply at small radii and the slope at large radii was a little too steep; however it did give a reasonable fit to the broad peak.

The estimate of p_4' had to be adjusted in the light of the new estimate for $p_3' = 2.0$ since the slope at large radii depends on both p_3 and p_4. This was done by substitution in Eq. (14a) which gave $p_4' = 2.5$. The only parameter left to be estimated was p_2' which can be found from Eq. (5b). Since $r_m' = 6.5 \times 10^{-3}$ for these data, substitution for r_m', p_3', and p_4' in Eq. (5b) gives $p_2' = 0.013$. The accuracy of this estimate was confirmed by estimating p_2' from the catalog. The DT was overlaid on the p_2-CG (Fig. 2A.1), and translated vertically so that the point (10^{-2}, 8×10^5) on the DT coincided with (10^{-2}, 1.0) on the CG. It was evident that the p_2 for the data

was less than 0.05. The estimate for p_2' was found by substitution in Eq. (14b). Substituting p_2 (=0.05) and r_m (=0.022) for closest catalog plot and r_m' (= 0.0065) for the data points, yielded $p_2' = 0.015$. However, $p_3 = 2.0$, $p_4 = 3.0$ on the CG and the estimates for the data were $p_3' = 2.0$, $p_4' = 2.5$; thus, the p_2' estimate obtained had to be adjusted by using Eq. (14c), which gave $p_2' = 0.013$, the same as the earlier estimate.

These estimates ($p_2' = 0.013$, $p_3' = 2.0$, $p_4' = 2.5$) were used as the initial estimates for a nonlinear least squares (NLLS) fit. The results are given in Fig. (11) and the best fit estimates are $p_2' = 3.172 \times 10^{-2}$, $p_3' = 1.82$, $p_4' = 2.65$. It can be seen that the initial parameter estimates represent the SD slope and the curvature quite well. Note that the estimated curve has the right shape but is too far to the left of the data points. This is due to the broad peak, the estimate of p_2' was too low, since the actual r_m value was used. It might have been more accurate to take r_m = mid point of peak region. The final best-fit values, obtained by the NLLS method, give a good analytic fit to the SD data. It should be noted that the greatest change occurred in p_2', which effectively gave a higher r_m value.

Model 4: Since the IMGD behaves as a power law for large 4, it is a suitable model for the Junge data (0-3 km). From the data points the slope as $r \to \infty$ was found to be -4; thus the estimate for p_2' was 4.0. To confirm this estimate, the DT was overlaid on the p_2-CG (Fig. 4A.1) so that the DT point (10^{-3}, 1.0) coincided with the CG point (2×10^{-2}, 10^{-5}), their respective x- and y-axes remaining mutually parallel. It was noted that the data points lay along the $p_2 = 4.0$ CP.

The DT was then overlaid on the p_4- CG (Fig. 4A.4) so that the point (10^{-3}, 8.0) coincided with the CG point (0.3, 10^{-5}). The data maximum then coincided with the maximum for the p_4 = 2.0 CP and the data points in the region of the peak fell on that curve. Thus, $p_4' = 2.0$ was the estimate.

Substituting the estimates for p_2' and p_4' and r_m' - 6.5 x 10^{-3} in Eq. (7b) gave $p_3' = 8.45 \times 10^{-5}$. To confirm the p_3 estimate, the DT was overlayed on the p_3- CG (Fig. 4A.3) so that the DT point (10^{-2}, 8 x 10^{+5}) coincided with the CG point (10^{-2}, 1.0). From this, it was evident $p_3 << 1.0$. Substituting r_m' for the data, and p_3 and r_m for the closest CP plot in Eq. (16a) gave $p_3' = 4.23 \times 10^{-5}$. However, ($p_2$, p_4) for the CG were different from the (p_2', p_4') estimates for the data; thus, the final estimate for p_3 was found by substitution in Eq. (16b), which gave $p_3' = 8.45 \times 10^{-5}$, the same as the earlier estimate. Figure 12 shows the results, the final estimates were $p_2' = 4.43$, $p_3' = 0.788$, $p_4' = 0.514$.

Model 5: Since these data fall off as a power law for large r, the log-normal distribution is not the most appropriate model to use. However, it is used here in order to illustrate the poor fit one obtains when the model chosen is inappropriate and also to illustrate that such a model can sometimes be used to fit the data in a portion of the data range.

The DT was overlaid on the p_3- CG (Fig. 5A.3) and then translated horizontally and vertically so that the DT point (10^{-3}, 8.0) coincided with the CG point (6 x 10^{-2}, 10^{-5}). At this point, the maxima for the data and the CP for p_3 = 1.0 coincided. The data points lay almost exactly along the p_3 = 1.0 CP, except for very small r. Thus, $p_3' = 1.0$ was the estimate.

The parameter p_2' was then estimated by using Eq. (8b) and $r_m' = 6.5 \times 10^{-3}$. Substitution in this equation gave $p_2' = 0.0176$. To confirm this estimate from the catalog plots, the DT was overlaid on the p_2- CG (Fig. 5A.2) so that $(10^{-2}, 8 \times 10^5)$ on the DT coincided with $(10^{-2}, 1.0)$ on the CG. It was noted that p_2 for the data was less than 0.1; thus, in order to obtain an estimate for p_2, an extrapolation was made by Eq. (17b). Substitution of the p_2 and r_m values for the closest CP and r_m' for the data gave $p_2' = 0.0176$, the same as the previous estimate. Thus, the parameter estimated for this model were $p_2' - 0.0176$, $p_3' = 1.0$.

Figure 13 shows the results of an NLLS fit using these parameter estimates. The best fit estimates were $p_2' = 1.208 \times 10^{-2}$ $p_3' = 1.21$. The initial estimate provides a good fit to the data up to about 2μm, beyond which it falls off too steeply. The final best-fit values give a much better fit in the region 0.2μm - 30μm, but do not fit the peak region. As was mentioned earlier, the log normal model is not as suitable for these data as Models 2 and 4. However, if only a portion of the size range covered is of interest, say up to 2μm, or beyond 0.2 m, then this model is as good as any of the others.

Model 8B: Since Model 8B behaves as a power law for large r it is a suitable model for the Junge data. It also has the advantage of being able to model broad peaks. To determine p_2', the DT was overlaid on the p_2- CG (Fig. 8D.1) so that the point $(10^{-2}$, $8 \times 10^5)$ coincides with 10^{-2}, 1.0) on the CG. It was then noted that the data points lay about halfway between the 10^{-4} and 10^{-5} CP's. The estimate for p_2' was thus 5×10^{-5}.

To determine p_3', the DT was overlaid on the p_3- CG (Fig. 8D.2) so that the point $(5 \times 10^{-3}, 8 \times 10^5)$ coincided with the

point (2×10^{-2}, 1.0) on the CG. The data points coincided with the $p_3 = 40.0$ CP; thus, the estimate was $p_3' = 40.0$.

The parameter p_4' was determined by overlaying the DT on the P_4- CG (Fig. 8D.3) so that the point (10^{-2}, 10^6) coincided with (2×10^{-2}, 10.0) on the CG. Since the data points lay along the $p_4 = 4.0$ CP, the estimate for p_4' was 4.0.

Thus, the parameter estimates for this model were $p_2' = 5 \times 10^{-5}$, $p_3' = 40.0$, $p_4' = 4.0$. The results of the NLLS fit to this data, using these estimates, are given in Fig. 14. The best fit estimates were $p_2' = 4.700 \times 10^{-5}$, $p_3' = 38.8$, $p_4' = 4.03$. As can be seen from Fig. 14 the initial estimates represent the shape of the data quite well but the n(r) values are consistently too low. The final estimates give a very good fit to the data and model the broad peak very well.

Cumulative Size Distribution: The SD data was obtained over Alaska at an altitude of 13 km, by Quartz Crystal Measurement (QCM) method.[1] The SD is in the form of the cumulative.

Model 2: The data points fell on a straight line as $r \to \infty$; thus, Model 2 is an appropriate model. In this case, p_2' was determined first, and then p_3' and p_4' which control the slope for large r. The first step was to extrapolate the data to r = 0.01. This gave a value 8×10^3 for N(0).

The DT was overlaid on the p_2- CG (Fig. 2C.1) so that N(0) for the DT coincided with N(r) = 1.0 on the CG. It was noted that in this case the rate of fall-off of the data for large r was

---

[1] *D. Woods, private communication.*

the same as for the CP's but that the data lay between the 3×10^{-2} and 5×10^{-2} CP's. By using the interpolation formula in Eq. (14e) at $N(r) = 3 \times 10^{-4}$ (on the CG), assuming $s = s'$ and substituting $r = 0.4$, $r' = 0.3$ and $p_2 = 0.05$, the estimate $p_2' = 0.0375$ was obtained. To obtain an estimate for p_4', the data values $N(p_2')$ and $N(0)$ were substituted in Eq. (14f). This gave $p_4' = 4$.

The DT was then overlaid on the p_3- CG (Fig. 2C.3) so that the point $(0.5, 10^4)$ coincided with the point (40, 10) on the CG. The data points lay on the $p_3 = 2.0$ CP making $p_3' = 2.0$ the estimate. However, both p_3 and p_4 affect the slope as $r \to \infty$, and p_4 on the CG was different from the p_4' estimated above, thus the estimate for p_3' was adjusted by using Eq. (14a). Substitution gave $p_3' = 1.33$ as the final estimate.

Thus, the parameter estimates were $p_2' = 0.0375$, $p_3' = 1.33$, $p_4' = 4.0$. Figure 15 shows the results of an NLLS fit using the estimates for p_2, p_3 and p_4 given above; the best estimates for the parameters were $p_2' = 0.0434$, $p_3' = 1.29$ and $p_4' = 4.31$. As can be seen from the plot, the initial estimate explains the data very well and the final estimates for the parameters are very similar to the original estimates.

Model 3: The DT was overlaid on the p_2- CG (Fig. 3C.1) so that the point $(10^{-2}, 8 \times 10^3)$ coincided with the point $(10^{-2}, 1.0)$ on the CG. The shape of the data curve in the region where it curves was very similar to the shape for the CP's, however, $p_2' < 1.0$. In the absence of any reliable extrapolation formula, $p_2' = 1.0$ was used as the best estimate.

The DT was then overlaid on the p_4- CG (Fig. 3C.5) so that the point (10^{-2}, 10^{-1}) coincided with (3.0, 10^{-5}) on the CG. The data lay close to the $p_4 = 0.3$ CP so $p_4' = 0.3$ was used.

To obtain an estimate for p_3', the DT was overlaid on the p_3- CG (Fig. 3C.3) so that the point (10^{-2}, 8×10^3) coincided with the point (10^{-2}, 1.0) on the CG. The data points lay closest to the $p_3 = 30.0$ CP; so this was taken as the estimate for p_3'.

Thus, the estimates for the model are $p_2' = 1.0$, $p_3' = 30.0$, and $p_4' = 0.3$. Figure 16 shows the results of an NLLS fit to the data using these estimates; the best estimates were $p_2' = 0.999$, $p_3' = 30.0$, $p_4' = 0.249$. The initial estimate gave a reasonable fit to the data, and the final estimate fitted the data very well.

Model 5: When fitting cumulative data with the LND, it is generally best to extrapolate the data to obtain N(0), and use this to calculate p_2. Extrapolation of the data gave $N(0) \sim 8 \times 10^3$, and by using $N(p_2')/N(0) = 0.5$, it was found that $N(r) = 4 \times 10^3$ at $r = 0.02$ and gave a first estimate for p_2'.

The DT was then overlaid on the p_3- CG (Fig. 5C.3) so that (2×10^{-2}, 4×10^{-3}) coincided with (1.0, 0.5) on the CG (i.e. the median points coincided). This suggested $0.5 < p_3 < 1.0$, since the data points lay between the CP's having those values. Looking at the behavior as $r \to \infty$, it was noted that the CP for $p_3 = 0.5$ fell off much more sharply than the data. The DT was translated horizontally and vertically

This Page Intentionally Left Blank

The DT was overlaid on the p_4- CG (Fig. 3A.4) so that the point (10^{-2}, 6 x 10^2) coincided with the point (3 x 10^{-2}, 10) on the CG. Then, by looking at the behavior as $r \to \infty$, it was noted that the data points lay on a line which was approximately parallel to the p_4 = 1.0 CP. The DT was translated horizontally so that the point (20.0, 6 x 10^3) coincided with the point (10^2, 10) on the CP. The data points did, in fact, lie close to the p_4 = 1.0 curve and thus confirm the estimate p_4' = 1.0. The parameter p_3' was then estimated from r_m', p_2', and p_4', by substituting into Eq. (6b); by taking r_m' = 0.1275, this gave p_3' = 78.4.

To confirm the estimate for p_3' the DT was overlaid on the p_3- CG (Fig. 3A.2) so that the point (10^{-2}, 6 x 10^2) coincided with the point (10^{-2}, 10) on the CG. The maximum for the data occurred at the same r as that for the p_3 = 10.0 CP; however, p_2 and p_4 for the CG were different from the estimates p_2' and p_4' so that p_3' estimate was adjusted by using Eq. (15b). Substituting p_2, p_3, p_4 for the CG and p_2', p_4' for the data gave p_3' = 62.5. Thus, the original estimate for p_3' seemed reasonable. Therefore, the estimates for this model were p_2' = 10.0, p_3 = 78.4, and p_4 = 1.0. Figure 18 shows the best fit obtained; the final estimates were p_2' = 8.38, p_3' = 64.7, and p_4' = 0.758.

Bimodal Size Distributions: The data used in this example were collected as part of an investigation of high temperature combustion aerosols (Ref. 17). The original data were in the form of the aerosol mass in each of eight diameter groups, ranging from 0.43 μm to 20 μm. For this example, the masses have been converted to number of particles by assuming spherical particles with density 1 $\mu g/cm^3$ and average diameter equal to the midpoint of the diameter group in question.

Figure 19 shows the original data, with a probably curve for the second mode dotted in. It was not possible to dot in a probable curve for the first mode because no information was available about the turning point for this mode. The bimodal data can be represented by two terms as in Eq. (18a). Both modes exhibit straight line behavior in the large r region, so the RPL (Model 2), was chosen as being suitable for both modes. The model fitted takes the form

$$n(r) = p_1 \left\{ \frac{(r/p_2)^{p_3-1}}{p_2(1+(r/p_2)^{p_3})^{p_4}} + \frac{p_5\,(r/p_6)^{p_7-1}}{p_6(1+(r/p_6)^{p_7})^{p_8}} \right\}$$

where p_2, p_3 and p_4 are parameters for the first mode, and p_5, p_6, p_7, and p_8 are parameters for the second mode.

Model 2: p_3' could not be determined from the data for either mode. The DT was overlaid on the p_4- CG (Fig. 2A.4) and translated vertically and horizontally until the point $(10^{-2}, 2 \times 10^{2})$ coincided with the CG point (0.3, 1.0). The data points for the first mode lay along the $p_4 = 2.0$ CP and, in the absence of any information about p_3', the values $p_3' = 3.0$, $p_4' = 2.0$ were taken as the best estimates of these parameters for the first term.

To determine p_8' for the second mode, the DT was translated so that (35.0, 3.0) coincided with the CG point $(10^{2}, 10)$. The data points for the second mode lay along the $p_4 = 2.0$ CP, and since this CP fitted both the peak and the large r portion of the data curve, $p_7' = 3.0$, $p_8' = 2.0$ were taken as the estimates.

To confirm p_7' for the second mode, the DT was overlaid on the p_3- CG (Fig. 2A.3) and translated vertically and horizontally until the point (45.0, 2.5) coincided with the CG point

$(10^2, 10)$. The data points in the region of the peak for the second mode lay along the $p_3 = 3.0$ CP and confirmed the p_7' estimate.

The next step was to determine p_2' and p_6'. The DT was overlaid on the p_2- CG (Fig. 2A.1) so that the point $(10^{-2}, 5 \times 10^2)$ coincided with the point $(10^{-2}, 1.0)$ on the CG. The data points for the first mode lay between the $p_2 = 0.1$ CP and $p_2 = 0.5$ CP and in the absence of any information about the mode radius, $p_2' = 0.1$ was taken as the estimate for the first mode. (The value 0.27, which is the smallest r for which data are available, is too high since there is no sign of any curvature at this point.)

To determine p_6' for the second mode, the DT was translated vertically until the point $(10^{-2}, 3.0)$ coincided with the point $(10^{-2}, 10)$ on the CG. In this case, interpolation was necessary since the data lay between the $p_2 = 1.0$ and $p_2 = 3.0$ CPs. Using Eq. (14b) with $r_m' = 1.6$ gave $p_6' = 3.58$ for the second mode.

The (p_3, p_4) values for the CG differ from $(p_3', p_4'$ and (p_7', p_8'); thus, the p_2' and p_6' estimates had to be adjusted by using Eq. (14c). Substituting in this equation gave $p_2' = 0.06$ for the first mode and $p_6' = 2.04$ for the second mode.

The final step was to determine the relative proportions of the two modes by determining the scaling factor p_1' for each mode. Since the peak values of the two modes differ by several orders of magnitude, it was decided to determine the scaling factors independently, by calculating them at radii where only one mode made a significant contribution to n(r) and using Eqs. (18d and 18e) to determine the scaling factors a_1', a_2' for each individual mode. This gave $a_1' = 1225$ for

the first mode (at r = 0.27) and $a_2' = 0.85$ for the second mode (at r = 4.5). Because of the form which the model fitted by the NLLS program takes, $a_1' = p_1'$, and $a_2' = p_1' \times p_5'$, and thus $p_5' = 6.9 \times 10^{-4}$. Thus, the initial estimates for this model are $p_1' = 1225.0$, $p_2' = 0.06$, $p_3' = 3.0$, $p_4' = 2.0$, $p_5' = 6.9 \times 10^{-4}$, $p_6' = 2.04$, $p_7' = 3.0$ and $p_8' = 2.0$. The results of the NLLS fit using these estimates are given in Fig. 19.

CONCLUDING REMARKS

The uses of the catalog are two-fold. Firstly, it provides a catalog of the shapes of the different distributions, illustrating such properties as the locations of mode radii, rates of fall-off and polydispersity. By providing a means for comparing distributions, it aids in selecting the model(s) most likely to give a good description of the experimental data to be fitted. Secondly, the catalog provides a means of estimating the likely values of the model parameters. Often these estimates will then be used as initial estimates for a nonlinear least-squares or other optimization code.

The catalog has been used successfully in fitting tropospheric and stratospheric aerosol data, bimodal data, and COSD data. It is importnat that the model chosen to fit the data be an appropriate one if useful results are to be obtained. In deciding whether a model is appropriate, mode radius, rates of fall-off, and polydispersity should be considered. Models which show different behavior for these properties from that of the data should be avoided.

As the examples showed, there are often several models which will adequately describe the data, although some may be better than others. Experience with the catalog has indicated that where there is a known relationship between a property of the model such as rate of fall-off and a particular parameter, that relationship should be used to get the best possible estimate for the parameter.

REFERENCES

1. Junge, C. E., "Air Chemistry and Radioactivity", Academic Press, New York (1963)

2. Kerker, Milton, "The Scattering of Light and other Electromagnetic Radiation", Academic Press, New York (1969).

3. Green, A. E. S., A. Deepak and B. J. Lipofsky, "Interpretation of the Sun's Aureole Based on Atmospheric Aerosol Models", Appl. Opt., 10, 1263 (1971)

4. Lidwell, O. M., Nature, 158, 61 (1946)

5. McGrath, E. J., et al, "Techniques for Efficient Monte Carlo Simulation: Selecting Probability Distributions", ORNL-RSIC-38 (Vol. 1) (1975).

6. Green, A. E. S., and P. J. Wyatt, "Atomic and Space Physics", Addison-Wesley, Reading, Mass. (1965).

7. Green, A. E. S., in "The Middle Ultraviolet: It's Science and Technology", A. E. S. Green, Ed., Wiley, New York (1966), Chap. 5, pp. 118-129.

8. Gradshteyn, I. S. and I. W. Ryzhik, "Table of Integrals, Series and Products", Academic Press, New York (1965)

9. Spiegel, Murray R., "Mathematical Handbook of Formulas and Tables", Schaum's Outline Series, McGraw-Hill, New York (1968).

10. Deirmendjian, D., "Electromagnetic Scattering on Spherical Polydispersions", Elsevier, New York (1969).

11. Abramowitz, Milton and Irene A. Stegun, "Handbook of Mathematical Functions", Dover Publications, New York (1965).

12. Twomey, S., "Atmospheric Aerosols", Elsevier, Amsterdam (1977).

13. Integraltafel (Bestimmte Integrale), Spinger Verlag, New York (1966).

14. Willeke, Klaus and Kenneth T. Whitby, "Atmospheric Aerosols: Size Distribution Interpretation", J. of the Air Pollution Control Assoc., 25, 529 (1975).

15. Patterson, E. M., and D. A. Gillette, "Commonalities in Measured Size Distributions for Aerosols Having a Soil Derived Component", J. Geophys. Res., 82, 2074 (1977).

REFERENCES (Continued)

16. Miranda, Henry A., Jr., "Balloon Measurements of Stratospheric Aerosol Size Distributions following a Volcanic Dust Incursion", AFCRL-TR-75-0518 (1975).

17. Singh, Jag J., "Trace Elemental Characteristics of Aerosols Emitted from Municipal Incinerators", NASA Technical Memorandum 78630 (1978).

APPENDIX I

SUMMARY TABLE FOR SIZE DISTRIBUTION MODELS

	Model 1 Power Law	Model 2 Regularized Power Law	Model 3 Modified Gamma
$n(r)$	$p_1 r^{-p_2}$	$\frac{p_1}{p_2} \frac{(r/p_2)^{p_3-1}}{(1+(r/p_2)^{p_3})^{p_4}}$	$p_1 r^{p_2} \exp(-p_3 r^{p_4})$
r_m	N. A.	$p_2 \left(\frac{p_3 - 1}{(1 + p_3(p_4-1)} \right)^{1/p_3}$	$(p_2/p_3 p_4)^{1/p_4}$
$n(r_m)$	N. A.	$\frac{p_1}{p_2} \frac{(p_3-1)^{\frac{p_3-1}{p_3}} (1+p_3(p_4-1))^{\frac{1+p_3(p_4-1)}{p_3}}}{(p_3 p_4)^{p_4}}$	$p_1 (\frac{p_2}{p_3 p_4})^{p_2/p_4} \exp(-p_2/p_4)$
As $r \to 0$, $n(r) \simeq$	$p_1 r^{-p_2}$	$\frac{p_1}{p_2} (r/p_2)^{p_3-1}$	$p_1 r^{p_2}$
As $r \to \infty$, $n(r) \sim$	$p_1 r^{-p_2}$	$\frac{p_1}{p_2} (r/p_2)^{-(1+p_3(p_4-1))}$	0
$N(r)$	$\frac{p_1}{p_2-1} (r^{1-p_2} - r_2^{1-p_2})$	$\frac{p_1 (1+(r/p_2)^{p_3})^{(1-p_4)}}{p_3(p_4-1)}$	$p_1 \lceil(p_{24}, p_3 r^{p_4}) / p_4 p_3^{p_{24}}$, $^*p_{24} = \frac{p_2+1}{p_4}$
As $r \to 0$, $N(r) \simeq$	$\frac{p_1}{p_2-1} (r^{1-p_2})$	$\frac{p_1 (1-(p_4-1)(r/p_2)^{p_3})}{p_3(p_4-1)}$	$p_1 \lceil(p_{24}) / p_4 p_3^{p_{24}}$
As $r \to \infty$, $N(r) \sim$	$\frac{p_1}{p_2-1} (r^{1-p_2})$	$\frac{p_1 (r/p_2)^{-p_3(p_4-1)}}{p_3(p_4-1)}$	0
M_k	$\frac{p_1}{(p_2-k-1)} (r_1^{1+k-p_2} - r_2^{1+k-p_2})$	$\frac{p_1 p_2^k}{p_3} \frac{\lceil(1+k/p_3) \lceil(p_4-1-k/p_3)}{\lceil(p_4)}$	$(p_1/p_4) p_3^{-(p_{24}+k/p_4)} \lceil(p_{24}+k/p_4)$

SUMMARY TABLE FOR SIZE DISTRIBUTION MODELS (CONTINUED)

	Model 4 Inverse Modified Gamma	Model 5 Log Normal Distribution	Model 6 Normal Distribution
$n(r)$	$p_1 \exp(-p_3/r^{p_4})/r^{p_2}$	$\frac{p_1}{\sqrt{2\pi}\, p_3 r} \exp\{-\frac{1}{2}(\frac{\ln r - \ln p_2}{p_3})^2\}$	$\frac{p_1}{\sqrt{2\pi}\, p_3} \exp\{-\frac{1}{2}(\frac{r-p_2}{p_3})^2\}$
r_m	$(p_3 p_4/p_2)^{1/p_4}$	$p_2 \exp(-p_3^2)$	p_2
$n(r_m)$	$p_1 (\frac{p_2}{p_3 p_4})^{p_2/p_4} \exp(-p_2/p_4)$	$\frac{p_1}{\sqrt{2\pi}\, p_2 p_3} \exp(p_3^2/2)$	$p_1 \Big/ \sqrt{2\pi}\, p_3$
As $r \to 0$, $n(r) \simeq$	0	0	$\frac{p_1}{\sqrt{2\pi}\, p_3} \exp\{-\frac{1}{2}(\frac{p_2}{p_3})^2\}(1+r p_2/p_3^2)$
As $r \to \infty$, $n(r) \sim$	$p_1 r^{-p_2}$	0	0
$N(r)$	$p_1 \gamma(p_{42}, p_3/r^{p_4})/p_4 p_3^{p_{42}}$ + , $+p_{42} = \frac{p_2-1}{p_4}$	$\frac{p_1}{2} \operatorname{erfc}\left(\frac{\ln r - \ln p_2}{\sqrt{2}\, p_3}\right)$	$\frac{p_1}{2} \operatorname{erfc}(\frac{r-p_2}{\sqrt{2}\, p_3})$
As $r \to 0$, $N(r) \simeq$	$p_1 \Gamma(p_{42}) / p_4 p_3^{p_{42}}$	0	$\frac{p_1}{2}\{1 - \sqrt{\frac{2}{\pi}}(\frac{r-p_2}{p_3})\}$
As $r \to \infty$, $N(r) \sim$	$p_1 r^{-(p_2-1)} / (p_2-1)$	0	0
M_k	$(p_1/p_4) p_3^{-(p_{42}-k/p_4)} \Gamma(p_{42}-k/p_4)$	$p_1 p_2^k \exp\left(\frac{p_3^2 k^2}{2}\right)$	see Eq. (9m)

	Model 7 Generalized Distribution Function	Model 8 Power Law - Generalized Distribution Function	Model 8B
$n(r)$	$\frac{p_1(1+p_2)^2\exp(r/p_3)}{(p_2+\exp(r/p_3))^2}$	$\frac{p_1\exp(p_2/r^{p_4})}{r^{p_4+1}(1+p_3(\exp(p_2/r^{p_4})-1))^2}$	$\frac{p_1\exp(p_2/r^2)}{r^{p_4}(1+p_3(\exp(p_2/r^2)-1))^2}$
r_m	$p_3 \ln p_2$	See Eq. (11b)	See Eq. (12b)
$n(r_m)$	$\frac{p_1(1+p_2)^2}{4\,p_2}$	See Eq. (11c)	See Eq. (12c)
As $r \to 0$, $n(r) \simeq$	$p_1(1+(\frac{p_2-1}{p_2+1})r/p_3)$	0	0
As $r \to \infty$, $n(r) \sim$	0	$p_1 r^{-(p_4+1)}$	$p_1 r^{-p_4}$
$N(r)$	$\frac{p_1(1+p_2)^2 p_3}{(p_2+\exp(r/p_3))}$	$\frac{p_1(\exp(p_2/r^{p_4})-1)}{p_2p_4(1+p_3(\exp(p_2/r^{p_4})-1))}$	N.A.
As $r \to 0$, $N(r) \simeq$	$p_1(1+p_2)p_3(1-r/p_3(1+p_2))$	$p_1/p_2p_3p_4$	N.A.
As $r \to \infty$, $N(r) \sim$	0	0	N.A.
M_k	N.A.	N.A.	$\frac{p_1}{2p_3^2p_2^{p_{4k}}}\Gamma(p_{4k})\sum_{i=0}^{\infty}(1-\frac{1}{p_3})^i(i+1)^{-(p_{4k}-1)}$ $p_{4k}=\frac{p_4-(k+1)}{2}$

PARAMETRIZED GRAPHICAL CATALOG OF SIZE DISTRIBUTION ANALYTIC MODELS

(*For List of Symbols and Acronyms see page vii-viii*)

- *Annotation on logarithmic axes gives the power of 10*
- *For semi-log graphs (Figures 6A.1 - 6C.3, 7A.1 - 7C.3) the annotation on the linear axis (X-axis) is the actual value.*
- *Blank log-log and semi-log graphs are reproduced on pages 156 and 157, respectively.*
- *Two transparencies of the blank log-log and semi-log graphs are attached at the end of the catalog.*

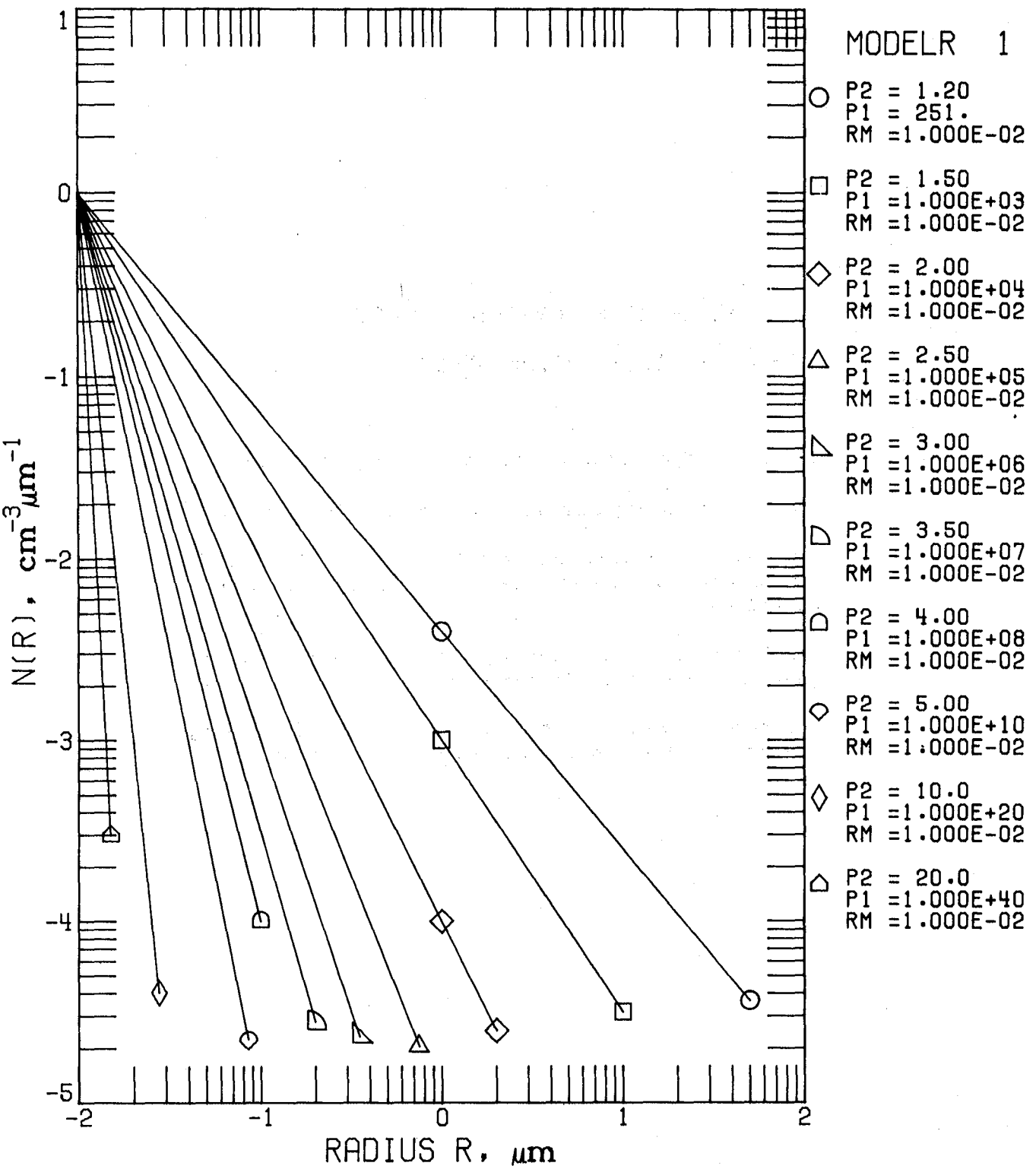

Figure 1A.1. Model 1 (power law) for n(r). Parameter Set 1.1: p_2 variable.

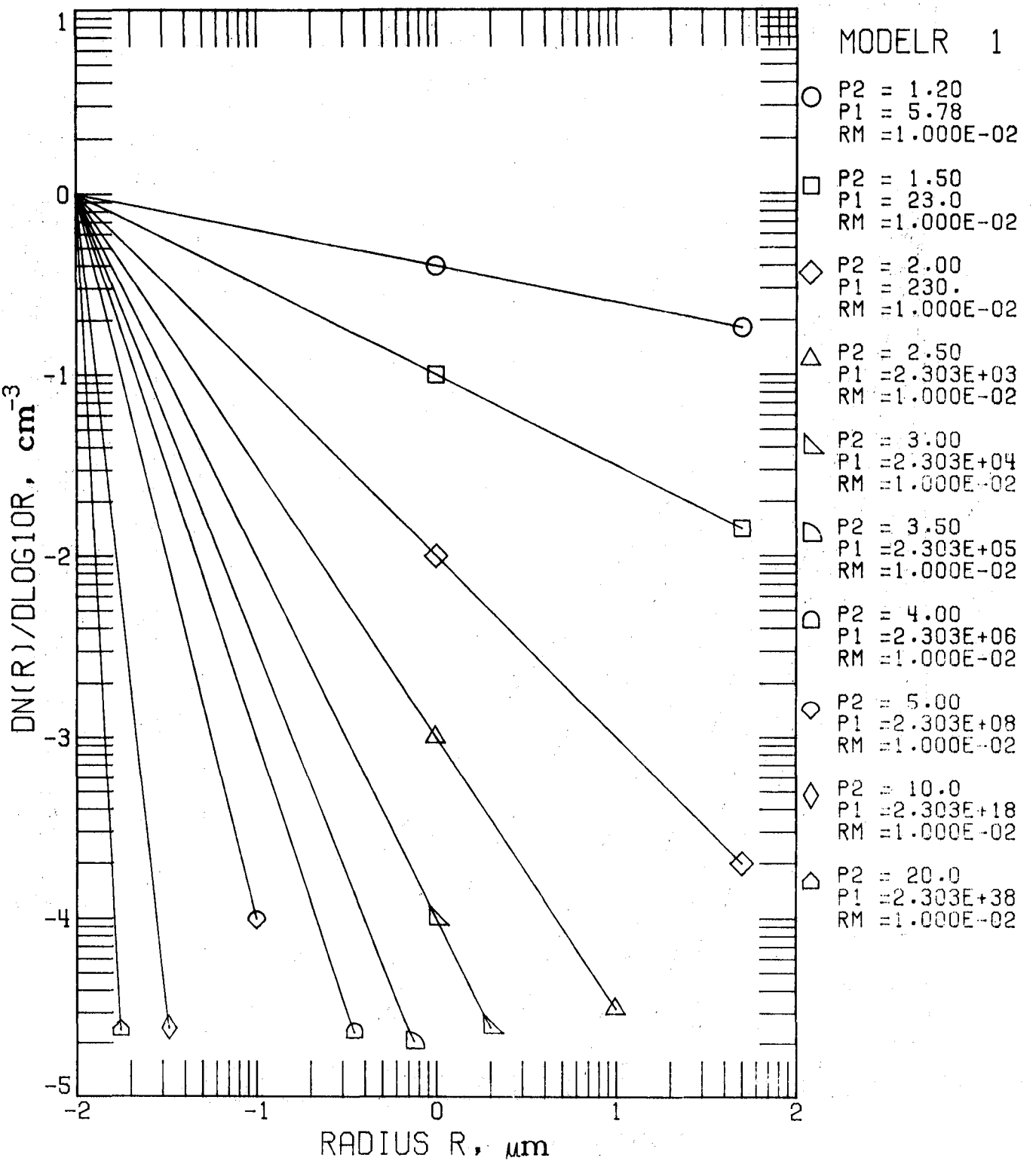

Figure 1B.1. Model 1 for $n_L(r)$.
Parameter Set 1.1.

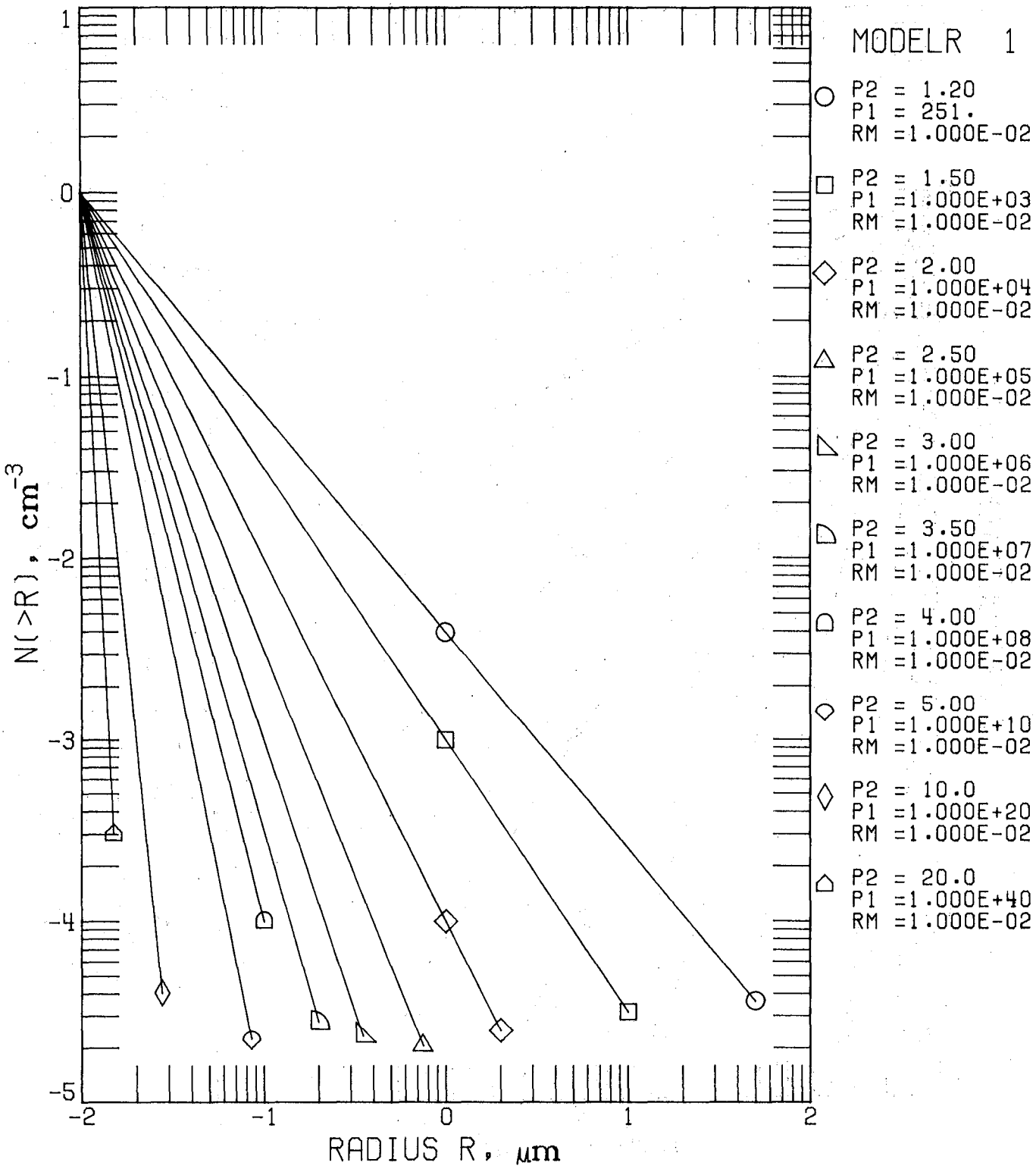

Figure 1C.1. Model 1 for N(>r).
Parameter Set 1.1.

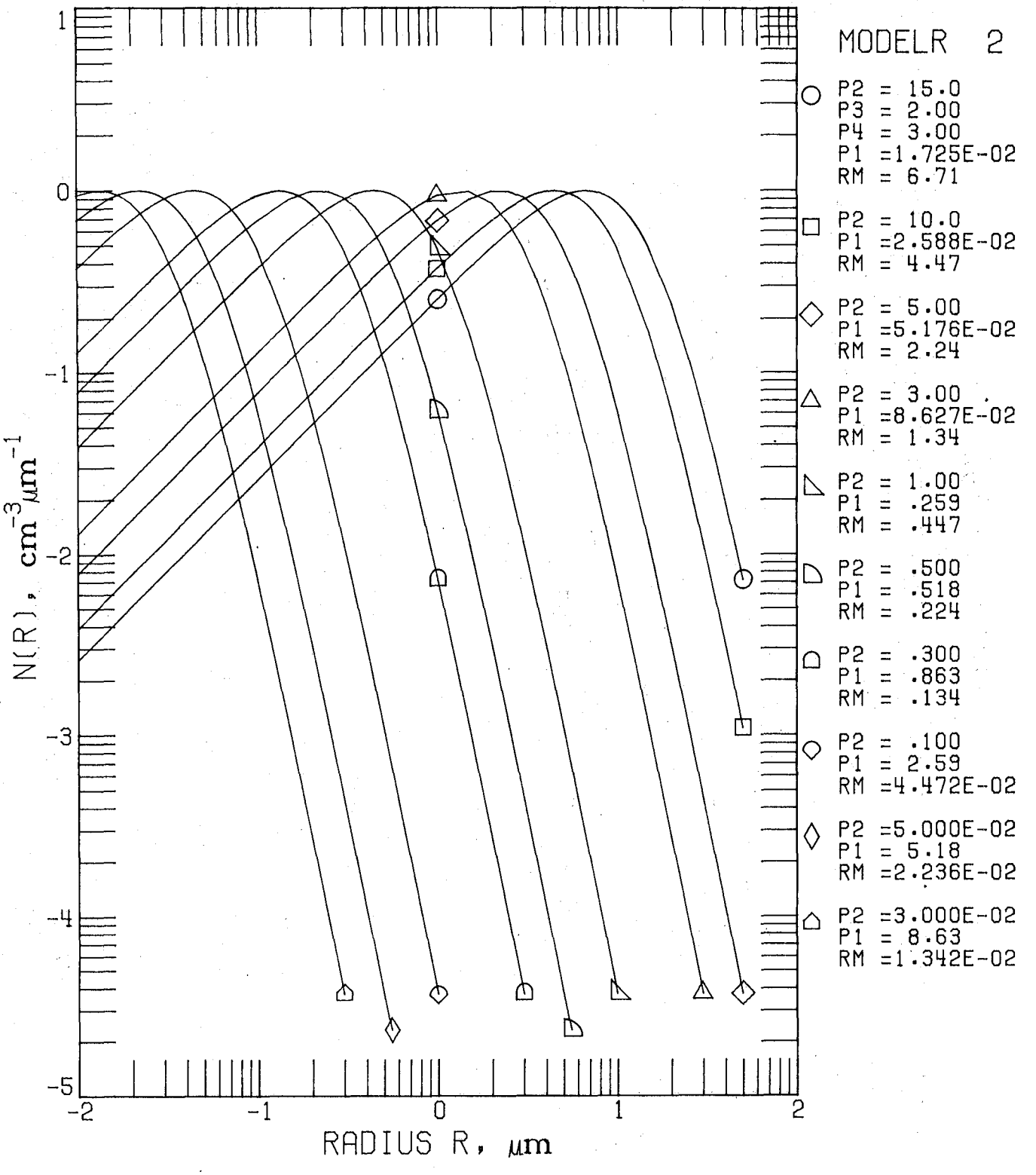

Figure 2A.1. Model 2 (Regularized Power Law) for n(r). Parameter Set 2.1: p_2 variable, p_3 = 2.0, p_4 = 3.0.

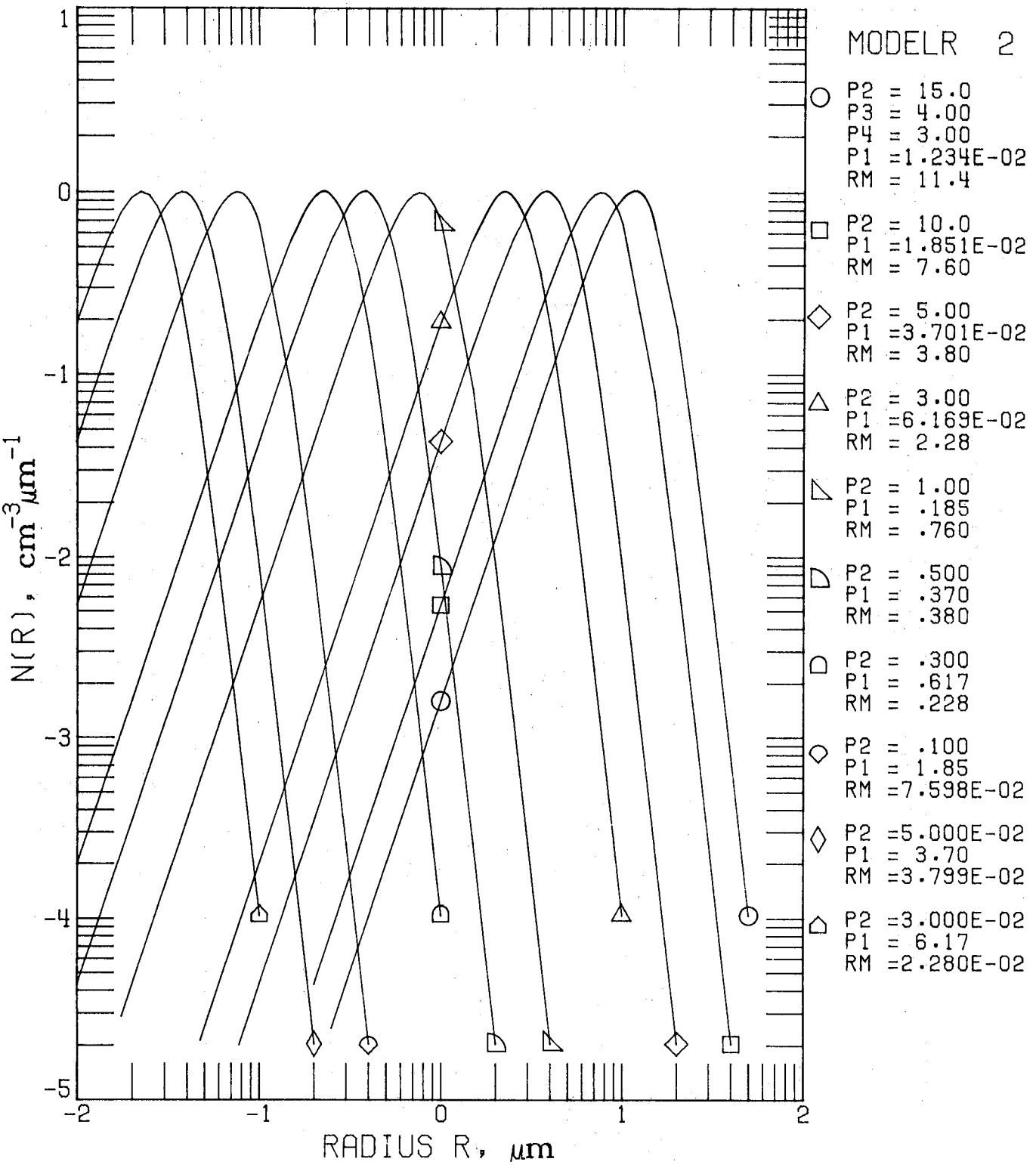

Figure 2A.2. Model 2 for n(r).
Parameter Set 2.2: p_2 variable,
$p_3 = 4.0$, $p_4 = 3.0$.

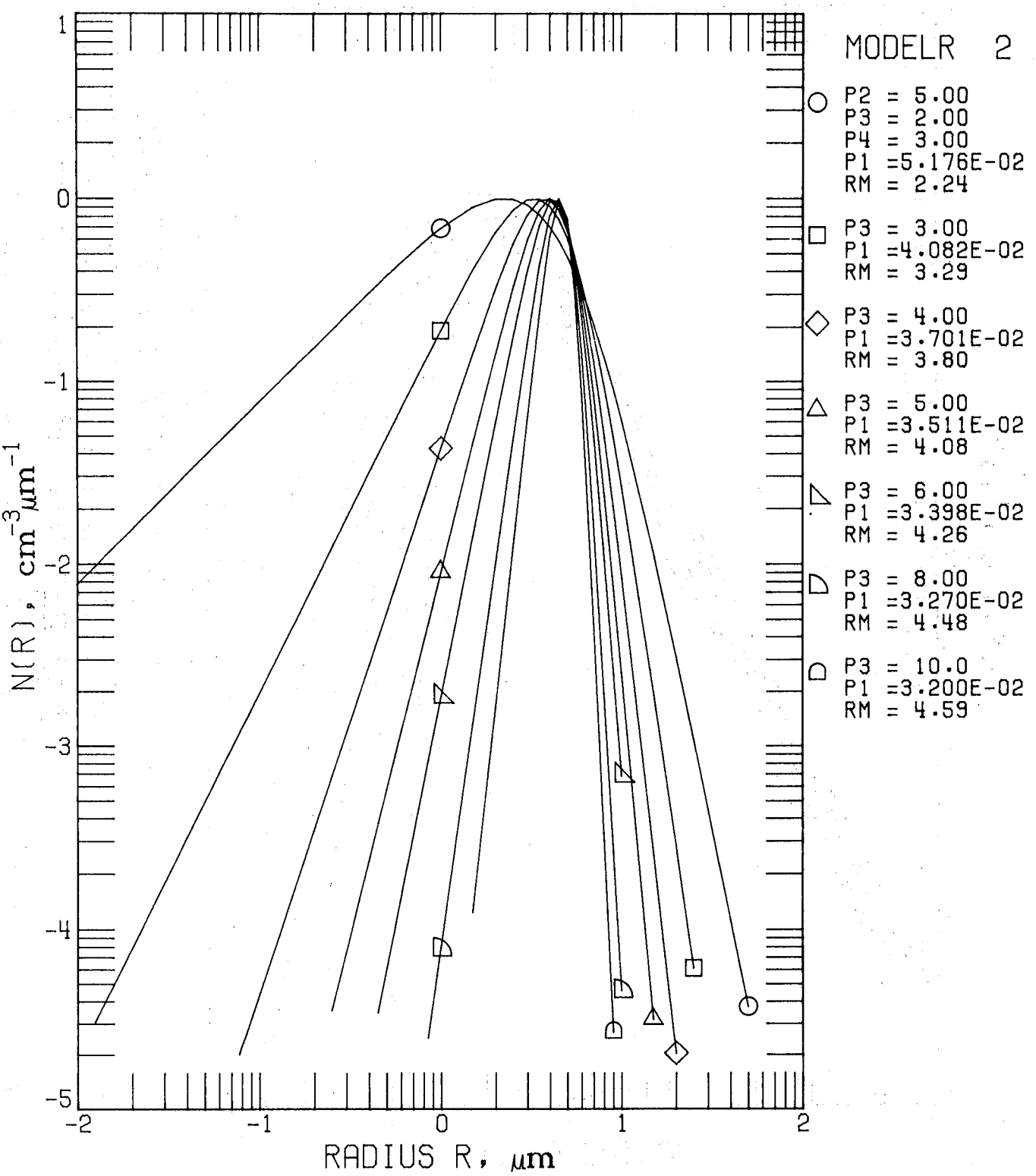

Figure 2A.3. Model 2 for n(r).
Parameter Set 2.3: p_3 variable,
p_2 = 5.0, p_4 = 3.0.

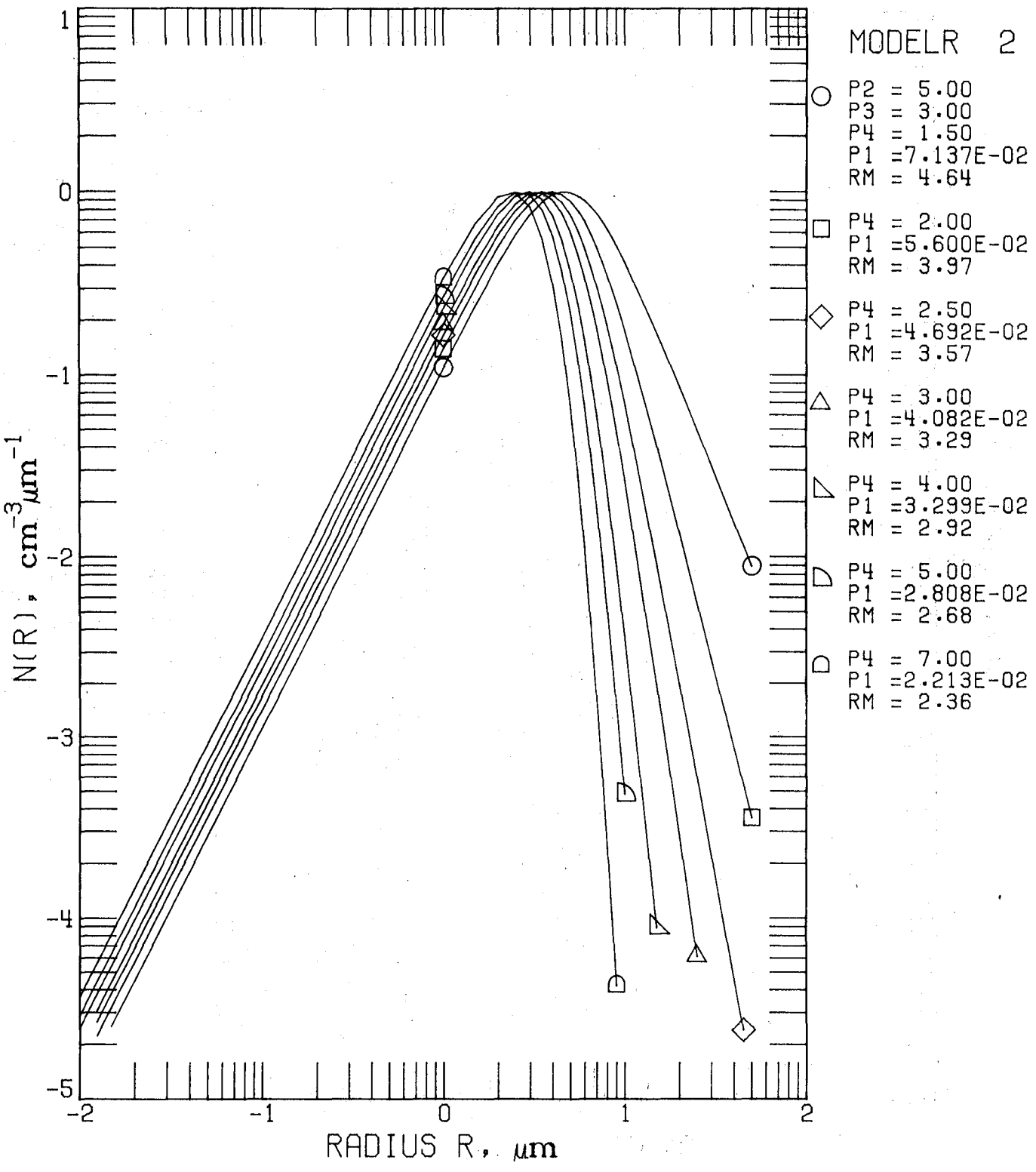

Figure 2A.4. Model 2 for n(r).
Parameter Set 2.4: p_4 variable,
$p_2 = 5.0$, $p_3 = 3.0$.

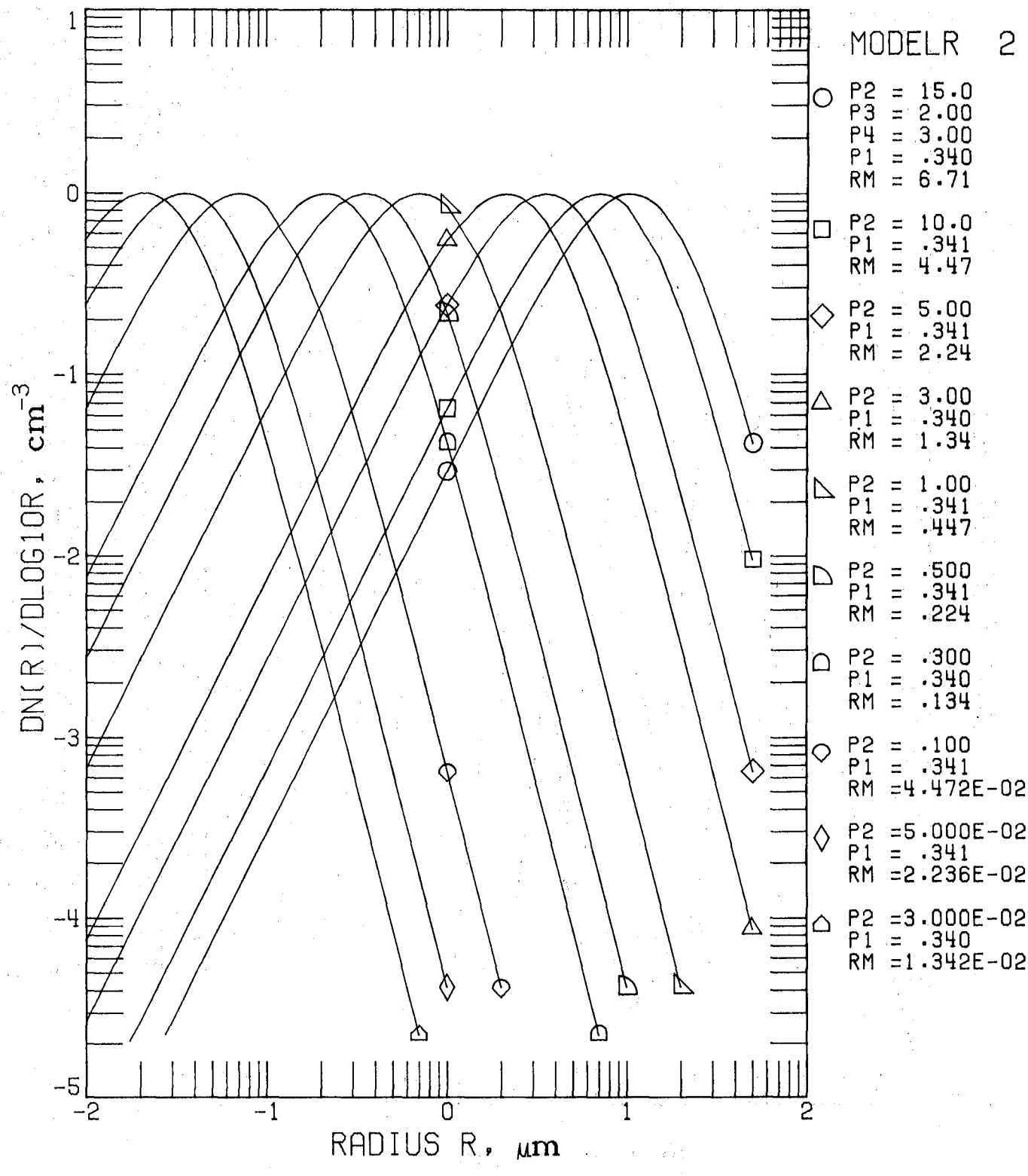

Figure 2B.1. Model 2 for $n_L(r)$.
Parameter Set 2.1.

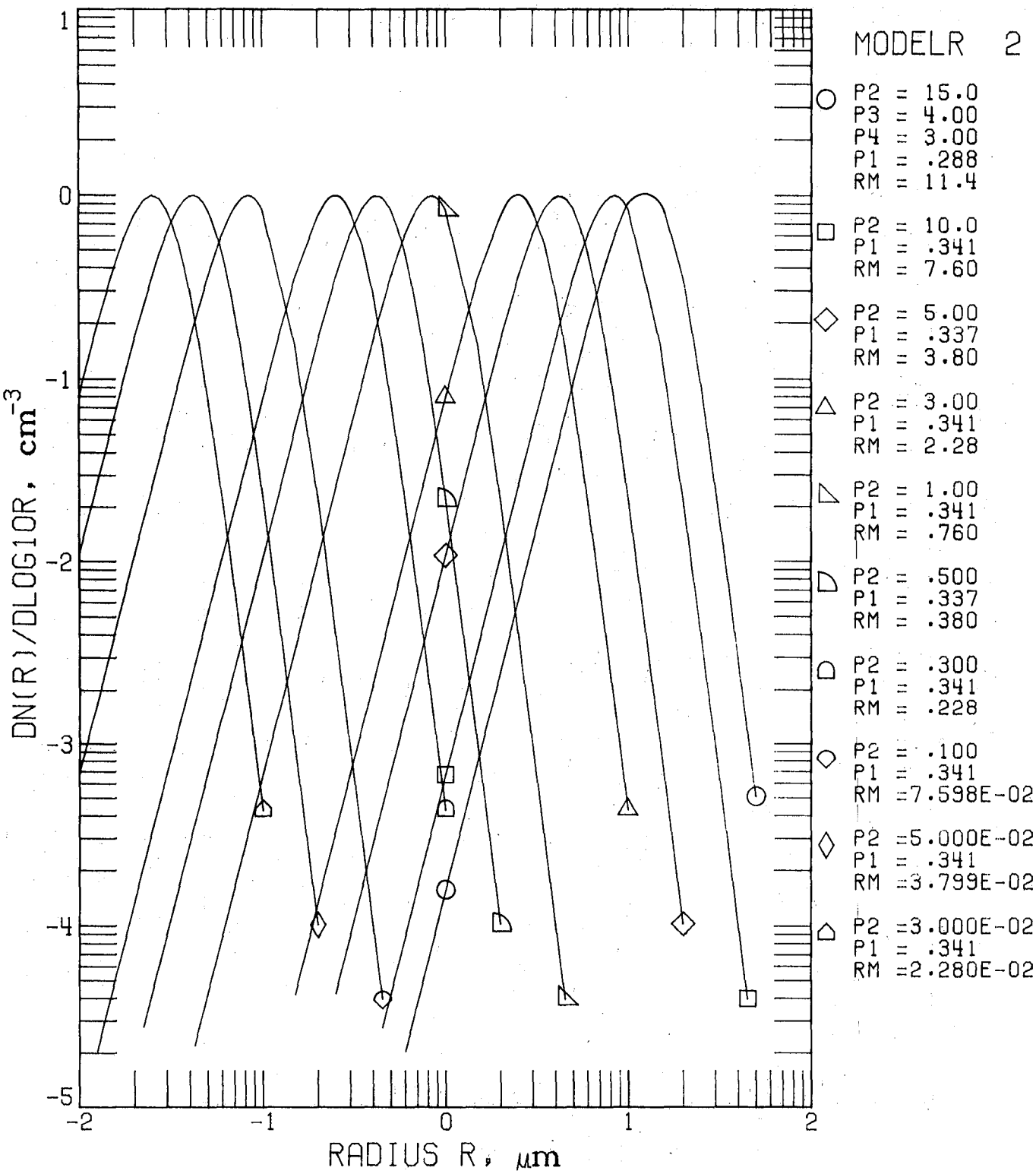

Figure. 2B.2. Model 2 for $n_L(r)$.
Parameter Set 2.2.

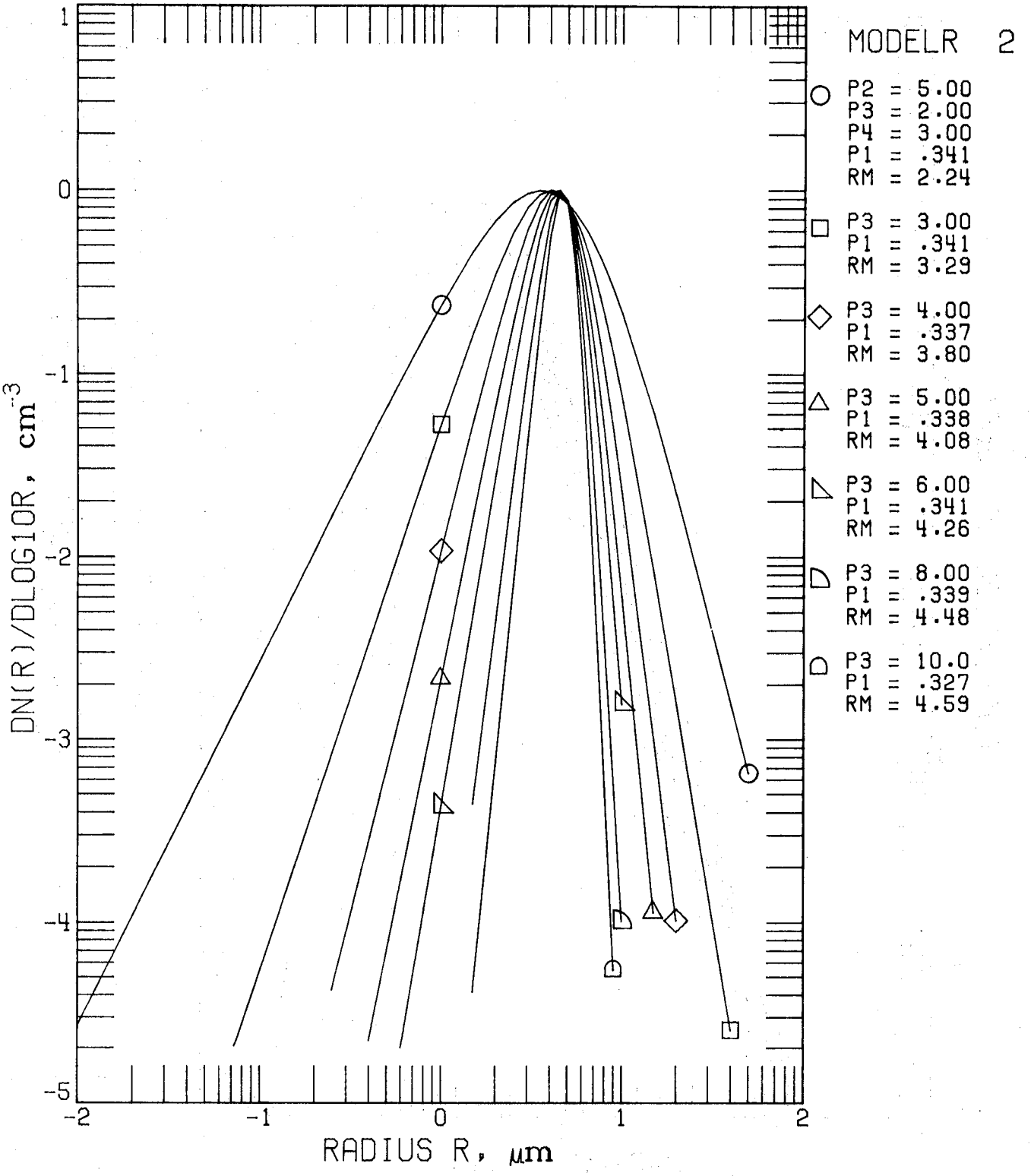

Figure 2B.3. Model 2 for $n_L(r)$.
Parameter Set 2.3.

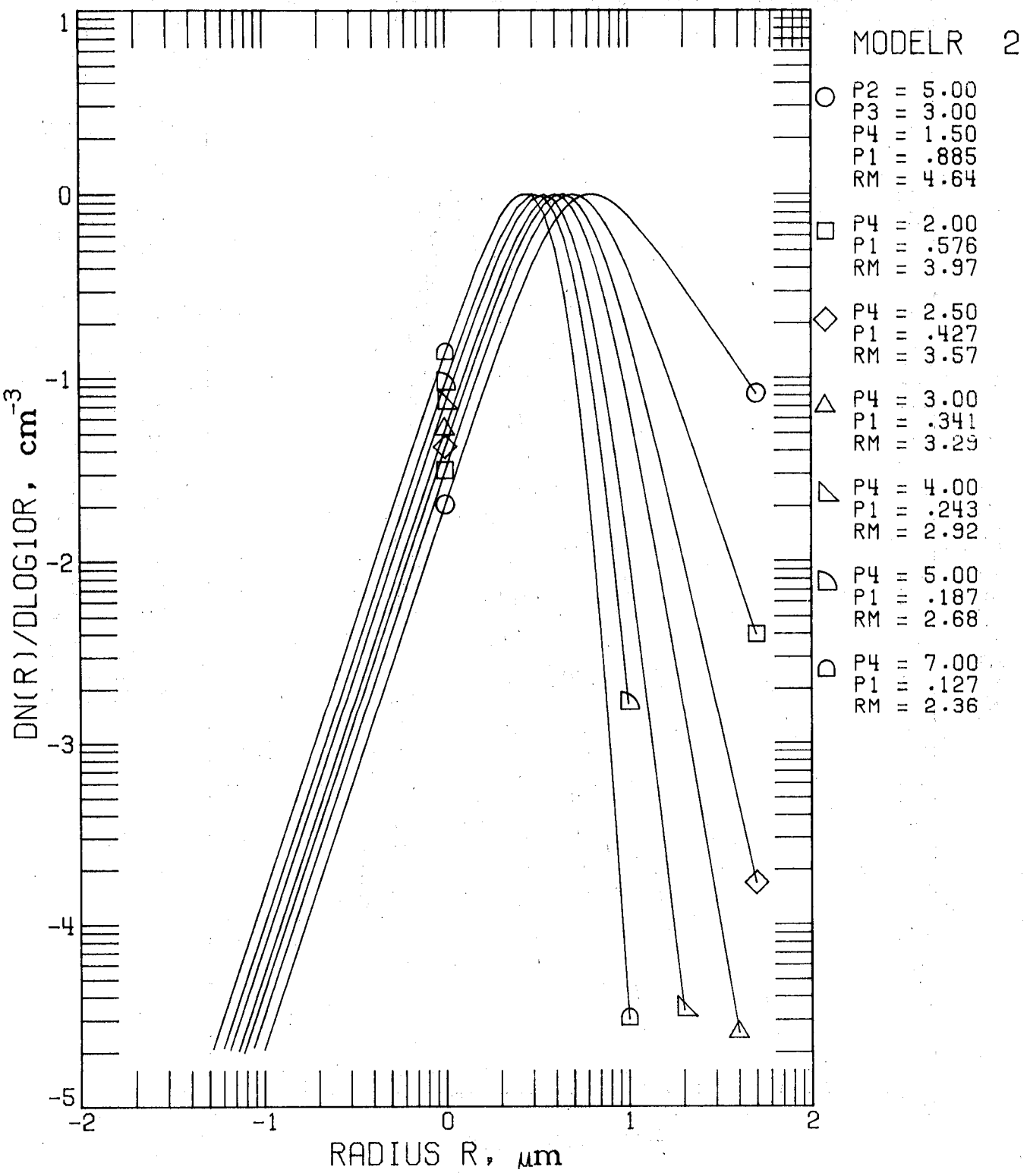

Figure 2B.4. Model 2 for $n_L(r)$.
Parameter Set 2.4.

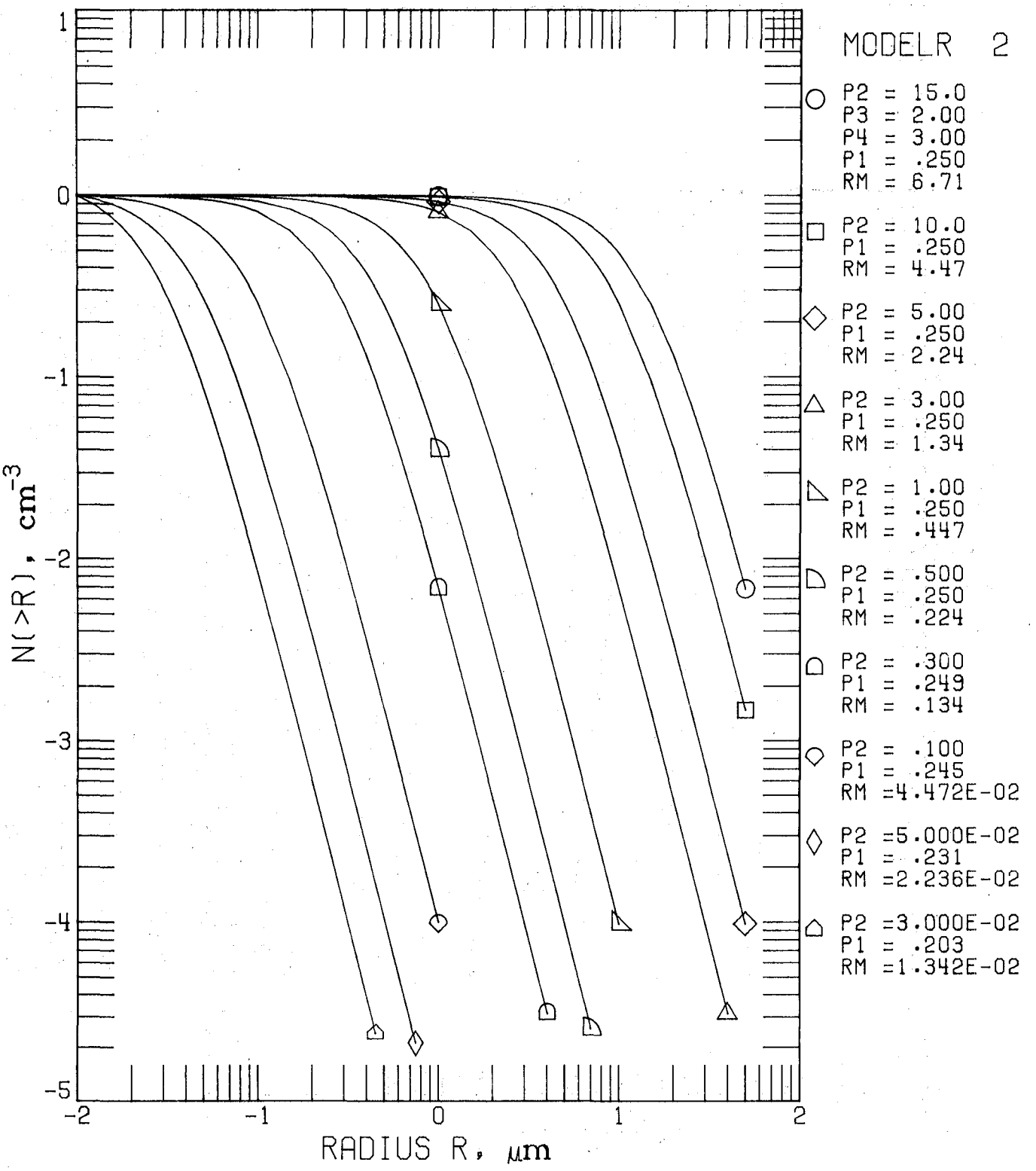

Figure 2C.1. Model 2 for N(>r).
Parameter Set 2.1.

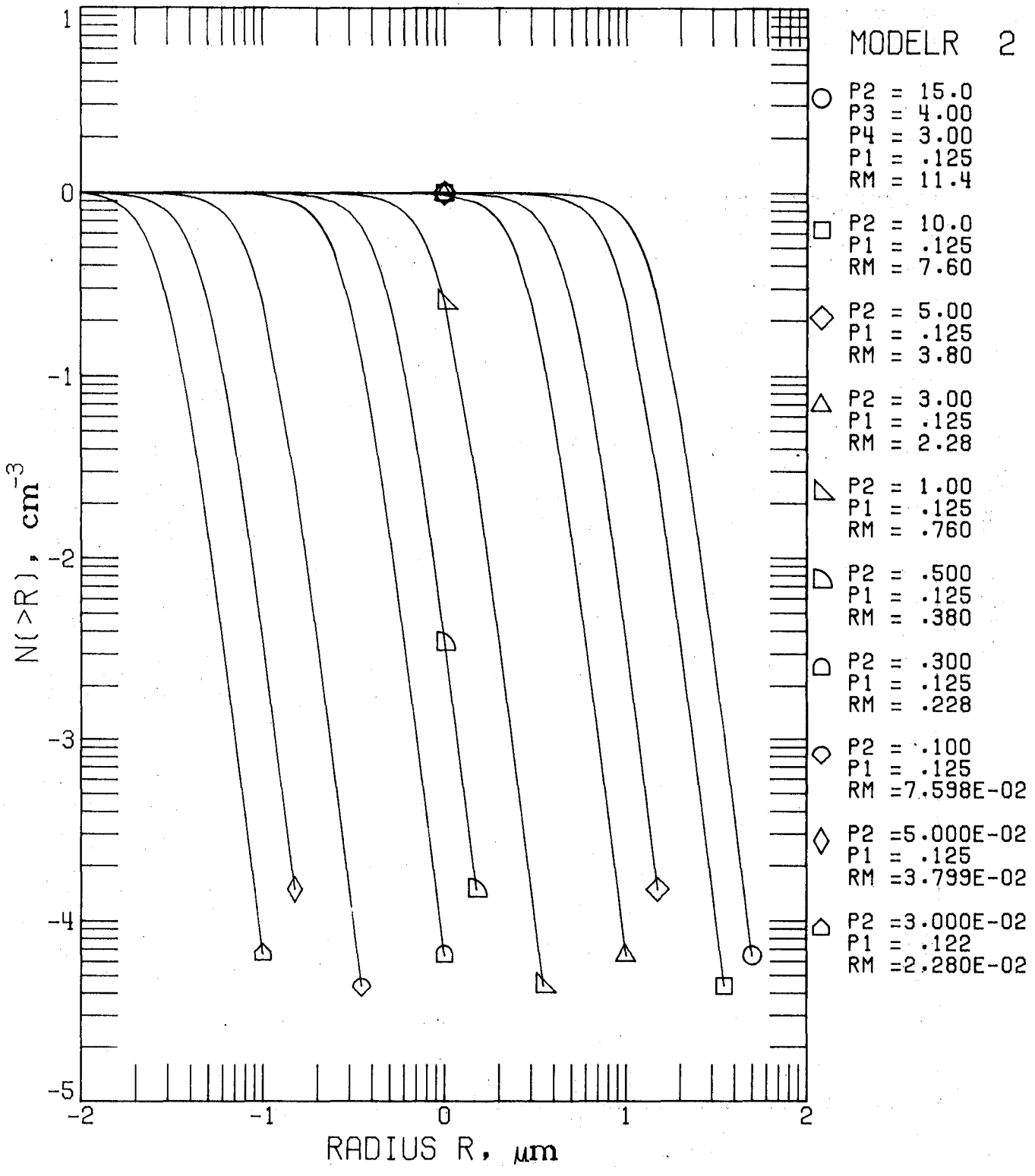

Figure 2C.2. Model 2 for N(>r).
Parameter Set 2.2.

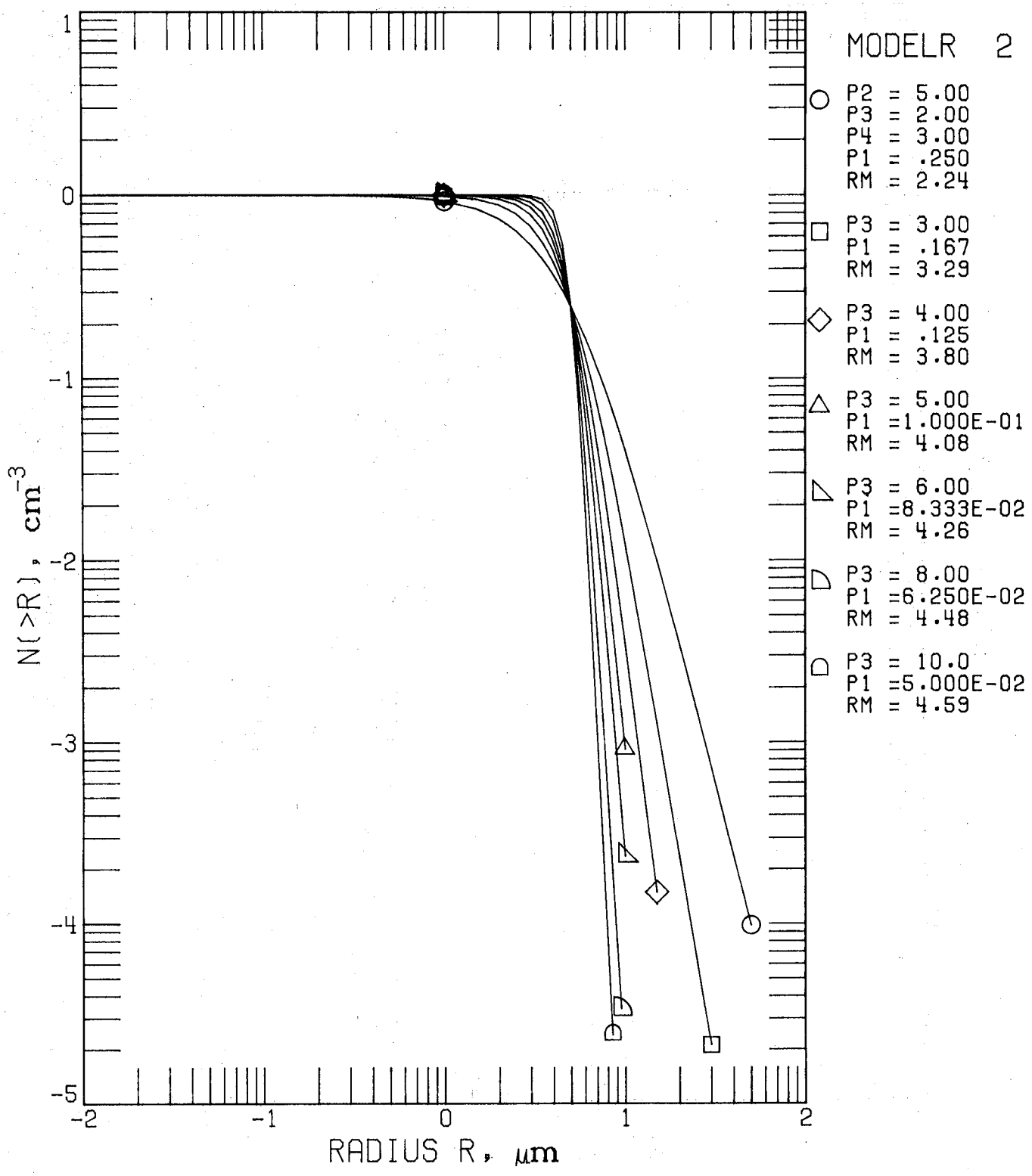

Figure 2C.3. Model 2 for N(>r).
Parameter Set 2.3.

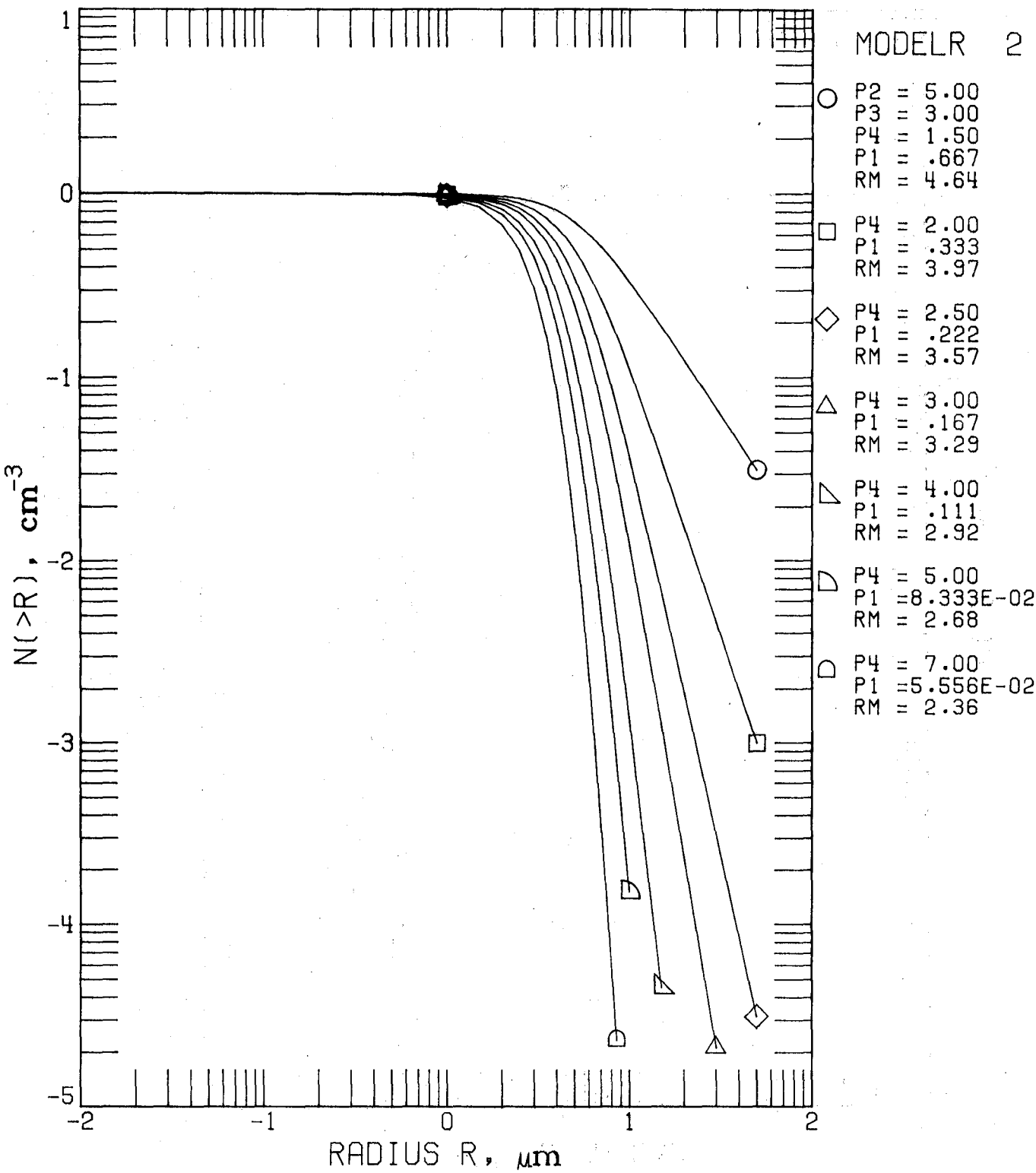

Figure 2C.4. Model 2 for N(>r).
Parameter Set 2.4.

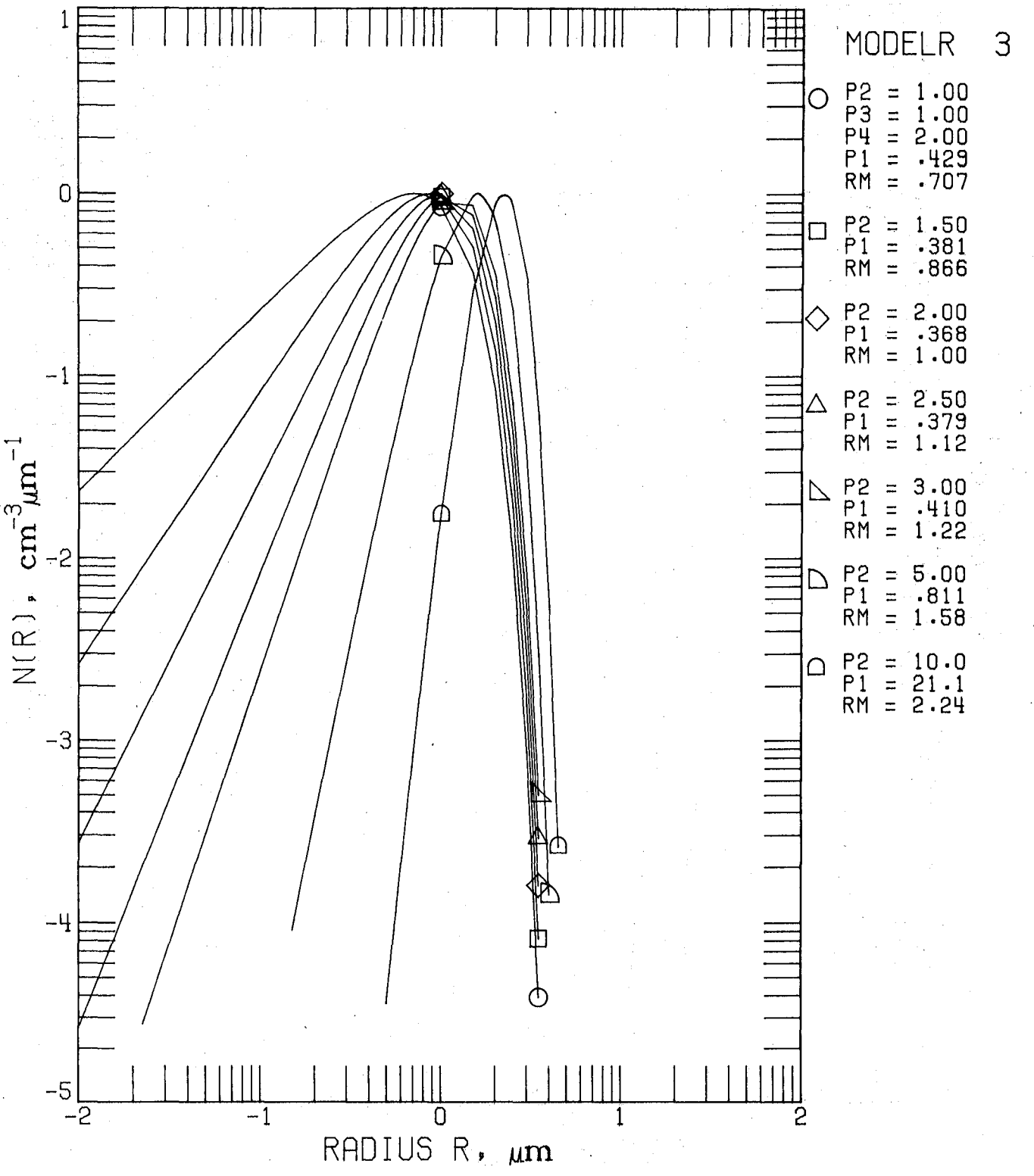

Figure 3A.1. Model 3 (Modified Gamma Distribution) for n(r). Parameter Set 3.1: p_2 variable, p_3 = 1.0, p_4 = 2.0.

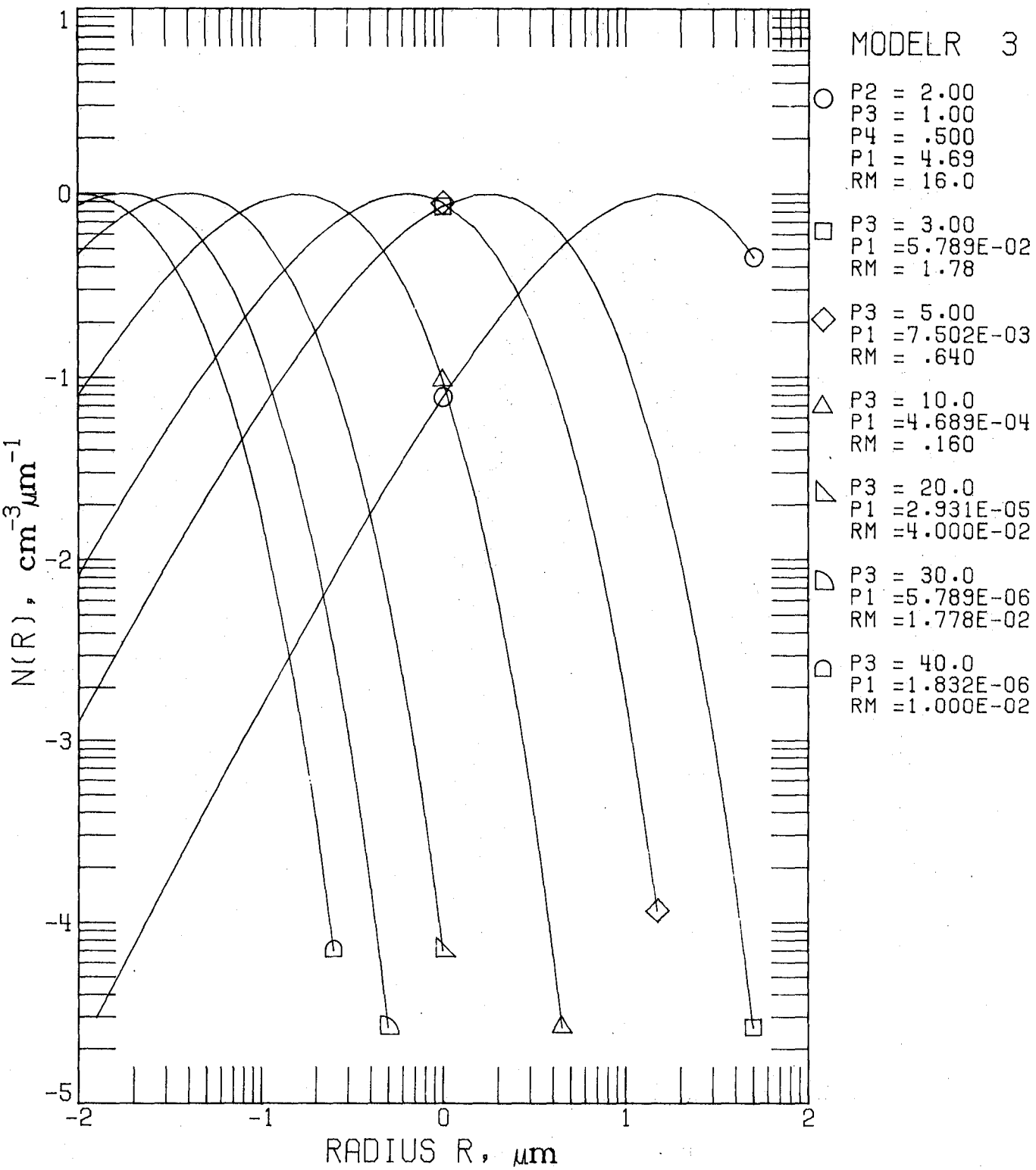

Figure 3A.2. Model 3 for n(r).
Parameter Set 3.2: p_3 variable,
p_2 = 2.0, p_4 = 0.5.

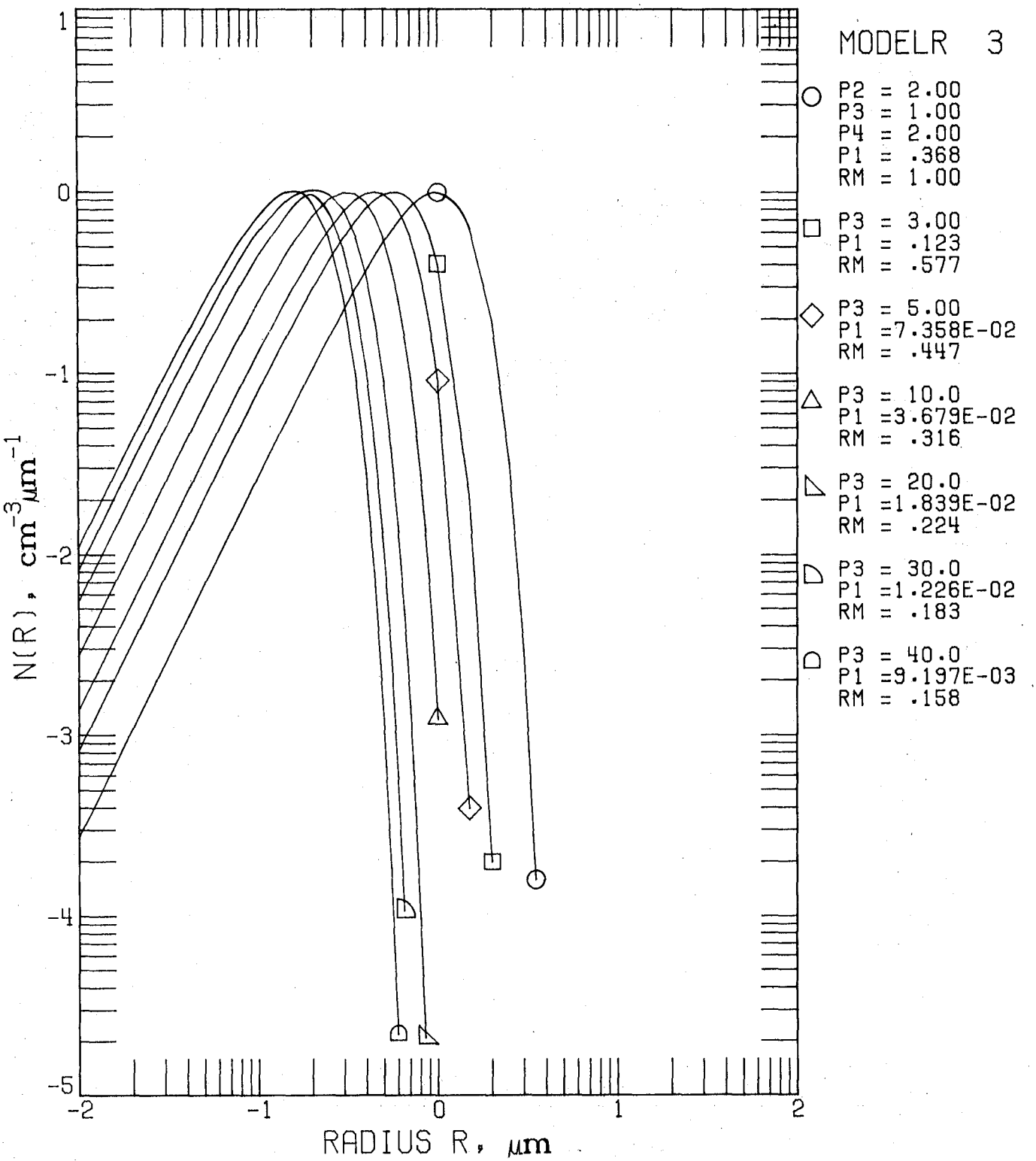

Figure 3A.3. Model 3 for n(r).
Parameter Set 3.3: p_3 variable,
$p_2 = 2.0$, $p_4 = 2.0$.

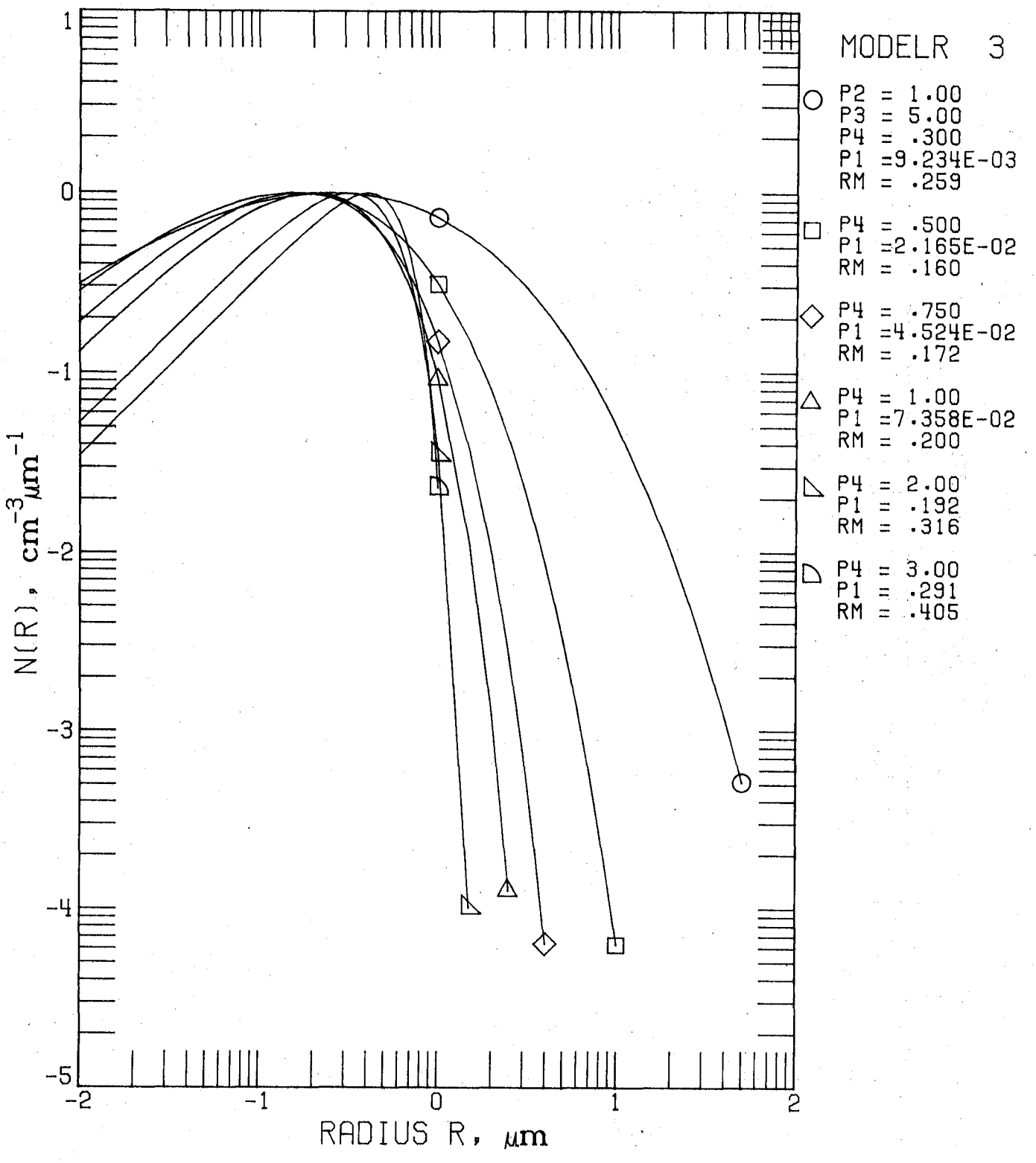

Figure 3A.4. Model 3 for n(r).
Parameter Set 3.4: p_4 variable,
$p_2 = 1.0$, $p_3 = 5.0$.

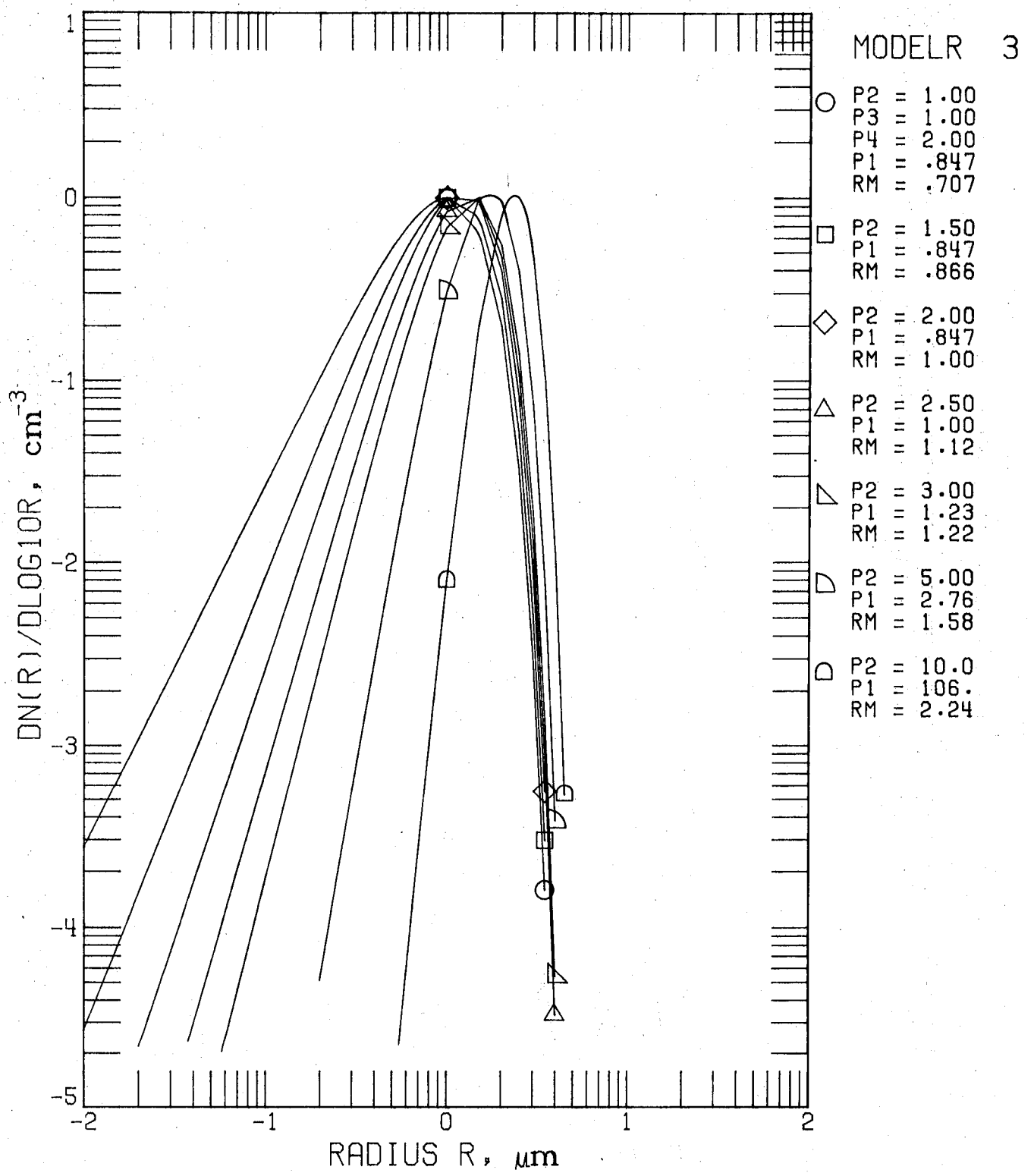

Figure 3B.1. Model 3 for $n_L(r)$.
Parameter Set 3.1.

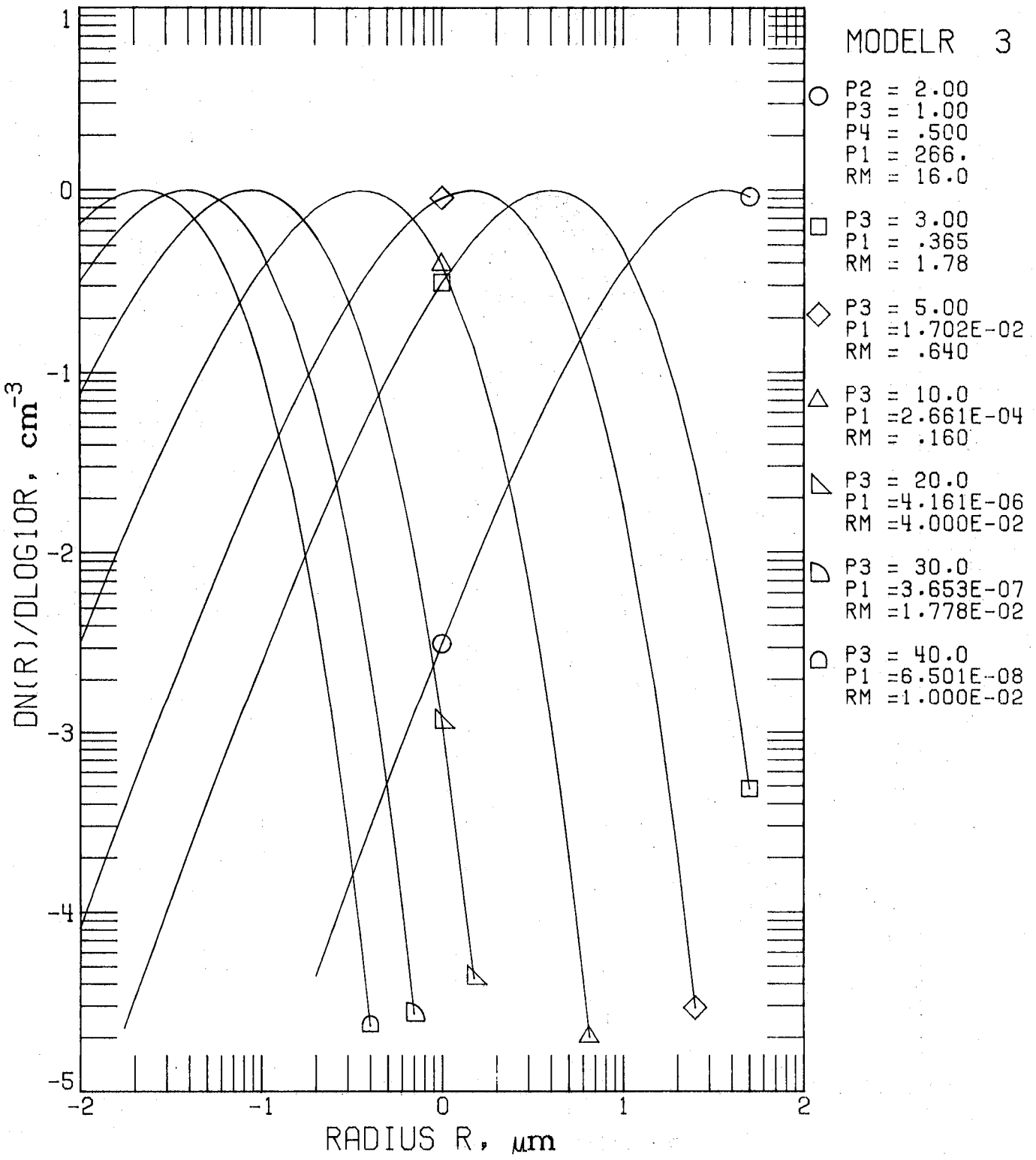

Figure 3B.2. Model 3 for $n_L(r)$.
Parameter Set 3.2.

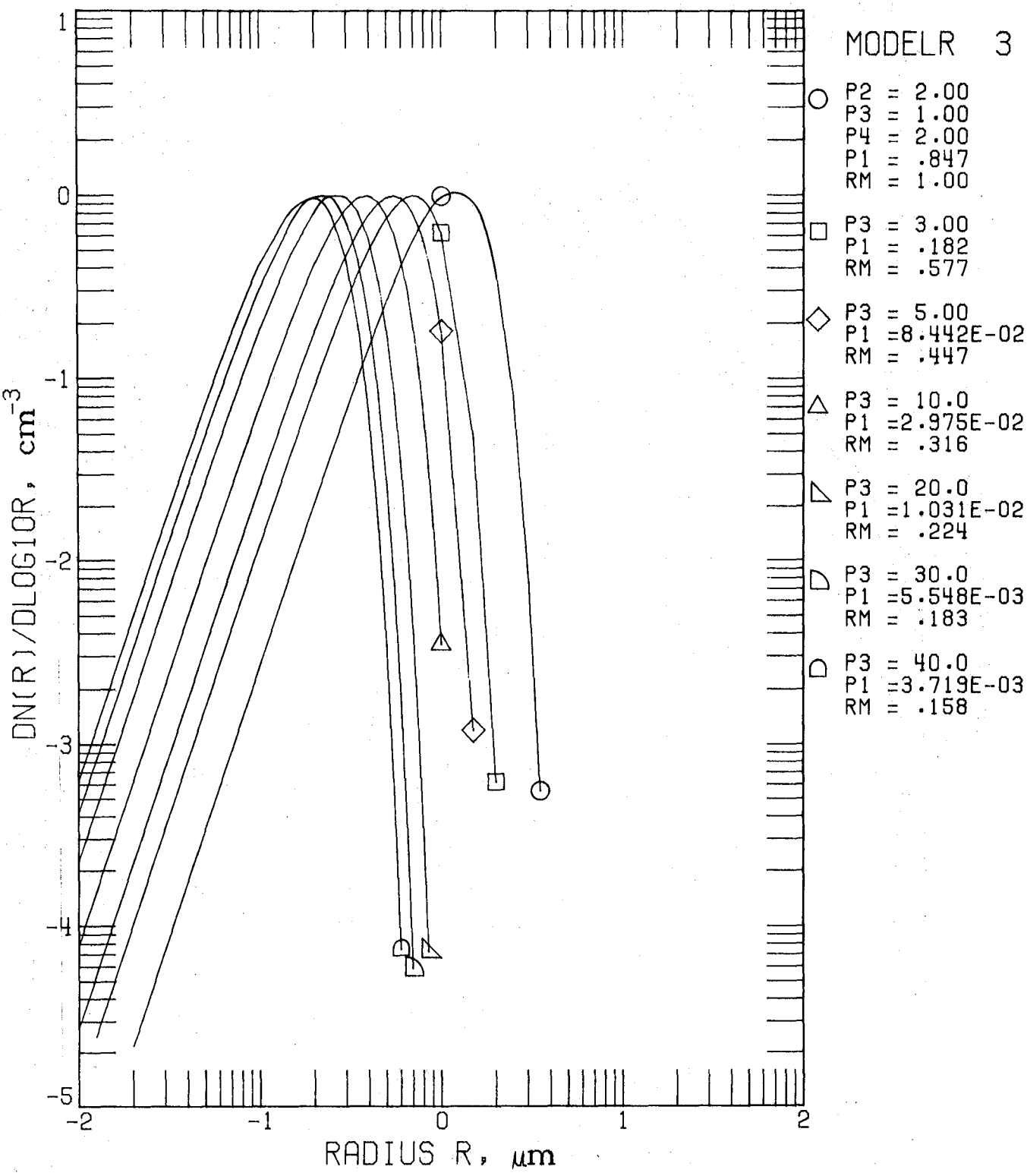

Figure 3B.3. Model 3 for $n_L(r)$.
Parameter Set 3.3.

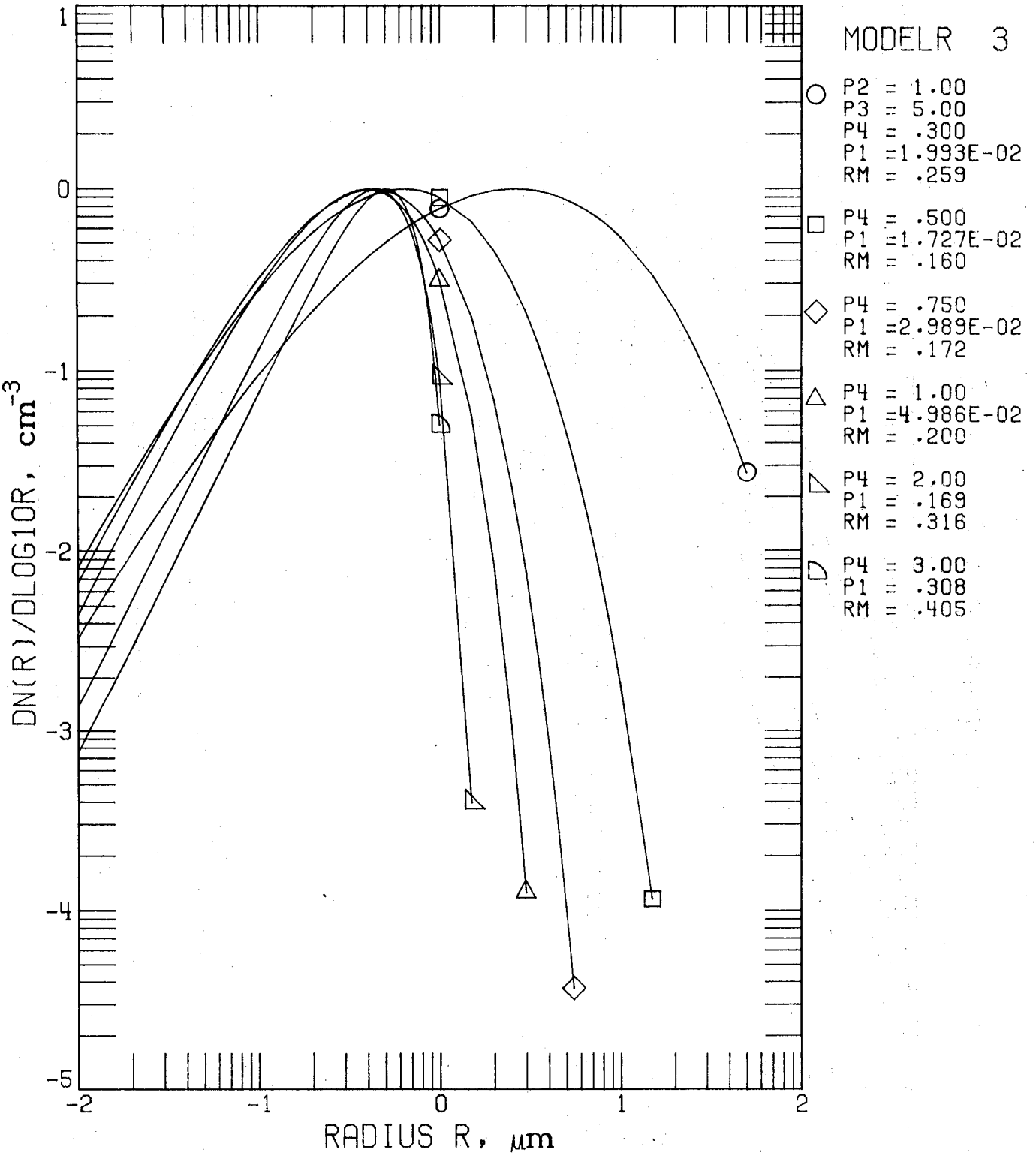

Figure 3B.4. Model 3 for $n_L(r)$.
Parameter Set 3.4.

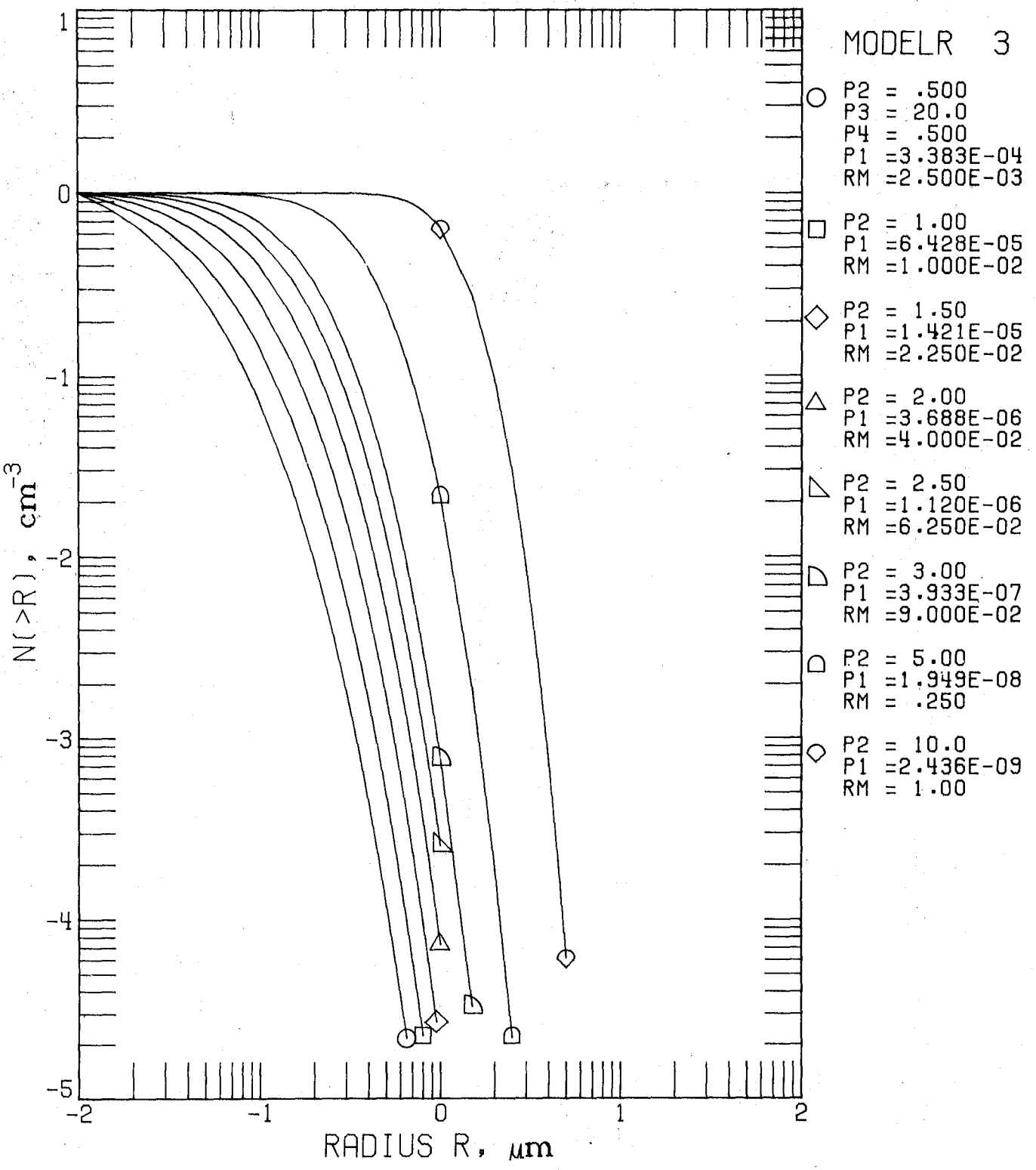

Figure 3C.1. Model 3 for N(>r).
Parameter Set 3.5: p_2 variable,
p_3 = 20.0, p_4 = 0.5.

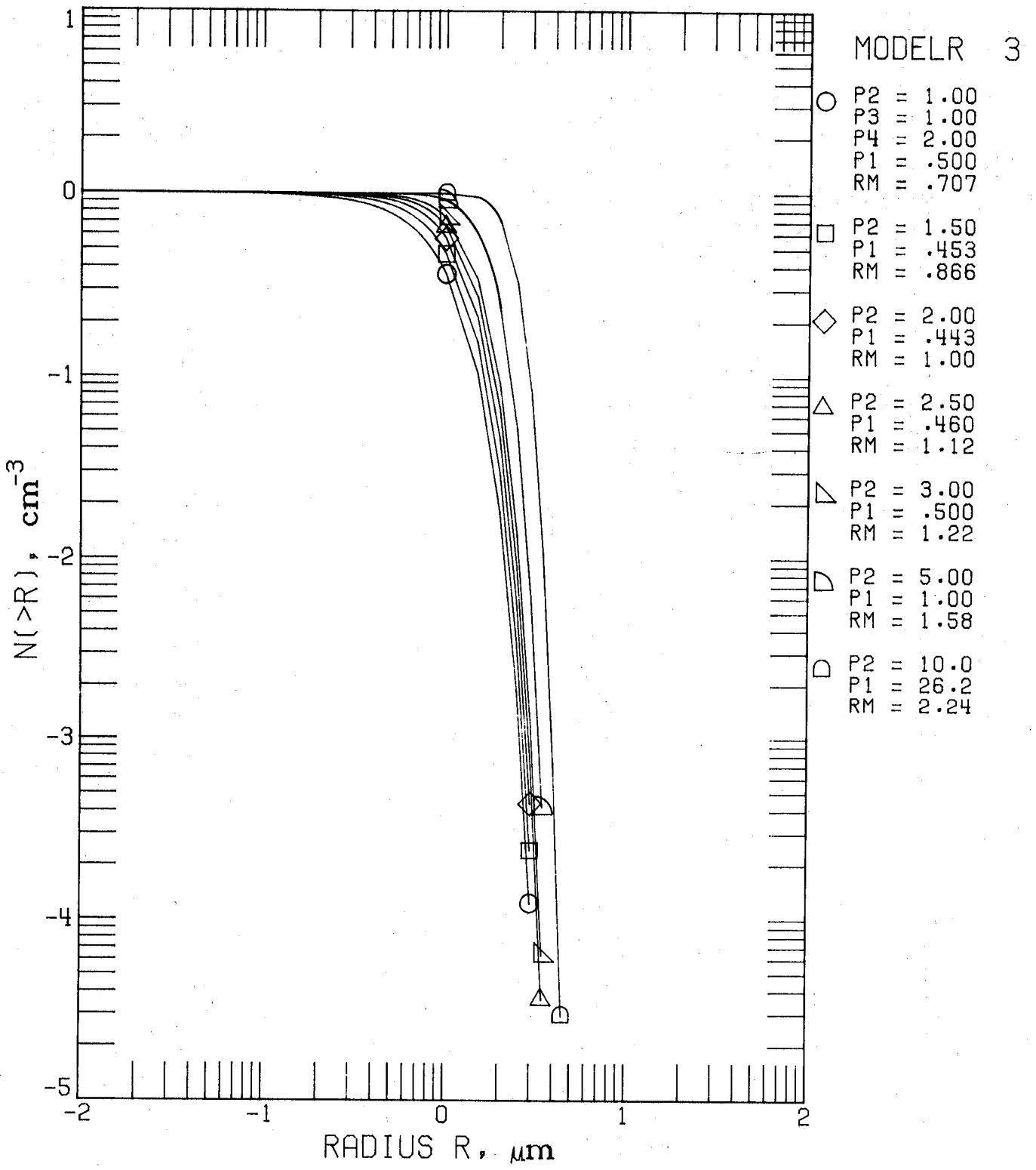

Figure 3C.2. Model 3 for N(>r).
Parameter Set 3.1.

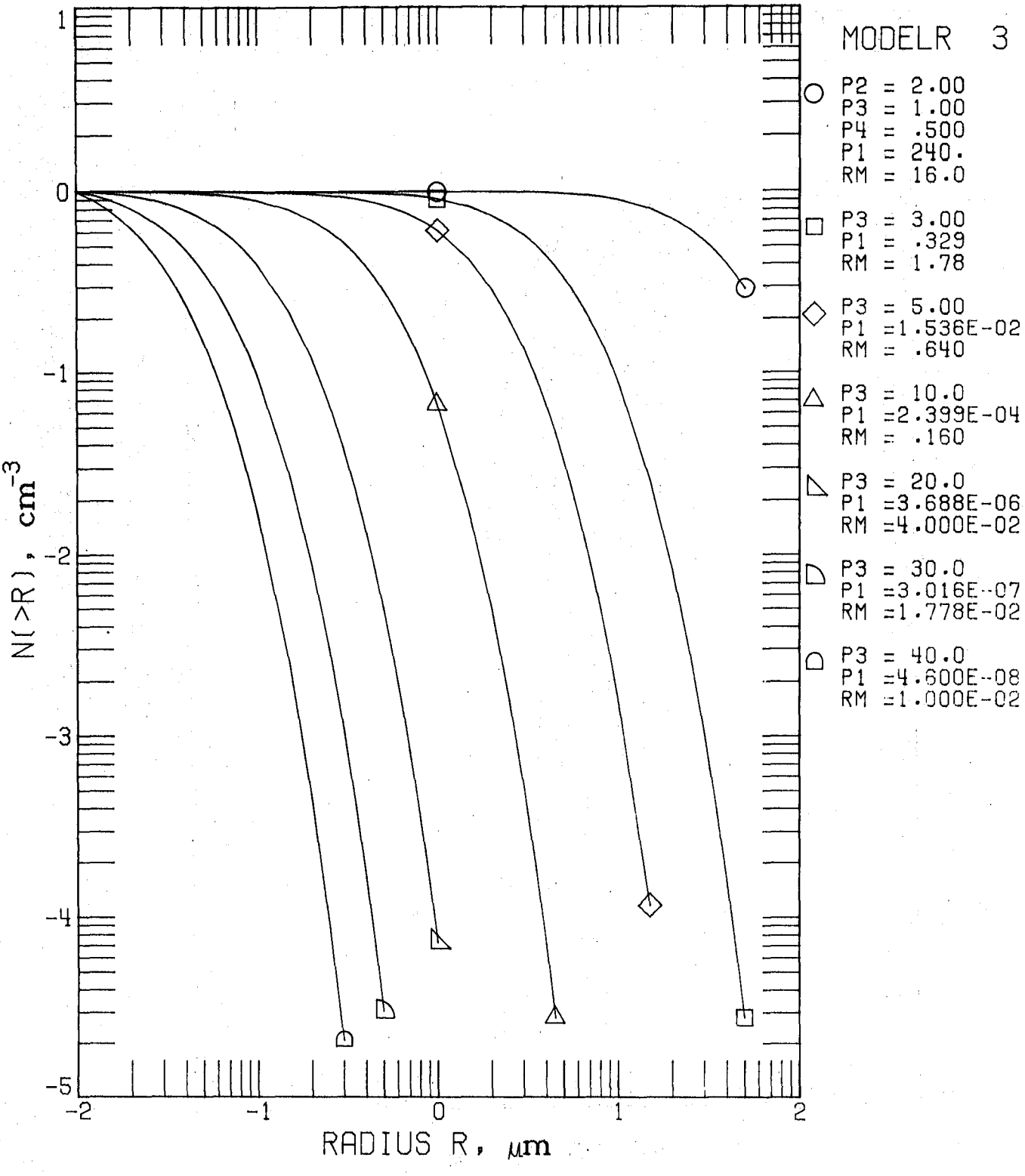

Figure 3C.3. Model 3 for N(>r).
Parameter Set 3.2.

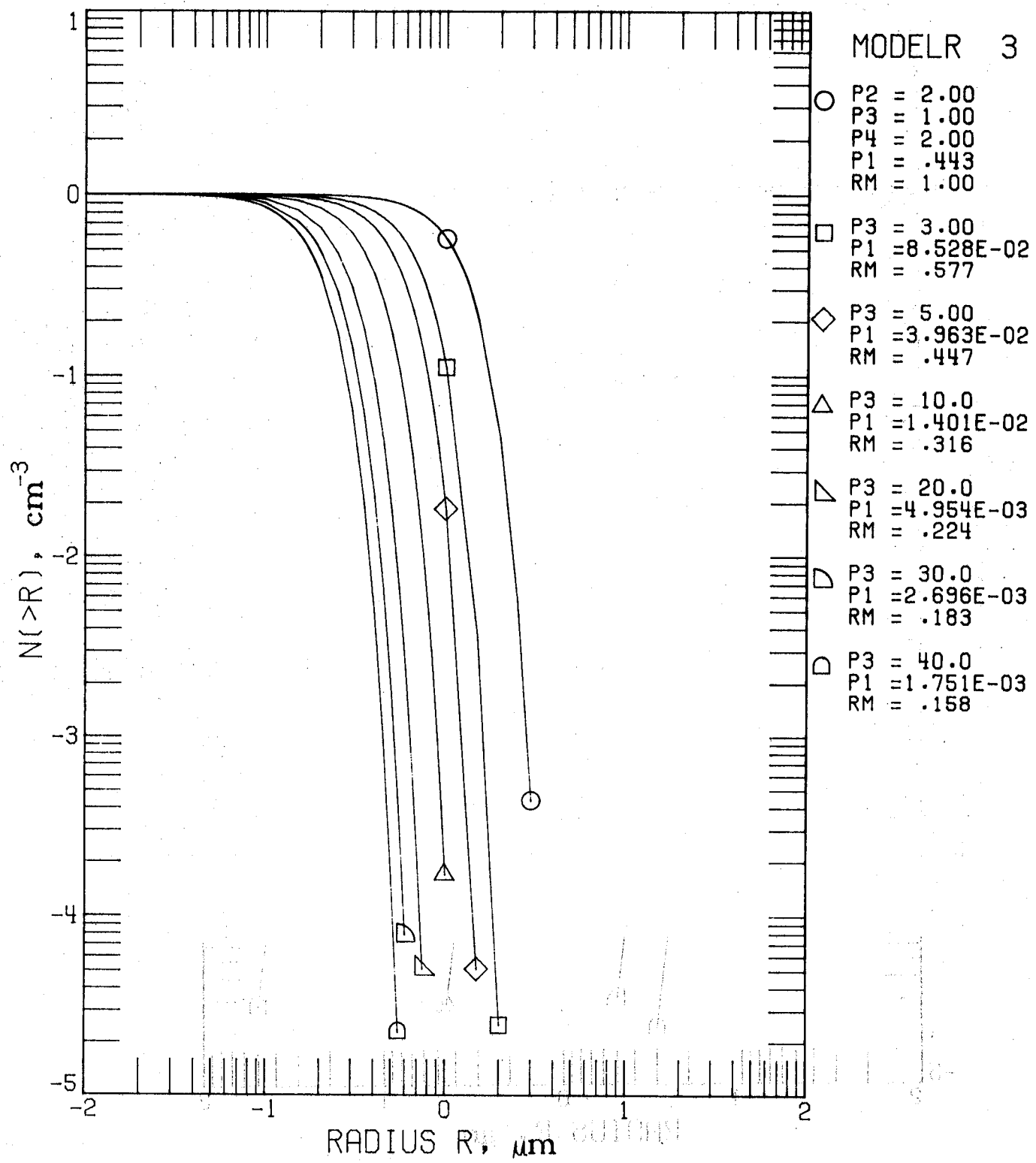

Figure 3C.4. Model 3 for N(>r).
Parameter Set 3.3.

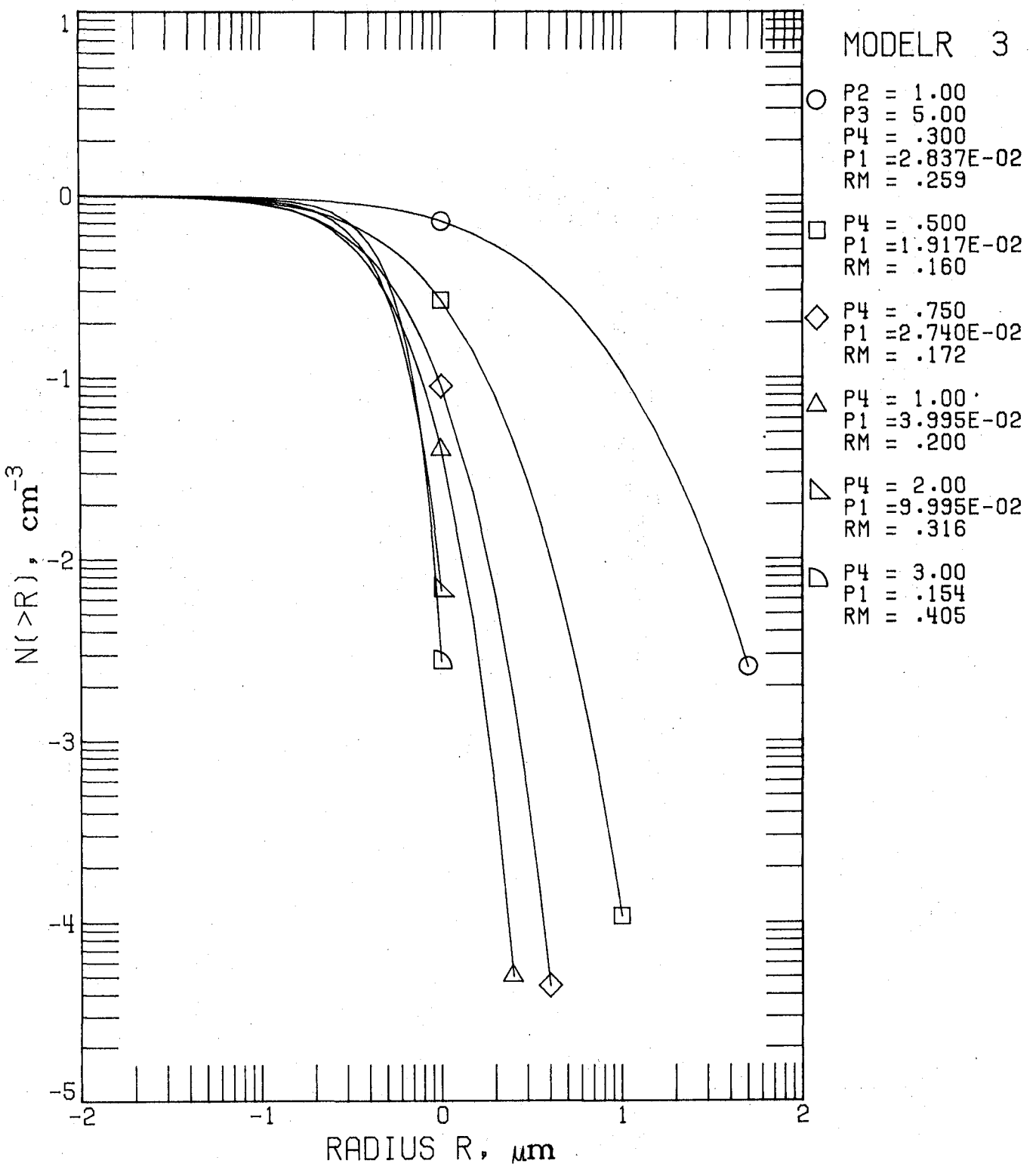

Figure 3C.5. Model 3 for N(>r).
Parameter Set 3.4.

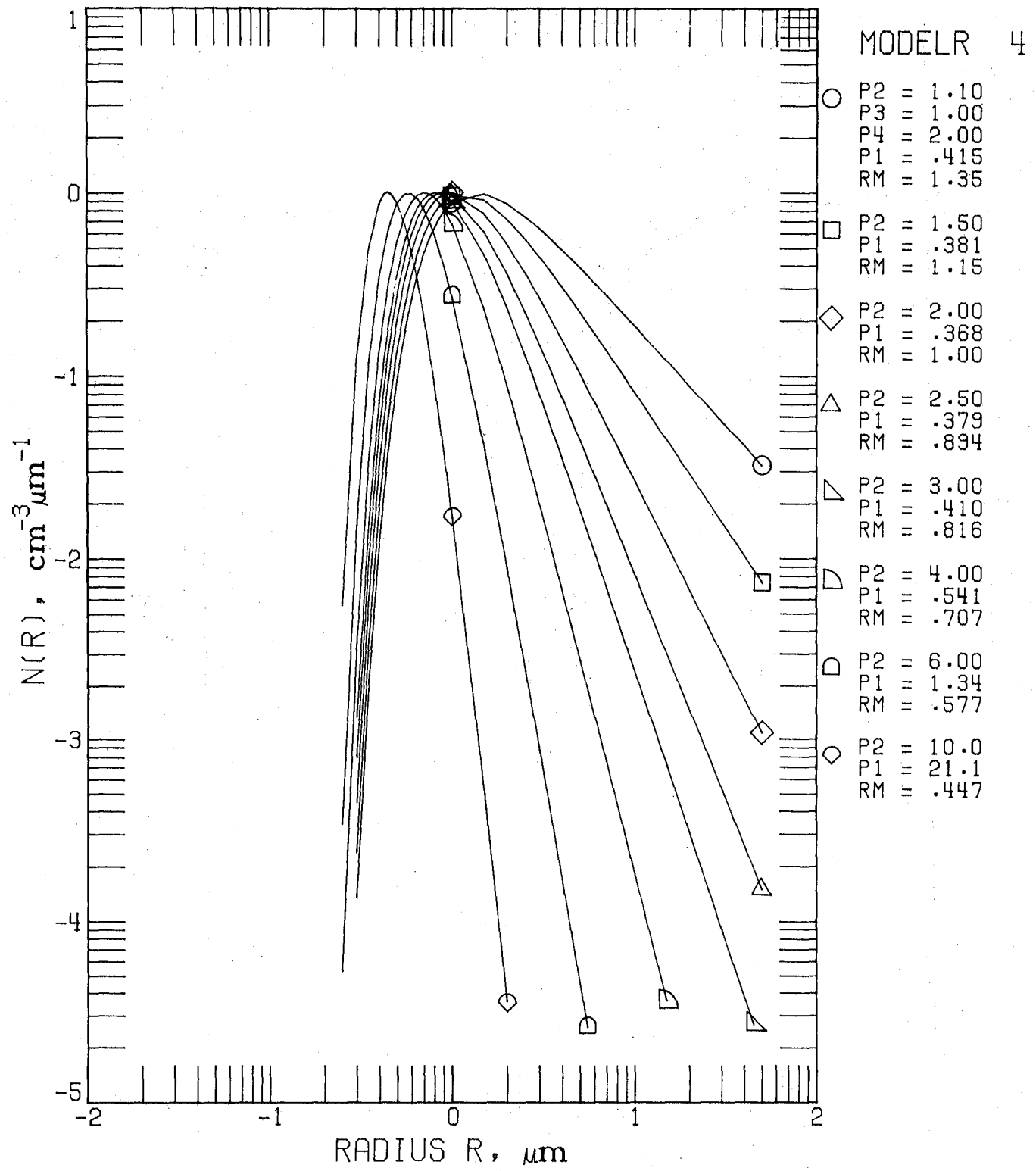

Figure 4A.1. Model 4 (Inverse Modified Gamma Distribution) for n(r). Parameter Set 4.1: p_2 variable, p_3 = 1.0, p_4 = 2.0.

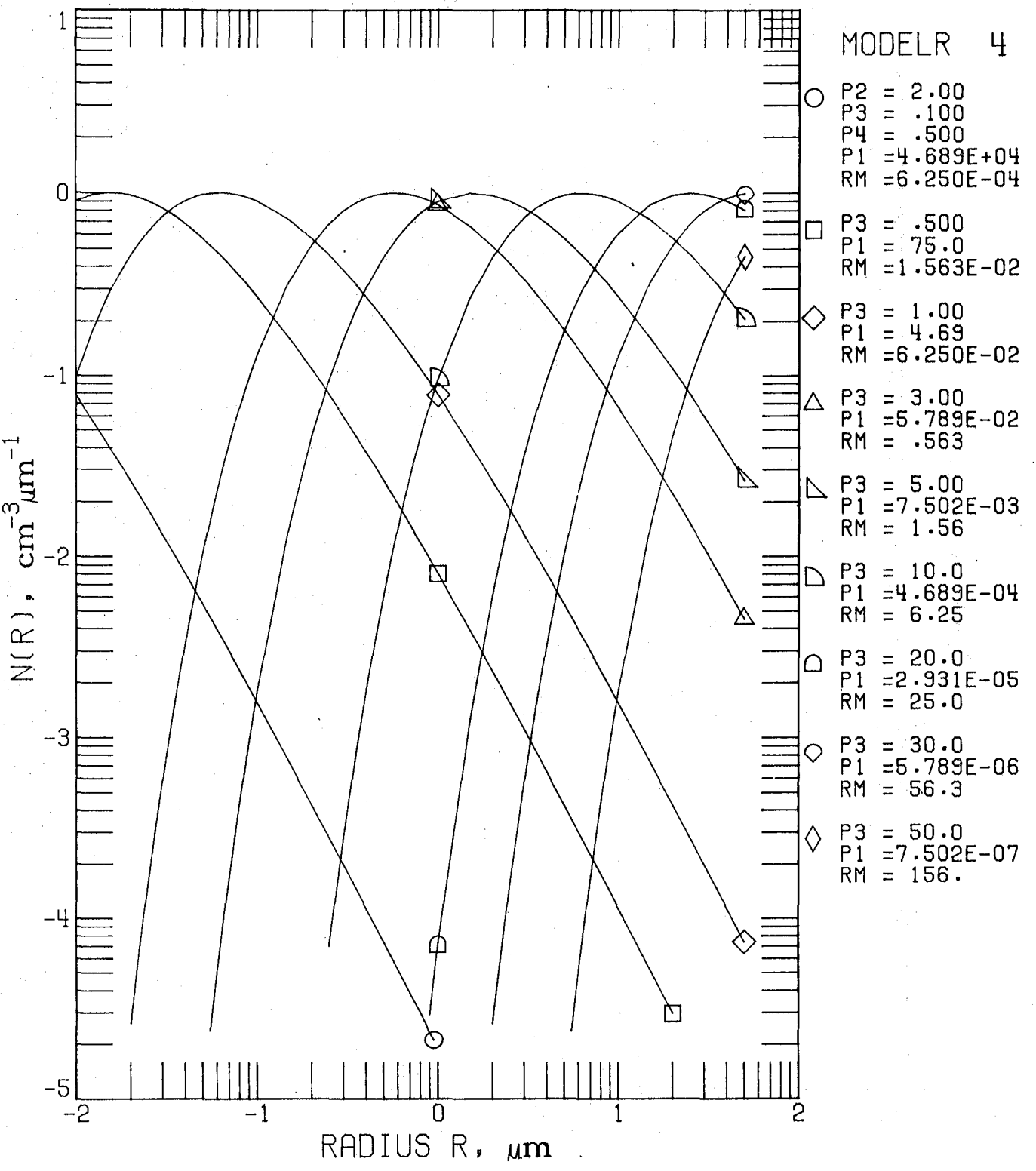

Figure 4A.2. Model 4 for n(r).
Parameter Set 4.2: p_3 variable,
$p_2 = 2.0$, $p_4 = 0.5$.

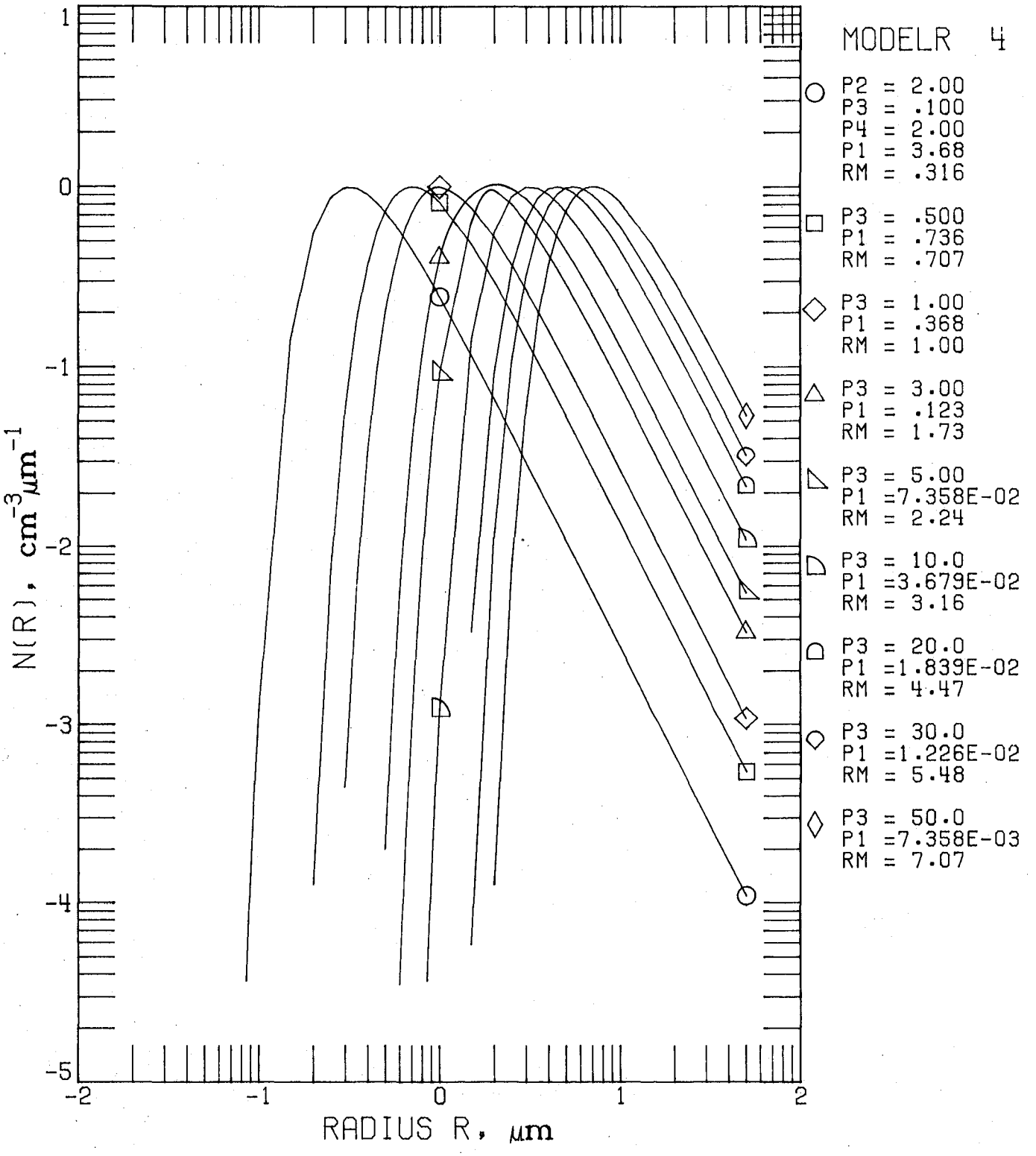

Figure 4A. 3. Model 4 for n(r).
Parameter Set 4.3: p_3 variable,
p_2 = 2.0, p_4 = 2.0.

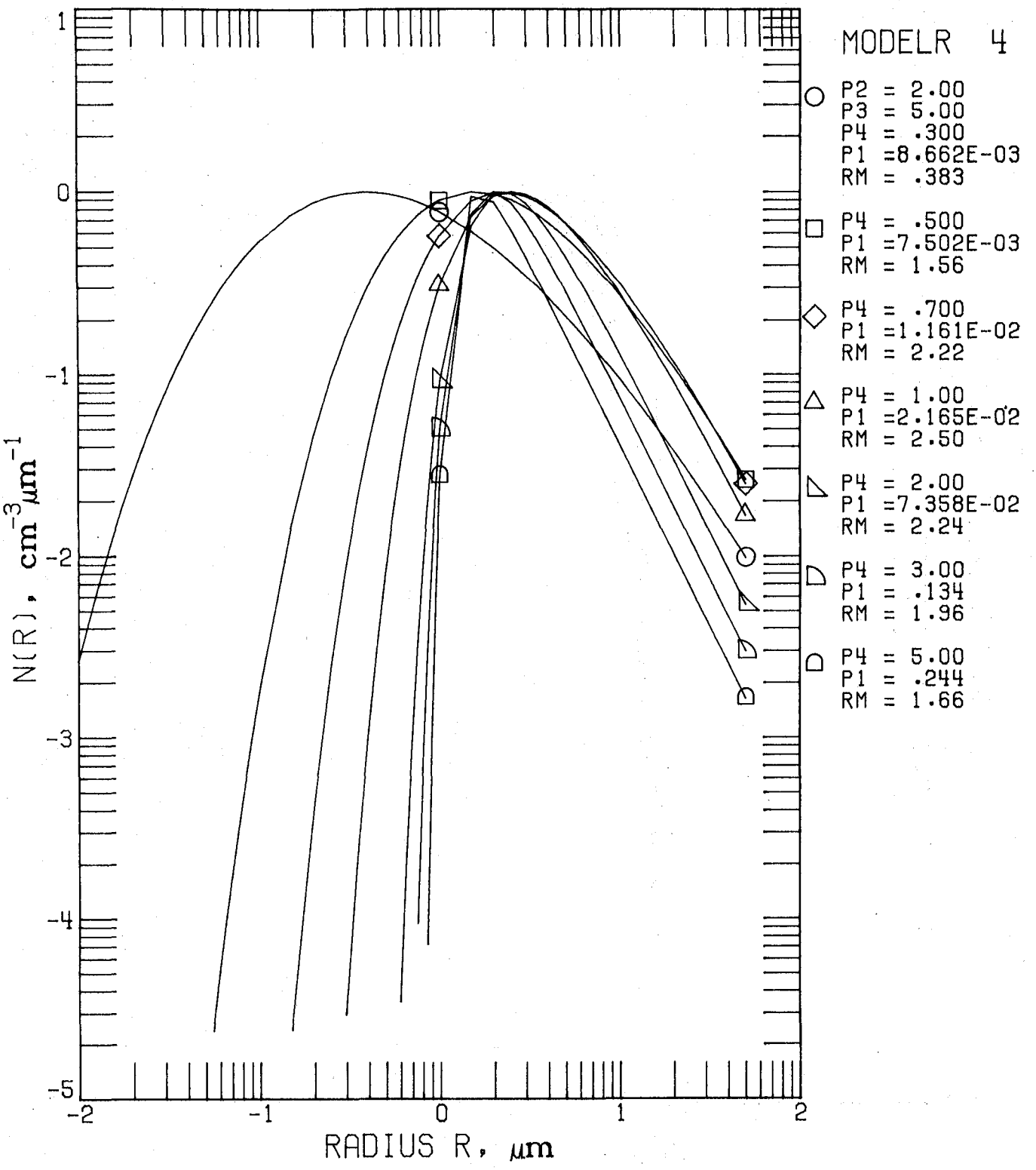

Figure 4A.4. Model 4 for n(r).
Parameter Set 4.4: p_4 variable,
p_2 = 2.0, p_3 = 5.0.

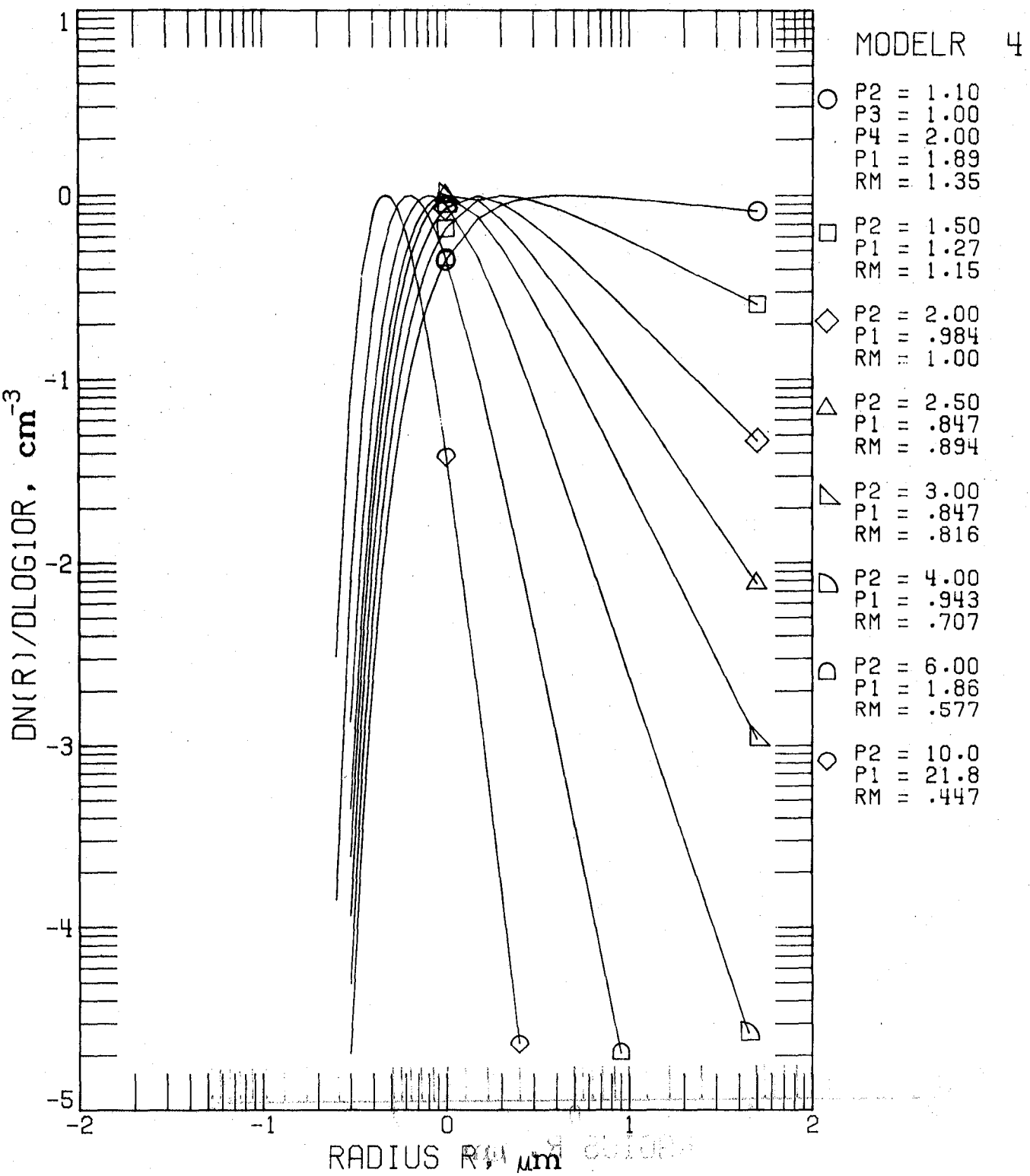

Figure 4B.1. Model 4 for $n_L(r)$. Parameter Set 4.1.

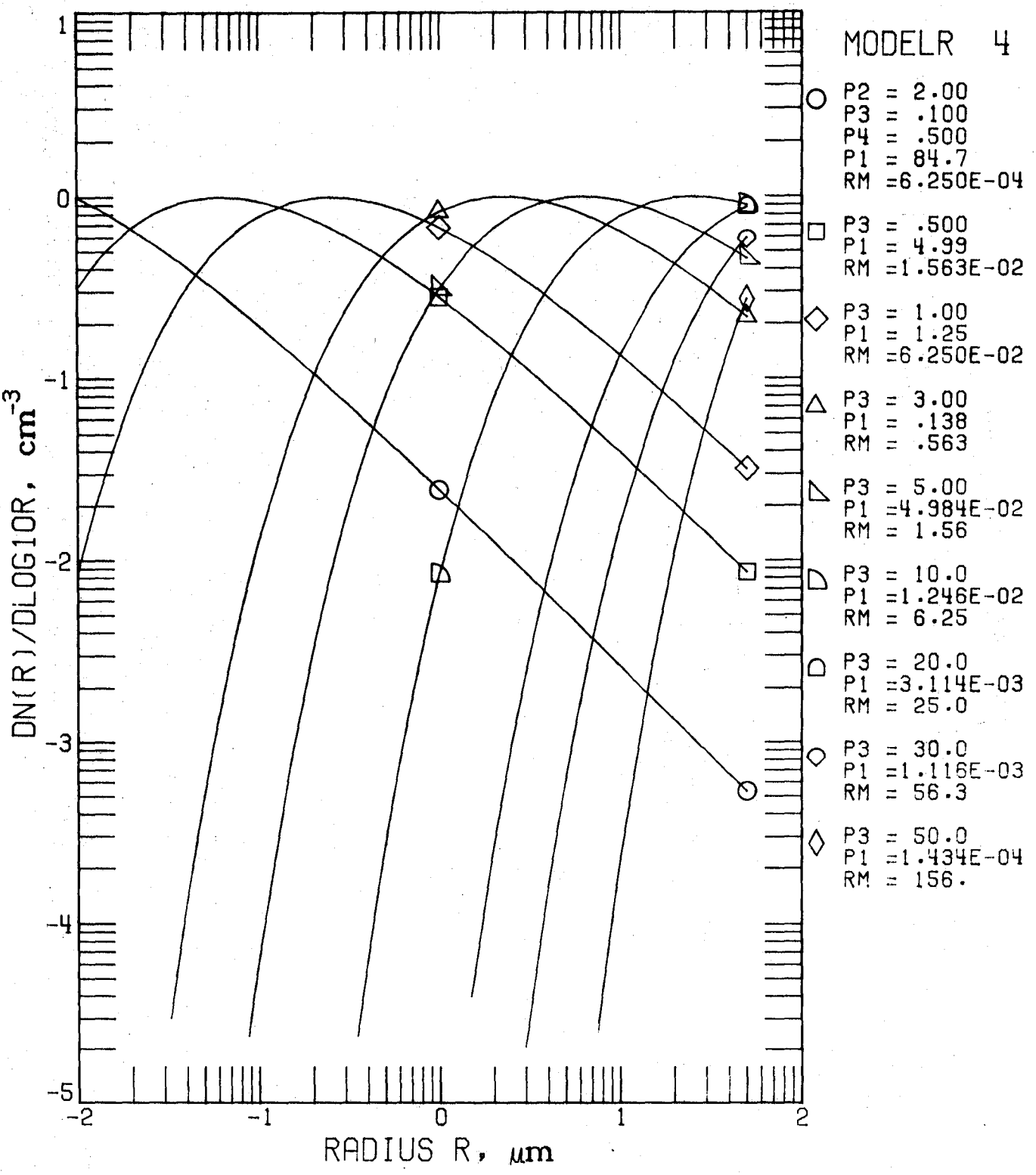

Figure 4B.2. Model 4 for $n_L(r)$.
Parameter Set 4.2.

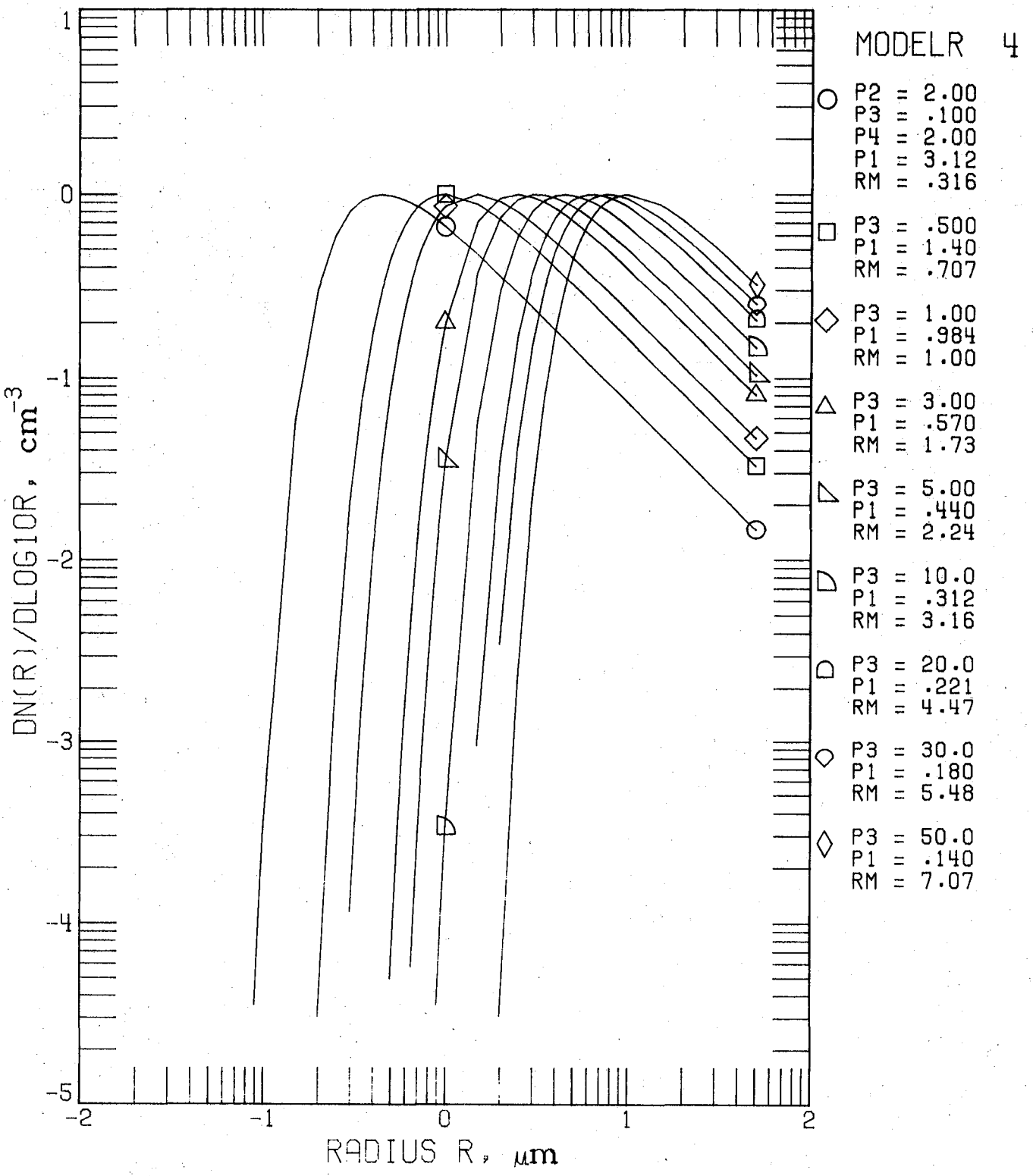

Figure 4B.3. Model 4 for $n_L(r)$
Parameter Set 4.3.

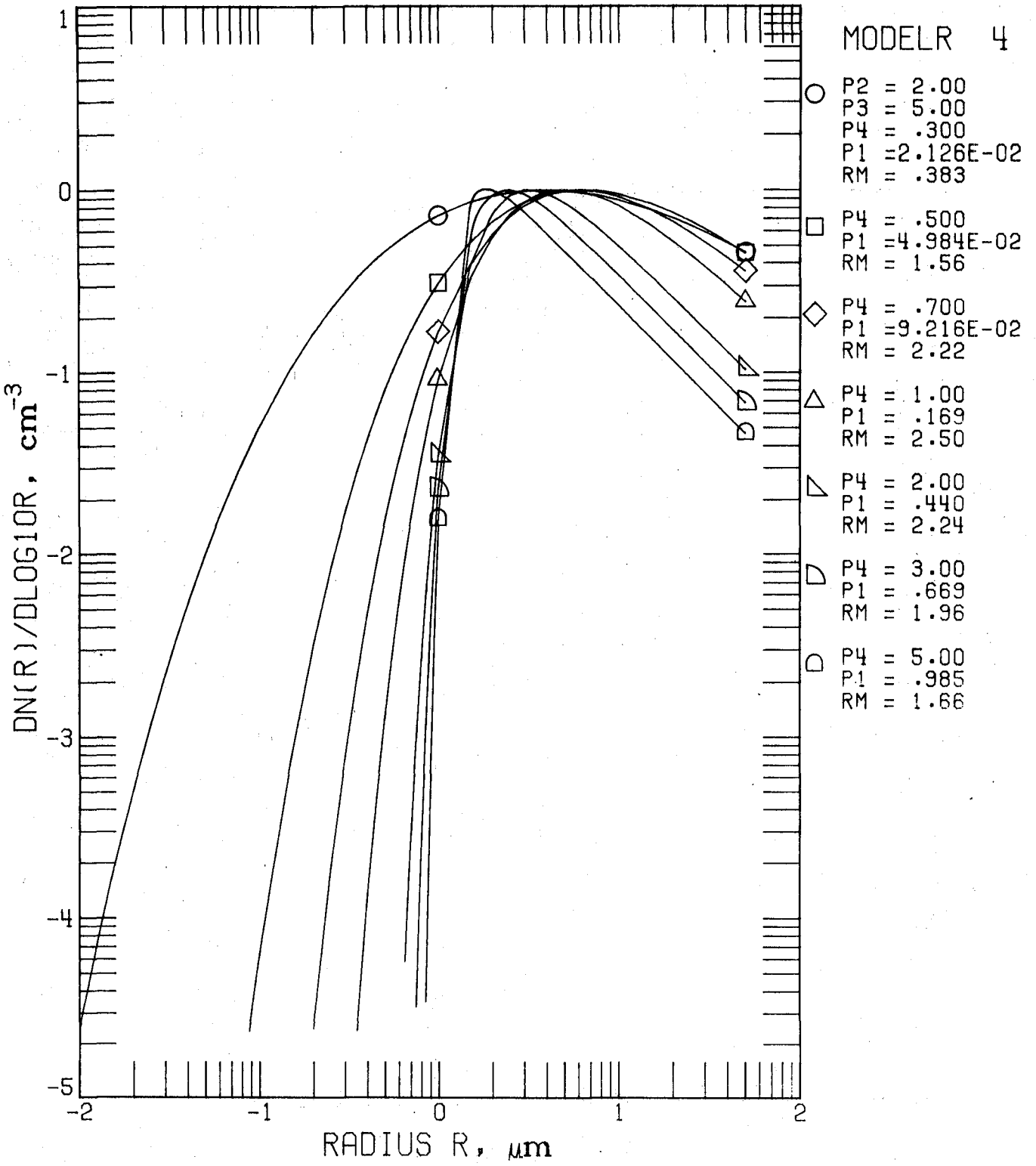

Figure 4B.4. Model 4 for $n_L(r)$.
Parameter Set 4.4.

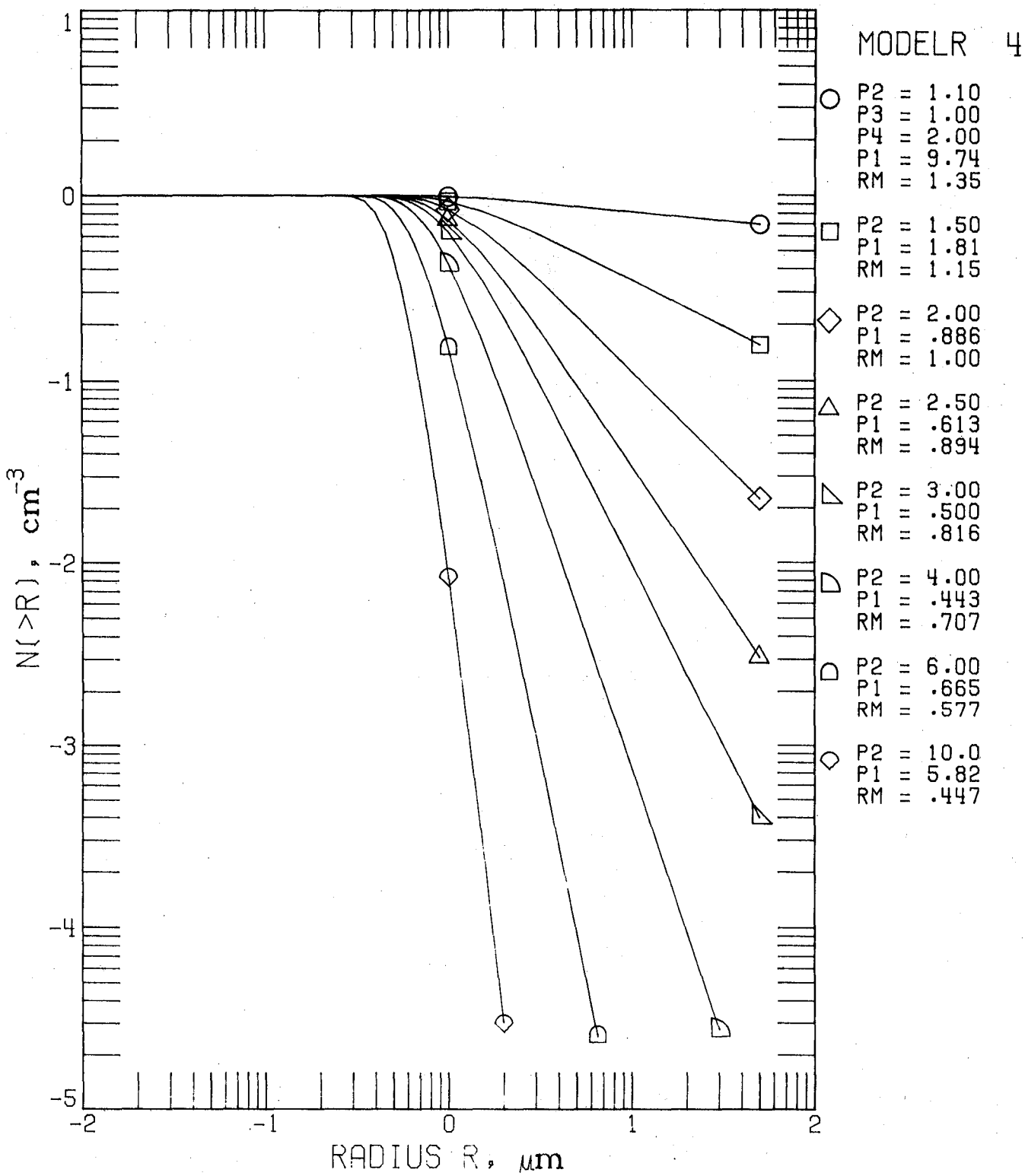

Figure 4C.1. Model 4 for N(>r).
Parameter Set 4.1.

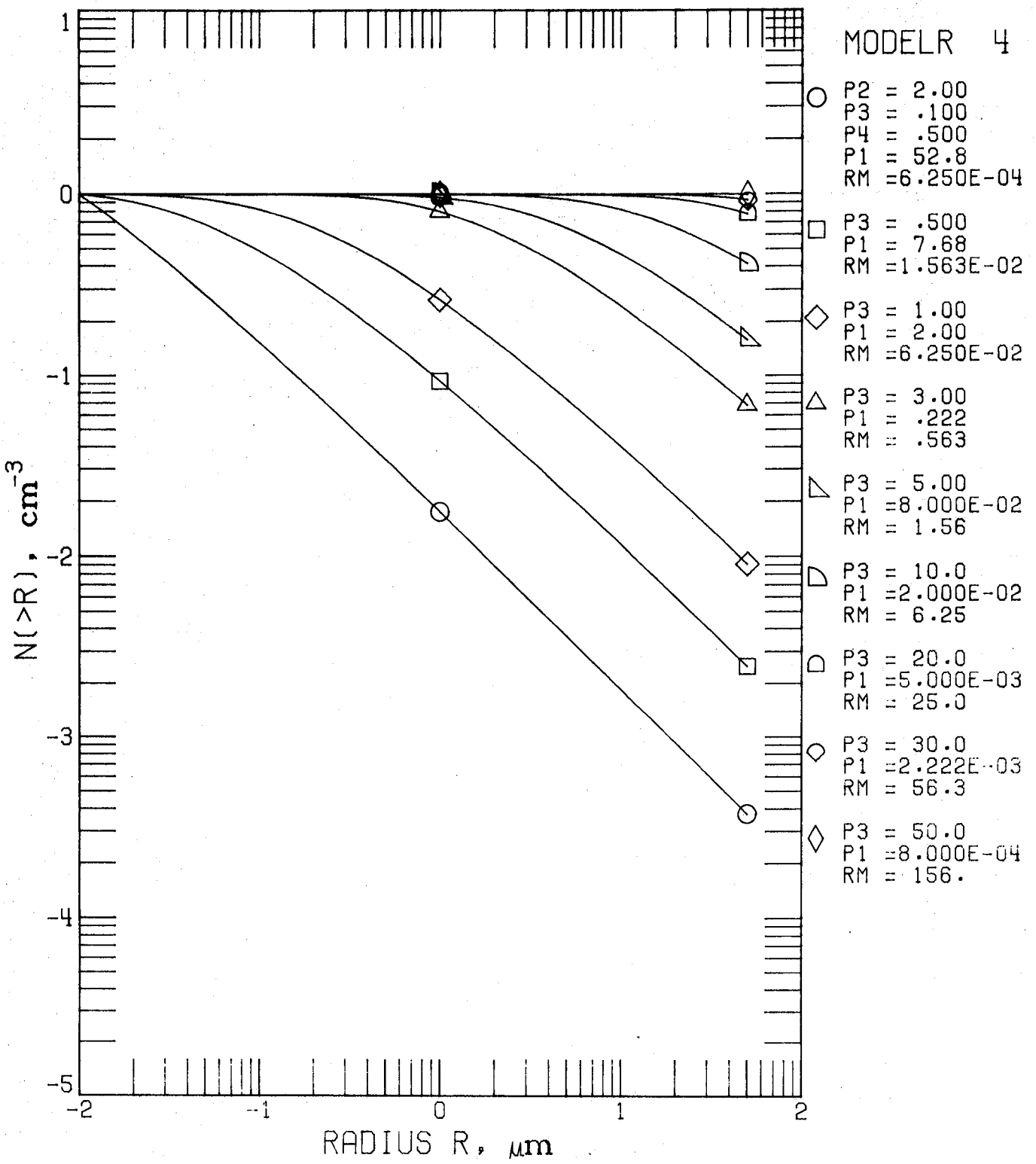

Figure 4C.2. Model 4 for N(>r).
Parameter Set 4.2.

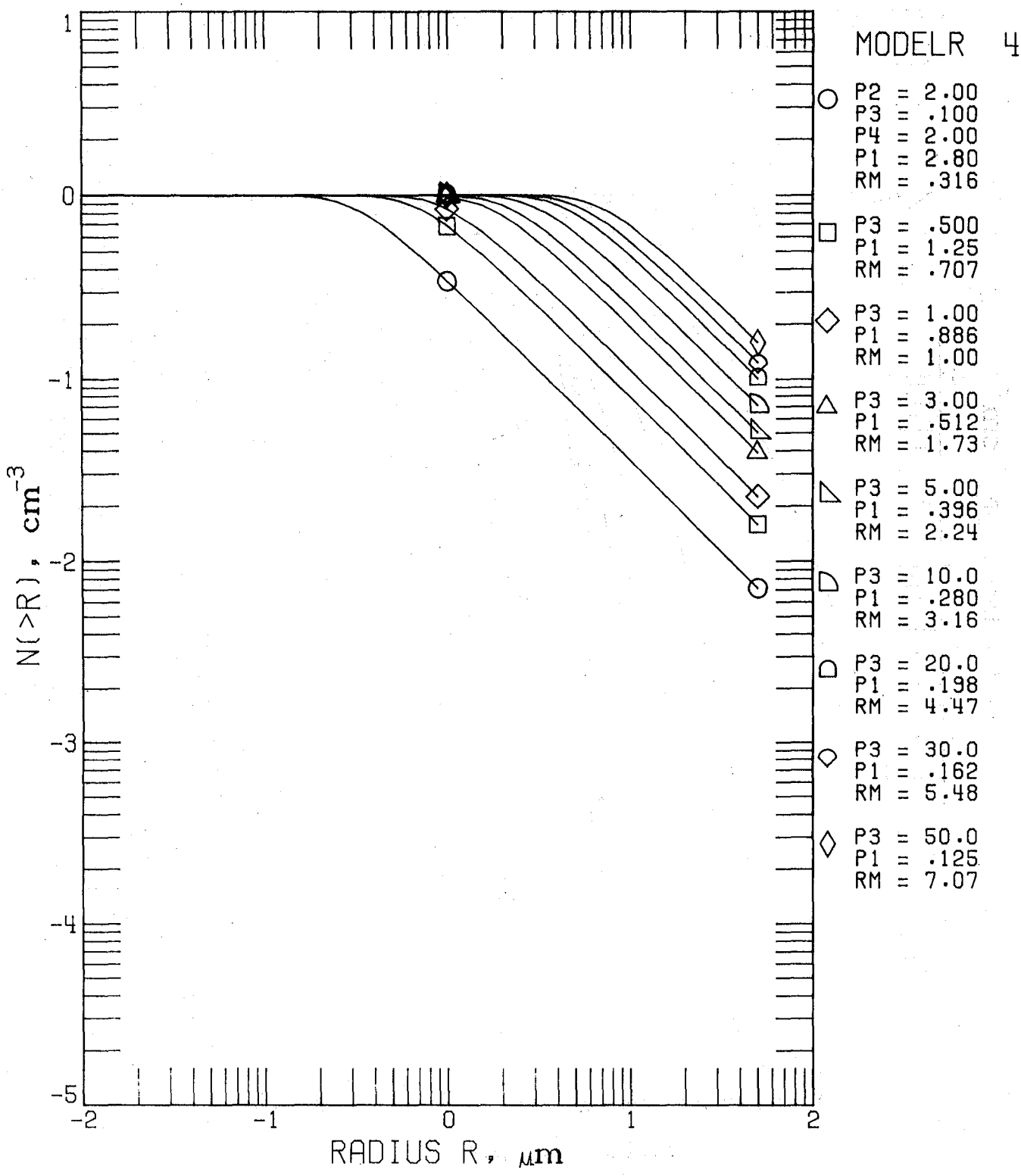

Figure 4C.3. Model 4 for N(>r).
Parameter Set 4.3.

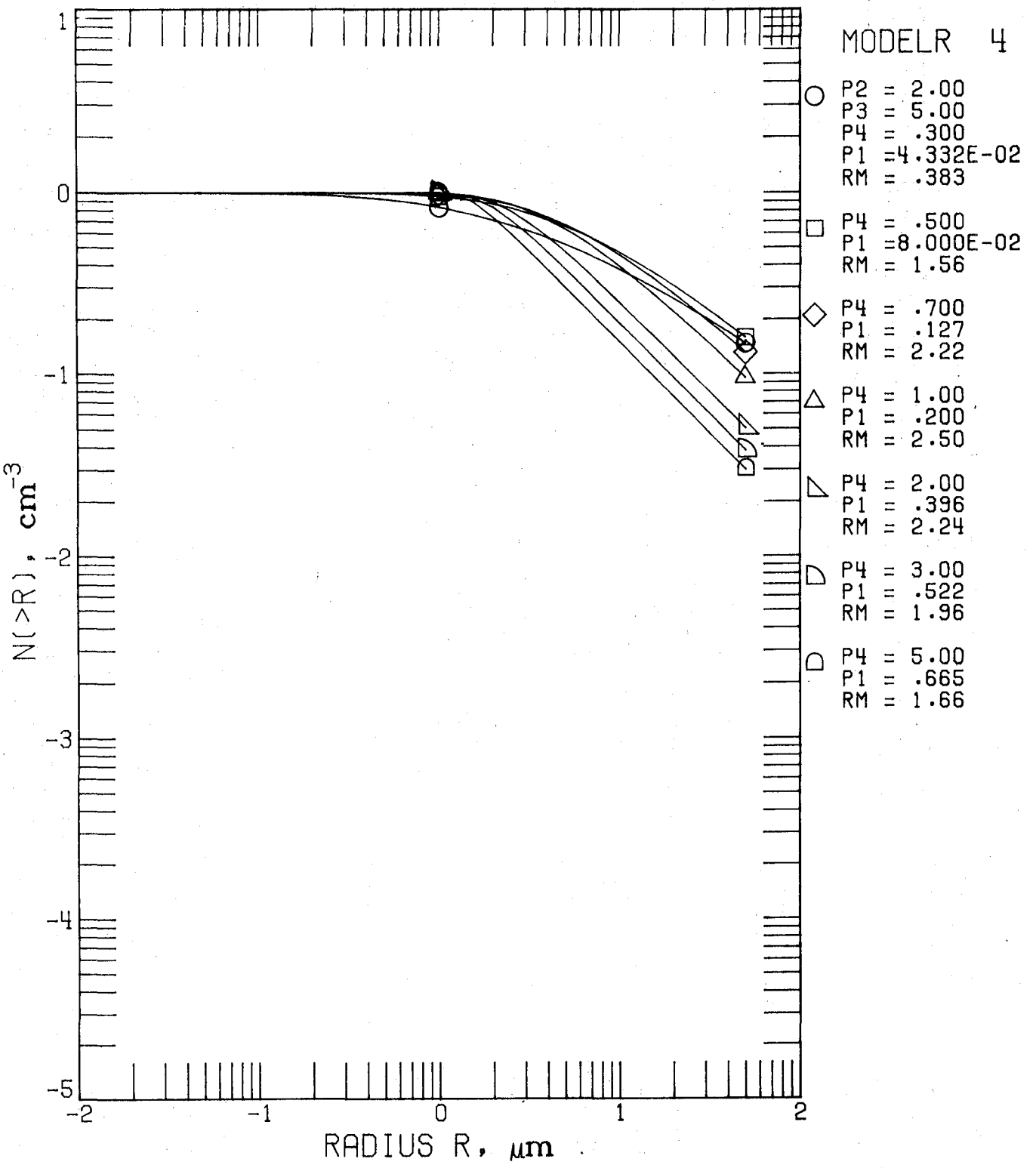

Figure 4C.4. Model 4 for N(>r).

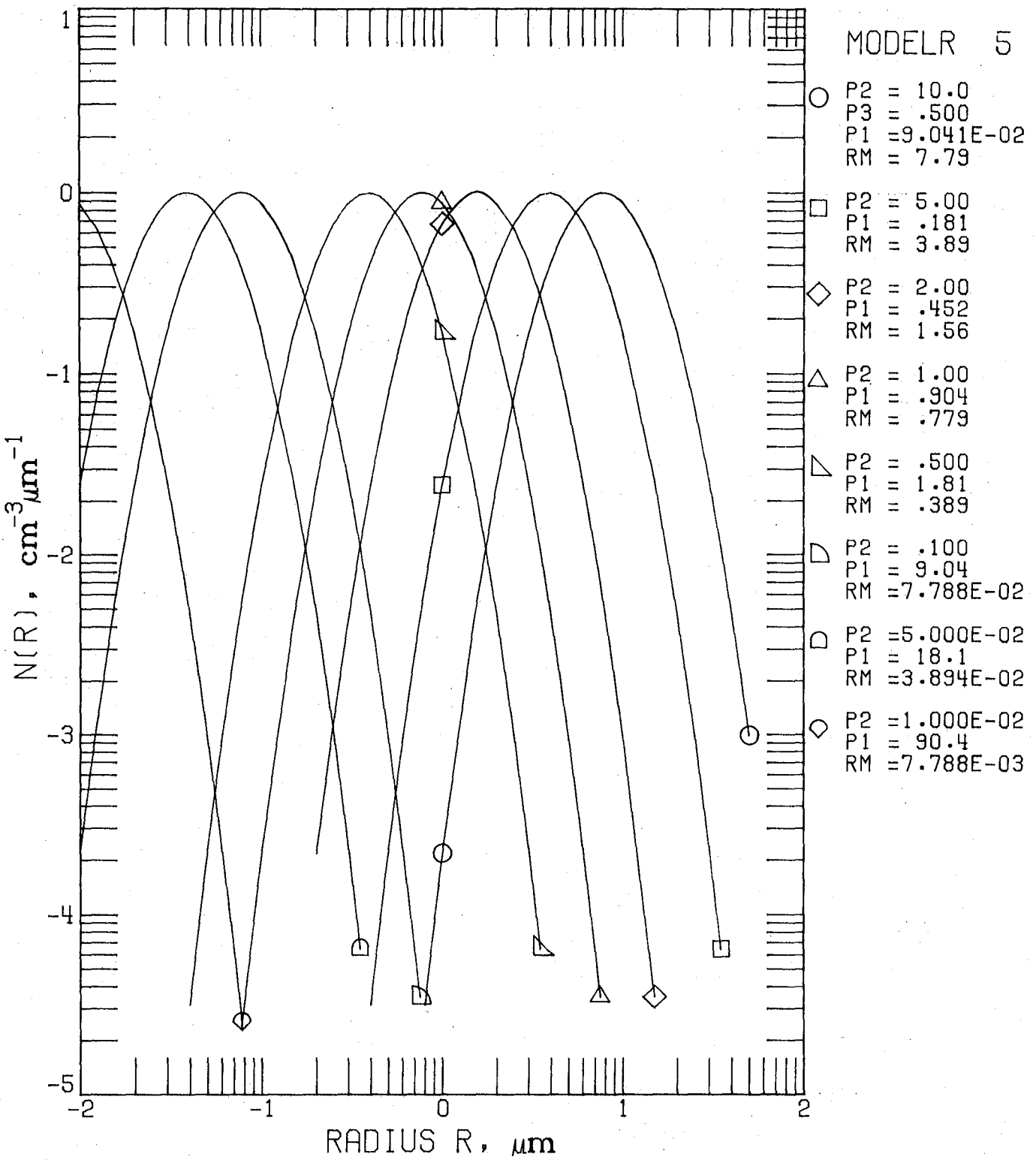

Figure 5A.1. Model 5 (Log Normal Distribution) for n(r). Parameter Set 5.1: p_2 variable, p_3 = 0.5.

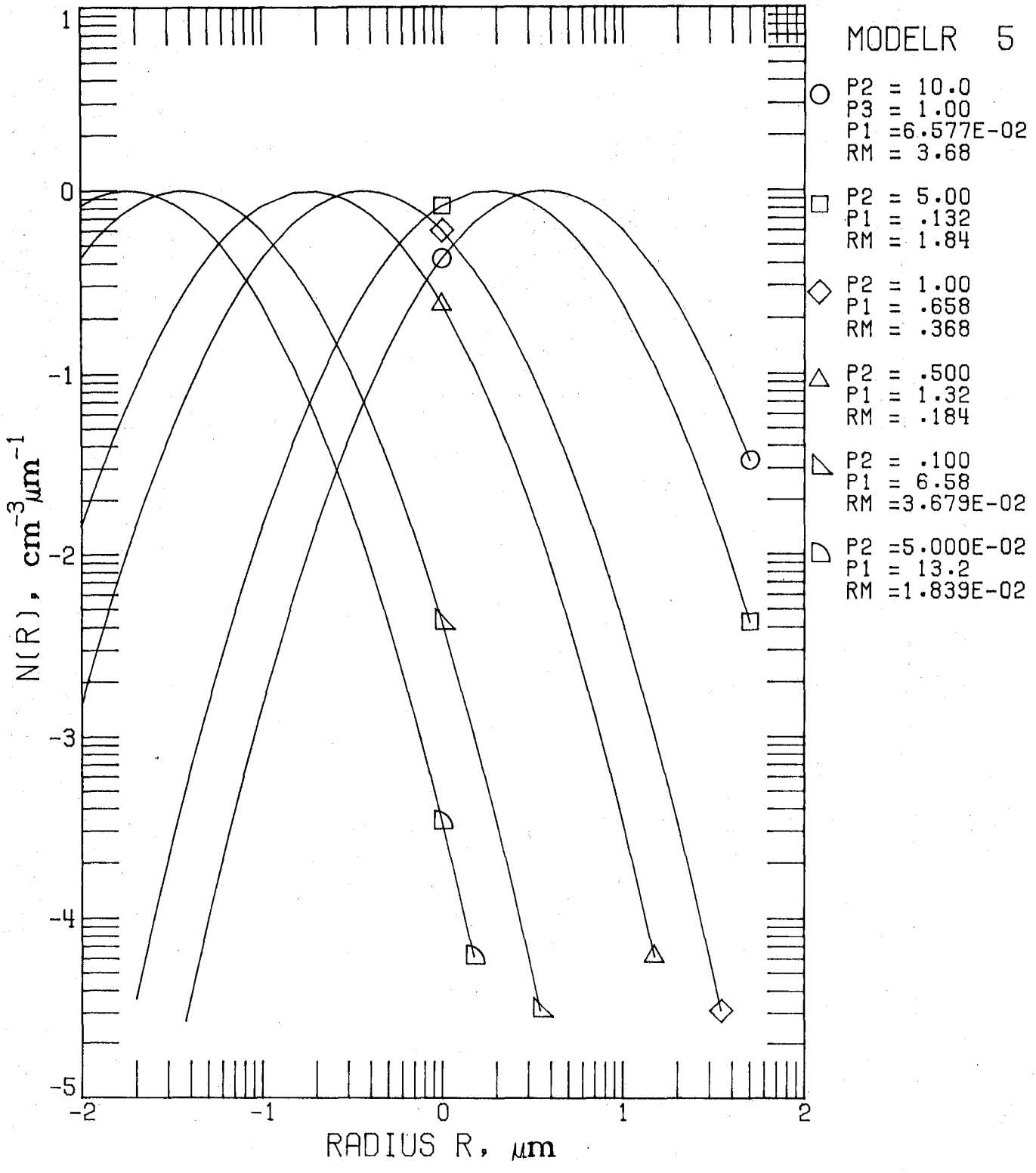

Figure 5A.2. Model 5 for n(r).
Parameter Set 5.2: p_2 variable,
p_3 = 1.0.

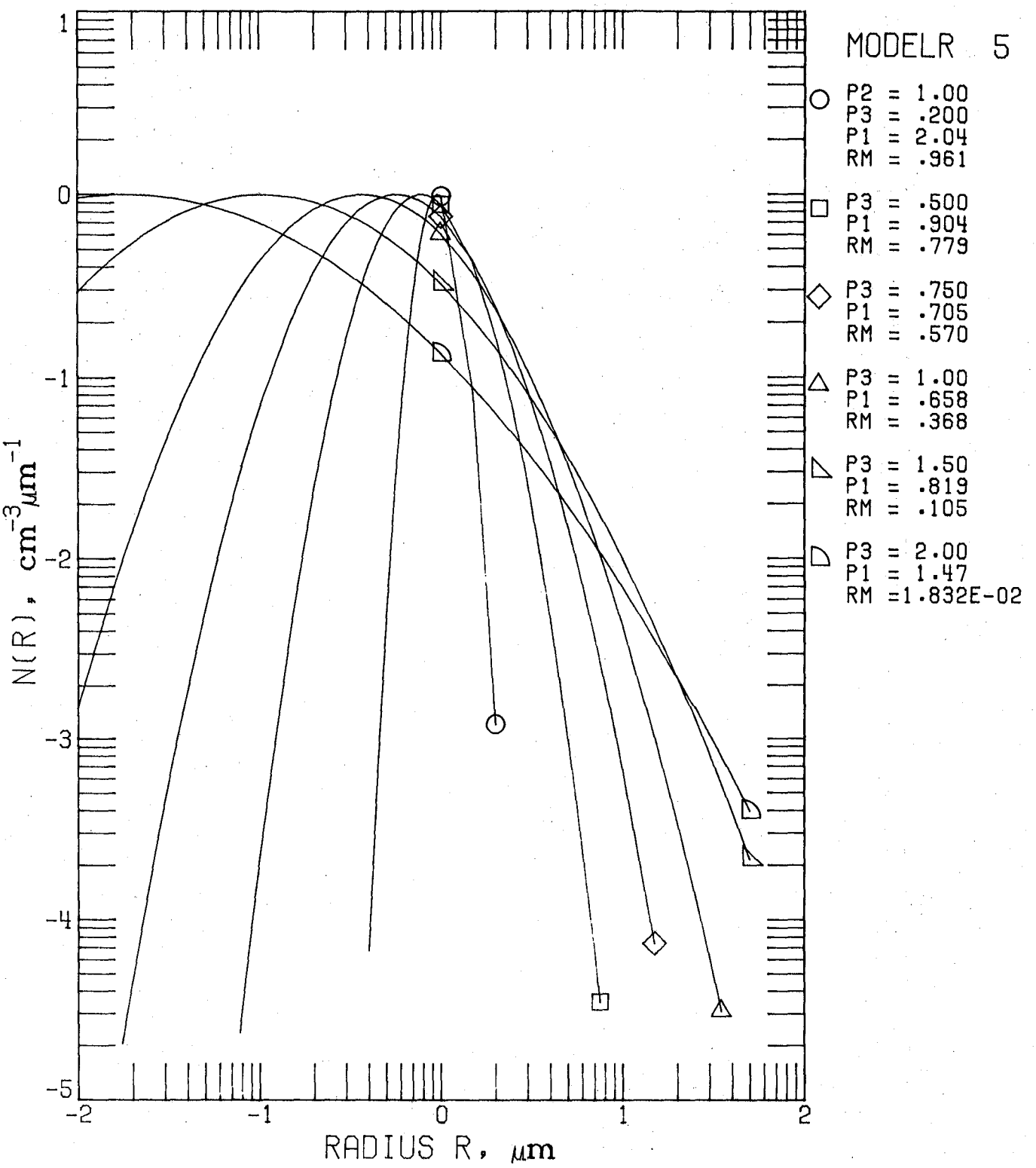

Figure 5A.3. Model 5 for n(r).
Parameter Set 5.3: p_3 variable,
p_2 = 1.0.

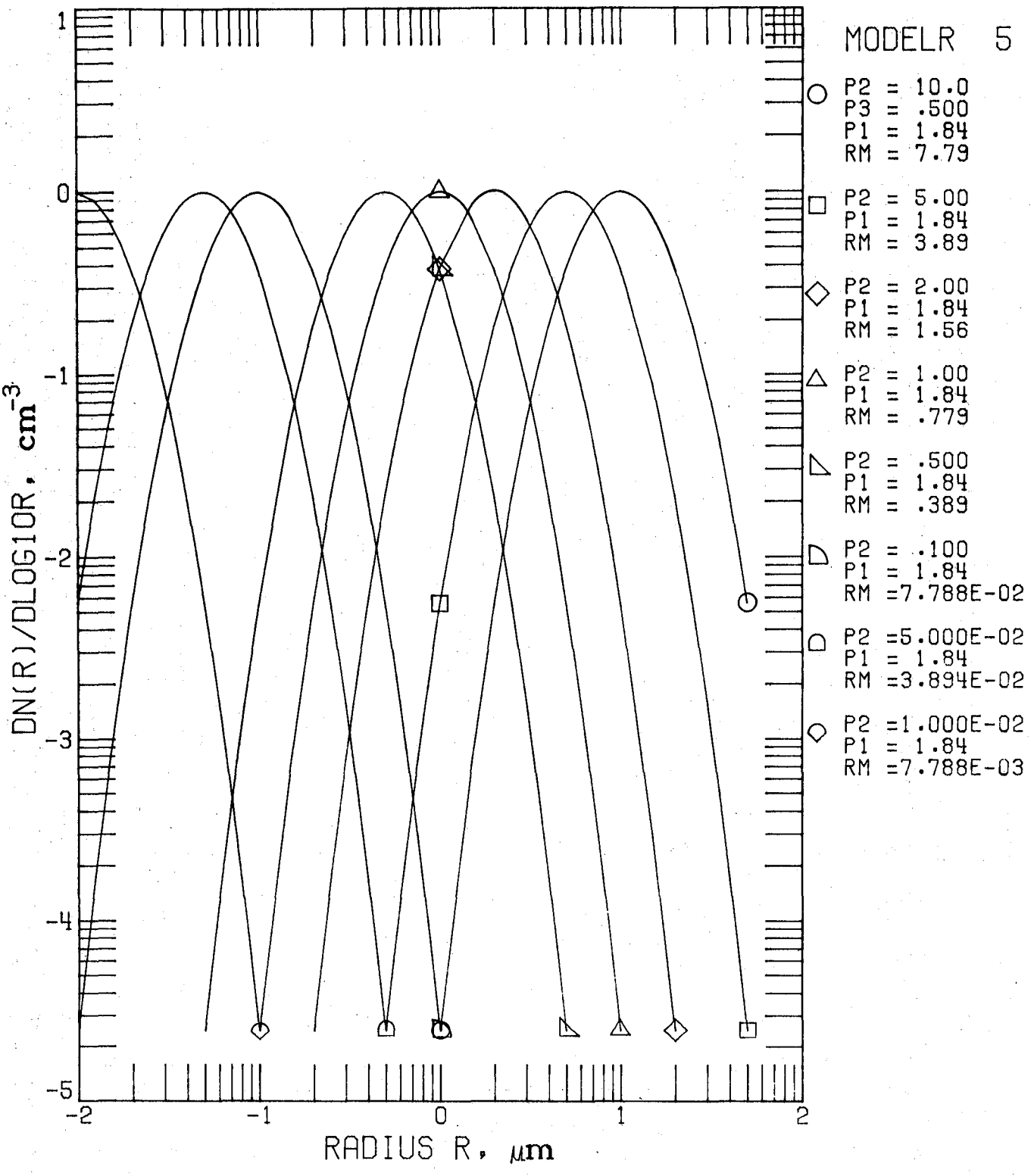

Figure 5B.1. Model 5 for $n_L(r)$.
Parameter Set 5.1.

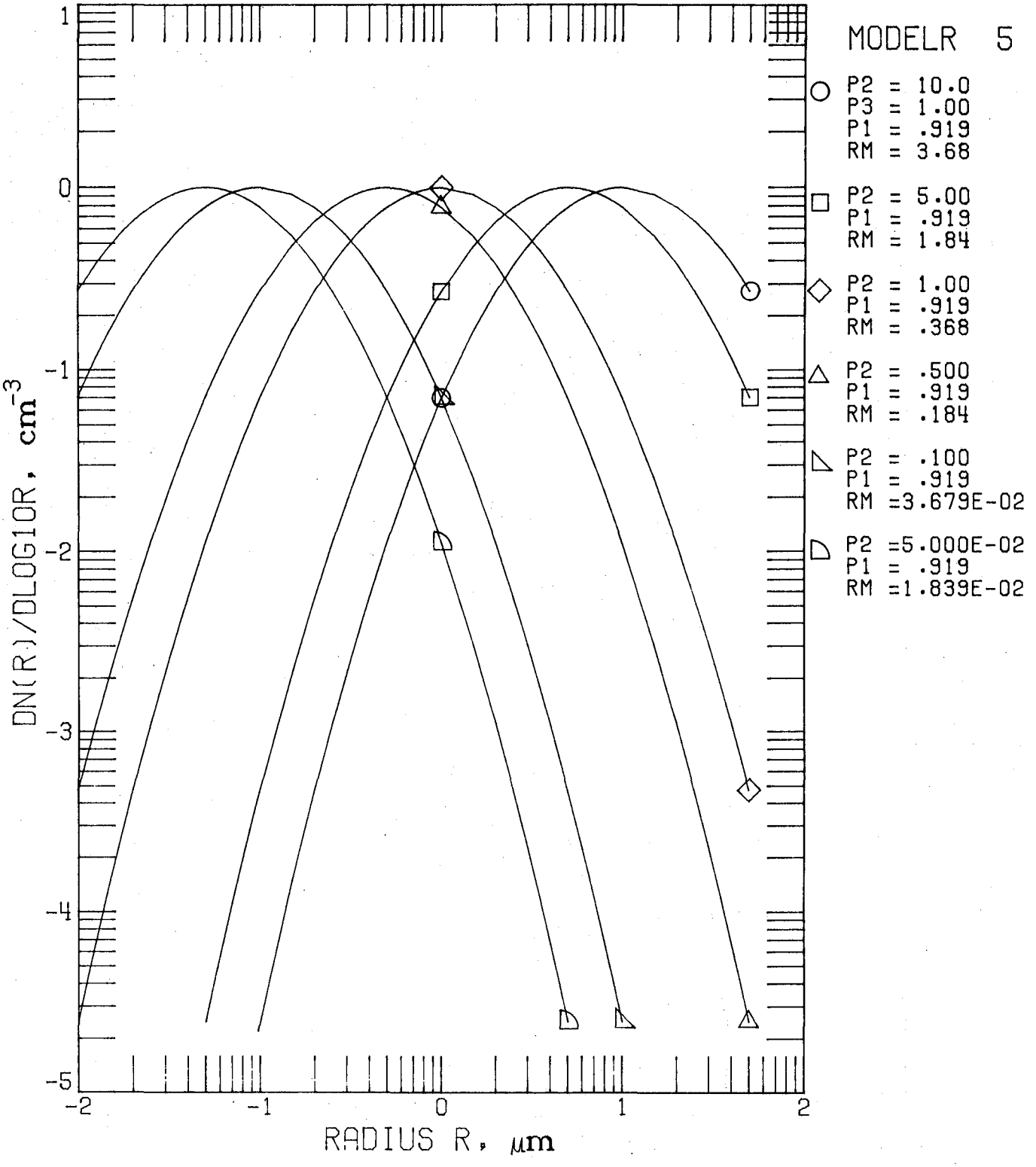

Figure 5B.2. Model 5 for $n_L(r)$.
Parameter Set 5.2.

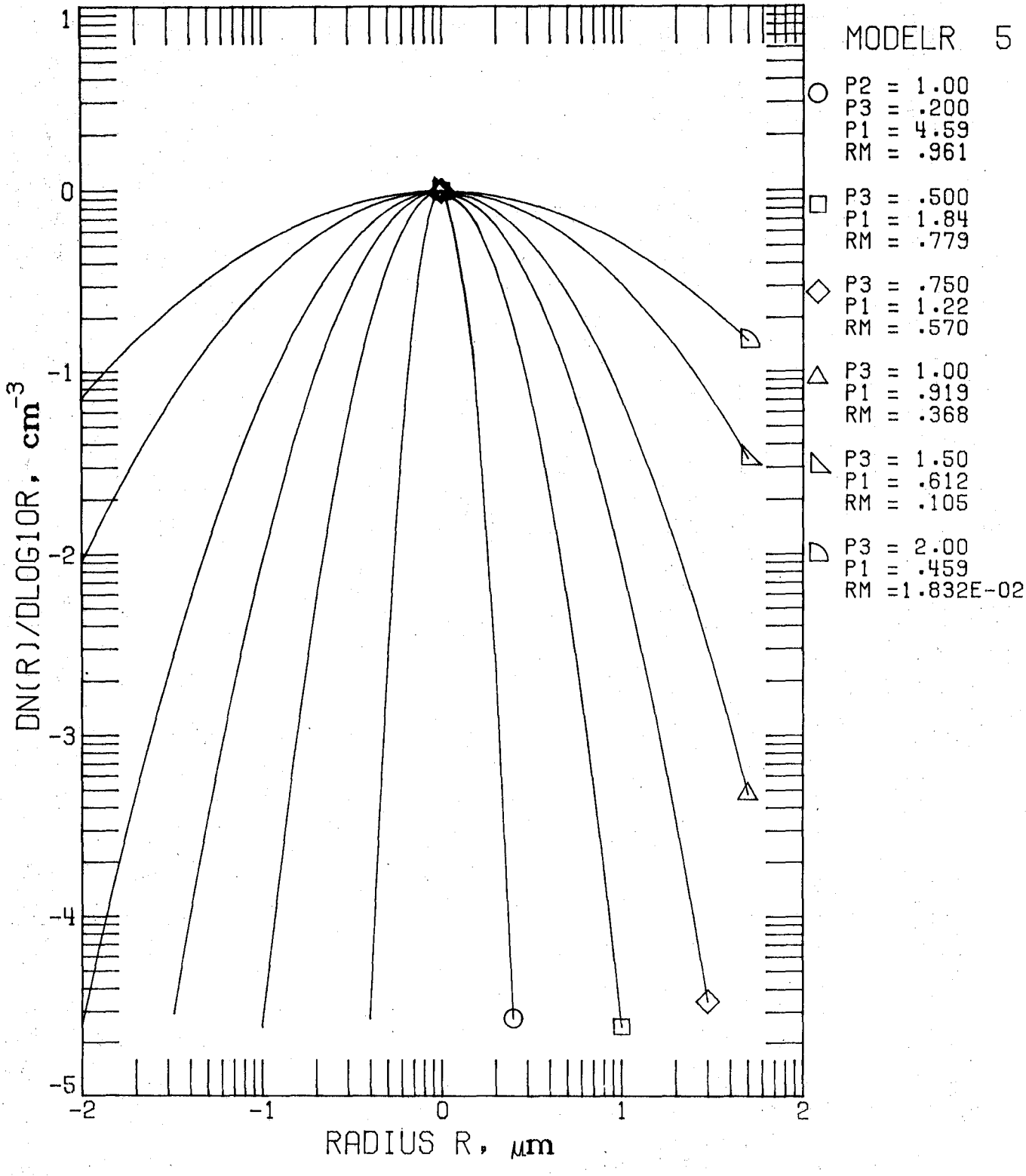

Figure 5B.3. Model 5 for $n_L(r)$.
Parameter Set 5.3.

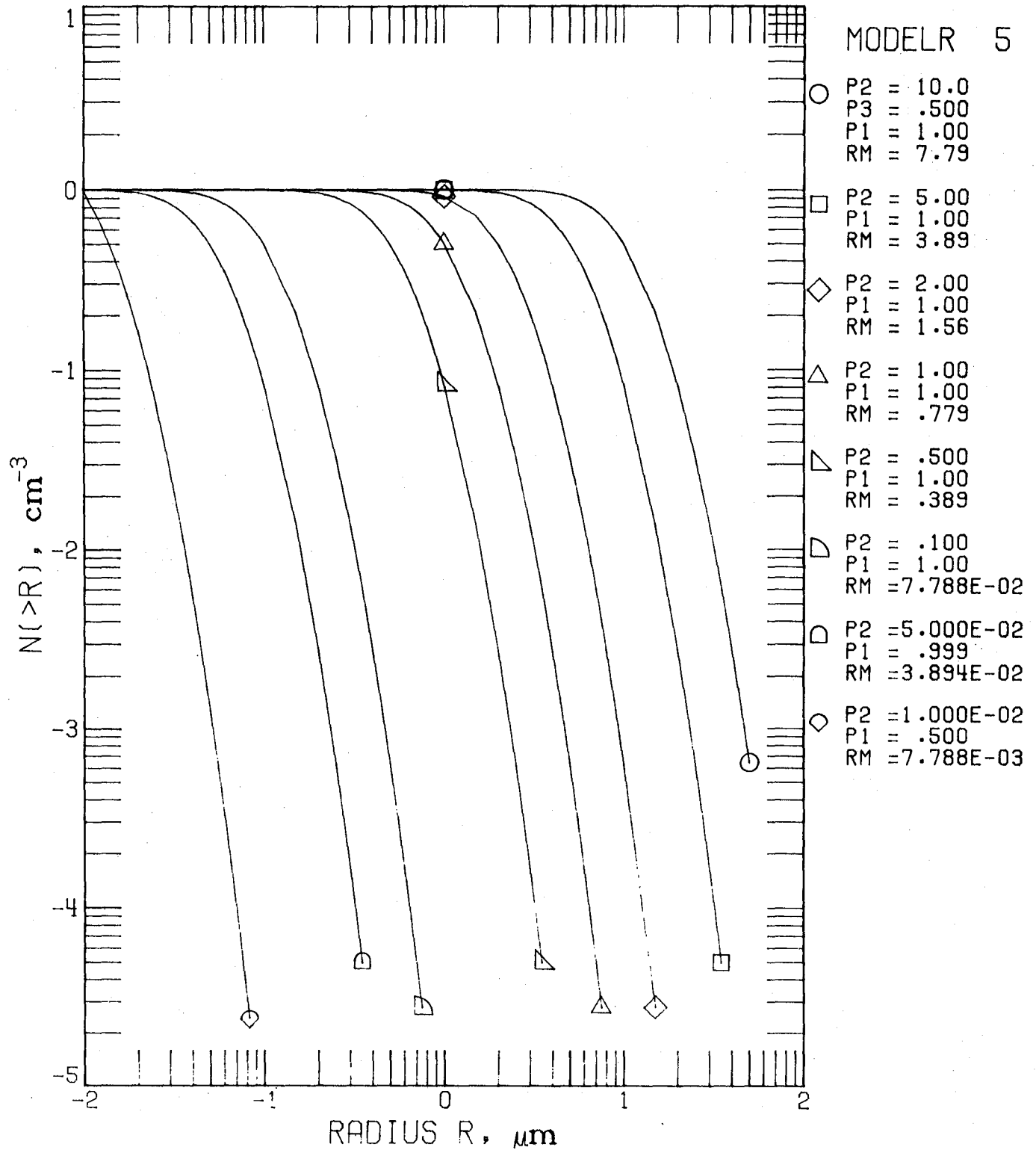

Figure 5C.1. Model 5 for N(>r).
Parameter Set 5.1.

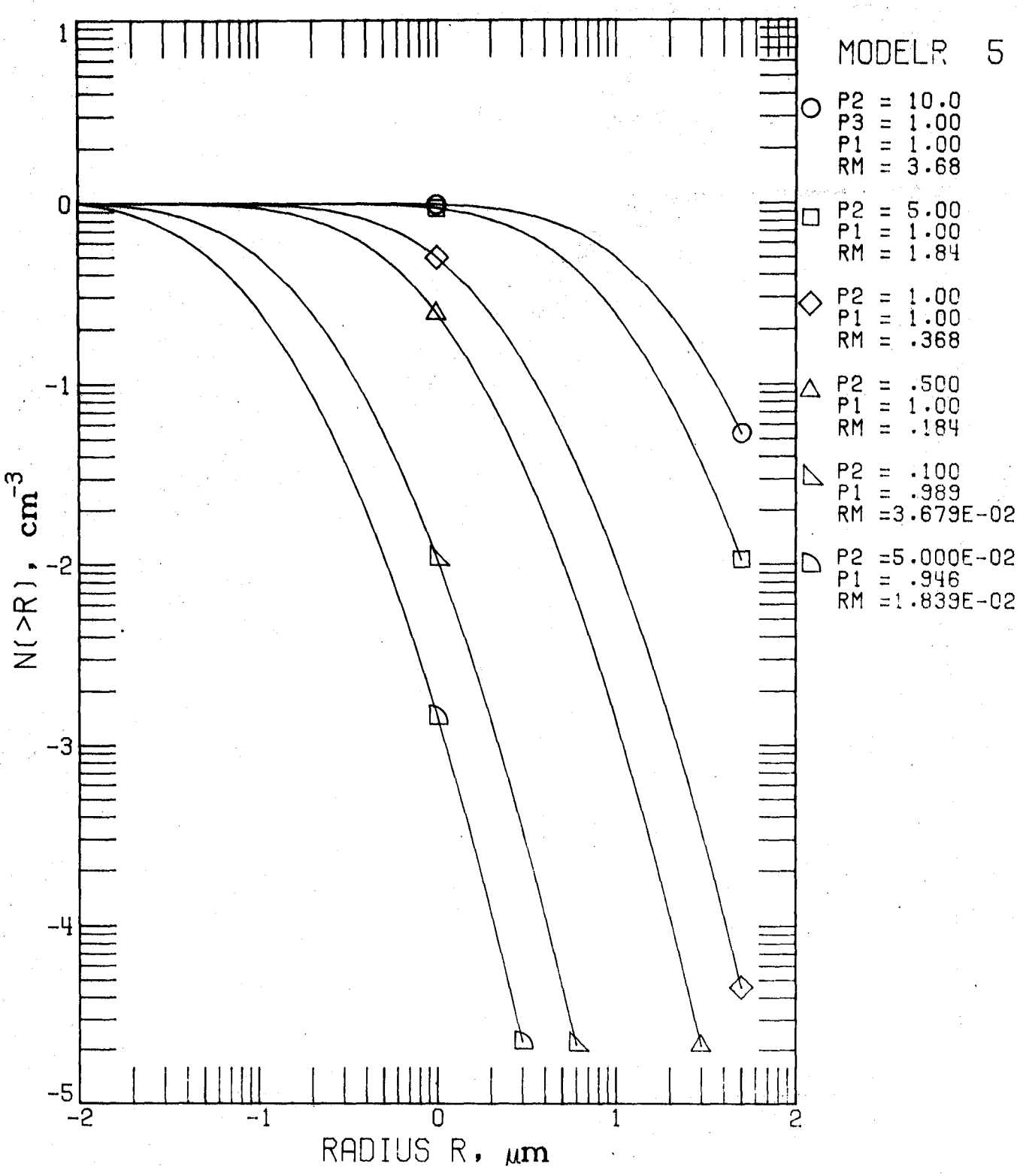

Figure 5C.2. Model 5 for N(>r).
Parameter Set 5.2.

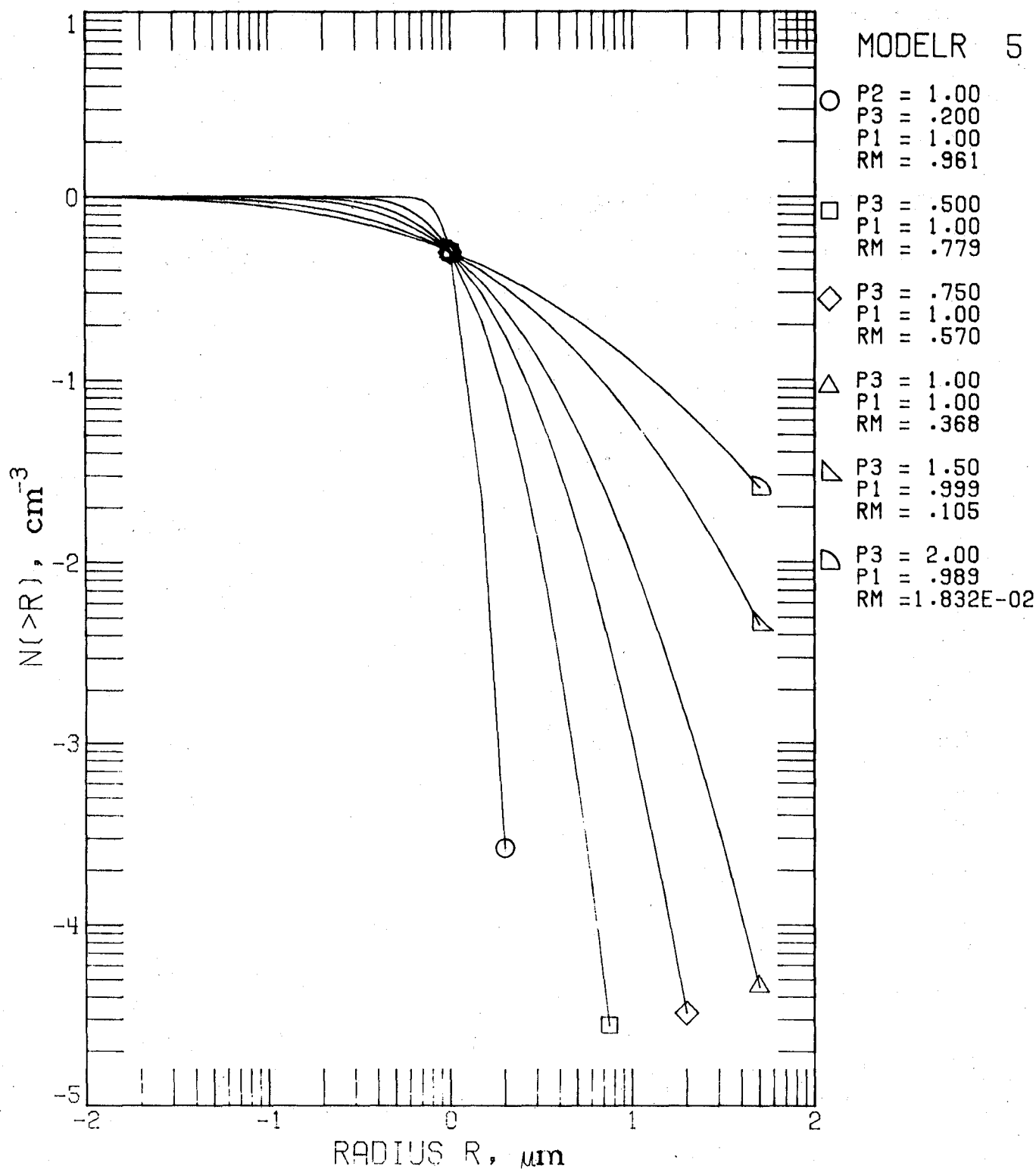

Figure 5C.3. Model 5 for N(>r).
Parameter Set 5.3.

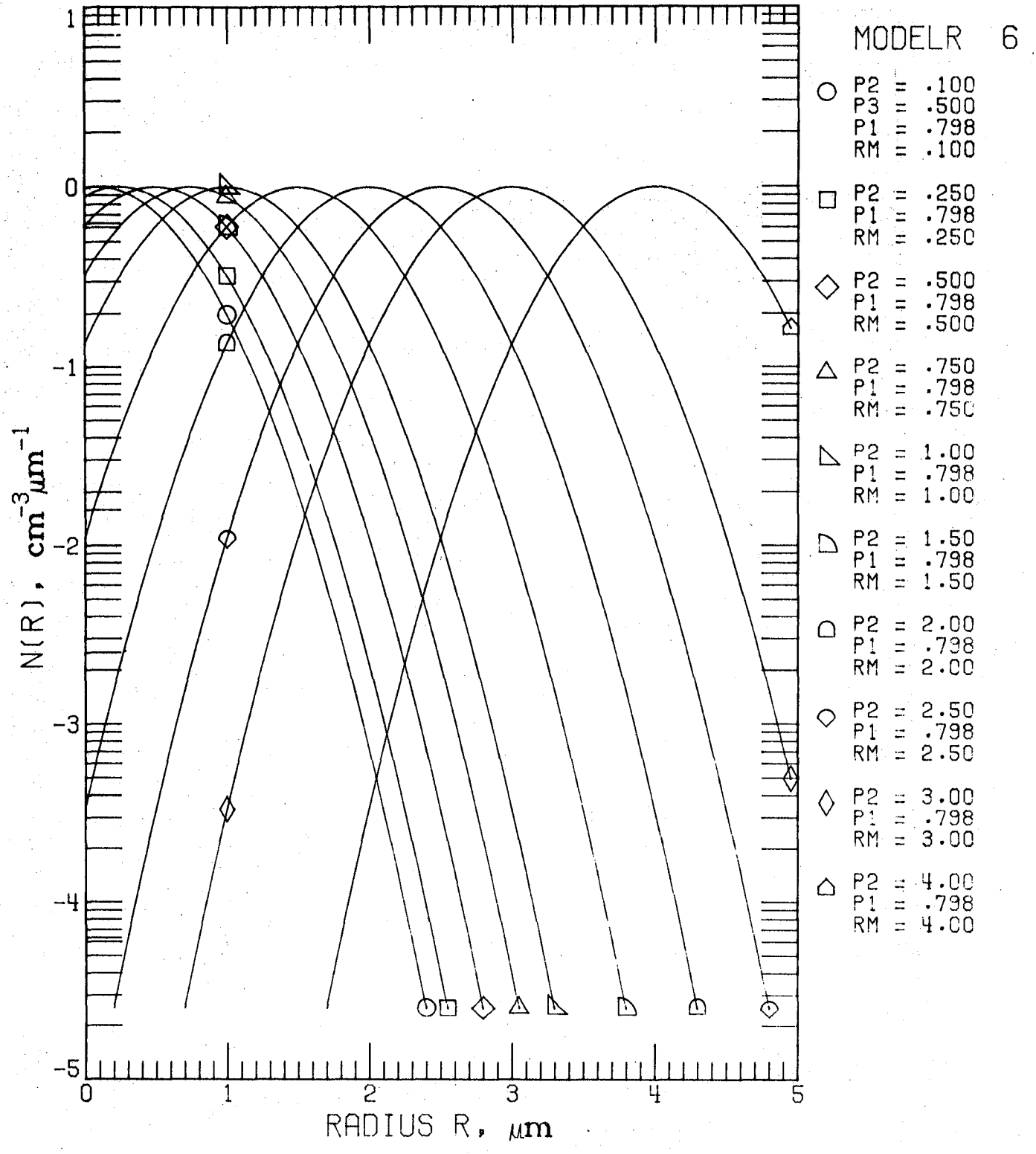

Figure 6A.1. Model 6 (Normal Distribution) for n(r). Parameter Set 6.1: p_2 variable, p_3 = 0.5.

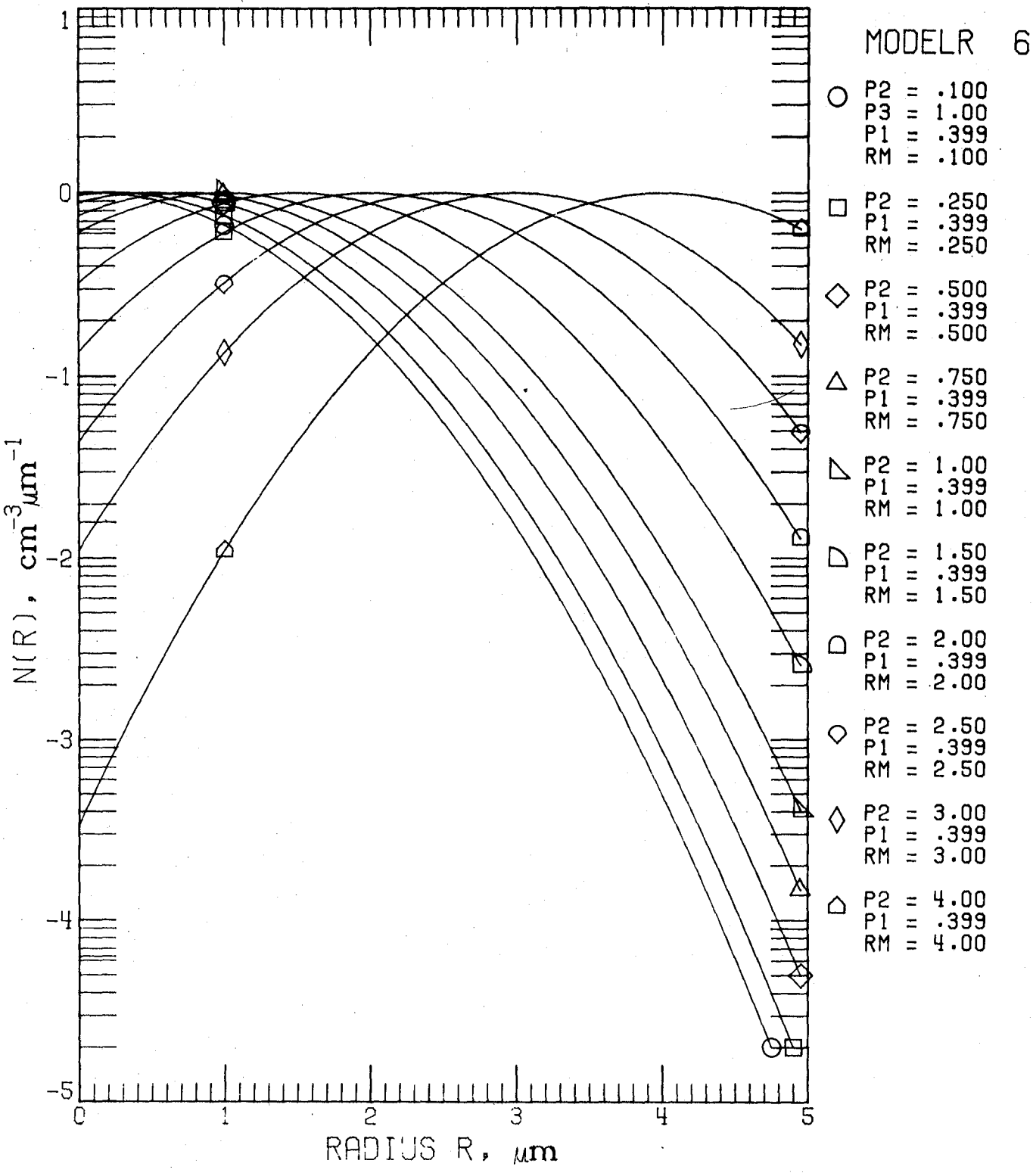

Figure 6A.2. Model 6 for n(r).
Parameter Set 6.2: p_2 variable,
p_3 = 1.0

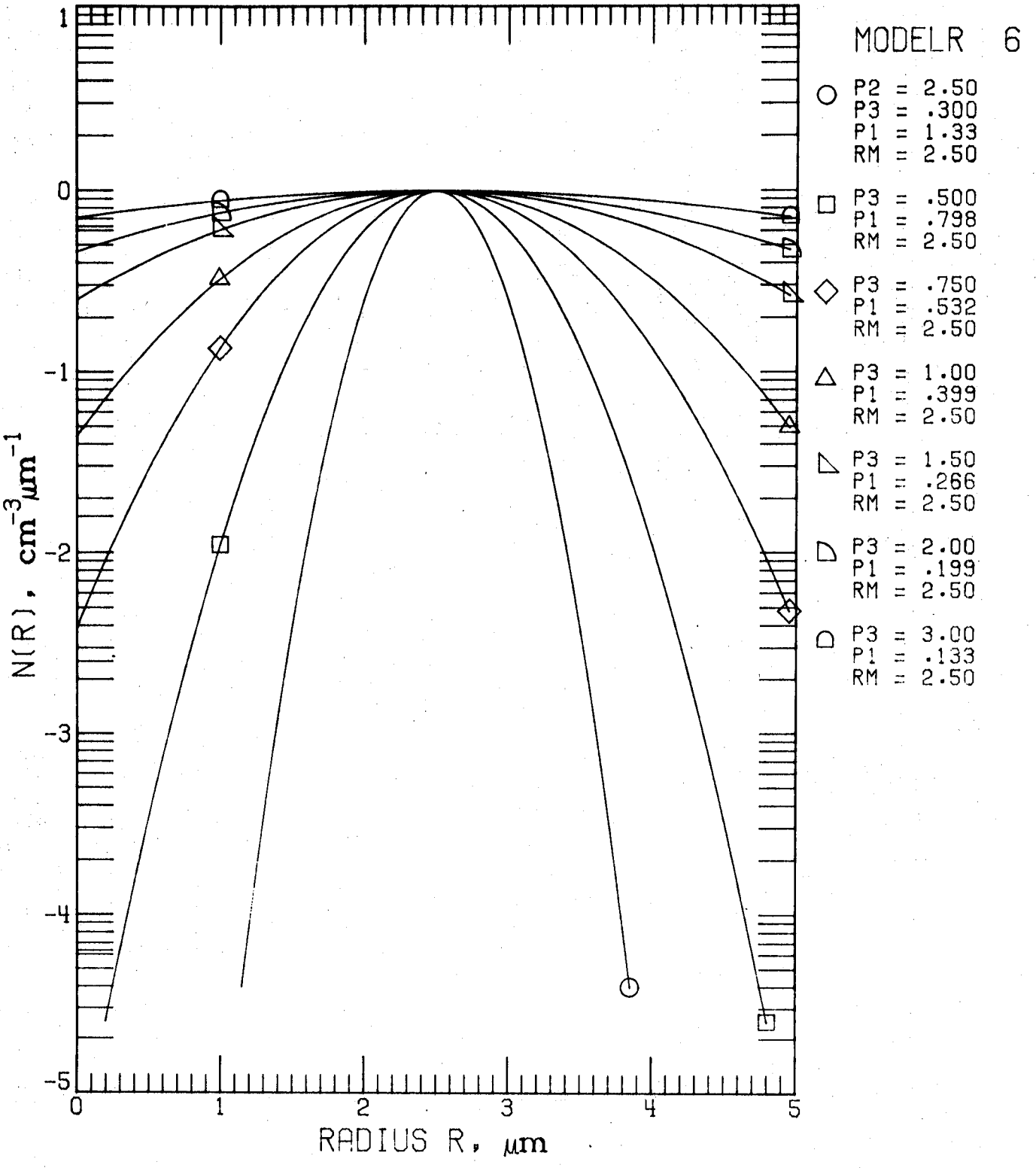

Figure 6A.3. Model 6 for n(r).
Parameter Set 6.3: p_3 variable,
p_2 = 2.5.

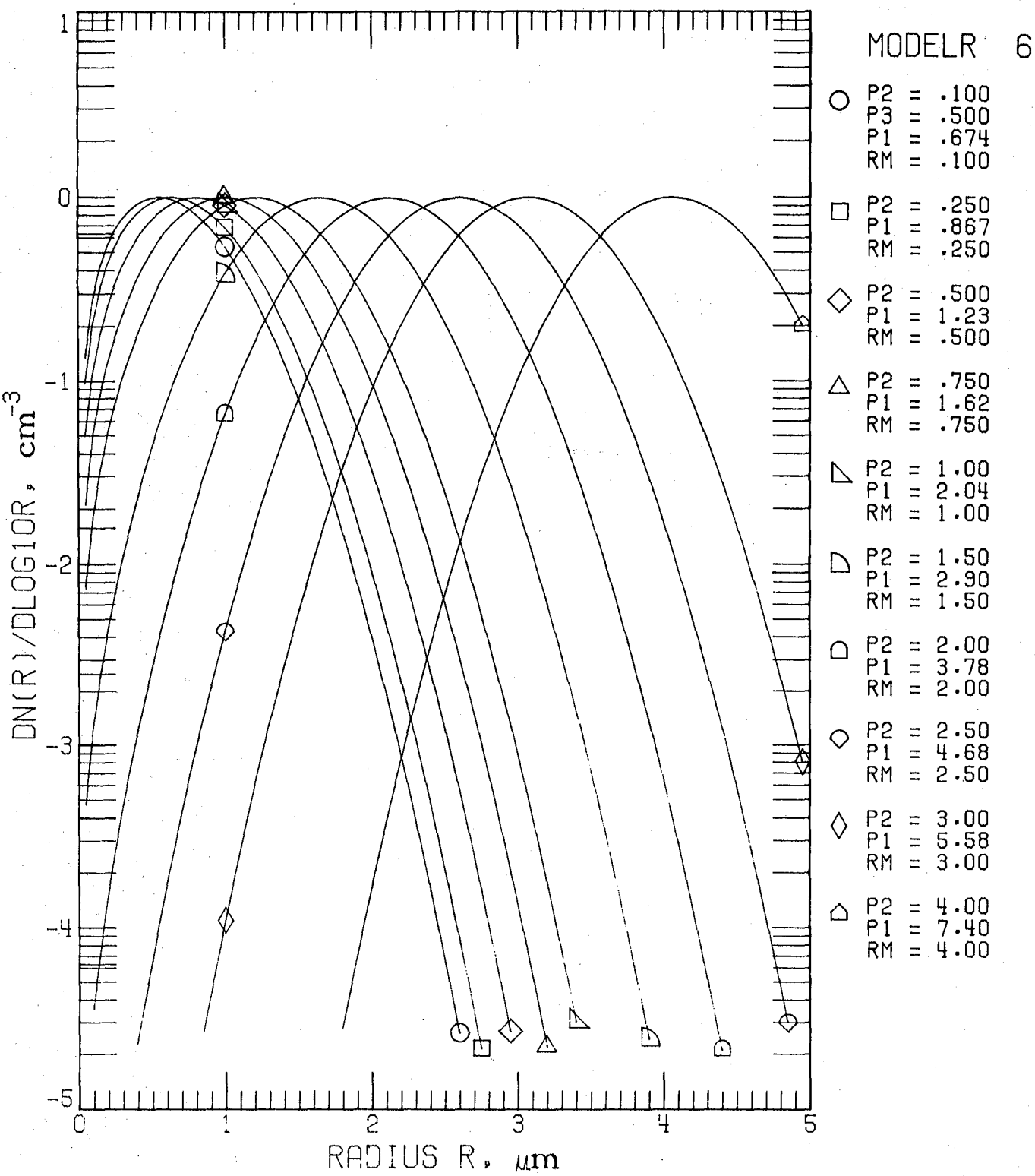

Figure 6B.1. Model 6 for $n_L(r)$.
Parameter Set 6.1.

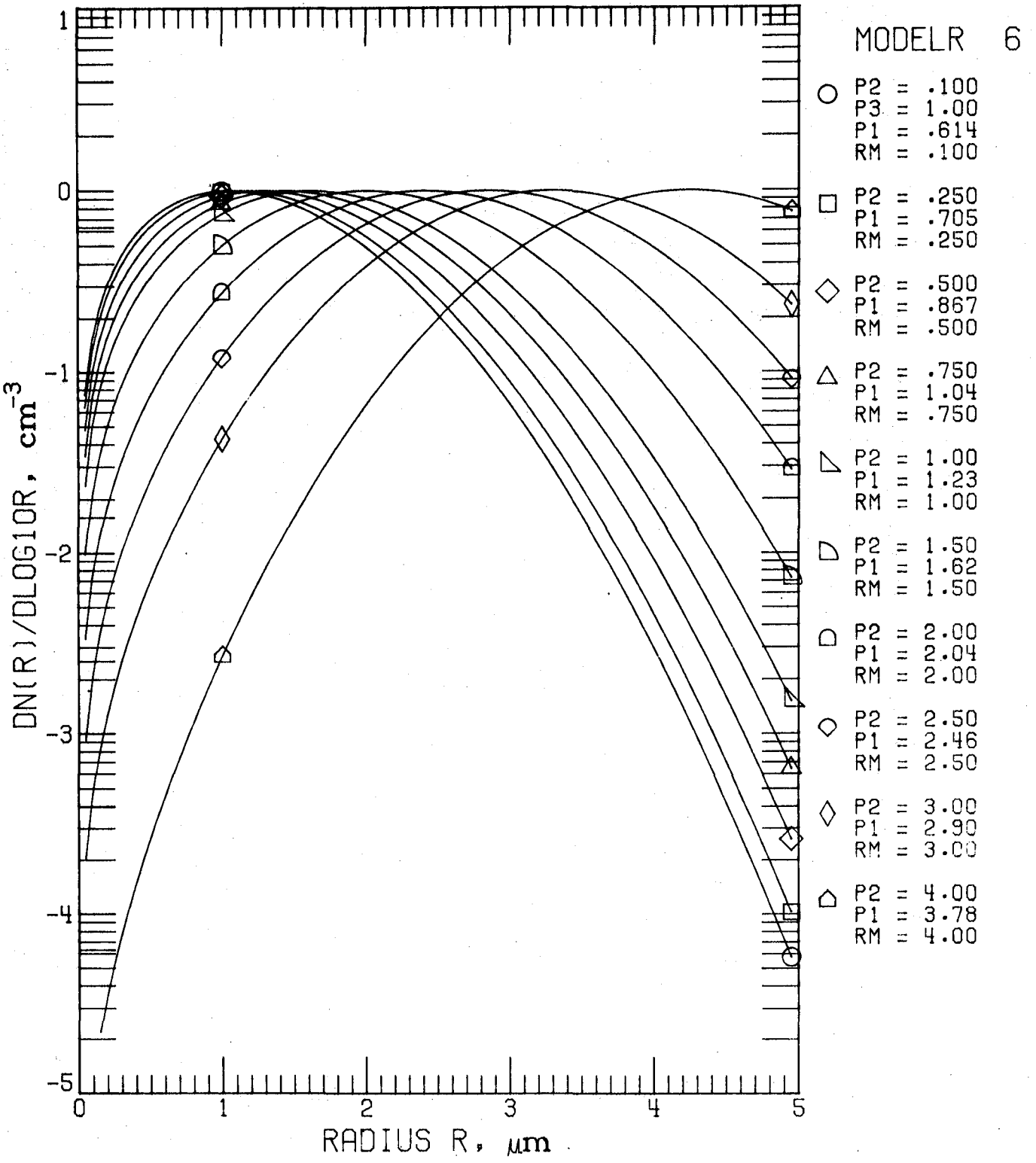

Figure 6B.2. Model 6 for $n_L(r)$.
Parameter Set 6.2.

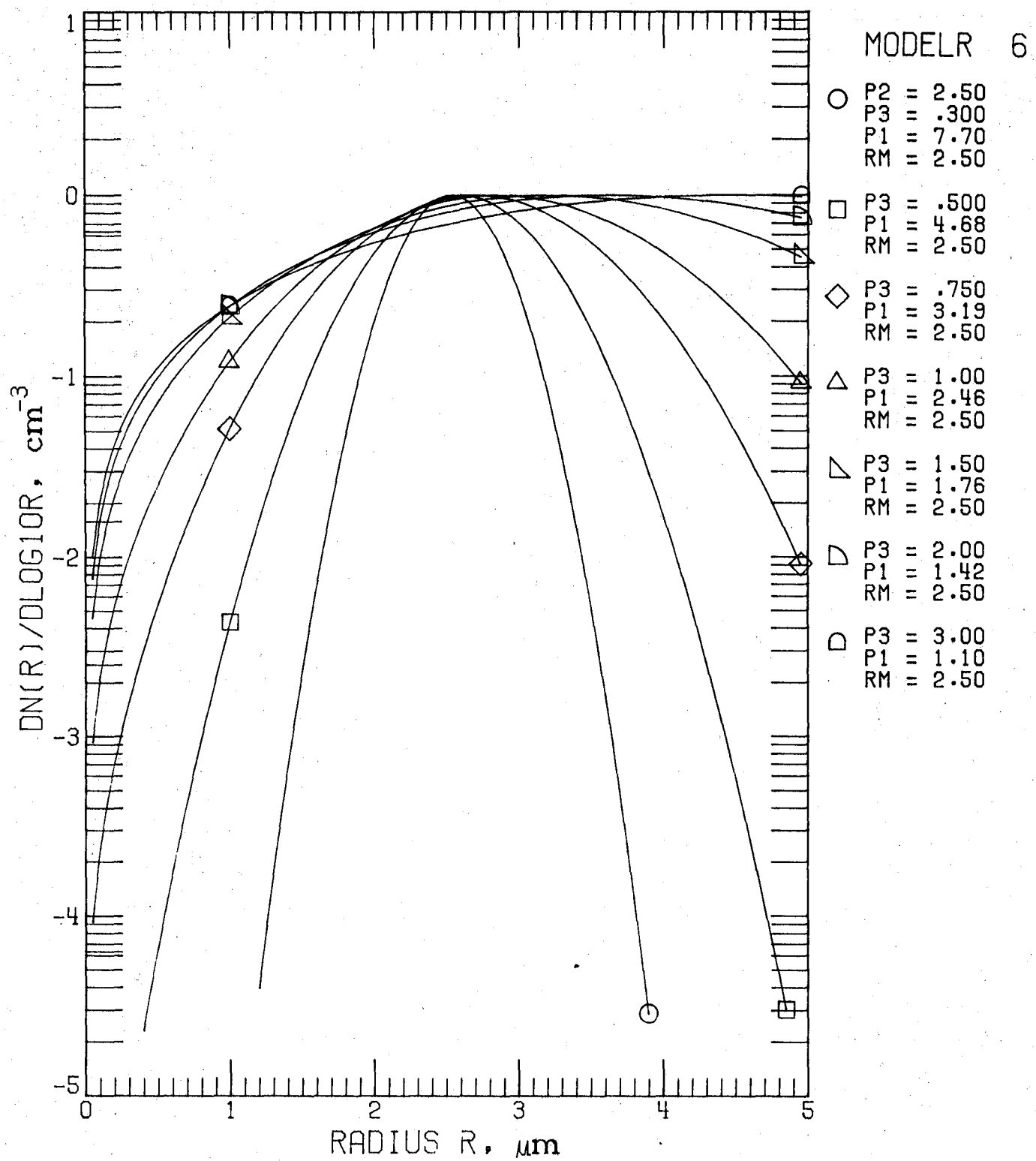

Figure 6B.3. Model 6 for $n_L(r)$.
Parameter Set 6.3.

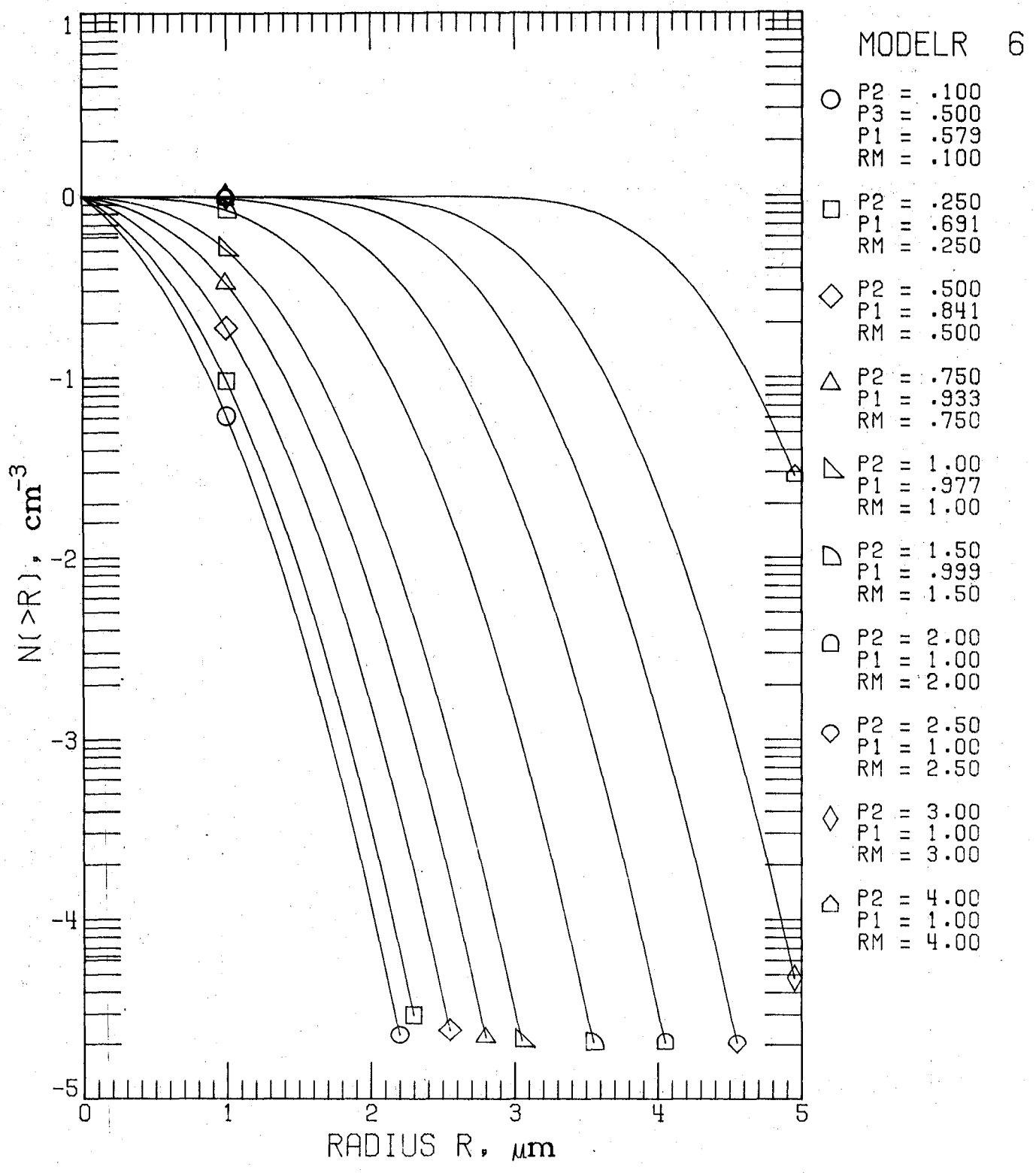

Figure 6C.1. Model 6 for N(>r).
Parameter Set 6.1.

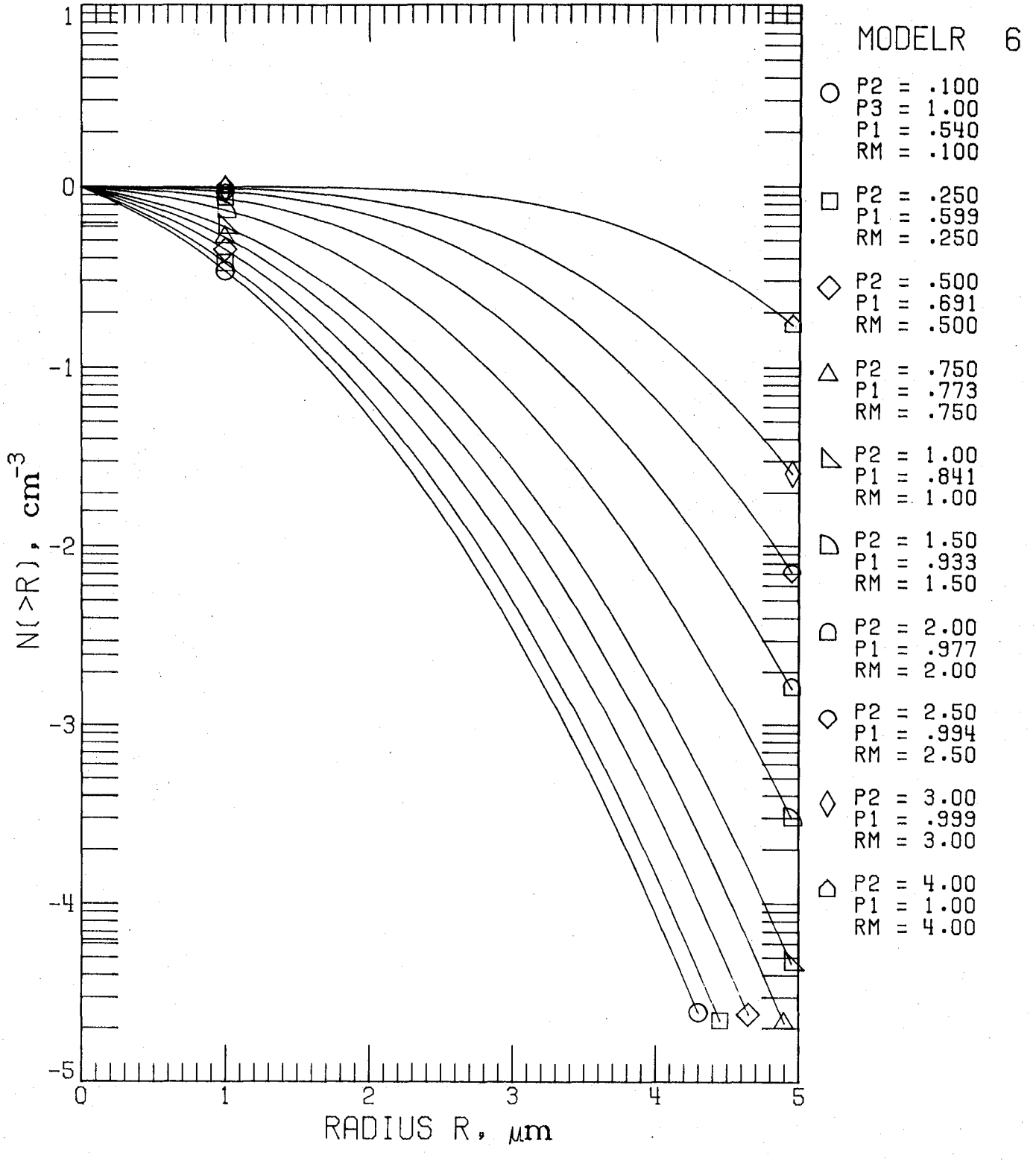

Figure 6C.2. Model 6 for N(>r).
Parameter Set 6.2.

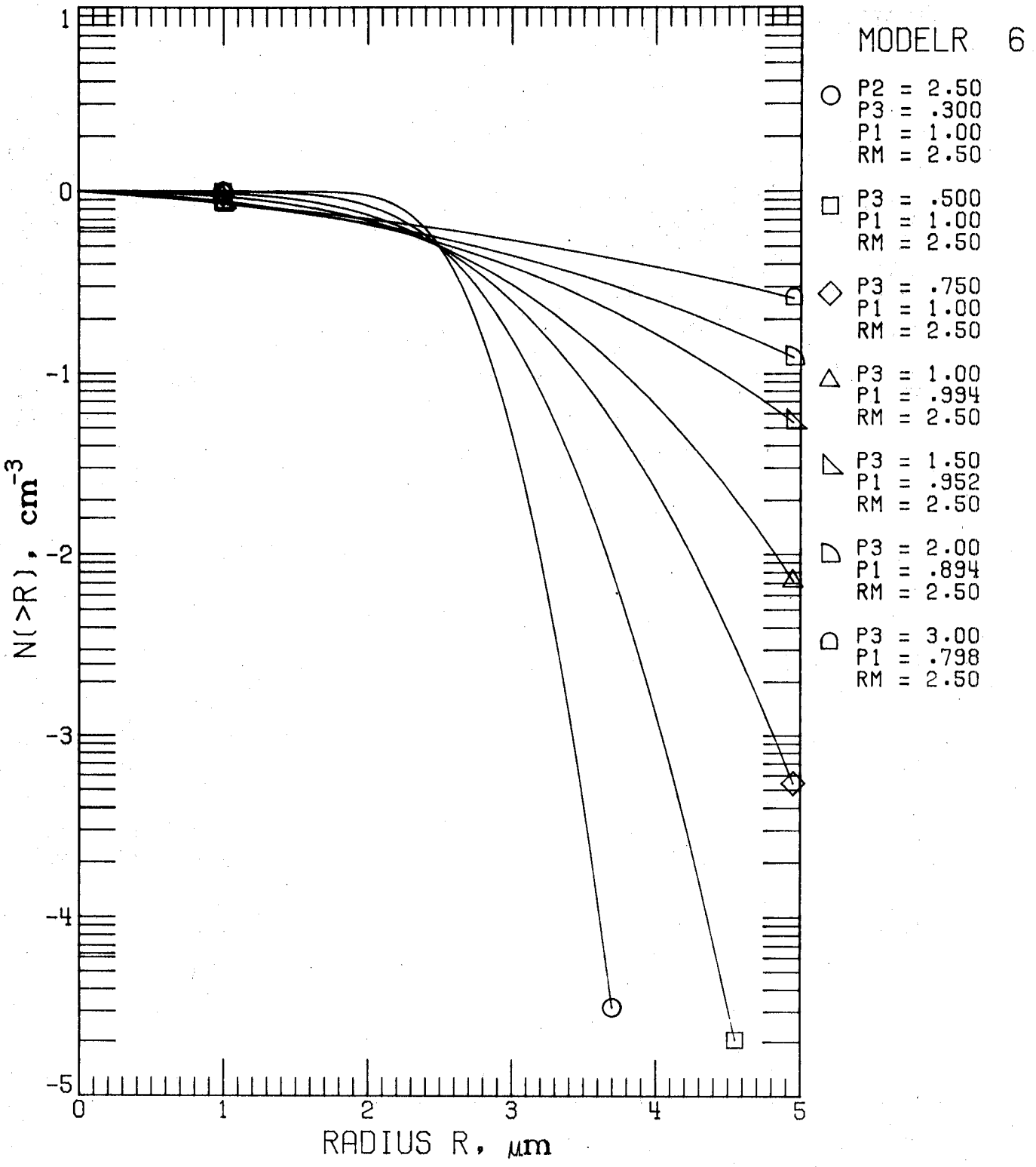

Figure 6C.3. Model 6 for N(>r).
Parameter Set 6.3.

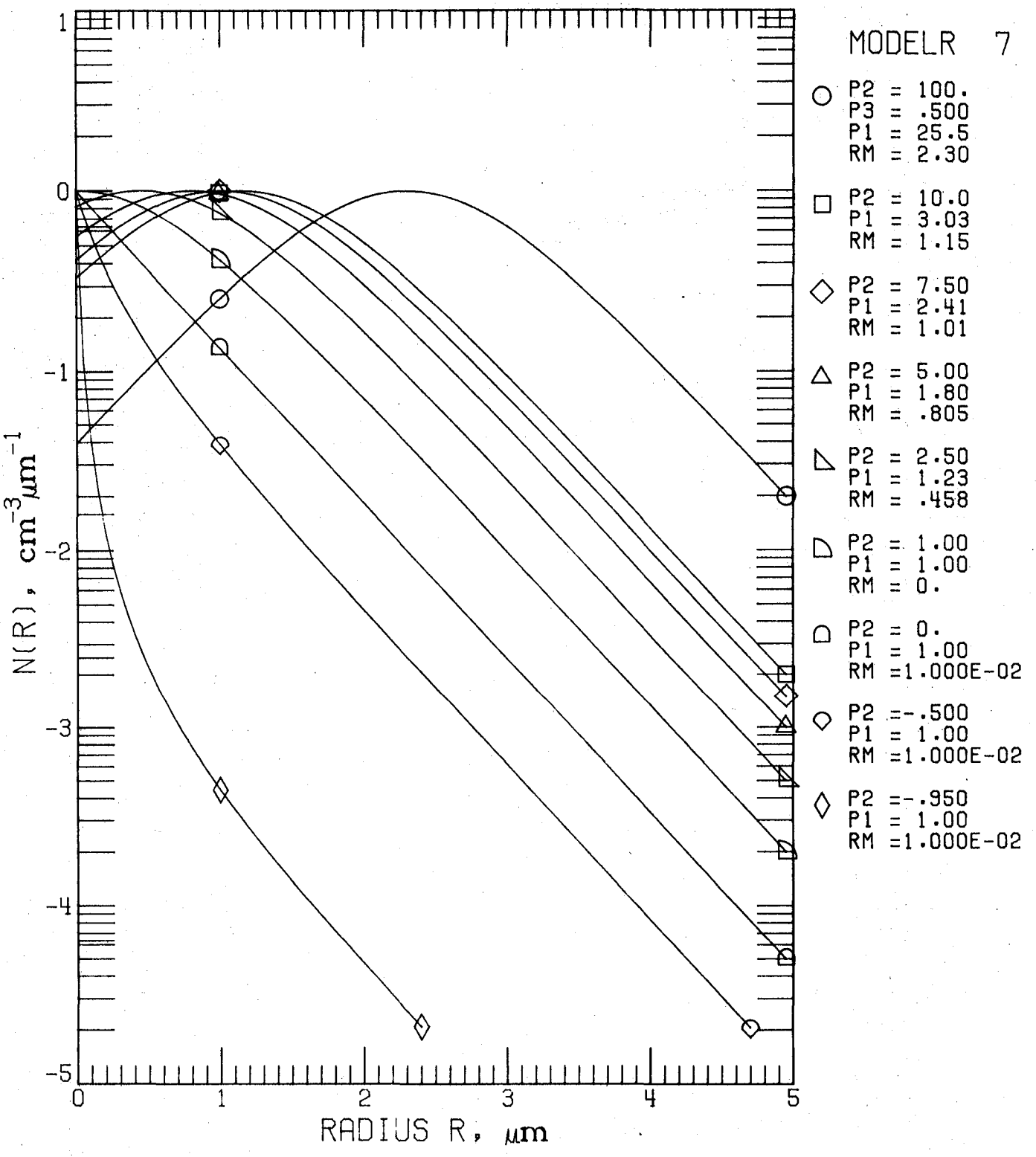

Figure 7A.1. Model 7 (Generalized Distribution Function) for n(r). Parameter Set 7.1: p_2 variable, p_3 = 0.5.

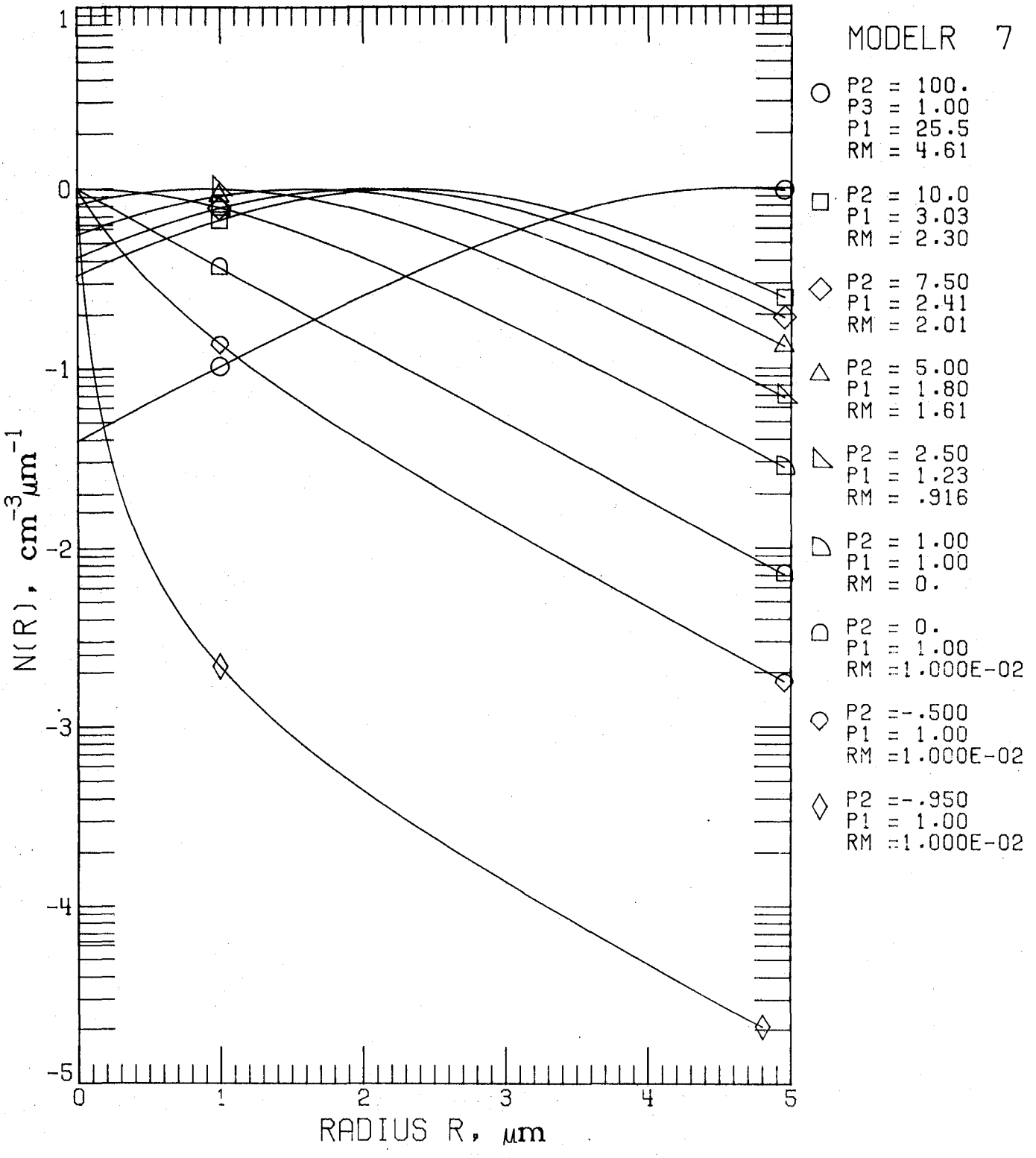

Figure 7A.2. Model 7 for n(r).
Parameter Set 7.2.: p_2 variable,
p_3 = 1.0.

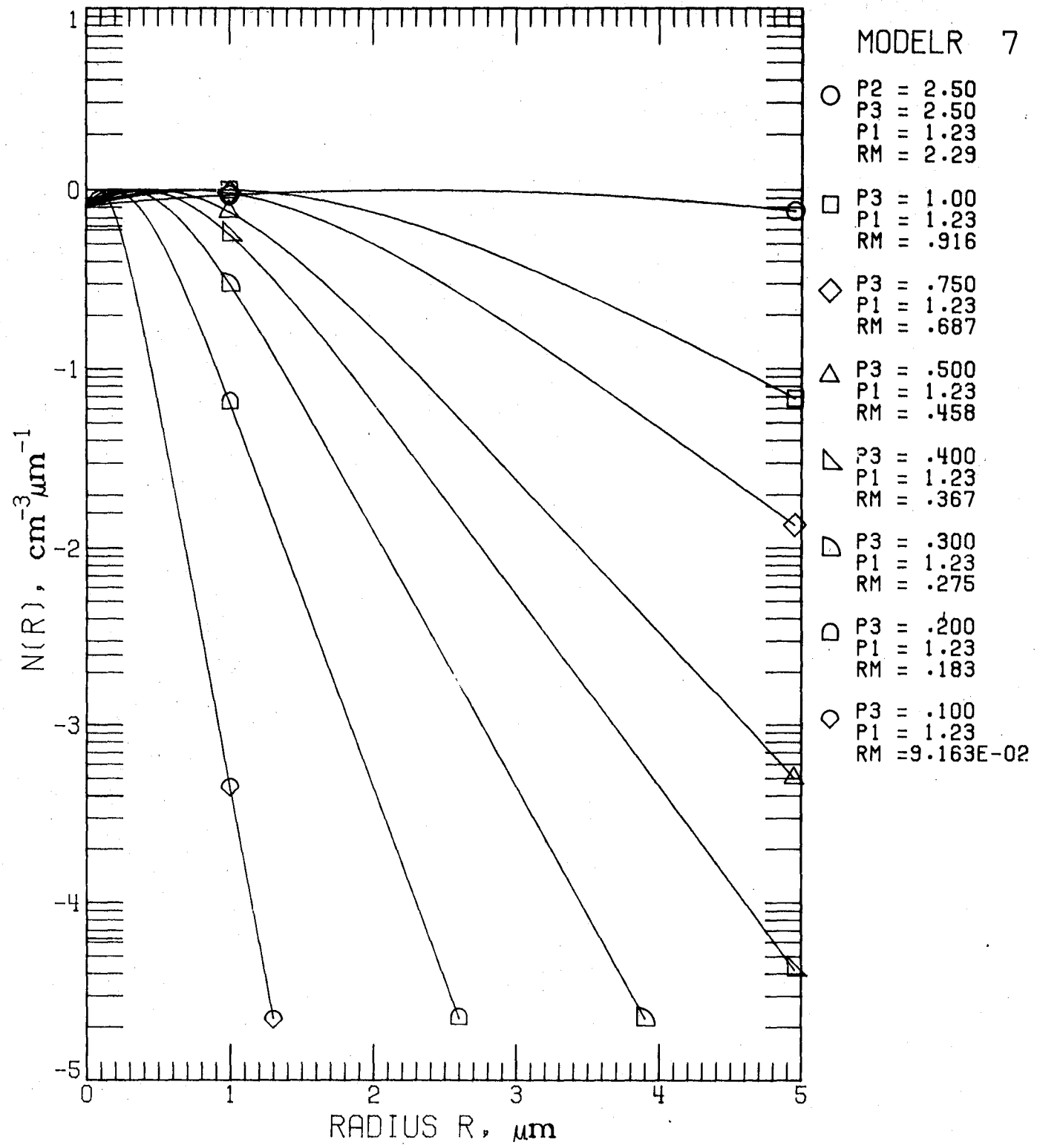

Figure 7A.3. Model 7 for n(r).
Parameter Set 7.3: p_3 variable,
p_2 = 2.5.

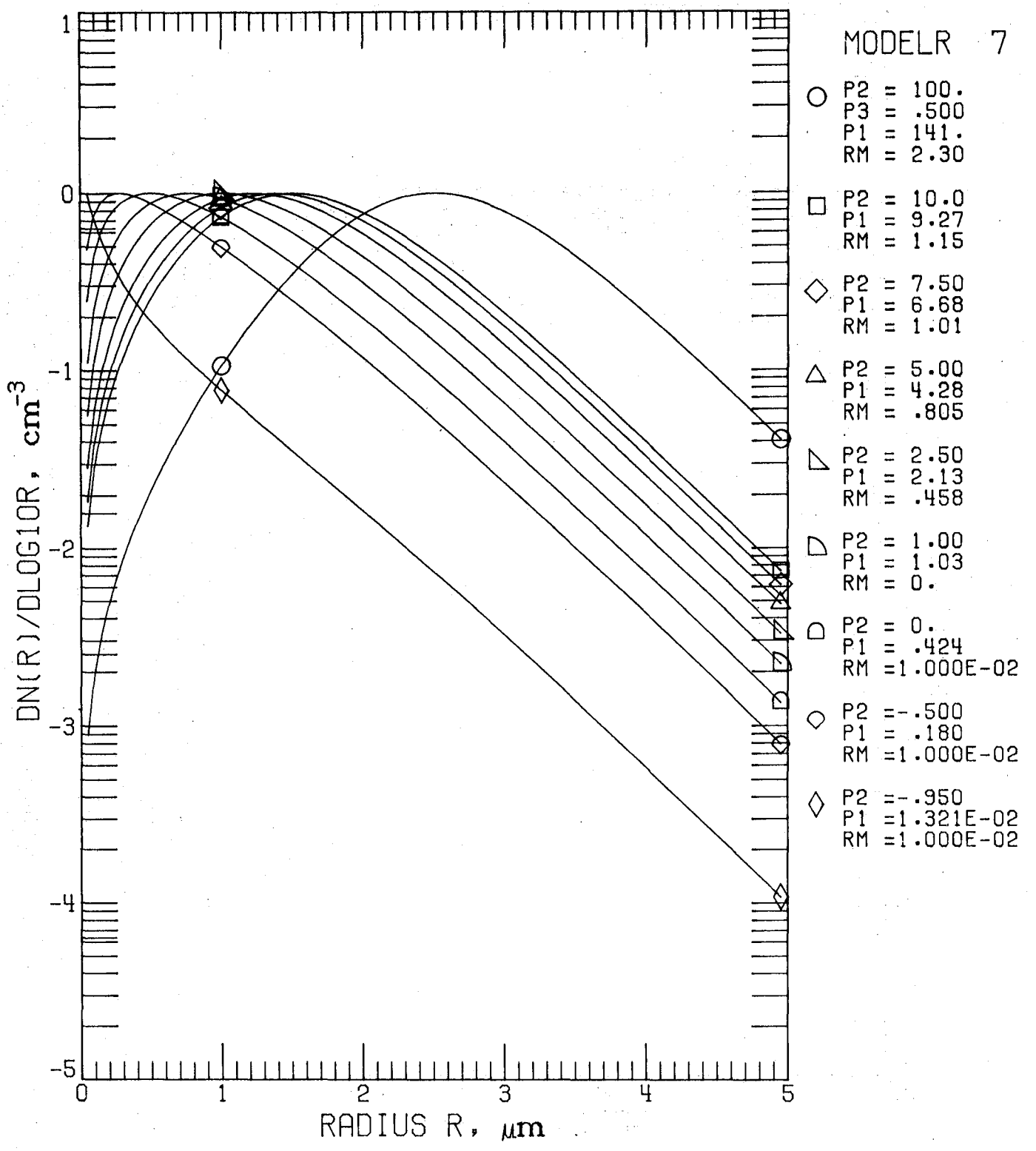

Figure 7B.1. Model 7 for $n_L(r)$.
Parameter Set 7.1.

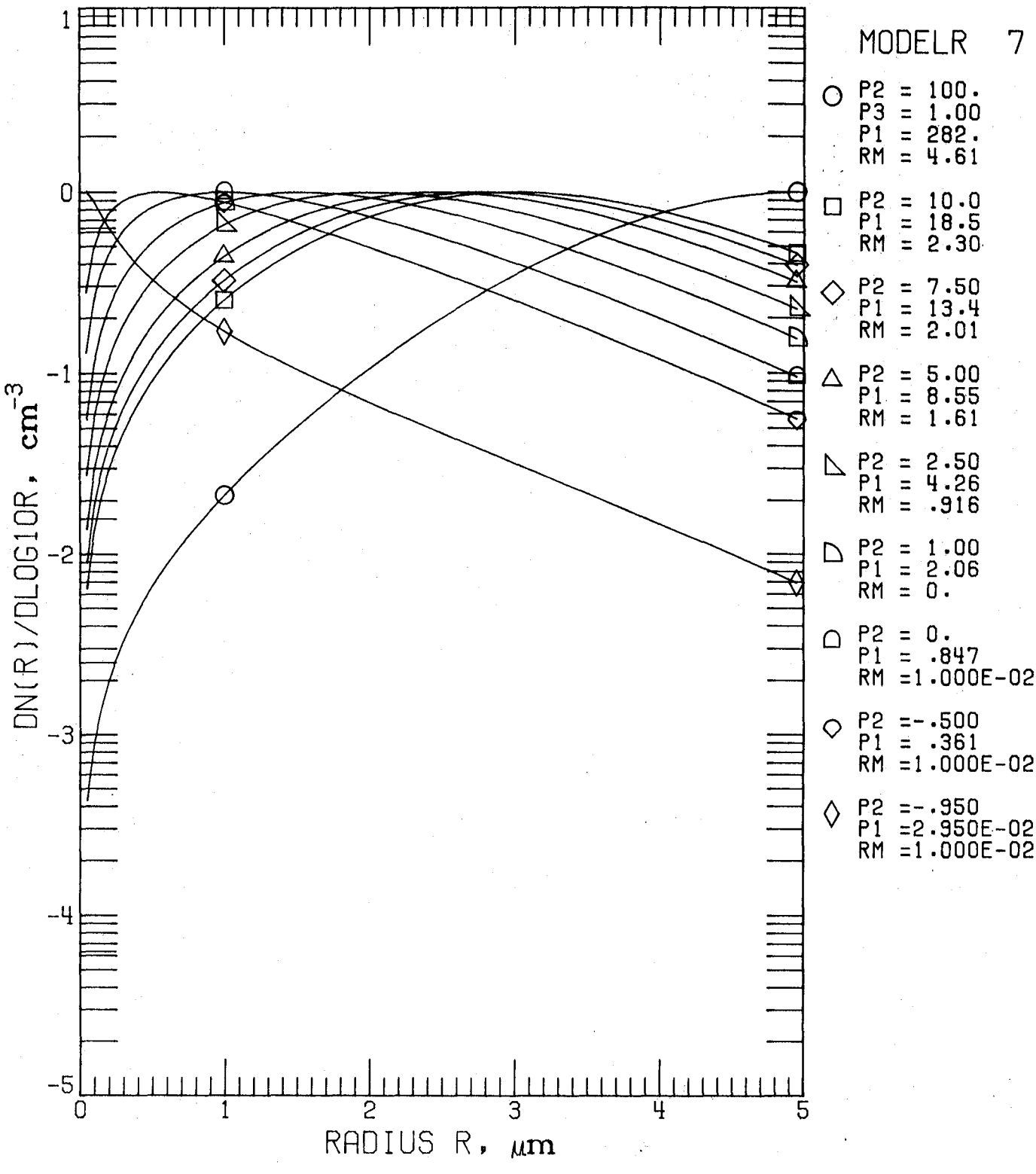

Figure 7B.2. Model 7 for $n_L(r)$.
Parameter Set 7.2.

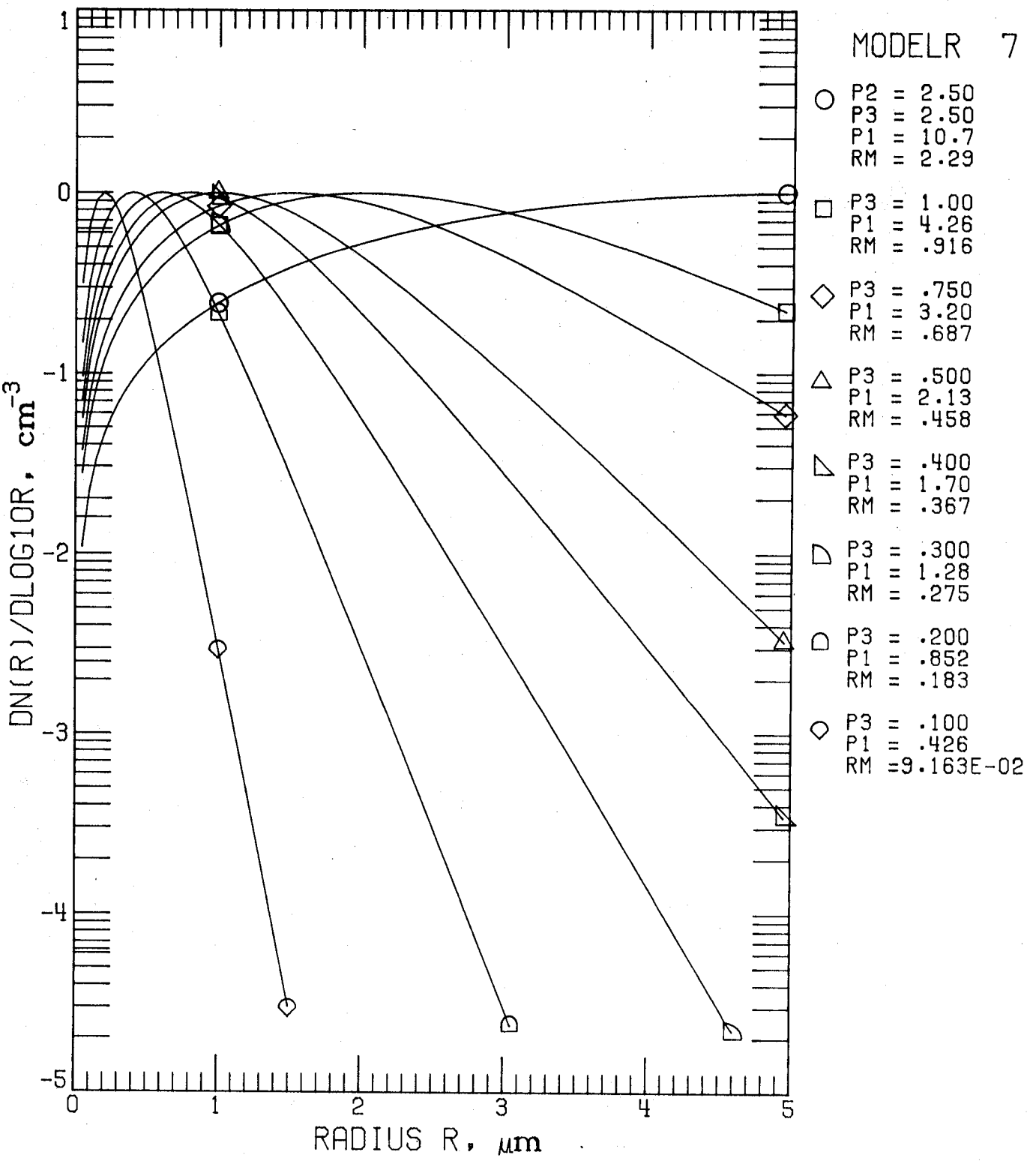

Figure 7B.3. Model 7 for $n_L(r)$.
Parameter Set 7.3.

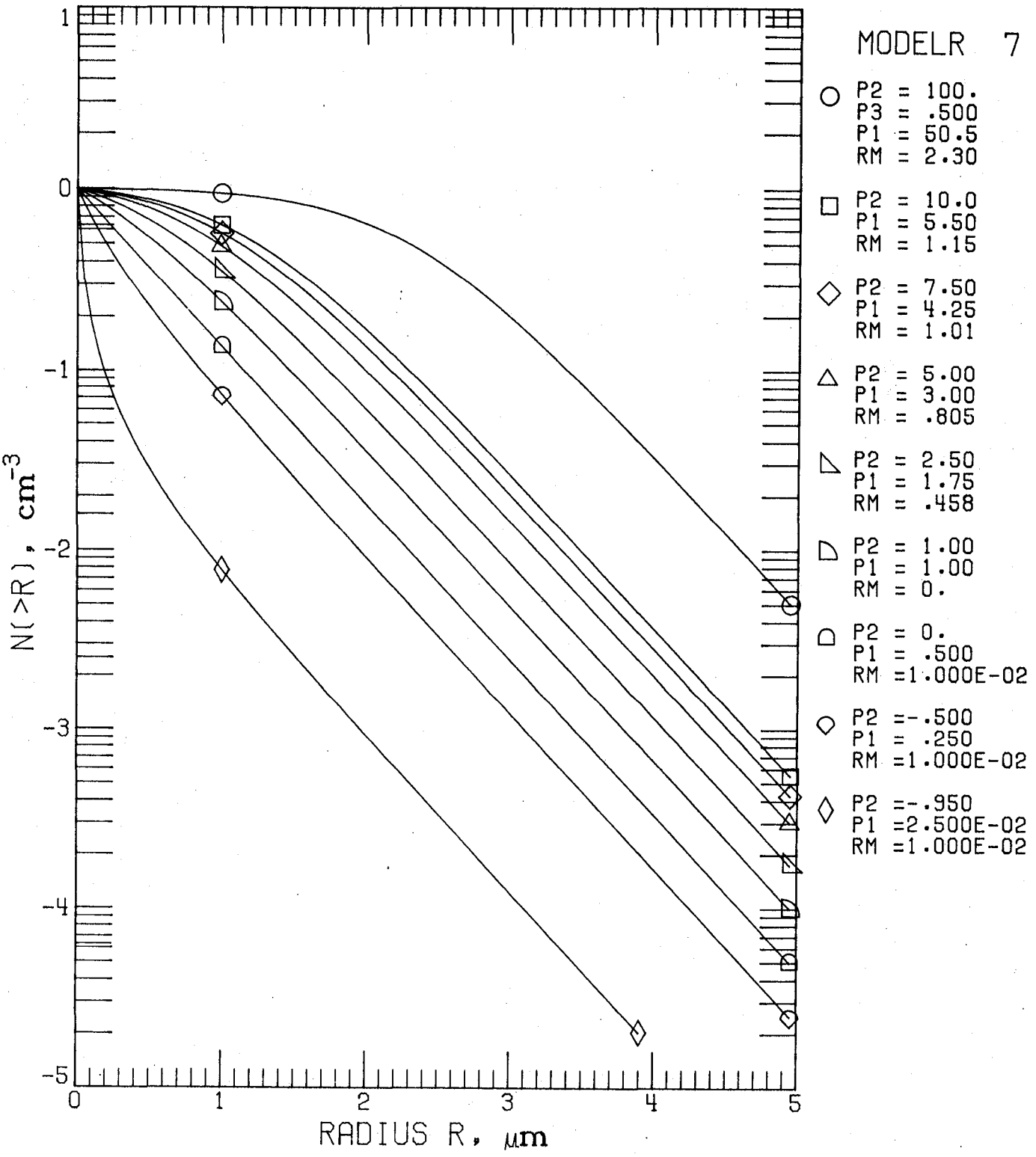

Figure 7C.1. Model 7 for N(>r).
Parameter Set 7.1.

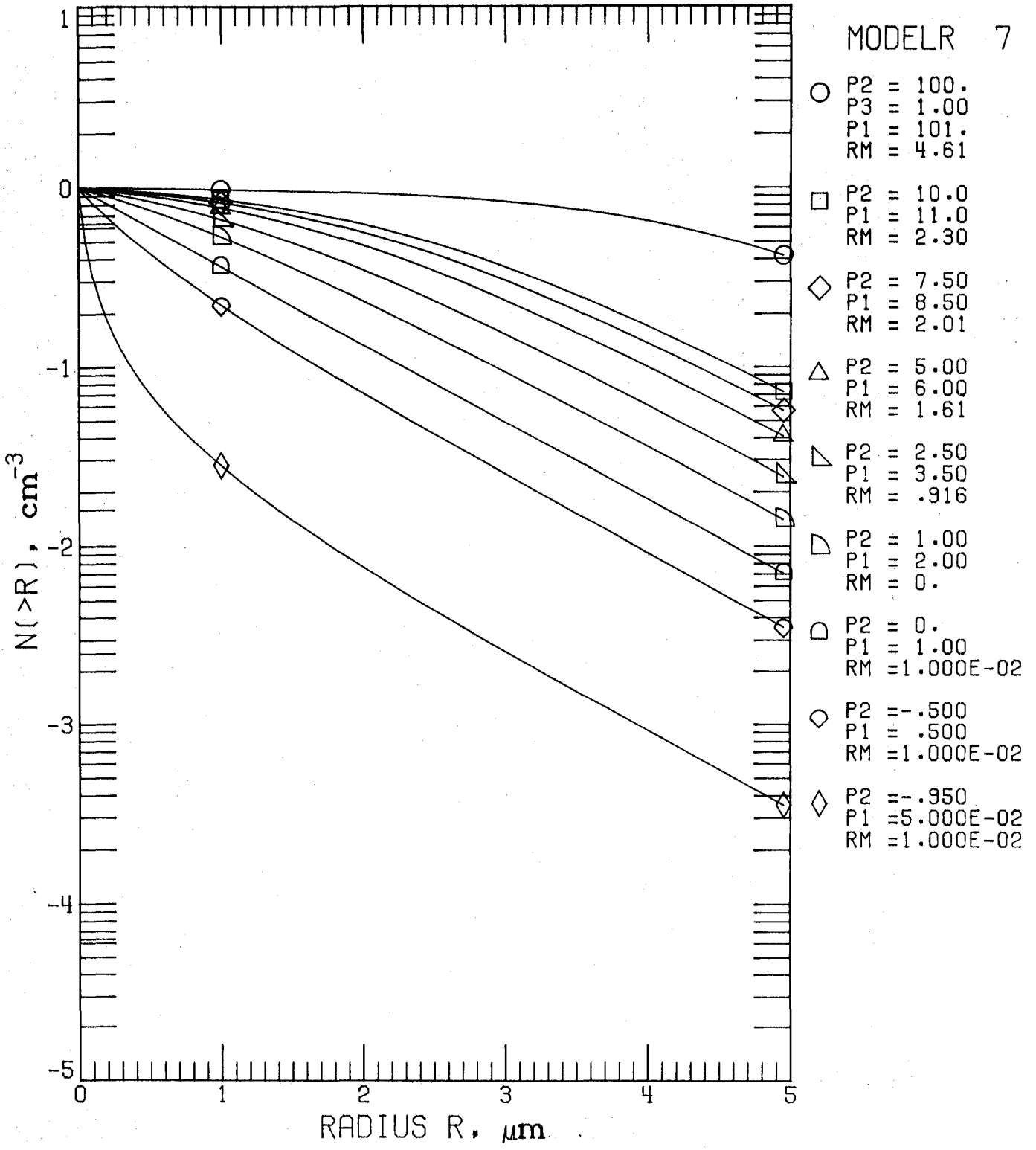

Figure 7C.2. Model 7 for N(>r).
Parameter Set 7.2.

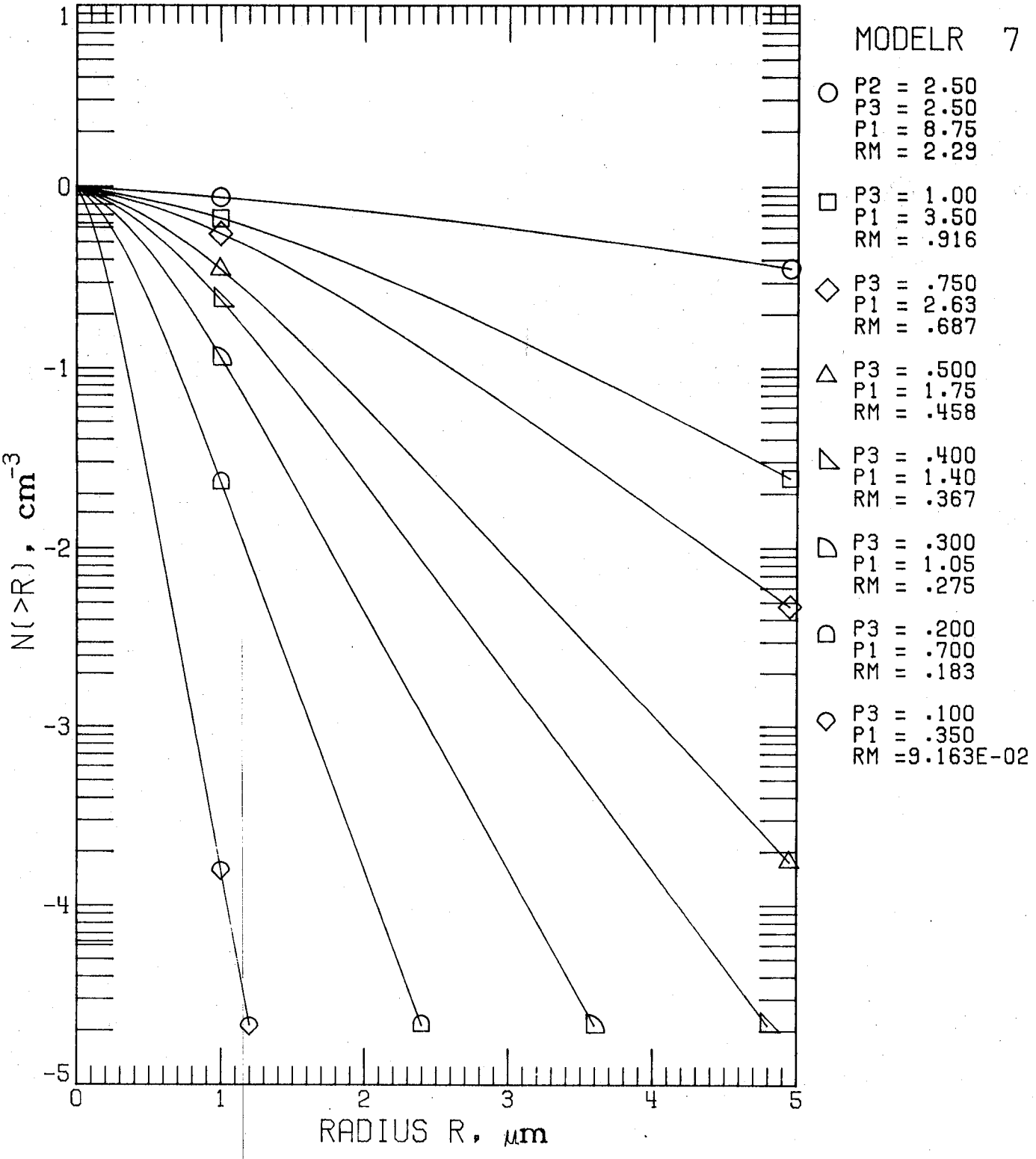

Figure 7C.3. Model 7 for N(>r).
Parameter Set 7.3.

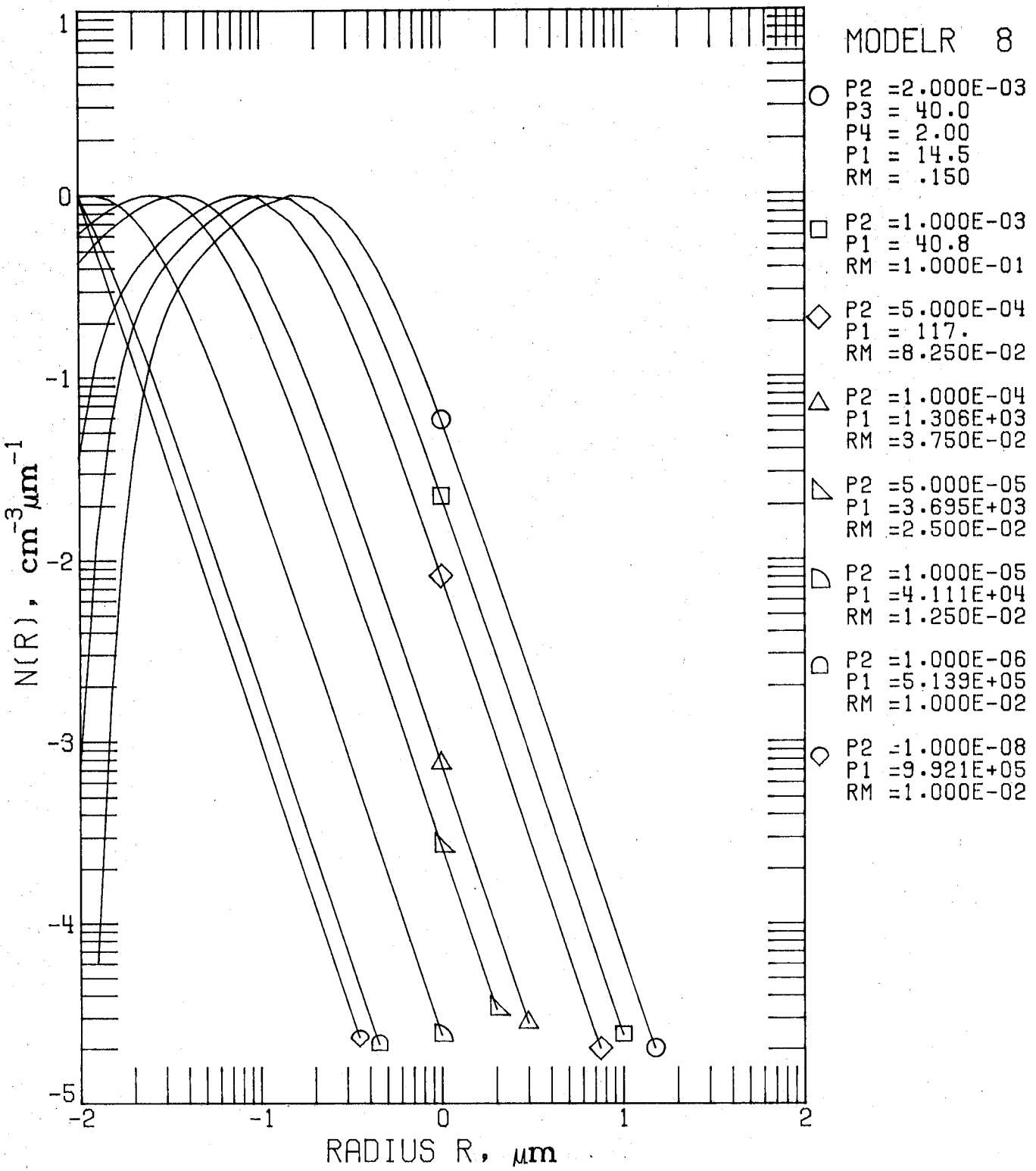

Figure 8A.1. Model 8 (Power Law--Generalized Distribution Function) for n(r). Parameter Set 8.1: p_2 variable, p_3 = 40.0, p_4 = 2.0.

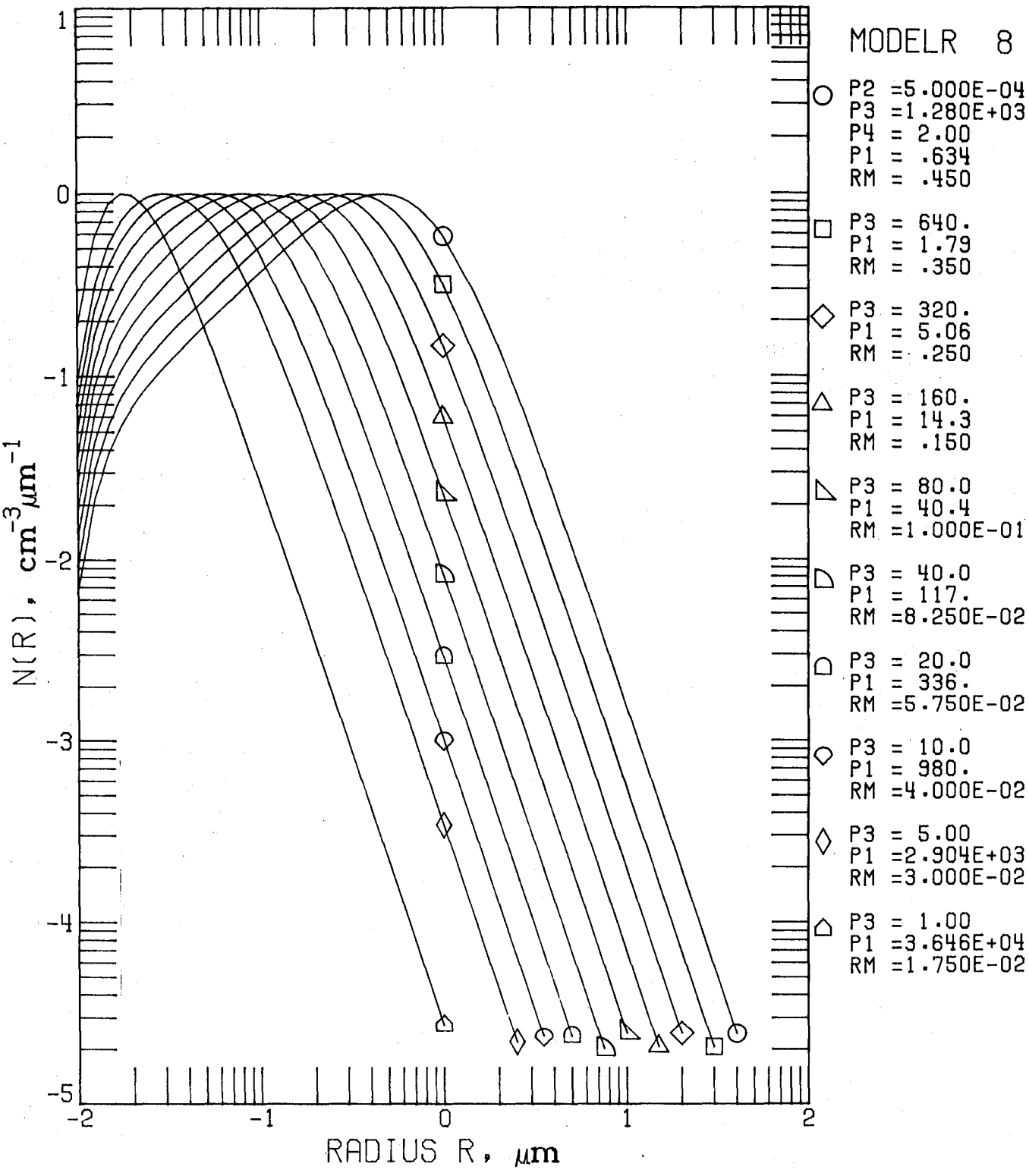

Figure 8A.2. Model 8 for n(r).
Parameter Set 8.2: p_3 variable,
$p_2 = 5.0 \times 10^{-4}$, $p_4 = 2.0$.

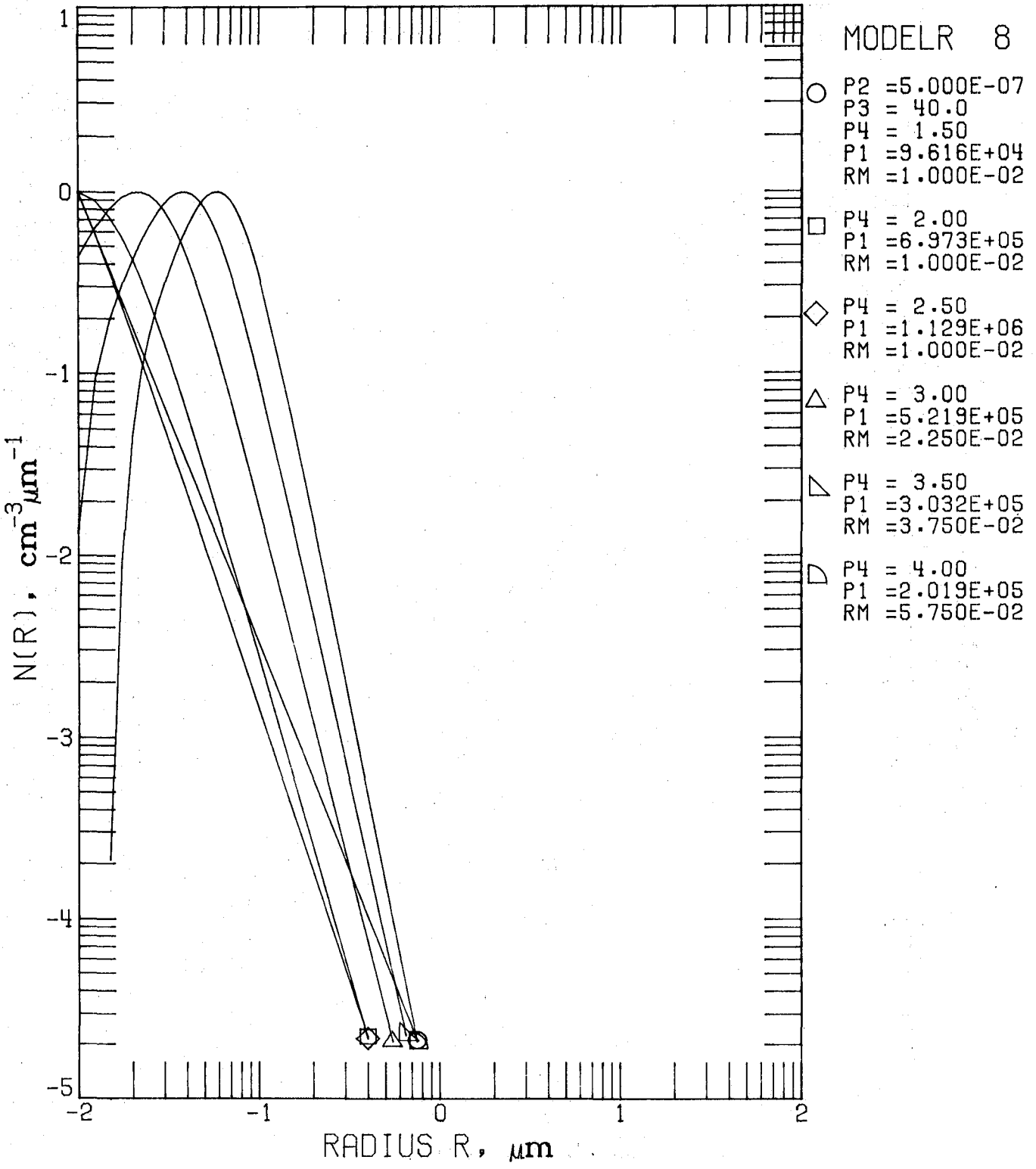

Figure 8A.3. Model 8 for n(r).
Parameter Set 8.3: p_4 variable,
$p_2 = 5.0 \times 10^{-4}$, $p_3 = 40.0$.

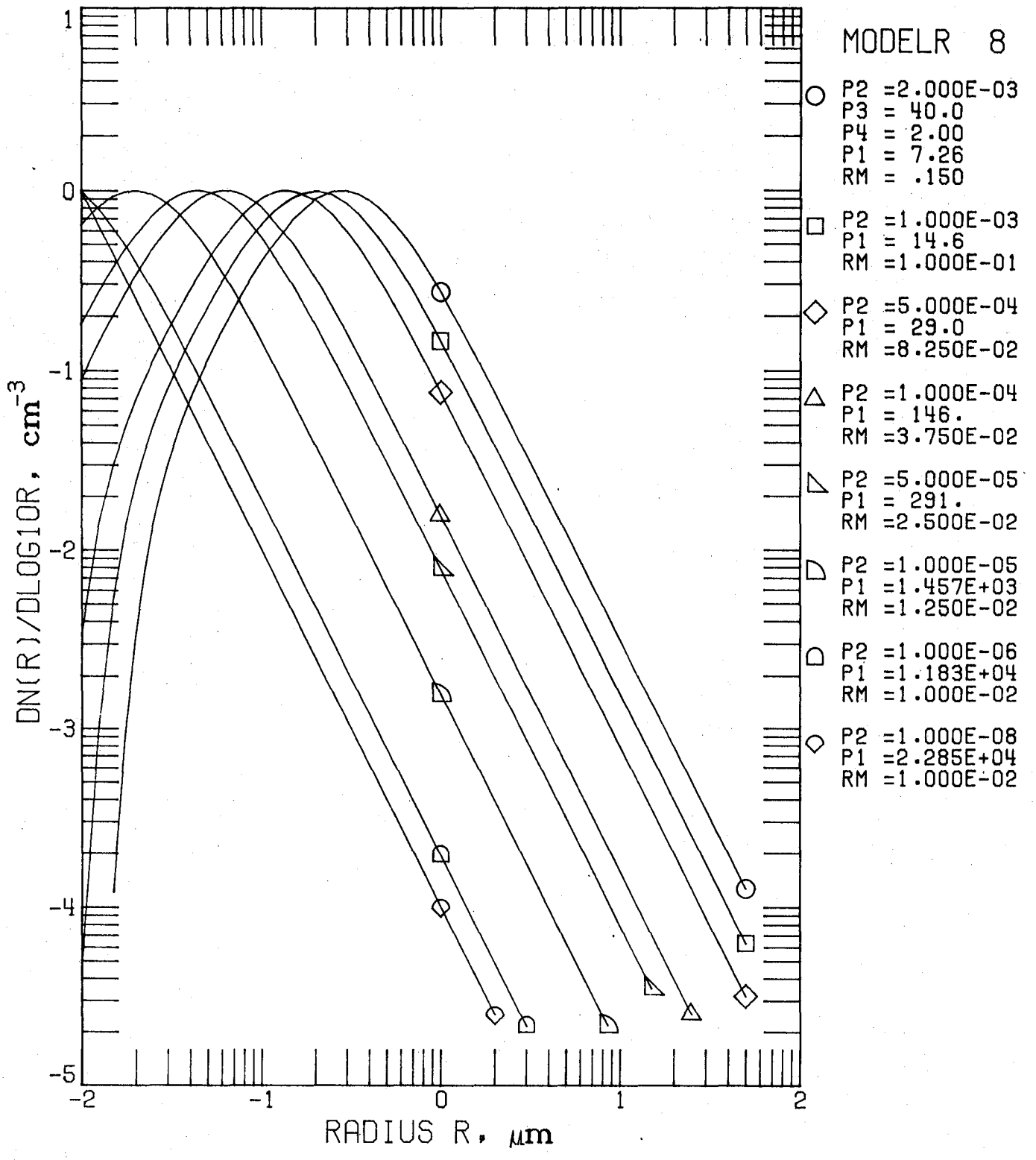

Figure 8B.1. Model 8 for $n_L(r)$.
Parameter Set 8.1.

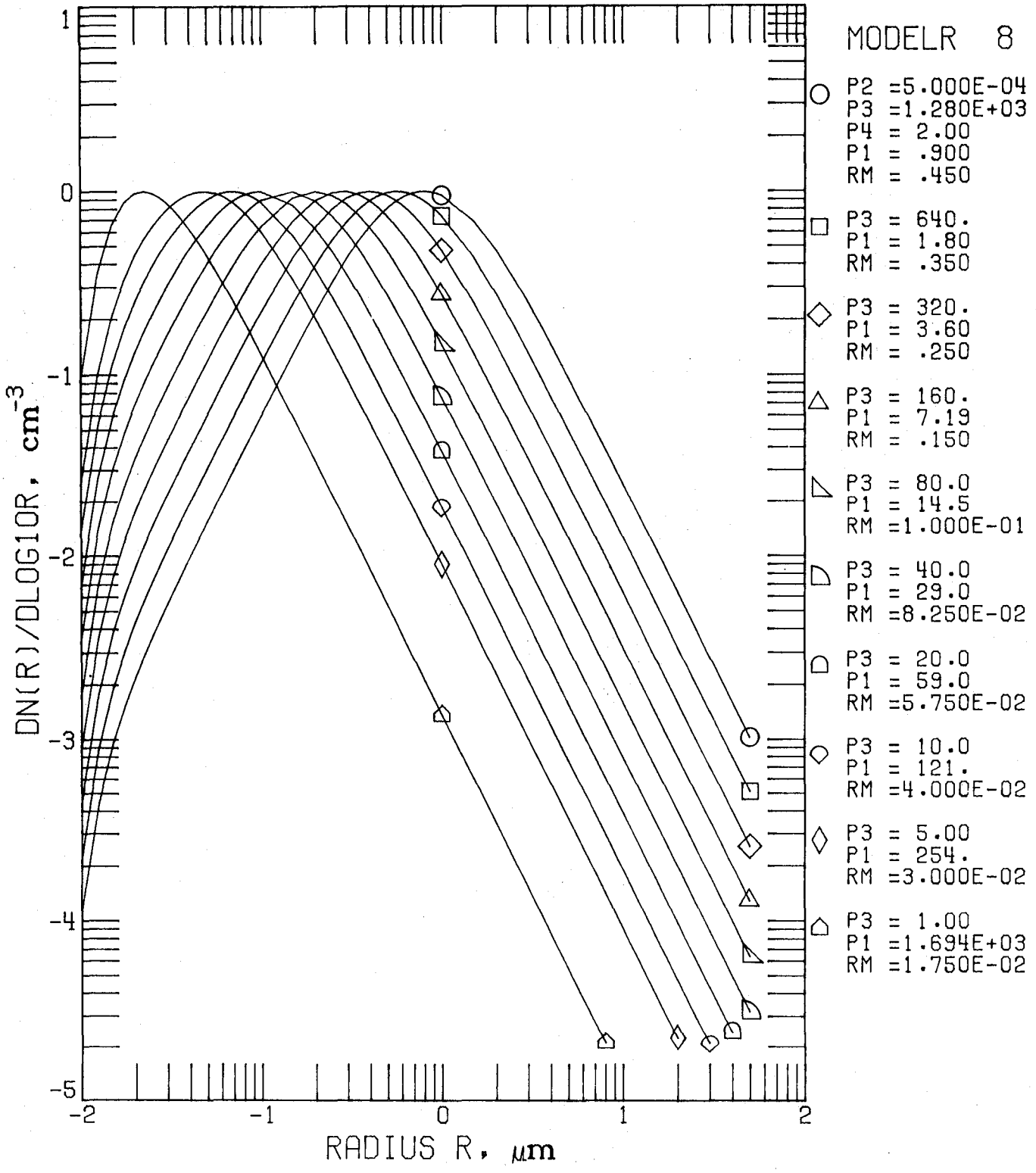

Figure 8B.2. Model 8 for $n_L(r)$.
Parameter Set 8.2.

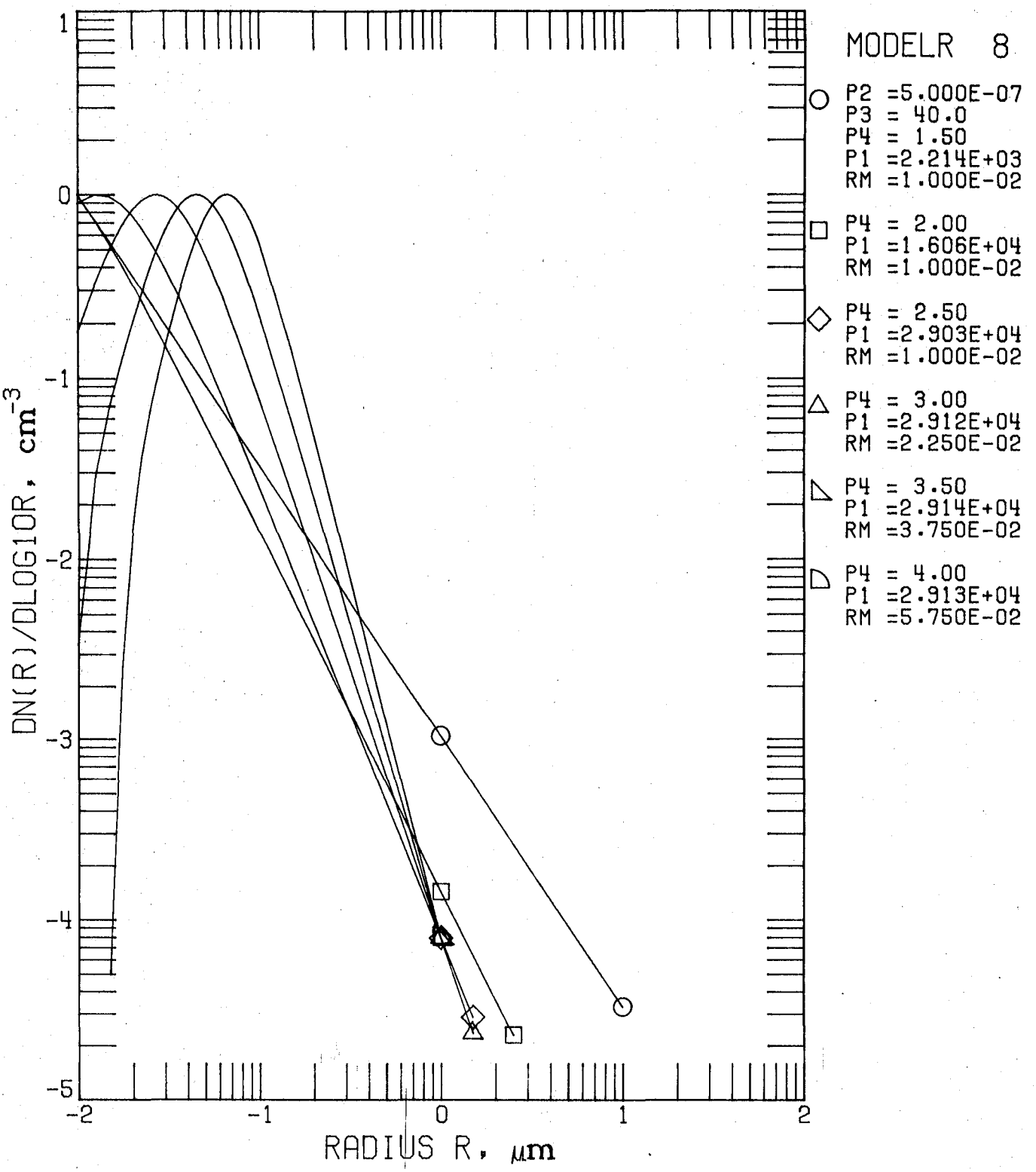

Figure 8B.3. Model 8 for $n_L(r)$.
Parameter Set 8.3.

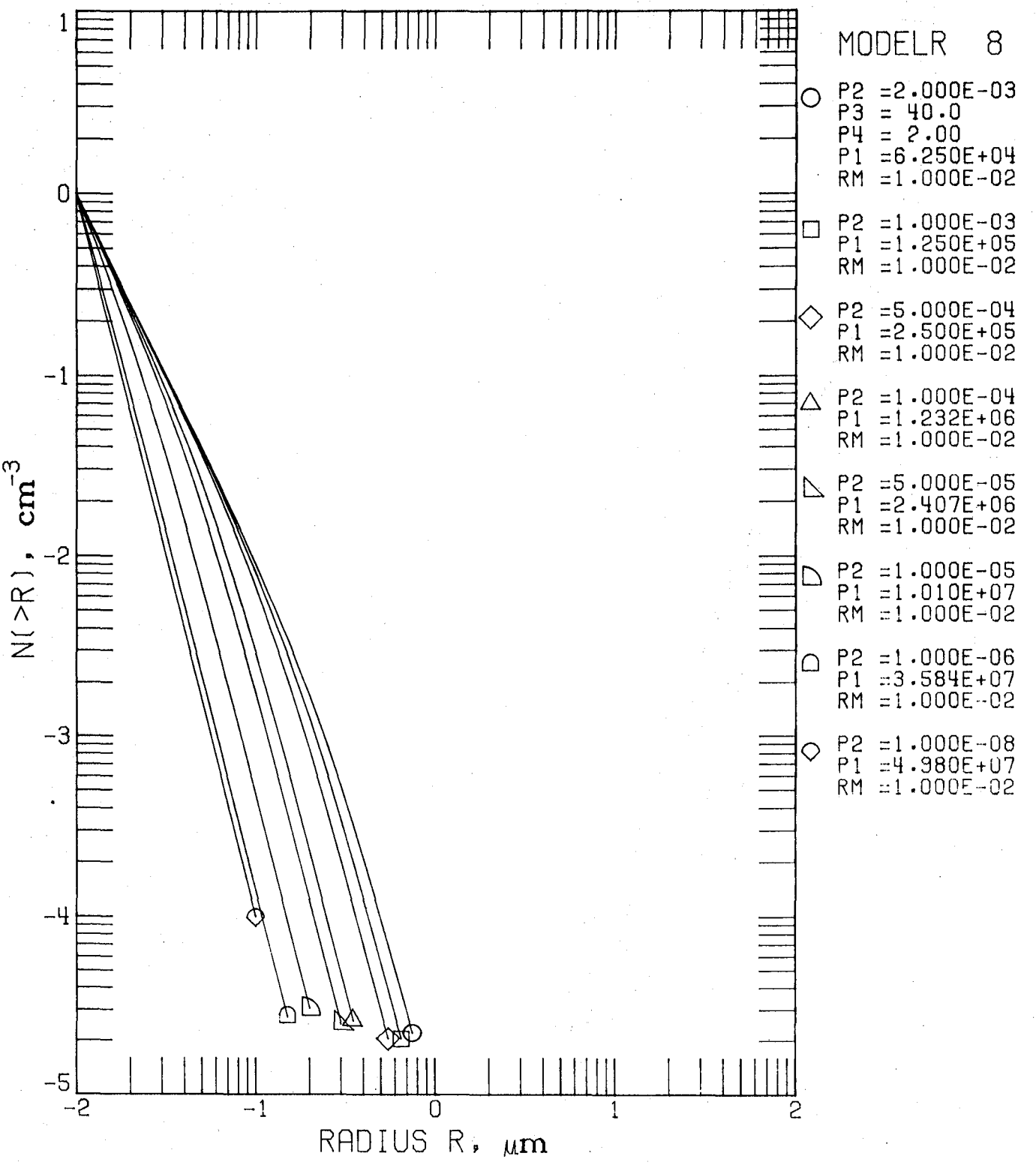

Figure 8C.1. Model 8 for N (>r).
Parameter Set 8.1.

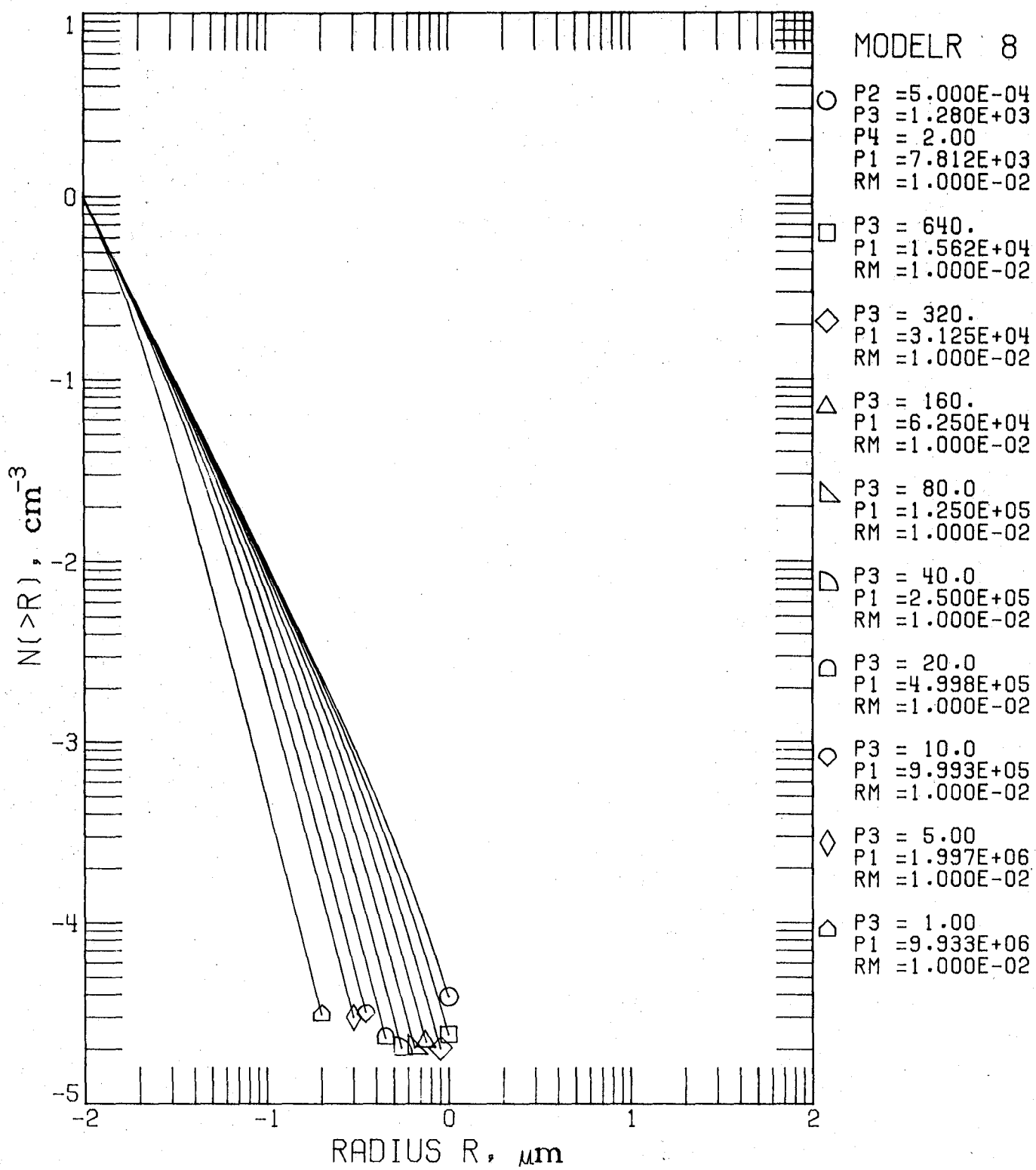

Figure 8C.2. Model 8 for N(>r).
Parameter Set 8.2.

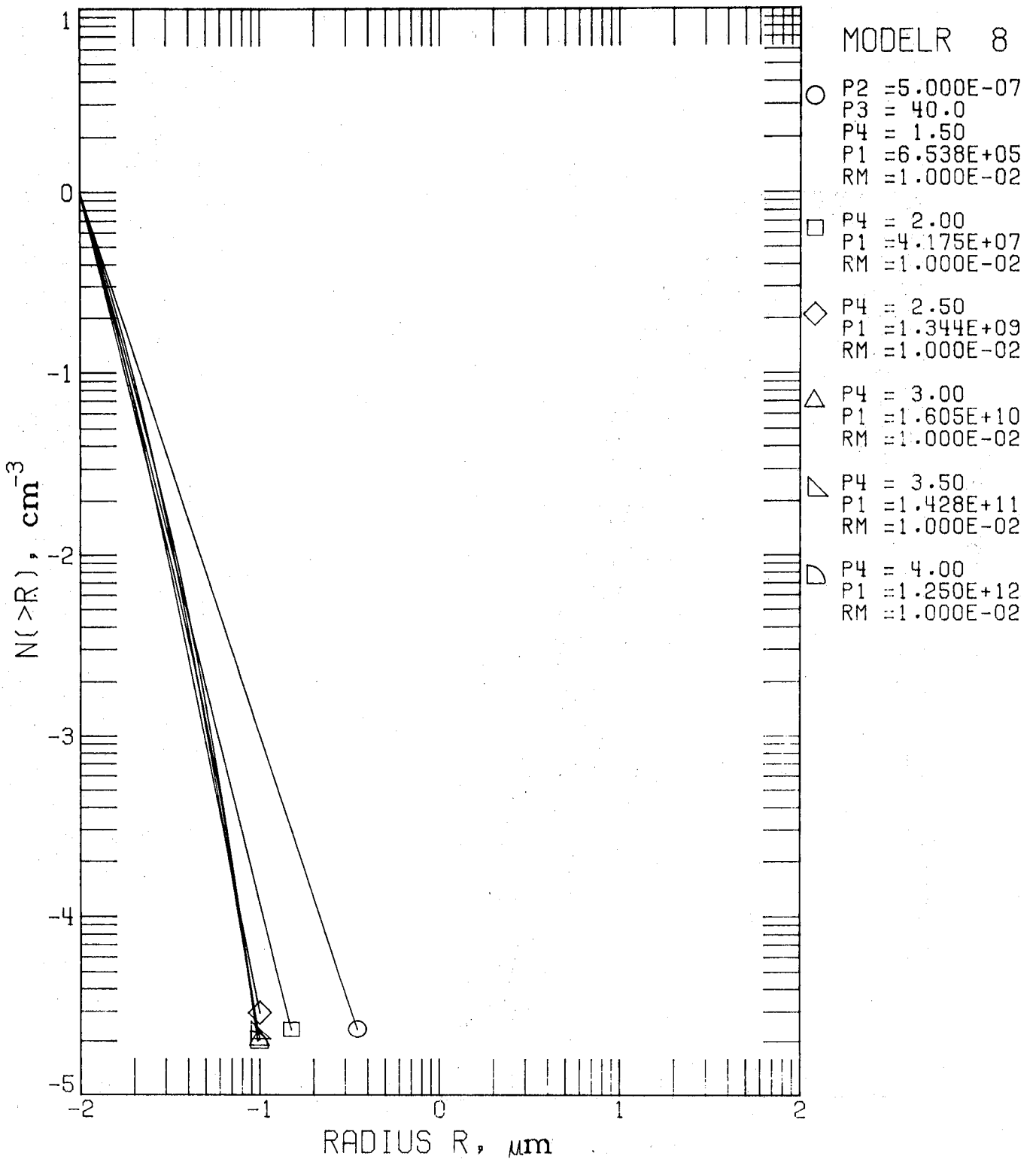

Figure 8C.3. Model 8 for N(>r).
Parameter Set 8.3.

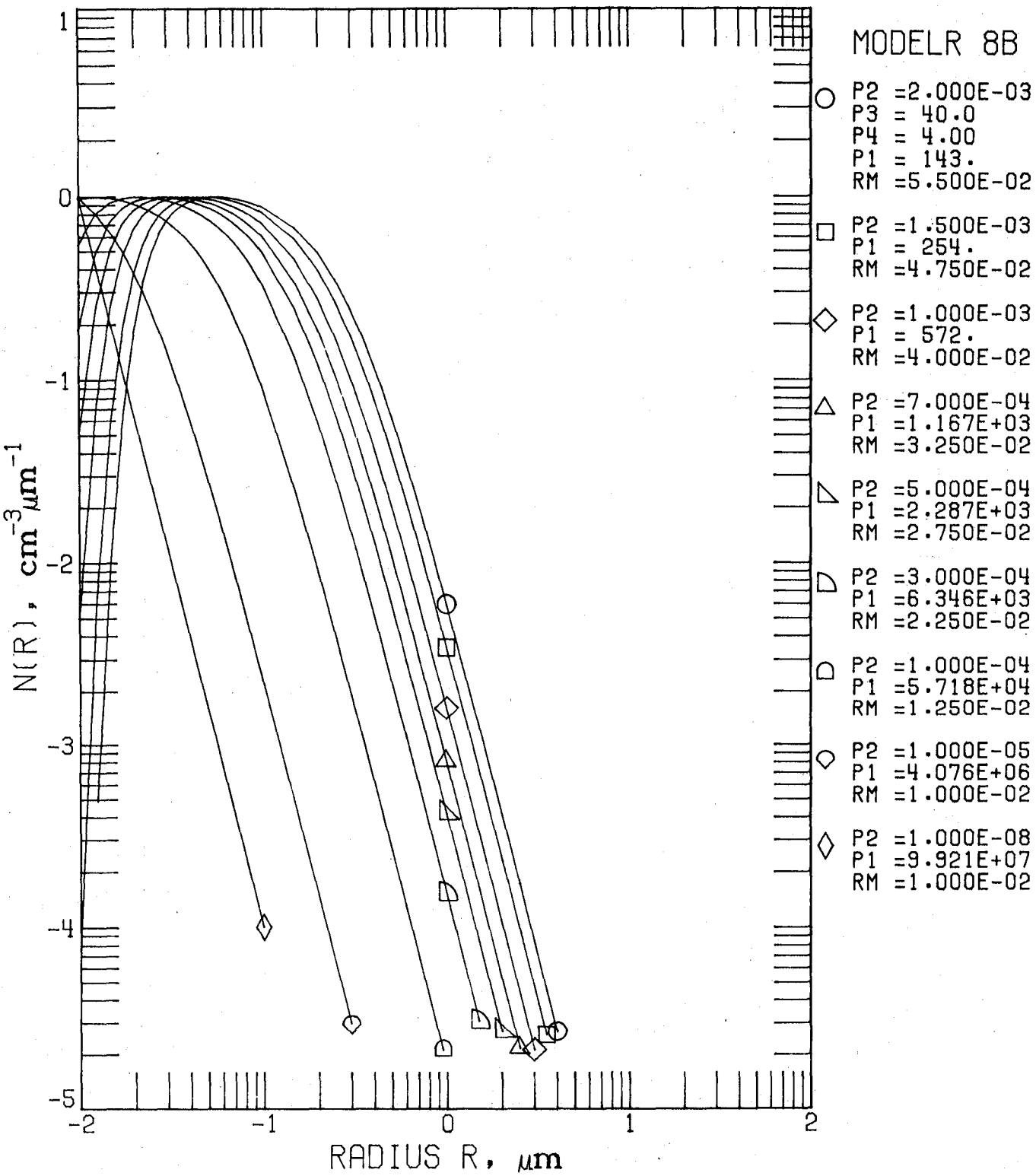

Figure 8D.1. Model 8B (Power Law--Generalized Distribution Function) for n(r). Parameter Set 8.4: p_2 variable, p_3 = 40.0, p_4 = 4.0.

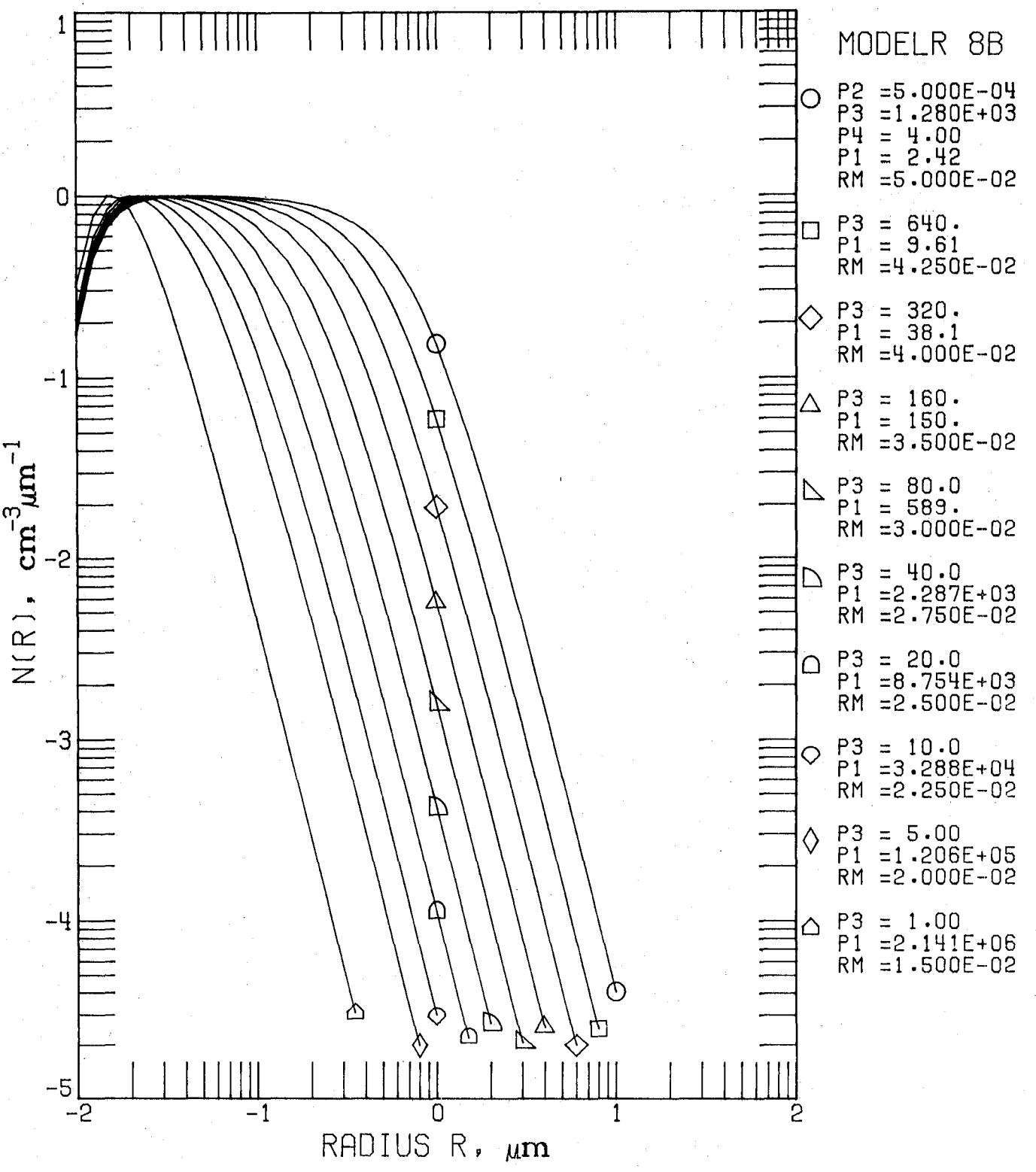

Figure 8D.2. Model 8B for n(r).
Parameter Set 8.5: p_3 variable,
$p_2 = 5.0 \times 10^{-4}$, $p_4 = 4.0$.

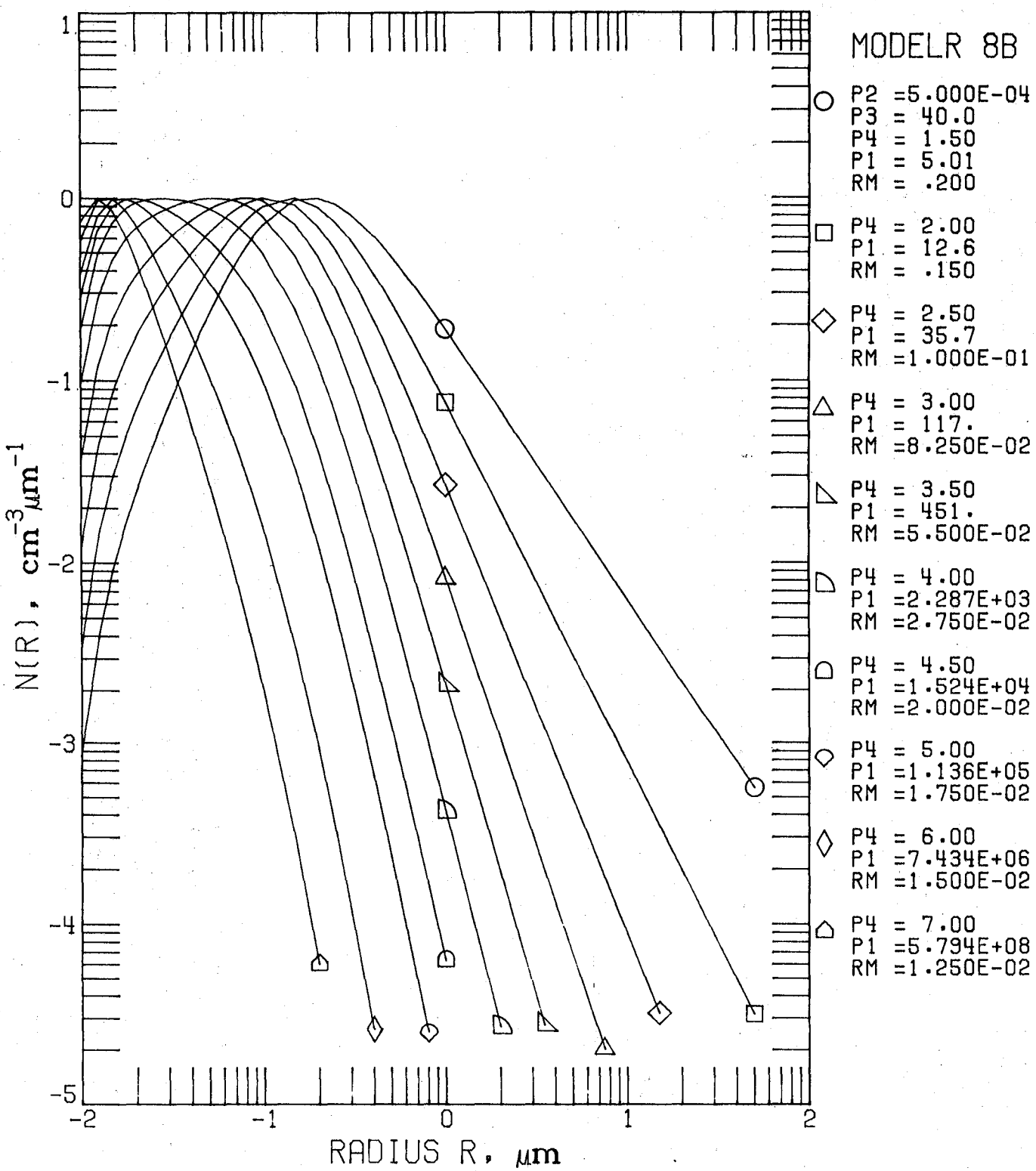

Figure 8D.3. Model 8B for n(r).
Parameter Set 8.6: p_4 variable,
$p_2 = 5.0 \times 10^{-4}$, $p_3 = 40.0$.

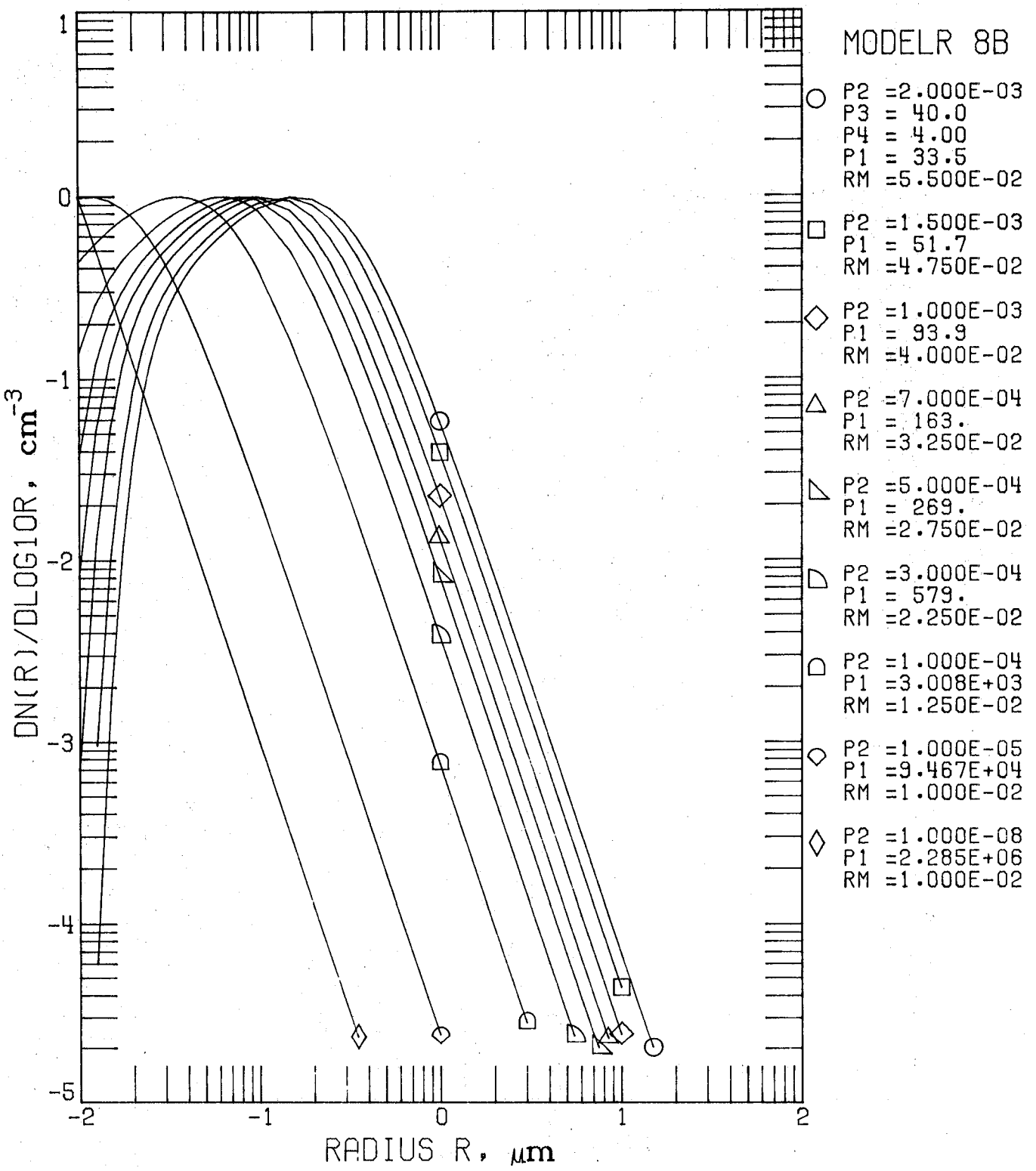

Figure 8E.1. Model 8B for $n_L(r)$.
Parameter Set 8.4.

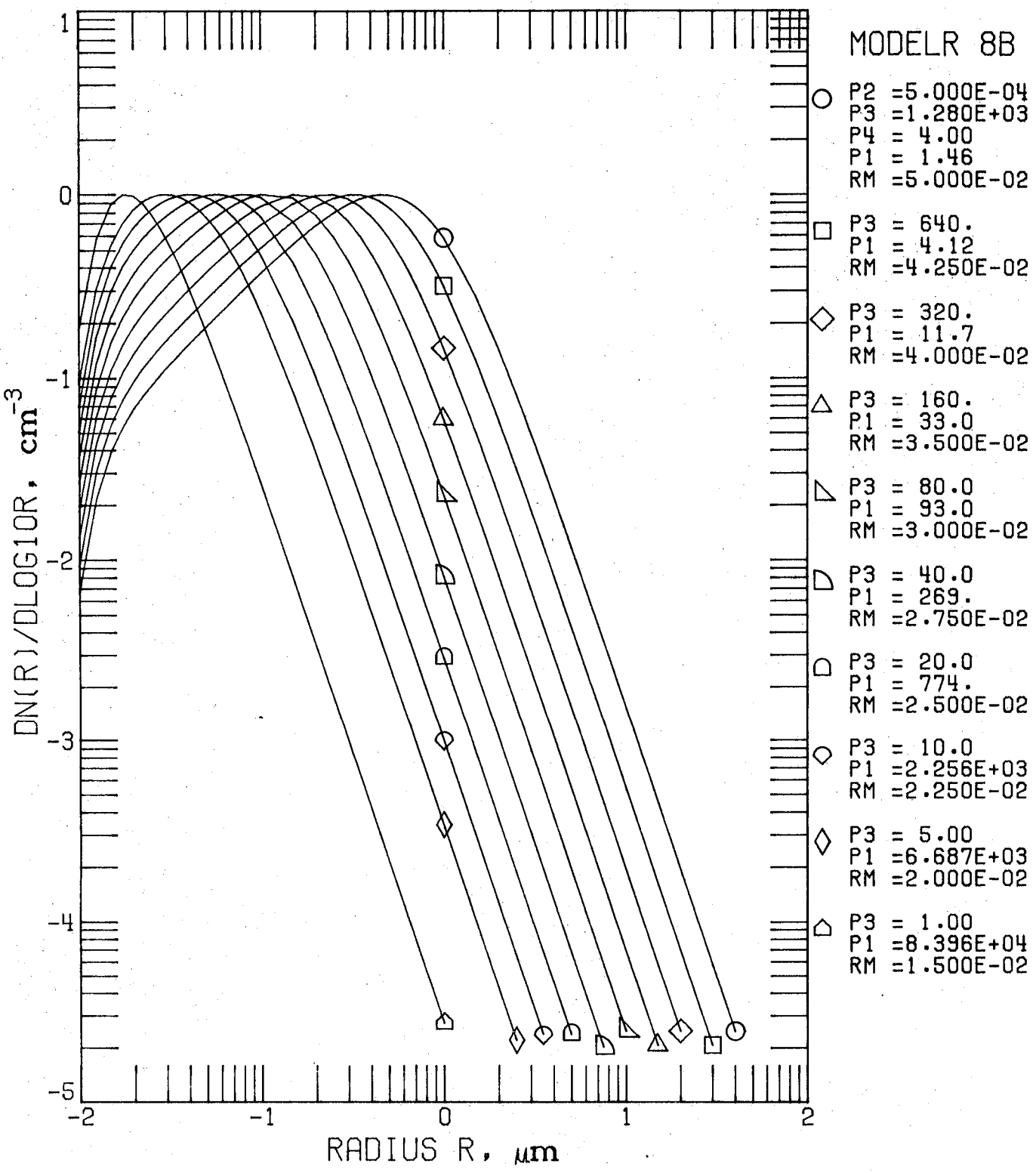

Figure 8E.2. Model 8B for $n_L(r)$.
Parameter Set 8.5.

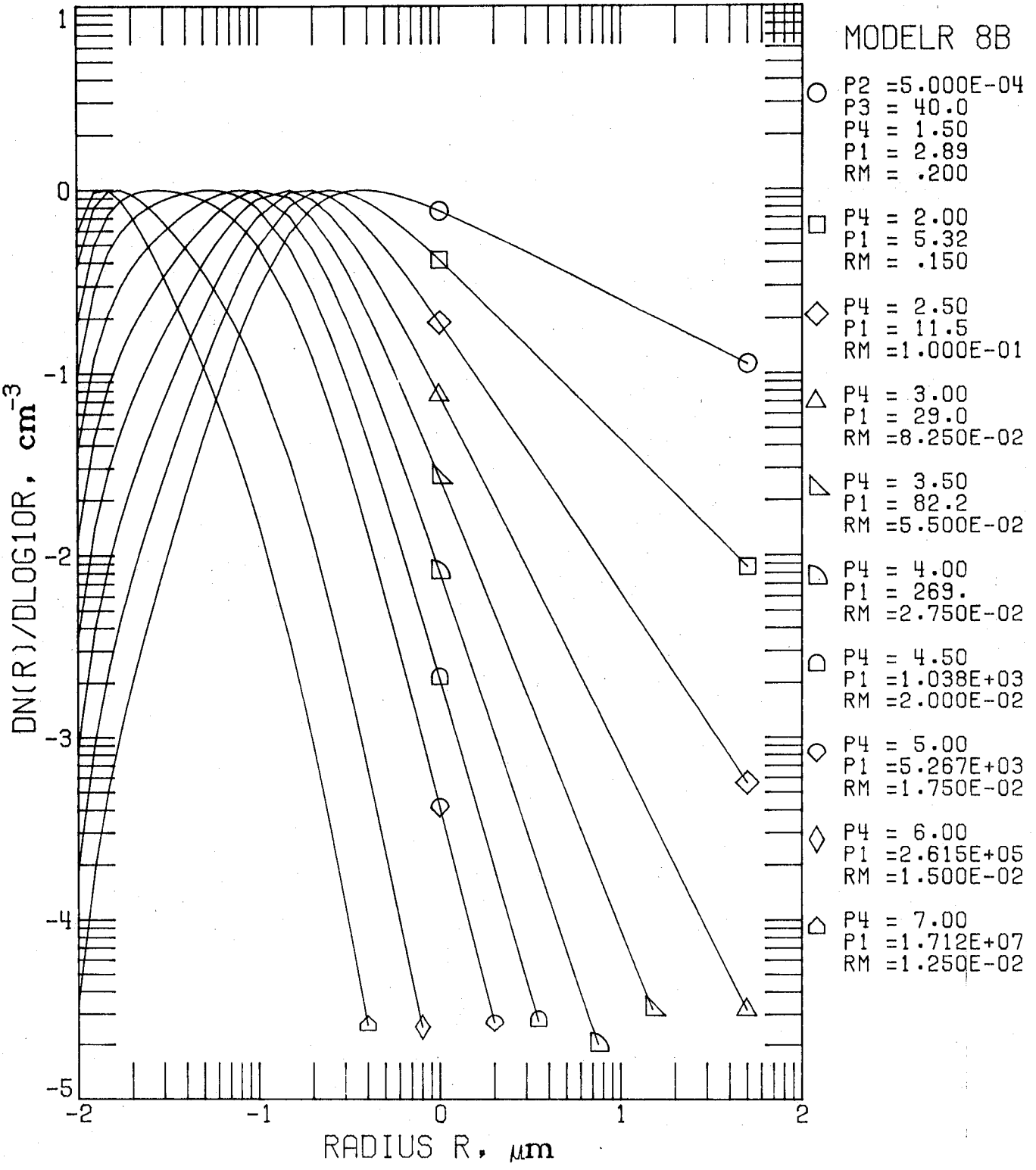

Figure 8E.3. Model 8B for $n_L(r)$.
Parameter Set 8.6.

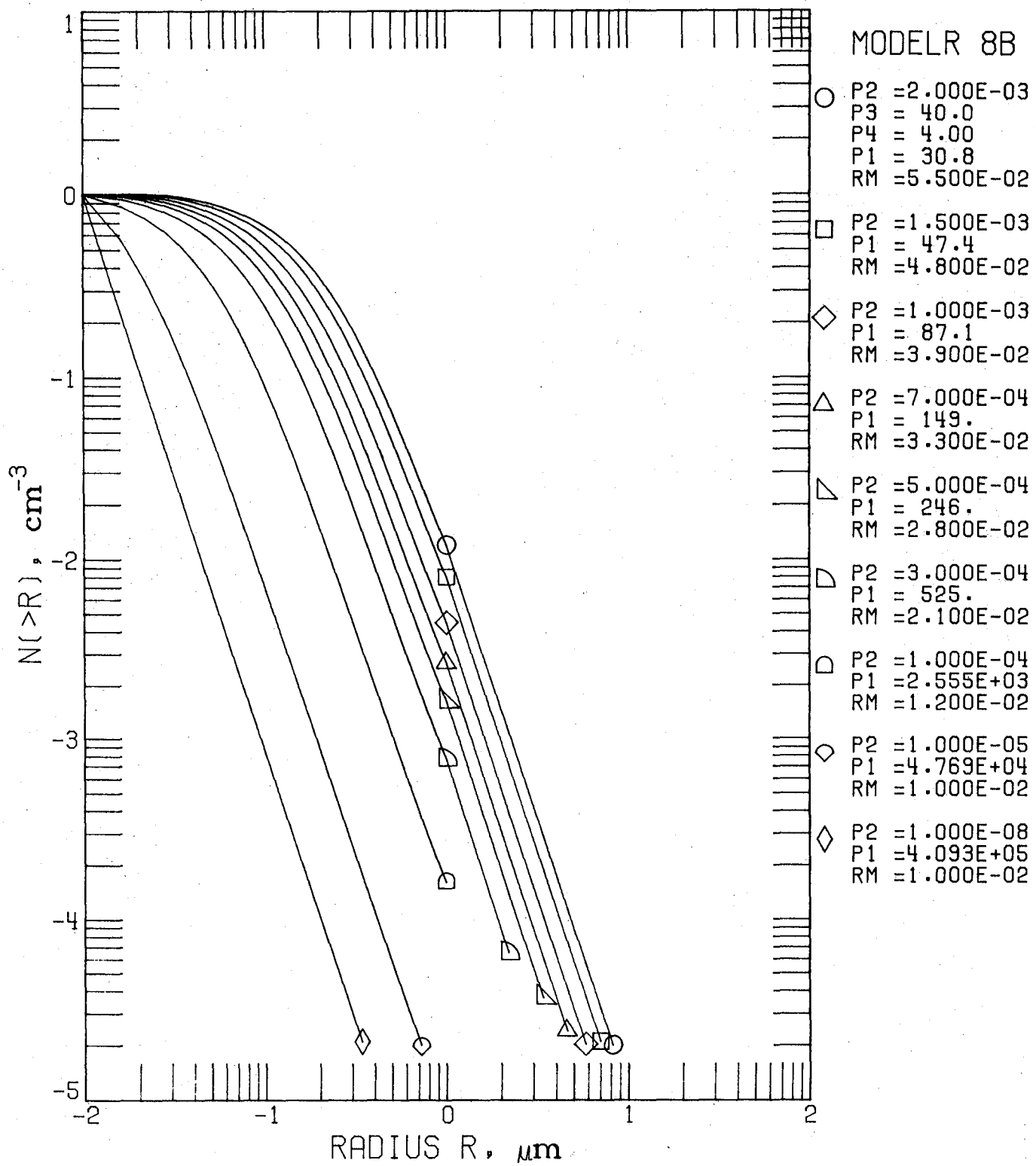

Figure 8F.1. Model 8B for N(>r).
Parameter Set 8.4.

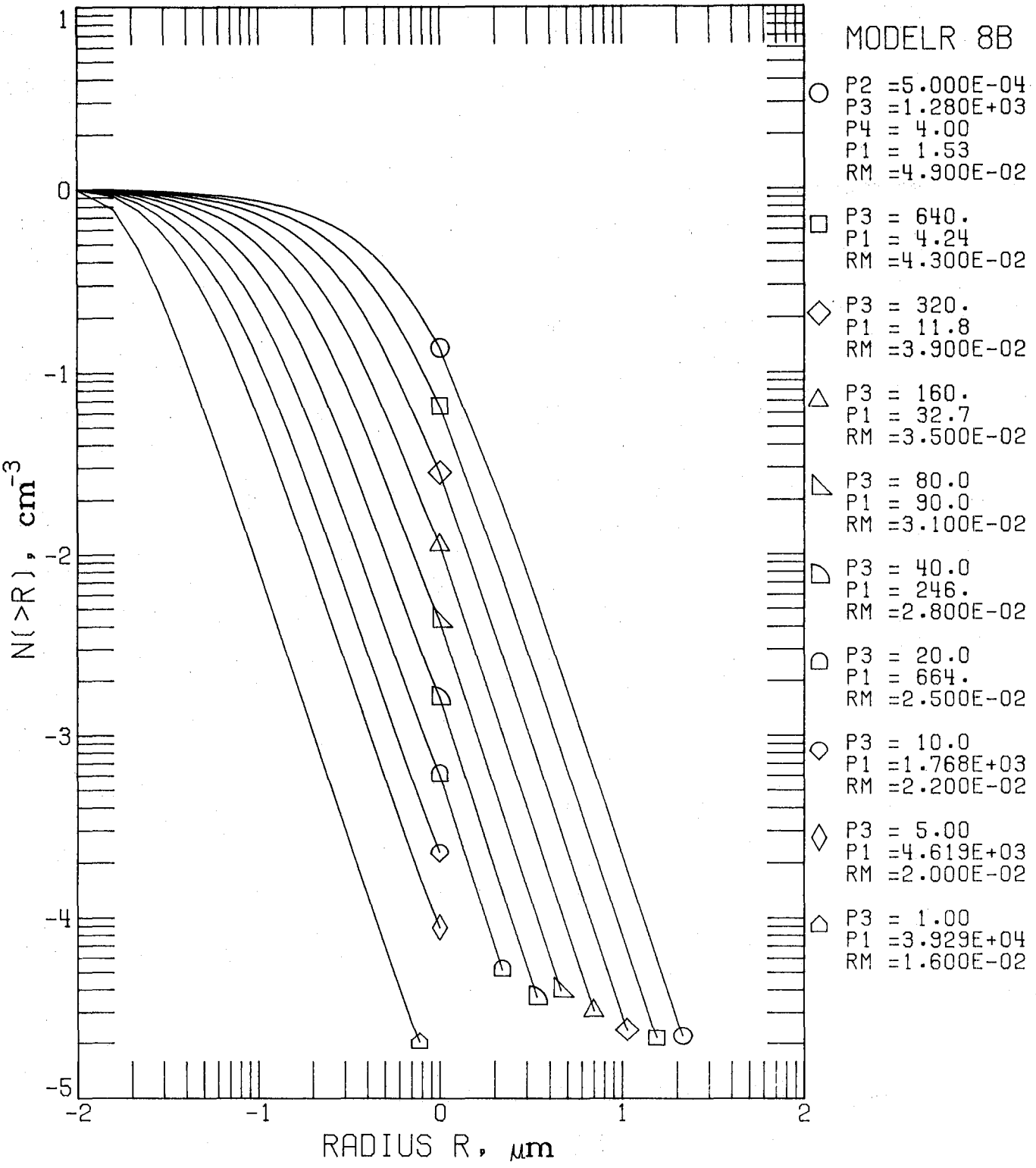

Figure 8F.2. Model 8B for N(>r).
Parameter Set 8.5.

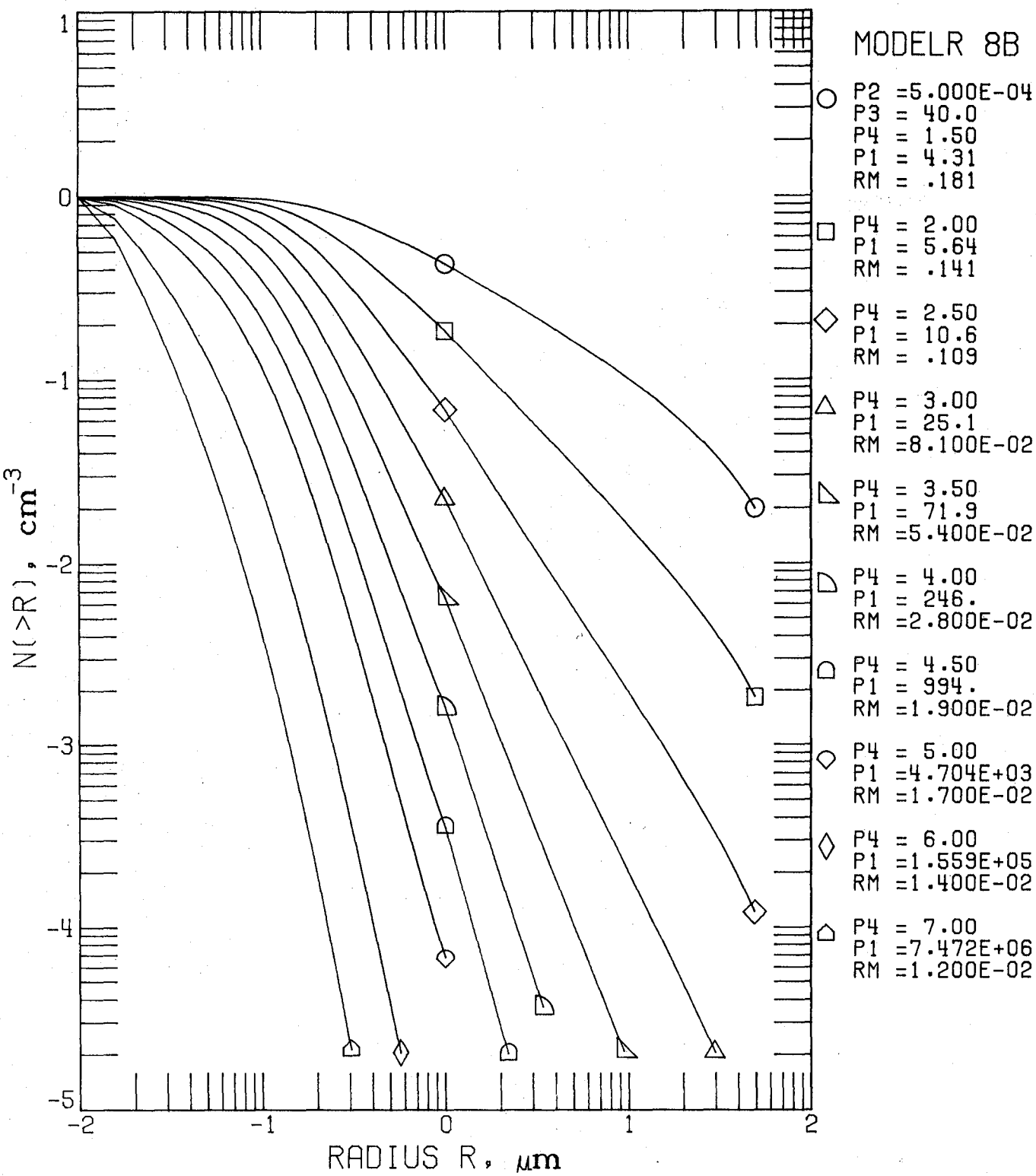

Figure 8F.3. Model 8B for N(>r).
Parameter Set 8.6.

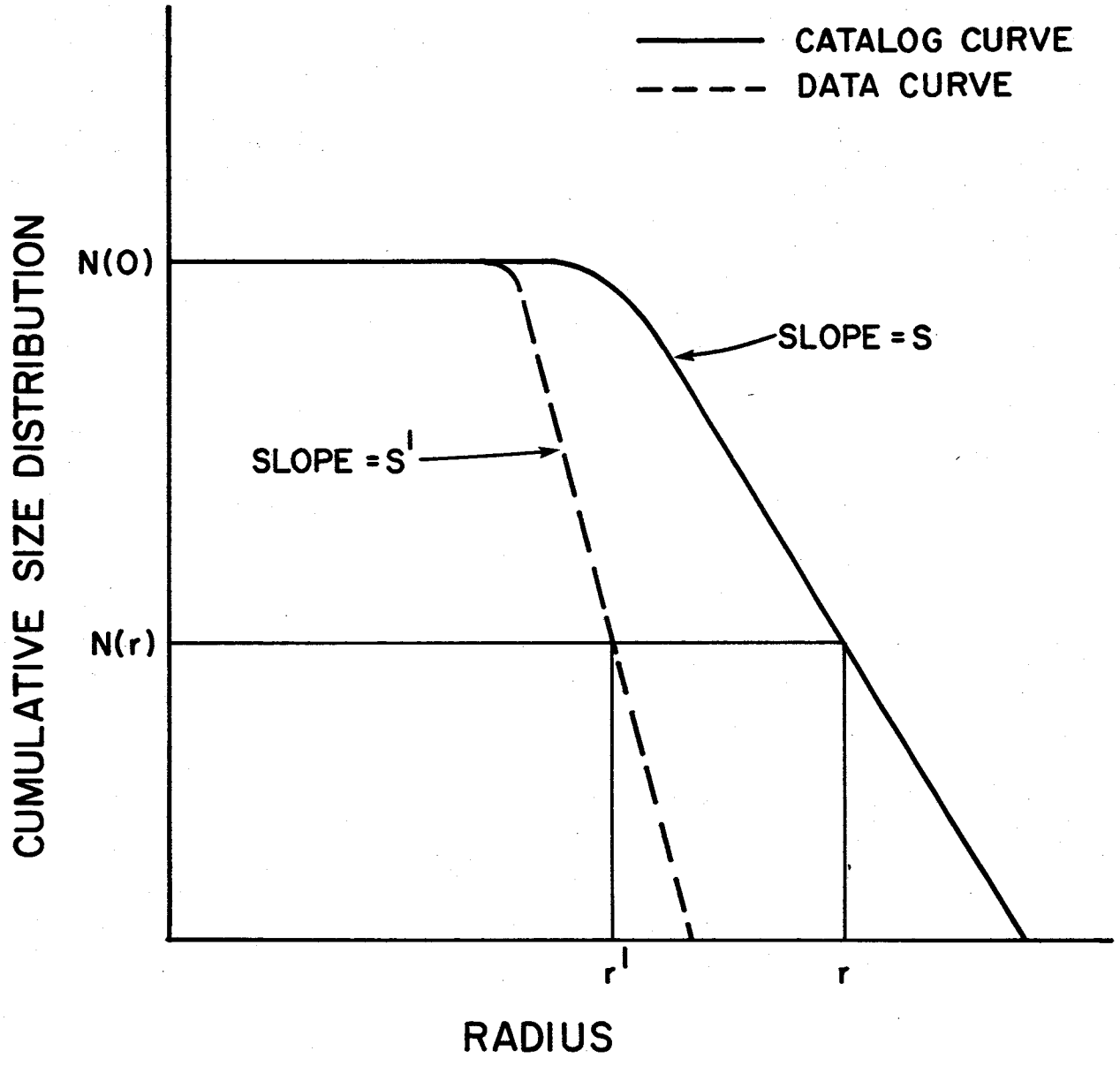

Fig. 9 Determination of the parameter p_2' from the catalog Model 2 for N(>r).

This Page Intentionally Left Blank

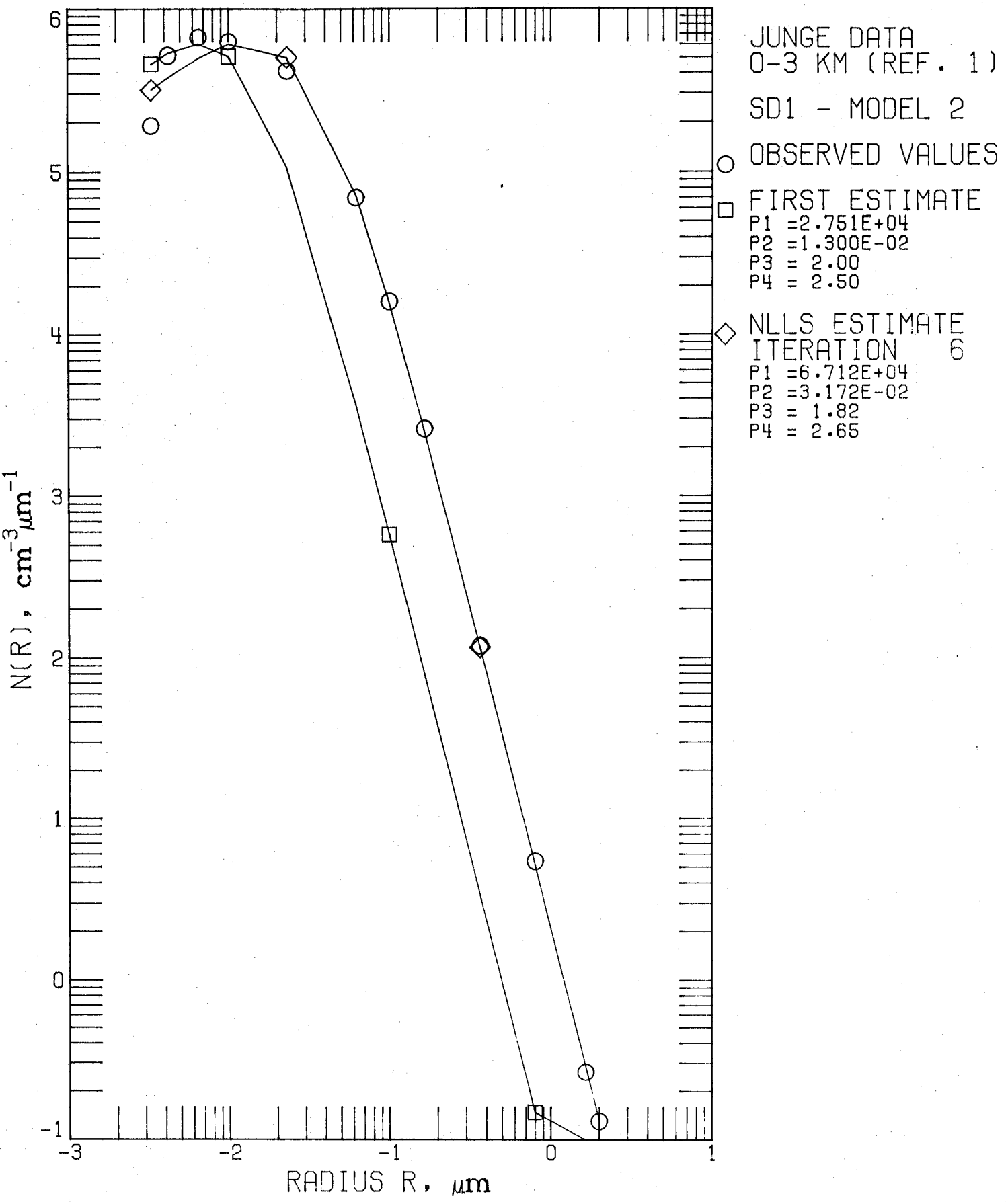

Figure 11. Example of fit to Junge data using Model 2. (Regularized Power Law).

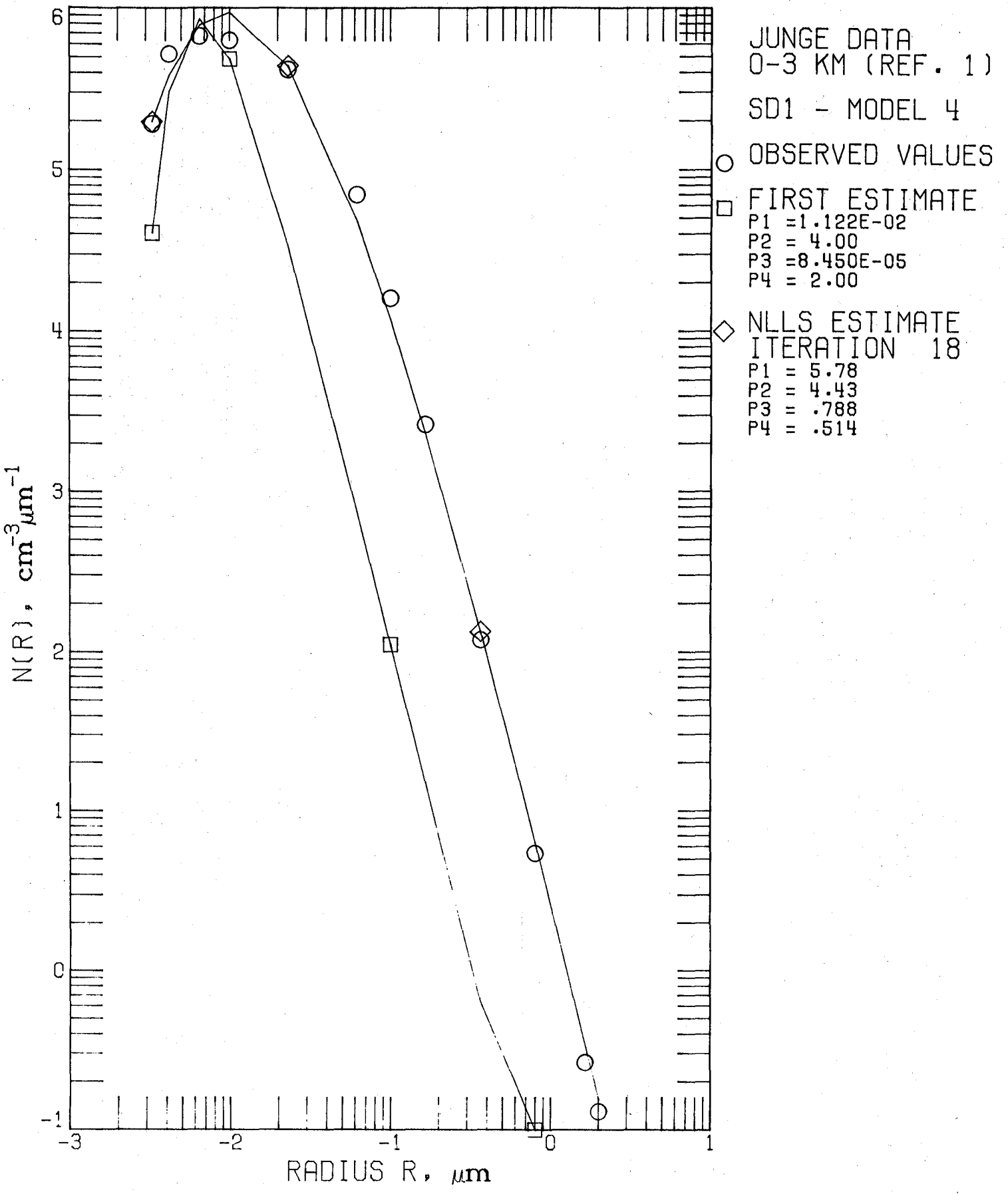

Figure 12. Example of fit to Junge data using Model 4. (Inverse Modified Gamma Distribution).

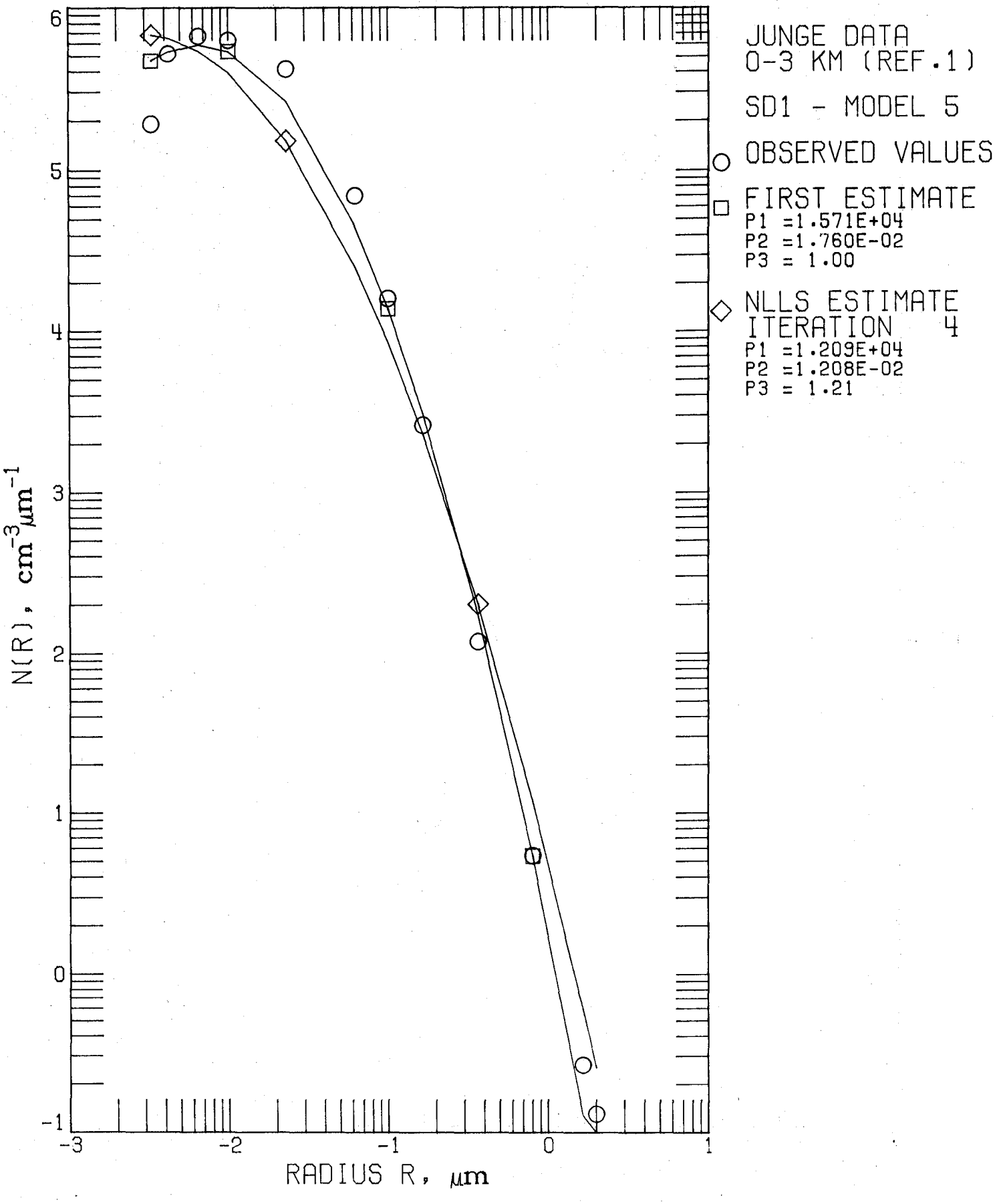

Figure 13. Example of fit to Junge data using Model 5. (Log Normal Distribution)

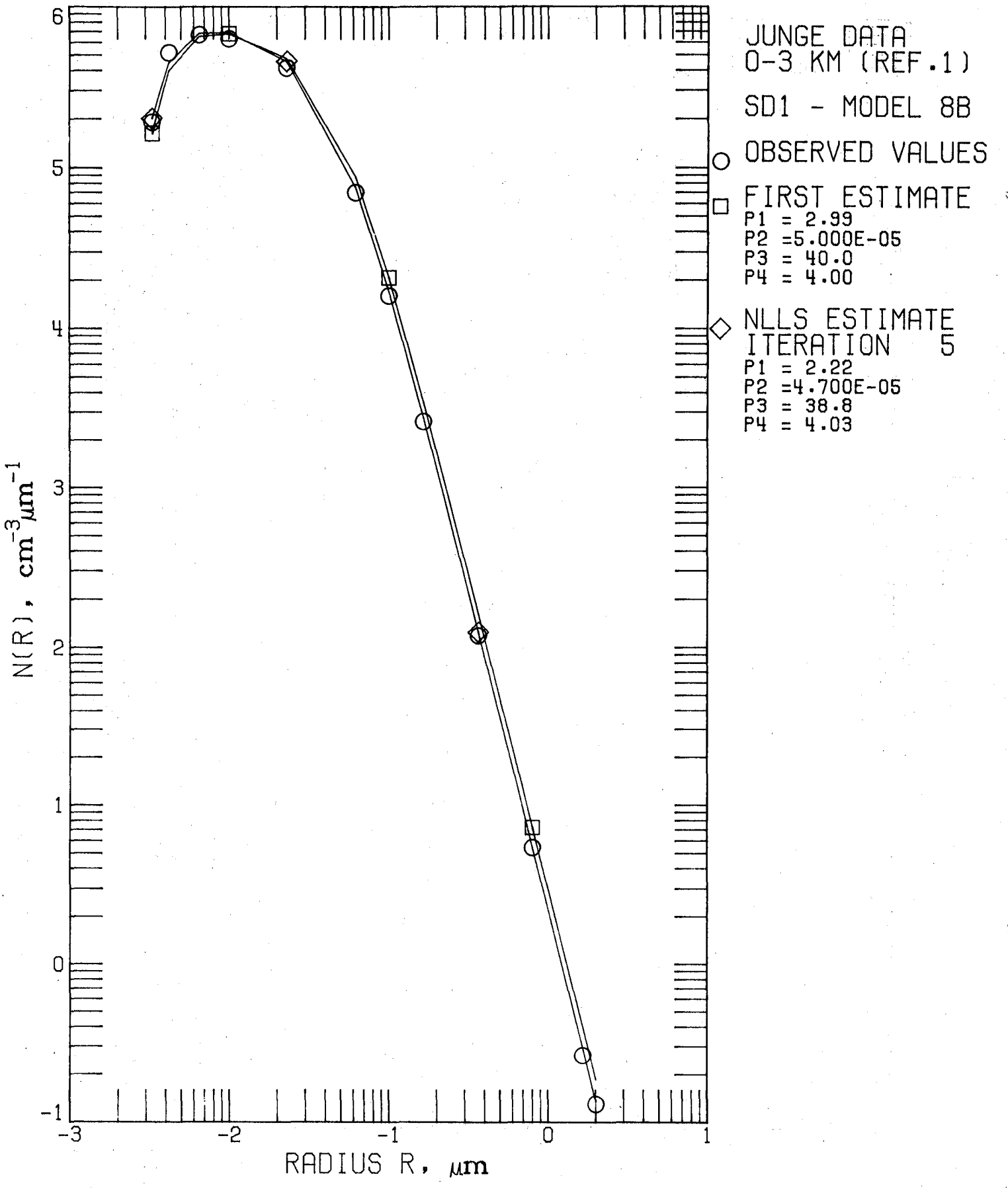

Figure 14. Example of fit to Junge data using Model 8B. (Power Law--Generalized Distribution Function)

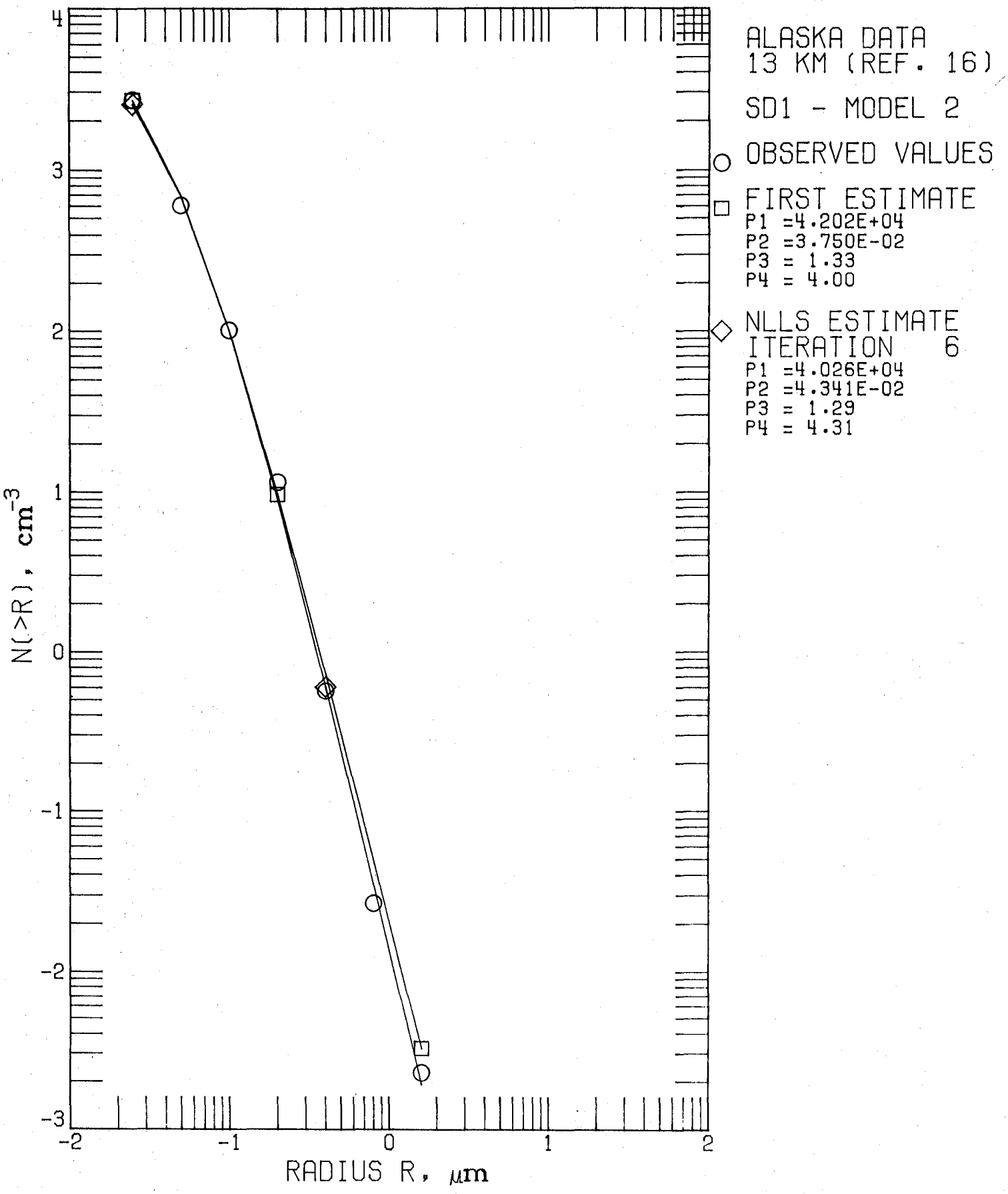

Figure 15. Example of fit to Alaska data using Model 2. (Regularized Power Law).

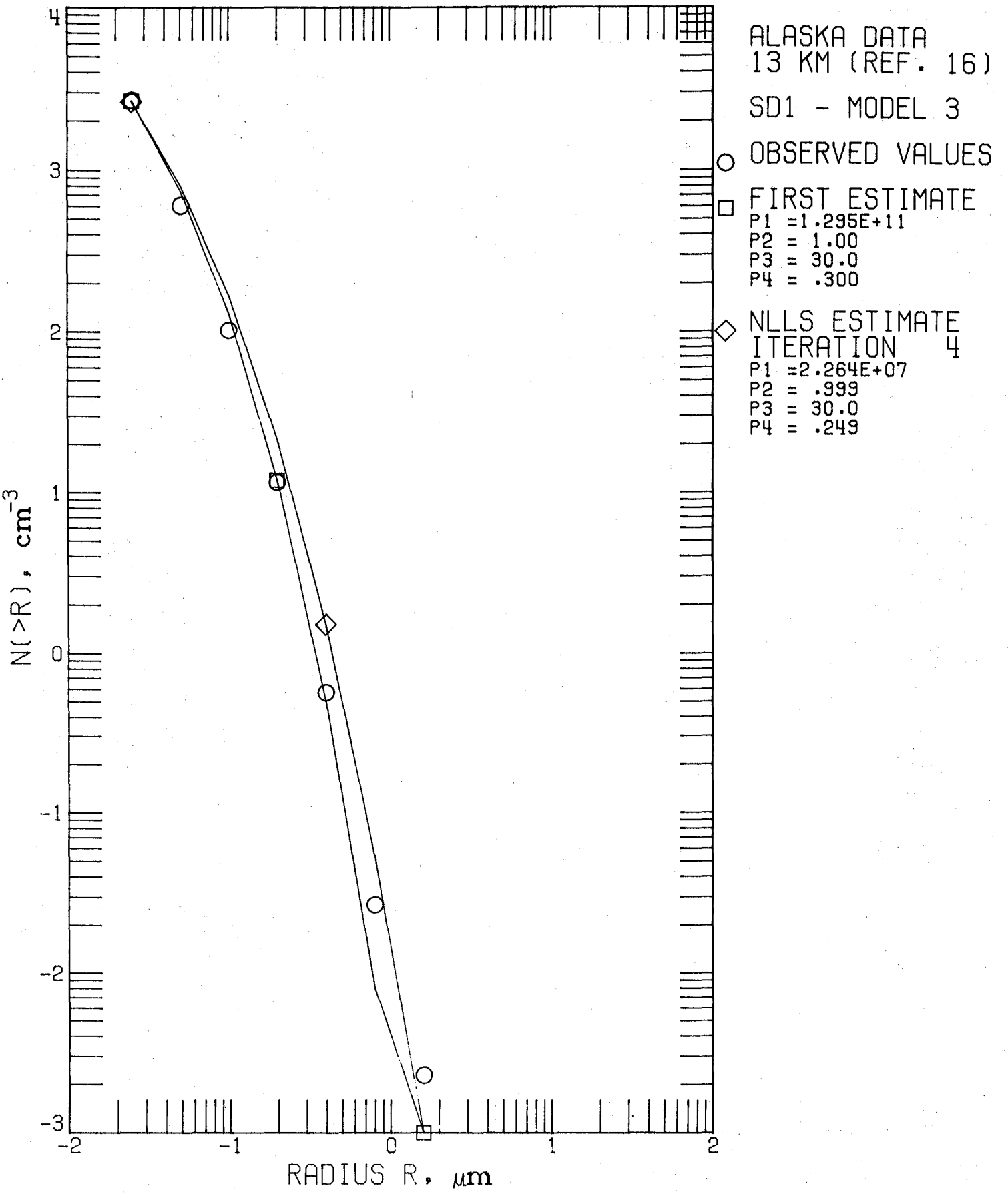

Figure 16. Example of fit to Alaska data using Model 3. (Modified Gamma Distribution).

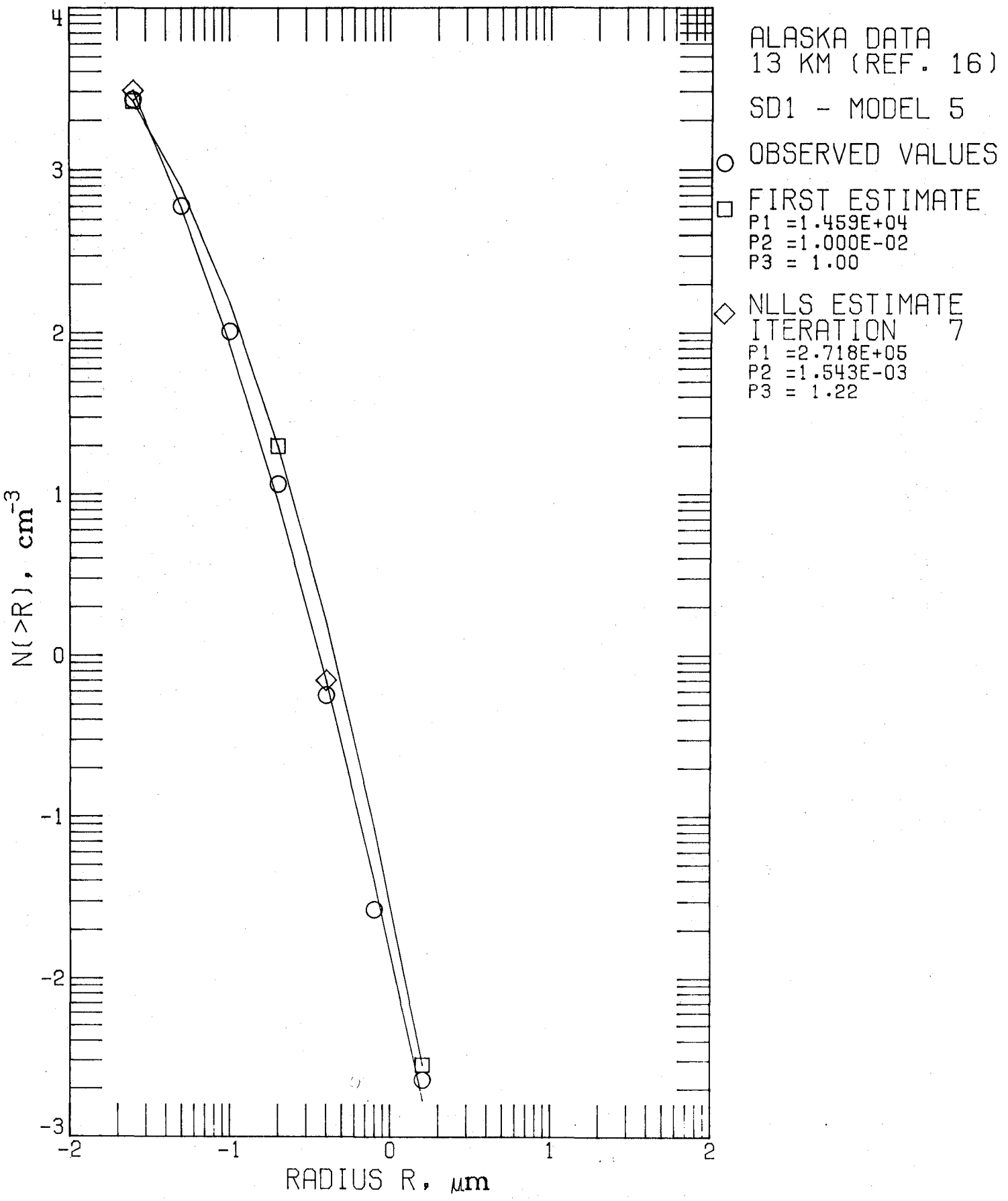

Figure 17. Example of fit to Alaksa data using Model 5. (Log Normal Distribution).

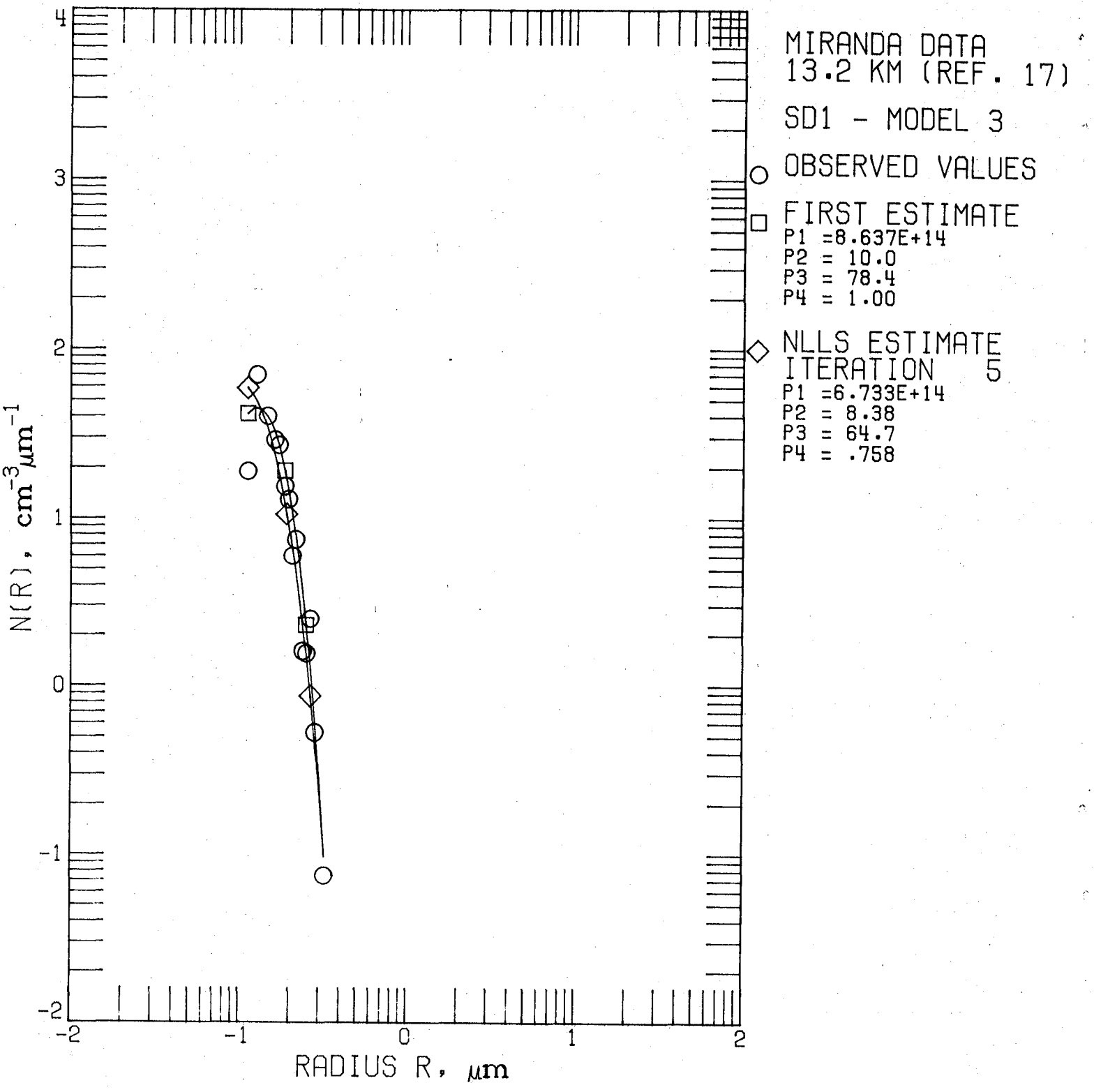

Figure 18. Example of fit to Miranda data using Model 3. (Modified Gamma Distribution).

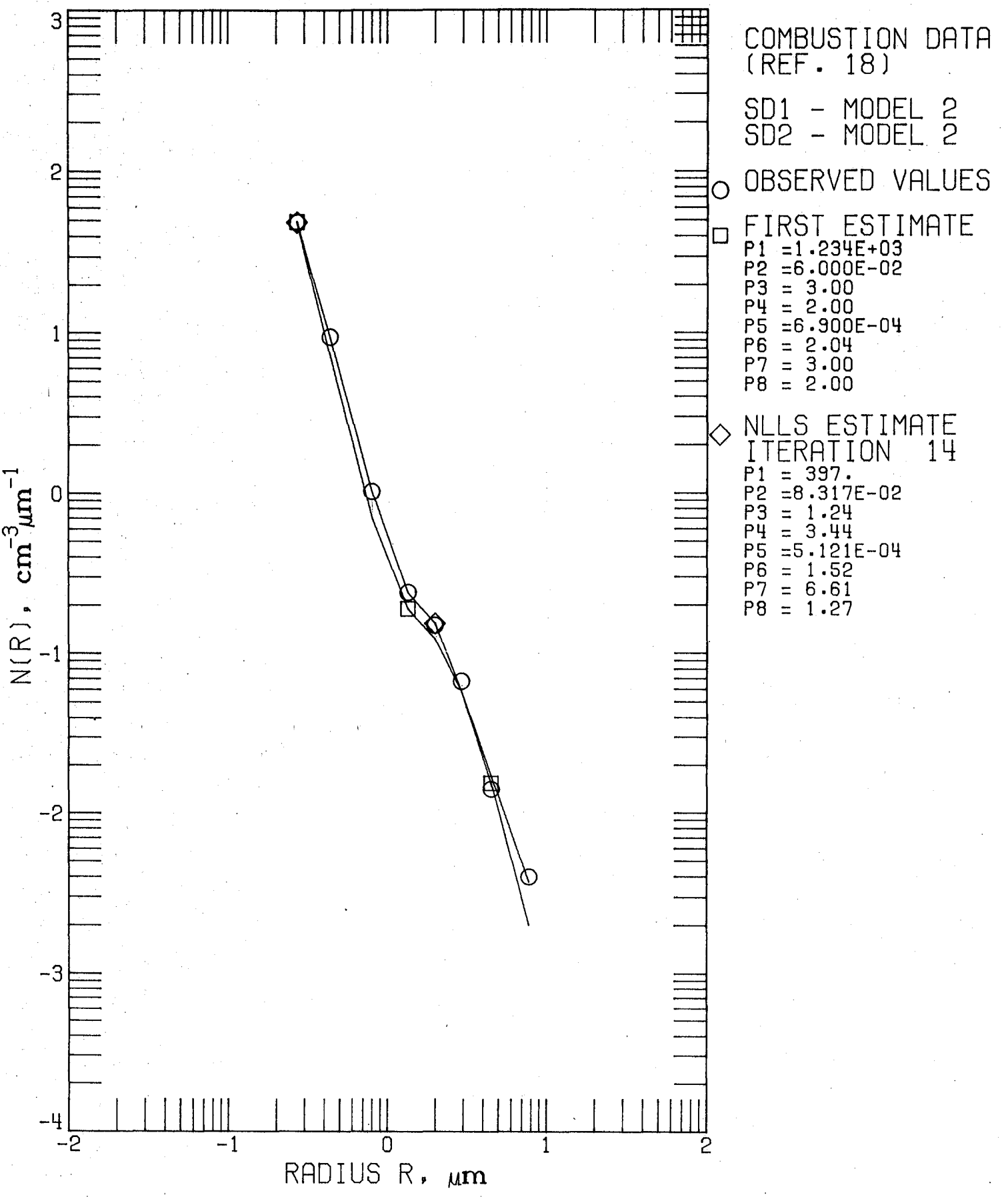

Figure 19. Example of fit to bimodal combustion data using sum of two Model 2's.

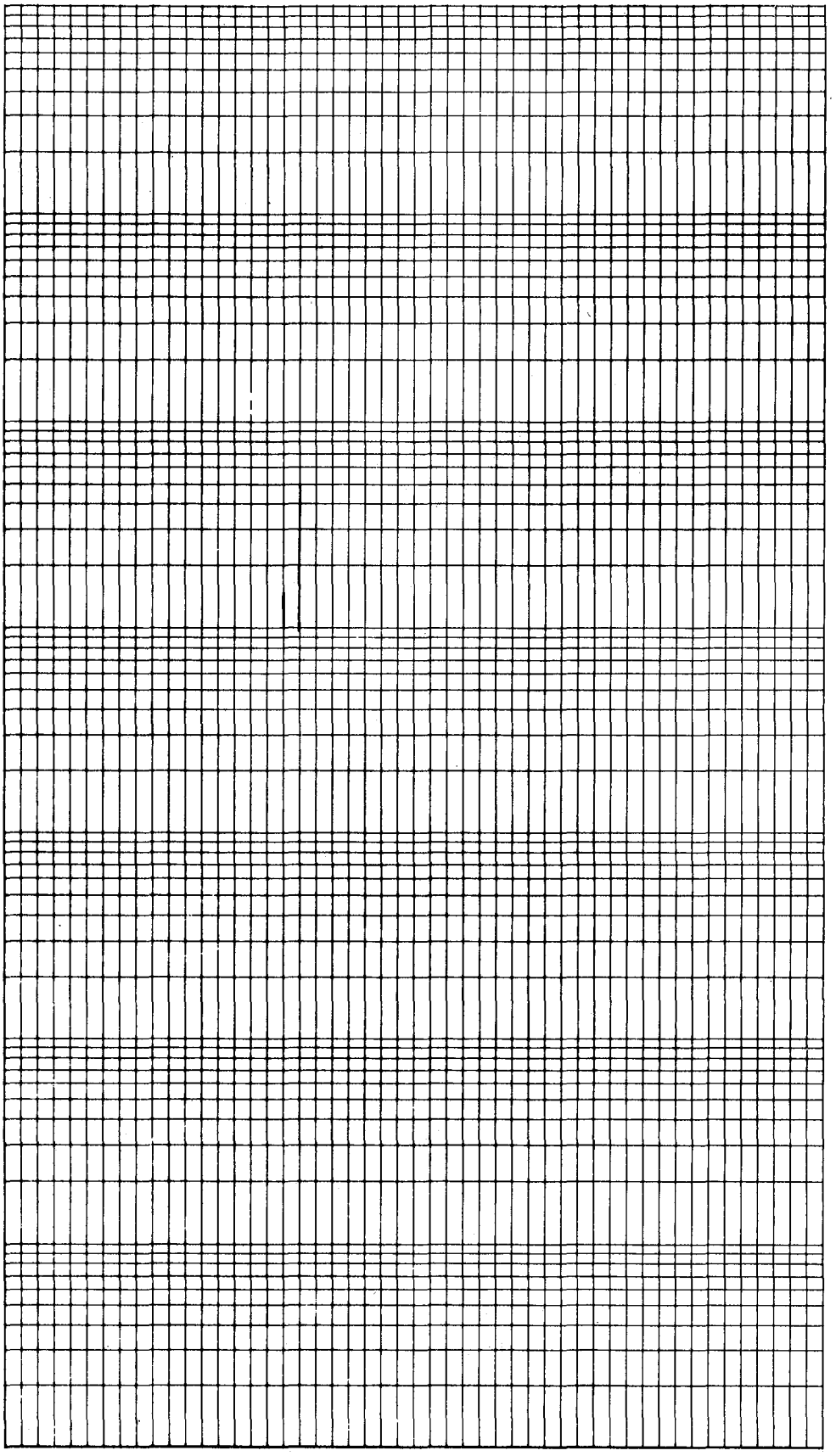

Institute for Atmospheric Optics and Remote Sensing
Post Office Box P, Hampton, Virginia 23666, USA

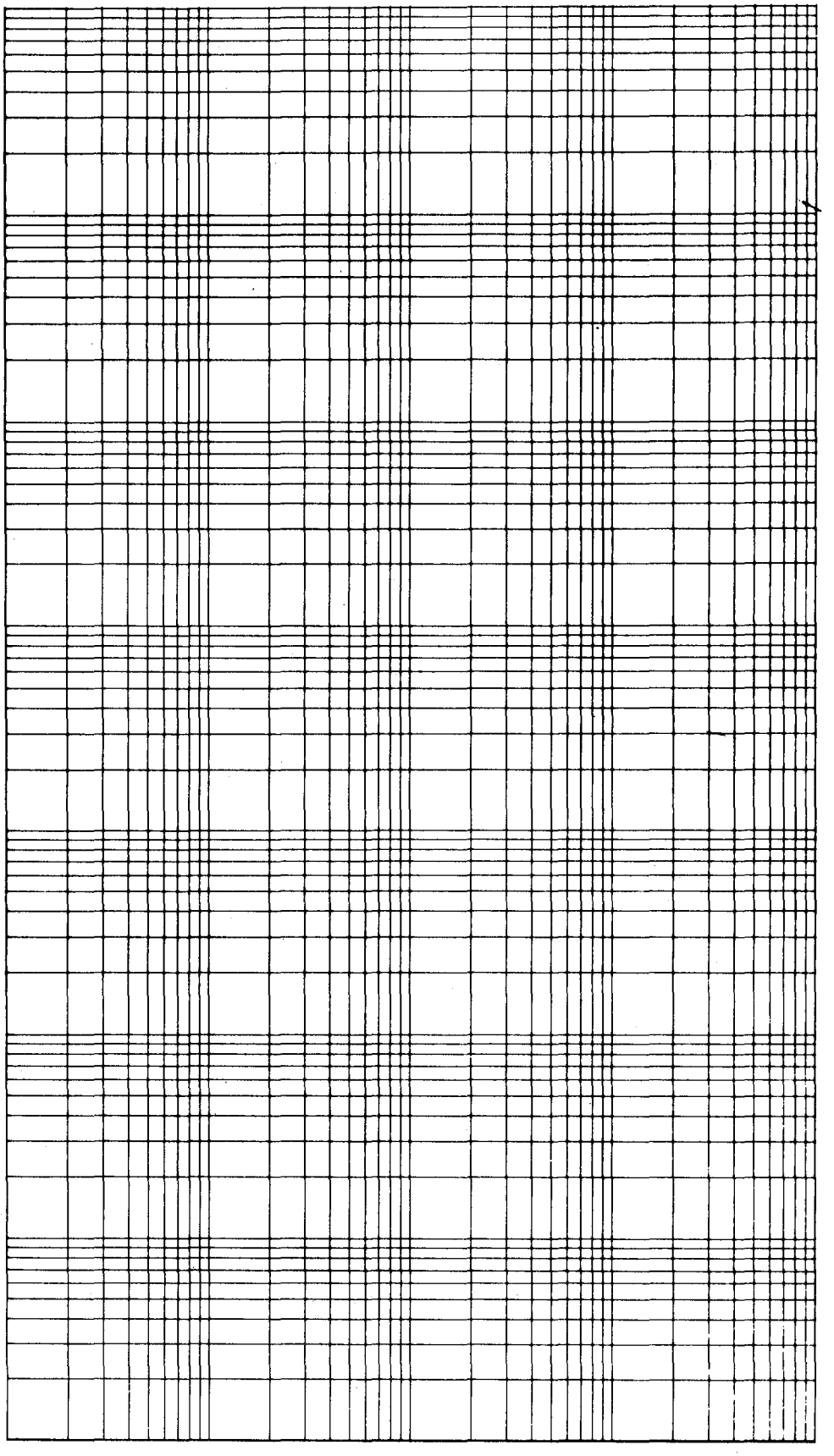

Institute for Atmospheric Optics and Remote Sensing
Post Office Box P, Hampton, Virginia 23666, USA

1. Report No.	2. Government Accession No.	3. Recipient's Catalog No.
NASA CR-159170		

4. Title and Subtitle	5. Report Date
Analytic Modeling of Aerosol Size Distributions	November 1979
	6. Performing Organization Code

7. Author(s)	8. Performing Organization Report No.
Adarsh Deepak and Gail P. Box	
	10. Work Unit No.

9. Performing Organization Name and Address	11. Contract or Grant No.
Institute for Atmospheric Optics & Remote Sensing Hampton, Virginia 23666	NAS1-15198
	13. Type of Report and Period Covered

12. Sponsoring Agency Name and Address	13. Type of Report and Period Covered
National Aeronautics and Space Administration Washington, DC 20546	Contractor Report
	14. Army Project No.

15. Supplementary Notes

Langley technical monitor: Kenneth H. Crumbly

16. Abstract

This report presents the results of a parametric study of some mathematical functions, with up to four parameters, that are commonly used for representing aerosol size distributions and describes methods by which best-fit estimates of these parameters can be obtained. Described in this connection, are a catalog of graphical plots, depicting the parametric behavior of the functions, and the procedures for obtaining analytical representations of size distribution data by visual matching of the data with one of the plots. Examples of fitting the same data with equal accuracy by more than one analytic model are also given.

17. Key Words (Suggested by Author(s))	18. Distribution Statement
Aerosol modeling Radiation	Unclassified - Unlimited

19. Security Classif. (of this report)	20. Security Classif. (of this page)	21. No. of Pages	22. Price*
Unclassified	Unclassified	162	$8.00

*For sale by the National Technical Information Service, Springfield, Virginia 22161